

Intracellular Regulation in Bacteria

**Control of Initiation of Chromosome Replication
Macrolide Antibiotics, Resistance Mechanisms and Bi-
stable Growth Rates**

Karin Nilsson

*Faculty of Natural Resources and Agricultural Sciences
Department of Biometry and Engineering
Uppsala*

**Doctoral thesis
Swedish University of Agricultural Sciences
Uppsala 2006**

Acta Universitatis Agriculturae Sueciae

2006: 72

ISSN 1652-6880
ISBN 91-576-7121-4
© 2006 Karin Nilsson, Uppsala
Tryck: SLU Service/Repro, Uppsala 2006

Abstract

Nilsson, K. 2006. *Intracellular Regulation in Bacteria: Control of Initiation of Chromosome Replication; Macrolide Antibiotics, Resistance Mechanisms and Bi-stable Growth Rates*. Doctor's dissertation.
ISSN 1652-6880, ISBN 91-576-7121-4.

Initiation of chromosome replication is a tightly controlled process. We have developed a stochastic model with all known major features of the regulation of the initiation in *Escherichia coli*, which automatically generates the correct initiation frequency and chromosome number, synchronous initiation of multiple origins and increasing cell size with increasing cell growth rate. We further suggest a principle for how an initiator may at the same time adequately regulate its own gene expression.

In Eubacteria, macrolide antibiotics bind at the entrance of the nascent peptide exit tunnel of the large ribosomal subunit and induce premature termination of translation by drop-off of peptidyl-tRNA. We have combined biochemical experiments and *in vivo* growth experiments with modelling to study peptide-mediated resistance against two different macrolides, erythromycin and josamycin. The mechanism behind resistance is different for the two drugs. In the case of erythromycin, we have verified that synthesis of a *cis*-acting peptide accelerates the rate of dissociation of erythromycin. In the case of josamycin, the drop-off rate of peptidyl-tRNA is considerably slowed down for a peptide sequence mediating resistance in relation to a control peptide sequence. We also show that peptide-mediated resistance requires the AcrAB-TolC efflux system in the cell membrane.

The most widely spread resistance mechanism against macrolides are a modification of the 23S rRNA by an Erm methylase which considerably lowers the affinity of macrolides to the ribosome. Induction of erythromycin resistance by ErmC requires ribosomes both with and without erythromycin. Modelling suggests that there exists a maximal induction rate of the synthesis of ErmC and resistant ribosomes at a certain concentration of the antibiotic.

We also derive how bi-stable growth rates may arise for bacterial cells growing exponentially at a fixed external antibiotic concentration as a consequence of low membrane permeability of the drug and high growth rate sensitivity to the intracellular concentration of the drug concentration.

Keywords: Enterobacteriaceae, replication control, 50S subunit, macrolides, resistance, bi-stability, stochastic, differential equation

Author's address: Karin Nilsson, Department of Biometry and Engineering, SLU, Box 7032, S-750 07 UPPSALA, Sweden. *E-mail:* Karin.Nilsson@bt.slu.se.

Contents

Chromosome replication in *Escherichia coli*, 7

Introduction, 7

The DnaA protein and its role in replication control, 7

The Dam methyltransferase, 16

The SeqA protein, 17

Control of initiation of chromosome replication, 19

Previous models, 19

Results and discussion, 20

A stochastic model of the regulation of initiation of replication, 20

Factors determining the initiation mass, 22

Regulation of the expression of the dnaA promoter, 22

Two tentative molecular mechanisms ending oriC sequestration, 23

Future modelling, 24

Macrolide antibiotics, 26

Introduction, 26

Four generations of macrolides, 26

Macrolide binding and mode of action, 28

Resistance mechanisms, 32

Results and discussion, 36

Validation of the “bottle-brush” mechanism, 36

Different mechanisms of peptide-mediated josamycin and erythromycin resistance, 38

Peptide-mediated macrolide resistance requires a fast outflow rate of the antibiotic over the cell membrane, 41

Erythromycin-induced methylation of 23S rRNA by ErmC, 42

Bi-stable growth rates generated by antibiotics with low membrane permeability, 44

Personal reflections on modelling, 45

References, 46

Acknowledgements, 54

Appendix

Papers I-V

The present thesis is based on the following papers, which will be referred to by their Roman numerals:

I. Nilsson, K., Elf, J., Ringheim, A., Dasgupta, S., Nordström, K. & Ehrenberg, M. Stochastic modelling of regulation of initiation of chromosome replication in single *Escherichia coli* cells. (Manuscript).

II. Lovmar, M, Nilsson, K., Vimberg, V., Nervall, M. & Ehrenberg, M. The molecular mechanism of peptide-mediated erythromycin resistance. 2006. *The Journal of Biological Chemistry* 281, 6742-6750.

III. Nilsson, K, Lovmar, M, Vimberg, V., Tenson, T. & Ehrenberg, M. Mechanisms and requirements of peptide-mediated macrolide resistance. (Manuscript).

IV. Nilsson, K., Tenson, T. & Ehrenberg, M. Traits of erythromycin-induced resistance by methylation of 23S rRNA. (Manuscript).

V. Elf, J., Nilsson, K., Tenson, T. & Ehrenberg, M. Bi-stable bacterial growth rates in response to antibiotics with low membrane permeability. (Submitted).

Paper **II** is reproduced by permission of the journal concerned.

Chromosome replication in *Escherichia coli*

Introduction

The regulation of chromosome replication in the gram-negative Enterobacteriaceae family member, *Escherichia coli*, is the most thoroughly studied within Eubacteria. The genome consists of a single circular chromosome and initiation of replication starts at a unique site, *oriC* (Marsh & Worcel, 1977). Two replication forks move along the chromosome bi-directionally from *oriC* to the *ter* sites in the terminus region (Hill, 1996). For generation times between 60 minutes down to the shortest generation time of 20 minutes, it takes about 40 minutes to complete one round of replication (the C-period) and another 20 minutes to complete cell division following termination of replication (the D-period). Since it takes 60 minutes to complete one cell cycle, the bacterium have overlapping cell cycles at generation times below 60 minutes, and also overlapping rounds of replication for generation times below 40 minutes (Fig. 1). A cell is then born with 2, 4 or 8 origins and replication initiates in the mother, grandmother or grand-grandmother generation, respectively. When the generation time is longer than 60 minutes there also exists a time period between cell birth and initiation of replication (the B-period) (Cooper & Helmstetter, 1968). Multiple origins initiate synchronously and initiation is triggered once every cell generation (Skarstad, Boye & Steen, 1986; Boye, Løbner-Olesen & Skarstad, 2000). Three proteins seem central for initiation control (see below). The DnaA protein binds at *oriC* and builds-up a nucleoprotein complex, which promotes strand opening and thereby initiates replication (Messer, 2002). Along the chromosome DnaA binding sites are scattered, where the *datA* locus reached by the replication fork eight minutes after initiation are known to titrate the highest number of DnaA molecules (Kitagawa *et al.*, 1996). DnaA exists in two forms, DnaA-ATP and DnaA-ADP and DnaA-ATP is active at initiation (Messer, 2002). Both forms of DnaA can repress the *dnaA* gene (Speck, Weigel & Messer, 1999). Conversion of DNA-bound DnaA-ATP to DnaA-ADP is stimulated by passage of the replication fork (called RIDA) (Katayama *et al.*, 1998). Following initiation *oriC* becomes hemi-methylated. The SeqA protein and the methyltransferase Dam regulate the methylation status of *oriC*. SeqA binds *oriC* after initiation and prevents immediate re-methylation by Dam (Lu *et al.*, 1994; von Freiesleben, Rasmussen & Schaechter, 1994; Løbner-Olesen, Skovgaard & Marinus, 2005). Fig. 2 shows the three proteins involvement in the control of replication initiation.

The DnaA protein and its role in replication control

DnaA binding sites

Along the chromosome are different types of DnaA binding sites scattered. The DnaA box is a 9-mer with the consensus sequence 5'-TT^T/_ATNCACA which both forms of DnaA bind with the same affinity (K_D between 0.6 and 50 nM) and constitutes a strong DnaA binding site (Messer, 2002). About 300 DnaA boxes of the stringent form are found on the *E.coli* genome (Roth and Messer, 1998). Less stringent definitions of the 9-mer also exist. In addition to DnaA boxes, DnaA-ATP

also binds 6-mer sequences called DnaA-ATP boxes. The affinity to the less stringent 9-mer DnaA boxes and to DnaA-ATP boxes is lower (K_D about 400 nM) than to the stringent strong DnaA box (Messer, 2002). In *oriC*, there is also weak 9-mer sequences, I-sites, which binds DnaA-ATP (Grimwade, Ryan & Leonard, 2000). All the weak boxes require an adjacent strong 9-mer DnaA box for DnaA binding (Messer, 2002; Leonard & Grimwade, 2005). Besides the primary nucleotide sequence of the DnaA box is the sequence surrounding the box of importance for DnaA binding efficiency (Schaper & Messer, 1995).

The site known to titrate the highest number of DnaA molecules (about 370 *in vitro*) is called *datA* (DnaA titration). It is located 470 kb from *oriC* and is reached by the replication fork approximately eight minutes after initiation (Kitagawa *et al.*, 1996). At initiation a nucleoprotein complex involving 20-30 DnaA monomers are formed (Messer, 2002). A fine-tuned sequential order of DnaA binding to boxes with varying affinity has been unravelled which suggest a switch, quickly creating strand opening once a high enough free concentration of the DnaA protein is reached (see orisome building below). Besides *datA* and *oriC* only four additional high-affinity binding sites, rather evenly distributed along the chromosome, have been found. No consensus as to the number and spacing of the DnaA boxes as well as the ± 40 bp sequences surrounding the DnaA boxes were found which could explain why these sites bind DnaA with high affinity (Roth & Messer, 1998).

Orisome building by DnaA

Binding of DnaA-ATP to the AT-rich region at the left border of *oriC* (Fig. 3) promotes strand opening followed by the consequent loading of the enzymes required for replication fork assembly and movement (DnaB helicase, DnaG primase and DNA polymerase III etc.) (Messer, 2002). Therefore, the building of a stable orisome (nucleoprotein complex at *oriC*) by binding of DnaA-ATP to the AT-rich region should be a key event to be tightly regulated to generate the correct timing of initiation of replication. Regulation by the rate of DnaA-ATP accumulation in the cell and by fine tuned differences in binding affinities of the DnaA binding sites in *oriC* appear as a straightforward way to achieve this, and is supported by experiments. Results from replication-synchronised cultures indicate that there may exist a cell cycle dependent oscillation of DnaA-ATP, where the fraction of DnaA in the ATP-form temporarily increases at the time of initiation (Kurokawa *et al.*, 1999). The affinity for DnaA of the different types of binding sites in *oriC* varies, and can be grouped in three classes: (i) strong sites (R1, R2, R4), (ii) weak sites (R5, R3, I1, I2, I3) and (iii) the single stranded DnaA-ATP box within the 13-mers in the AT-rich region (Leonard & Grimwade, 2005).

In addition to DnaA, the Fis (factor of inversion stimulation) and the IHF (integration host factor) proteins stand out as important in the control of orisome assembly. DnaA is bound to the strong sites R1, R2 and R4 most of the cell cycle (Samitt *et al.*, 1989) while DnaA binding to the other sites in *oriC* only occurs at the time of initiation (Ryan *et al.*, 2004). Similarly, Fis is bound most of the cell cycle at its primary binding site next to the R2 box while IHF only bind at the time of initiation (Cassler, Grimwade & Leonard, 1995). Foot printing studies *in vitro* showed that Fis suppresses IHF and DnaA binding to the weak sites but an

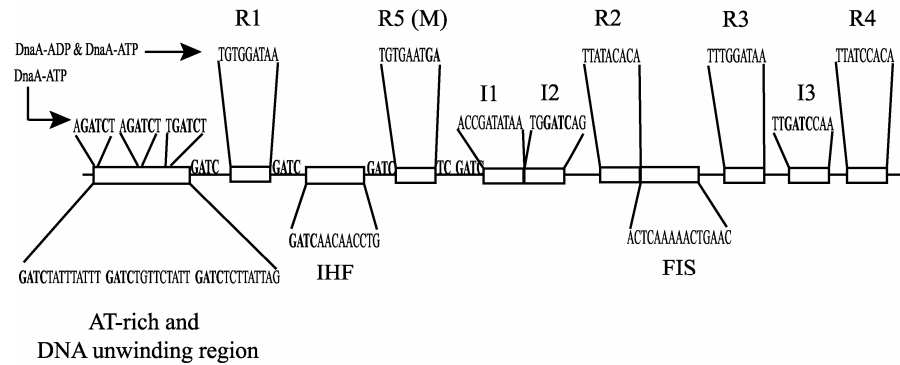


Figure 3. Binding sites of DnaA and SeqA and the primary binding sites of IHF and Fis within the *E. coli* replication origin, *oriC*. The sequences are all derived from the top DNA strand and are in the correct orientation on that strand. The 9-mer DnaA boxes (R1, R2, R3, R4, R5 (or M)) binds both DnaA-ADP and DnaA-ATP while the I-sites (I1, I2, I3) and 6-mer DnaA-ATP boxes in the AT-rich region only binds DnaA-ATP. The GATC sites, which binds SeqA when hemi-methylated, are shown in bold text. Adapted from Leonard & Grimwade (2005).

increased concentration of DnaA weakened Fis binding and allowed IHF to bind along with DnaA to the remaining R boxes, R5 and R3, and the I-sites. At this point the AT-rich region is unwound and DnaA-ATP binds to the ssDNA 13-mer sites ensuring stable strand separation (Ryan *et al.*, 2002; McGarry *et al.*, 2004; Ryan *et al.*, 2004). Taken together, it suggests that a raising level of DnaA-ATP can create a switch with the aid of Fis and IHF during orisome assembly to rapidly form a stable orisome once the DnaA-ATP concentration has reached a certain concentration.

DnaA as a repressor of transcription

The *dnaA* gene is transcribed from two promoters, *dnaAp1* and *dnaAp2*, where *dnaAp2* is the strongest (Hansen, Hansen & Atlung, 1982; Chiamarello & Zyskind, 1990). DnaA binding sites, two 9-mer DnaA boxes and three 6-mer DnaA-ATP boxes are located between the promoters (Speck, Weigel & Messer, 1999). Inactivation of DnaA in temperature-sensitive mutants derepresses *dnaA* transcription and DnaA overproduction leads to repression of the chromosomal *dnaA* expression (Atlung, Clausen & Hansen, 1985). Speck, Weigel & Messer (1999) studied expression of the two promoters *in vitro* in the presence of either DnaA-ATP or DnaA-ADP for concentrations between 0 and 300 nM. Transcription from the promoters decreases sharply and simultaneously from 100% to 40 % when adding DnaA-ATP up to 100 nM and is negligible at 300 nM. Expression from the two promoters also decreases synchronously when increasing the DnaA-ADP concentration but the change is less distinct than in the presence of DnaA-ATP. Up to 200 nM the expression level roughly decreases two-fold when doubling the DnaA-ADP concentration. At 300 nM the promoters still show approximately 35% activity. Thus, both forms of DnaA can repress transcription, and promoter activity is more sensitive to changes in the DnaA-ATP concentration than to the DnaA-ADP concentration (Speck, Weigel & Messer, 1999).

DnaA also represses the expression of other genes, *e.g.* the *mioC*, *uvrB* and *rpoH* genes. DnaA has also been reported to activate transcription of the *glpD* gene and the *nrd* operon (Messer & Weigel, 1997). However, DnaA was recently shown to repress the *nrd* operon (Gon *et al.*, 2006). The *nrd* operon encodes the two subunits of the ribonucleotide reductase (RNR) enzyme which catalyses the reduction of ribonucleotides to deoxyribonucleotides. The *nrd* promoter contains two 9-mer DnaA boxes as well as sequences for DnaA-ATP boxes (Gon *et al.*, 2006), similar to the region between the *dnaA* gene promoters.

Conversions between the two forms of the DnaA protein

Newly synthesised DnaA protein is expected to form complex with ATP since the ATP concentration in the cell is approximately ten times higher than the ADP concentration (Bochner & Ames, 1982). Spontaneous hydrolysis of ATP to ADP and exchange of nucleotides are slow in solution. The spontaneous rate of ATP hydrolysis corresponds to a 50% percent reduction of DnaA-ATP in 15 minutes. About 50% of the DnaA-ADP complexes had changed nucleotide after 30 minutes in excess ATP. Similar results were observed for the nucleotide exchange of DnaA-ATP (Sekimizu, Bramhill & Kornberg, 1987). Besides spontaneous conversions between the DnaA forms, there exists a regulated inactivation of DnaA-ATP to DnaA-ADP connected to the movement of the replication fork. Acidic phospholipids in the cell membrane can dissociate a nucleotide bound to DnaA, which offers a rejuvenation pathway of inactive DnaA-ADP to active DnaA-ATP, but its significance *in vivo* is unclear.

Regulatory inactivation of DnaA

Regulatory inactivation of DnaA (RIDA) accelerates the hydrolysis of ATP bound to DnaA, generating DnaA-ADP, which is incapable of triggering initiation of replication. The essential components of RIDA are the β -subunit of the DNA polymerase III holoenzyme, encoded by the *dnaN* gene, and the Hda (“homologous to DnaA”) protein (former named IdaB) (Katayama *et al.*, 1998; Kato & Katayama, 2001). The β -subunit is called the “the sliding clamp” because it forms a ring-shaped homodimer, which encircles and slides on DNA (Kuriyan & O’Donnell, 1993). Based on the *in vitro* observations that RIDA require dsDNA present *in cis* to the loaded β clamp, that the Hda protein forms a stable complex with the sliding clamp and that DnaA-ATP bound to DnaA boxes present *in trans* are less sensitive to RIDA than free DnaA-ATP, Su’etsugu *et al.* (2004) suggest that DnaA-ATP proteins bound to DnaA binding sites along the chromosome are released by passage of the replication fork and converted to DnaA-ADP by interacting with a dsDNA: β clamp:Hda complex.

In an asynchronous, exponentially growing wild-type culture only 15-30% of the DnaA protein exist in the ATP form. To sustain a high DnaA-ADP fraction ongoing replication is required as shown by comparing a wild-type culture to a *dnaN* temperature sensitive (Ts) mutant culture grown at the restrictive temperature. A high percentage DnaA-ADP also requires *de novo* synthesis of DnaA as demonstrated by the same *dnaN* (Ts) mutant grown at the restrictive temperature in the presence and absence of chloramphenicol, which inhibits translation (Kurokawa *et al.*, 1999). Cells with a deleted *hda* gene, Δhda , have an

asynchronous, over-initiating phenotype (Camara, Skarstad & Crooke, 2003; Camara *et al.*, 2005; Morigen, Molina & Skarstad, 2005). The DnaA/total protein ratio is only slightly increased while the *oriC*/terminus ratio is significantly increased (~ 2 times) in a Δhda strain compared to the wild-type (Camara *et al.*, 2005). Measurements of the *oriC*/terminus ratio in an *hda* (Ts) mutant gave the same qualitative results (Kato & Katayama, 2001). RIDA is usually assumed to be required for reducing the initiation potential following initiation, why the Δhda phenotype has been ascribed the cells expected inability to reduce the initiation potential (Morigen, Molina & Skarstad, 2005). However, the growth defect seen in a Δhda strain was overcome by overexpressing the ribonucleotide reductase (RNR) enzyme, which catalyses the reduction of ribonucleotides to deoxyribonucleotides (dNTPs). DnaA regulates the *nrd* genes encoding RNR, as described above. The apparent connection between Hda presence and RNR indicates that the distorted replication observed in Δhda cells at least partly is a consequence of an increased repression of the *nrd* expression by an increased concentration of DnaA-ATP in the cell, generating a lack of dNTPs and DNA fork stalling (Gon *et al.*, 2006). Perhaps the adverse effect on growth and the regulation of replication initiation observed in Δhda cells, mainly follow from altered gene expression of *dnaA* and *nrd*, both regulated by DnaA. Recently, Riber *et al.* (2006) showed a correlation between the Hda concentration in the cell and *dnaA* gene expression.

Acidic phospholipids

Acidic phospholipids *e.g.* cardiolipin, in a fluid phase membrane, accelerates the dissociation of either of the nucleotides in complex with DnaA and are responsible for the increased rate of nucleotide exchange detected *in vitro*. Phospholipid treated DnaA-ADP can be reactivated and trigger *in vitro* replication in the presence ATP, *oriC* DNA and replication enzymes (Sekimizu & Kornberg, 1988). Since the free ATP concentration in the cell is expected to be much higher than the free concentration of ADP, it suggests that phospholipids constitute a rejuvenation pathway for DnaA-ADP to DnaA-ATP. Recent *in vitro* experiments using DnaA-ATP interacting with membrane to study the exchange of DnaA bound nucleotides by phospholipids suggest that there exists a switch in the phospholipid/DnaA protein ratio at which the dissociation rate constant of phospholipid promoted nucleotide dissociation is changed. When the membrane occupancy is low enough, the rate of nucleotide dissociation is increased, which makes dissociation critically dependent on the crowding of total protein on the membrane (Aranovich *et al.*, 2006).

Initiation of replication is dependent on the presence of acidic phospholipids in the cell membrane. When the concentration of acidic phospholipids drops below a critical level, DnaA-dependent initiation of replication at *oriC* is inhibited and cell growth arrests (Xia & Dowhan, 1995; Zheng *et al.*, 2001). Constitutive replication initiated from *oriK* sites or mutated DnaA protein in the carboxyl region required for DnaA-phospholipid interactions *in vitro*, allows replication to proceed and restores cell growth (Xia & Dowhan, 1995; Zheng *et al.*, 2001). However, while this suggests that DnaA binding to acidic phospholipids in the membrane is essential for initiating replication it does not directly implicate that acidic phospholipids also are responsible for developing a high initiation potential by

accelerating the dissociation of ADP from DnaA at the time of initiation. Instead the DnaA-membrane interaction may be a control mechanism to promote proper chromosome segregation prior to cell division. Recently Li *et al.* (2005) showed that a mutant DnaA protein, which restores growth in phospholipid-deficient cells, does so independent of its capacity to bind and exchange nucleotides.

The initiation mass

For generation times between 60 and 20 minutes, the replication time of the chromosome (the C-period) and the time from termination of replication to cell division (the D-period) are approximately constant, 40 and 20 minutes, respectively (Cooper & Helmstetter, 1968). Donachie (1968) combined the findings by Cooper & Helmstetter with cell mass measurements of *Salmonella typhimurium* grown in different media (Schaechter, Maaløe & Kjeldgaard, 1958) to introduce the concept of a constant initiation mass, defined as cell mass/#chromosome origins, at the onset of one round of replication. Later estimates of the initiation mass question its constancy but instead indicate that the mass might vary considerably and increase with growth rate (B/r strain) (Churchward, Estiva & Bremer, 1981) in some strains of *E.coli* and stay approximately constant in others (K-12 strain) (Wold *et al.*, 1994). The initiation mass has most certainly been of conceptual help in the process of elucidating the regulation of chromosome replication but probably is its constancy of less importance for the bacterium. Instead focus should be on the factors determining the initiation mass (Herrick *et al.*, 1996). Many experiments point in the direction of the number of DnaA boxes and the number of DnaA molecules in the cell determining the initiation mass. Thus, the demand and supply of DnaA seem to set the initiation frequency, which determines the cell size at initiation and influences the initiation mass accordingly.

Phenotypes resulting from manipulations of the number of DnaA boxes and the DnaA concentration

Results from numerous experiments show that the amount of DnaA in relation to the number of DnaA binding sites on the chromosome by and large controls the initiation of replication. One way to manipulate the relation between DnaA and its binding sites in the cell is to change the concentration of the DnaA protein. When the DnaA concentration varies both below and above the normal concentration in cells completely dependent on plasmid-borne *dnaA* expression, the cell size is increased or decreased, respectively (Løbner-Olesen *et al.*, 1989). Overproduction of DnaA by controlling the expression of the *dnaA* gene carried on a plasmid increases the mini-chromosome copy number (Atlung, Løbner-Olesen & Hansen, 1987) and the chromosomal gene dosage of *oriC* proximal DNA but not the overall DNA content (Atlung, Løbner-Olesen & Hansen, 1987; Skarstad *et al.*, 1989). The response of cells subjected to a gradual elevating DnaA overproduction can be divided into 3 states (Atlung & Hansen, 1993). A slight overproduction (up to 1.5 times the normal DnaA concentration) generates a nearly proportional increase between *oriC* and DNA concentration. Between 1.5 to 3-fold normal DnaA concentration the *oriC* concentration increases more than the DNA concentration. Beyond a 3-fold increase in DnaA concentration there is no further increase of the

oriC concentration. Asynchronous initiations of multiple origin cells increase both at a lower and higher than normal concentration of DnaA (Løbner-Olesen *et al.*, 1989; Skarstad *et al.*, 1989; Atlung & Hansen, 1993) although retained synchrony in DnaA over-producing cells has also been reported (Løbner-Olesen *et al.*, 1989). DnaA overproduction also result in slowed down replication fork movement and stalled or collapsed replication forks (Atlung, Løbner-Olesen & Hansen, 1987; Løbner-Olesen *et al.*, 1989; Skarstad *et al.*, 1989; Atlung & Hansen, 1993; Simmons *et al.*, 2004), which may explain the disproportional increase between *oriC* and overall DNA concentration.

Another way to change the wild-type relation between the amount of DnaA and its binding sites is to change the number of binding boxes in the cell, either by deletion of boxes on the chromosome or by introducing extra boxes, usually carried on plasmids. Extra-chromosomal *oriC* boxes result in larger cells, increased asynchrony and derepression of the *dnaA* promoters (Christensen, Atlung and Hansen, 1999). A 4-fold increase in *datA* dosage (MiniR1-borne *datA*) or a 12-fold increase (pACYC177-borne *datA*) result in an increased cell size, a decreased DNA concentration and a lowered origin/terminus ratio compared to the wild-type. The differences accumulate with increasing *datA* copy number. Introduction of a DnaA-overproducing plasmid suppresses the effects of the extra *datA* sites (Morigen, Løbner-Olesen & Skarstad, 2003). With an increasing number of *datA* copies in the cell, increased initiation asynchrony and *dnaA* derepression also follow (Morigen *et al.*, 2001; Morigen, Løbner-Olesen & Skarstad, 2003). Interestingly, the 4-fold increase of *datA* dosage also resulted in a 2-fold increase in replication fork movement. A further increase in *datA* dosage (above 10-fold) induces the SOS response and slows down or inhibits replication fork movement. The *datA* locus has been suggested to be important for reducing the initiation potential following initiation because of its capacity of binding a high number of DnaA molecules. In line with this idea, deletion of *datA* was reported to generate an asynchronous phenotype (Kitagawa *et al.*, 1998). The fraction of cells containing an even number of chromosomes after replication run-out is a measure of how synchronously multiple origins fired in the cell. Rifampin blocks *de novo* initiation of replication by inhibiting primer formation but allows ongoing rounds of replication to finish. By increasing the concentration of rifampin added in replication run-out experiments Morigen, Molina & Skarstad (2005) demonstrated that the previously observed initiation asynchrony largely depends on rifampin-resistance in the $\Delta datA$ strain, allowing for extra rounds of replication to be initiated in replication run-out experiments. The cause of the observed rifampin-resistance is not clear. Besides a moderate increased initiation asynchrony, the $\Delta datA$ cells have on the average an 18% lower cell mass compared to wild-type cells (Morigen, Molina & Skarstad, 2005).

Hansen, Christensen & Atlung (1991) proposed that DnaA binds *oriC* and initiates replication when it has saturated all its binding sites outside *oriC* (the initiator titration model, see below). The observed changes in cell size when either the DnaA concentration or the concentration of DnaA boxes are changed is in line with this idea (Christensen, Atlung & Hansen, 1999; Morigen, Molina & Skarstad, 2005). An increased concentration of DnaA or deletion of *datA* generates smaller than normal cells as expected if the boxes are saturated faster than normal so that initiation takes place earlier during the cell cycle. The increased concentration of

oriC DNA in the DnaA over-producing cells is in line with an increased initiation frequency. A lower than normal concentration of DnaA or introduction of extra copies of *oriC* boxes or of the *datA* locus, result in larger cells as expected if it takes a longer time to saturate the DnaA binding sites and initiation therefore occurs later than normal during the cell cycle.

The observed change in replication fork movement is not directly explained by alterations in the DnaA protein-DnaA box relation, but it may create changes in gene expression of DnaA regulated promoters. If the replication fork movement is mainly limited by the supply of dNTPs an altered *nrd* gene expression may explain the effects on fork movement. Overproduction of DnaA slows down the speed of replication forks in line with the idea that the free concentration of DnaA-ATP is elevated, which represses *nrd* expression more than normal in these cells. An elevated copy number of *oriC* boxes or of *datA* seem to cause derepression of the *dnaA* promoters and likewise the *nrd* promoter might become further derepressed, increasing the RNR synthesis and thereby dNTPs production. This may allow a faster than normal fork movement, which would explain why replication forks in cells with a 4-fold increase in *datA* dosage moves with twice the speed of wild-type replication forks. A changed speed of the replication forks should also change the rate DnaA boxes become duplicated and the rate of DnaA-ATP conversion to DnaA-ADP by RIDA, which in turn feeds back and affects the DnaA regulated gene expression.

The observed increased asynchrony when the wild-type relation between the amount of DnaA protein and DnaA boxes is altered may be generated in at least three different ways. Generally, plasmids replicate throughout the division cycle to keep a constant plasmid concentration in the host cell. Thus, accumulation of DnaA boxes in proportion to the cell volume increase, if carried on plasmids, may interfere and disrupt the build-up of an initiation potential, leaving some origins fired and others unfired (Christensen, Atlung & Hansen, 1999). Asynchrony in cells with a DnaA synthesis below the wild-type level may be generated by a peak in the free concentration of DnaA-ATP less distinct at the time of initiation, while asynchrony in cells with a DnaA synthesis above the wild-type level may be a result of failed *oriC* sequestration following initiation. Yet another explanation may be the disturbed movement of replication forks. Both a high enough DnaA overproduction and a high enough *datA* dosage result in replication fork stalling and collapse, which would make cells appear asynchronous in replication run-out experiments even if initiation occurred synchronously.

Mini-chromosomes

The attention that mini-chromosomes, plasmids replicating exclusively from a cloned *oriC* copy, have received originates from several seemingly puzzling properties. Mini-chromosomes are not only compatible with the chromosome but replication is initiated in synchrony with the chromosome and a high copy number of mini-chromosomes can be maintained within the cell although at high loss frequencies (Helmstetter & Leonard, 1987; Løbner-Olesen, 1999). Therefore, it seems that *E.coli* cells do not control mini-chromosomal number and that there does not exist a copy number control of the chromosomal origin (Jensen, Løbner-Olesen & Rasmussen, 1990). However, mini-chromosomes only contain the DNA

sequence required for replication initiation and lacks the *dnaA* gene and the DnaA boxes along the chromosome, both of which potentially control initiation of replication (Dasgupta & Løbner-Olesen, 2004). Thus, the apparent lack of incompatibility of mini-chromosomes only demonstrates that the copy number of the origin is not directly regulated but it does not exclude that some other control element, with a copy number proportional to the origin, may be regulated. Many mini-chromosomes of other species of bacteria show a high incompatibility with the chromosomal origin. However, these bacteria also contain a high number of DnaA boxes in the origin, which may bind a high number of DnaA molecules (Dasgupta & Løbner-Olesen, 2004), suggesting that the origin acts as a control element. The high loss frequencies of mini-chromosomes, has been attributed to a lack of partition mechanism (Jensen, Løbner-Olesen & Rasmussen, 1990) but may also be a consequence of the chromosome determining the initiation potential. Once the chromosomal origin has fired among all the *oriC* copies in the cell, *dnaA* expression is shut-off and DnaA will bind to boxes along the chromosome, especially the *data* locus. Thus, mini-chromosomes that did not fire prior to the chromosomal *oriC* will not fire, why mini-chromosomes copy number will vary from generation to generation dependent on when the chromosomal origin fired.

The Dam methyltransferase

Dam methylation of GATC sites

The *dam* gene encodes a DNA methyltransferase (DamMT), which transfers methyl groups from S-adenosyl-L-methionine to the adenine residues in the sequence 5'-GATC-3' in double-stranded DNA so that they contain an N⁶-methyladenine (Marinus, 1996). Methylation lags behind the replication fork why newly synthesised DNA exists in a hemi-methylated state (Campbell & Kleckner, 1990). Dam methylation affects post-replicative mismatch repair, nucleoid structure, control of DNA replication and gene regulation (Løbner-Olesen, Skovgaard & Marinus, 2005). Initiation of replication is prevented from a hemi-methylated *oriC* (Russell & Zinder, 1987). The Dam enzyme acts as a functional monomer and only one strand is modified in each DNA binding event (Urig *et al.*, 2002). From *in vitro* experiments, Dam was estimated to scan 3000 GATC sites and to methylate 55 sites on the average per binding event in a random walk on 48 502 base-pairs of λ -DNA containing 116 GATC sites (Urig *et al.*, 2002). The highly processive reaction of Dam greatly speeds up DNA methylation, which may explain why a low number of Dam molecules (20-130) in the cell can sustain GATC methylation during replication (Boye, Marinus & Løbner-Olesen, 1992; Szyf *et al.*, 1984; Urig *et al.*, 2002). Processive methylation of DNA also results in DNA stretches completely methylated alternated by completely unmethylated stretches (Urig *et al.*, 2002). The concentration of Dam is critical for coordination of initiations. The cellular level of Dam was controlled using a plasmid-borne *dam* gene with a temperature-inducible promoter and the effect on the regulation of replication initiation was studied (Boye & Løbner-Olesen, 1990). Initiation synchrony was found only within a narrow temperature range. Most GATC sites become methylated within 1-2 minutes, except for the sites in *oriC* and in the *dnaA* promoter region, which stays hemi-methylated a prolonged period of time (Campbell & Kleckner, 1990). Exactly how long *oriC* and *dnaA* are sequestered

following initiation is not known. Campbell and Kleckner (1990) estimated the time period from the average value in a non-synchronised culture at two different growth rates. The calculated sequestration times for two individual GATC sites in *oriC* was approximately 30% for a generation time of about 28 minutes and approximately 40% for a generation time of about 53 minutes. This is so often cited in the literature as a sequestration period of one-third of a cell cycle independent of growth rate. However, one may argue that estimated times from only two different generation times might be too uncertain and too scarce data to generalise from. The sequestration time of the studied GATC site in *dnaA* promoter region was about 50% shorter than for the sites in *oriC*. In a synchronised culture the same GATC sites in *oriC* and in the *dnaA* promoter became methylated approximately after the same time, 13 minutes following initiation. (Campbell & Kleckner, 1990; Lu *et al.*, 1994). Thus, there is a discrepancy between the sequestration periods of *oriC* and of the *dnaA* promoter in the non-synchronised and synchronised culture. This may be a result of a bad estimate of the sequestration time from average values in the non-synchronised culture or there really is a difference in length dependent of growth rate and manipulation when synchronising the culture may generate a longer sequestration period of the *dnaA* promoter. Thus, how the sequestration period varies with the generation time is not clear.

The SeqA protein

SeqA negatively controls initiation of chromosome replication

The molecule responsible for the prolonged sequestration time of *oriC* and *dnaA* is the SeqA protein (Lu *et al.*, 1994). In a *seqA* null mutant the hemi-methylated state was reduced from 13 to 5 minutes for GATC sites in *oriC* and the *dnaA* promoter in a synchronised culture (Campbell & Kleckner, 1990; Lu *et al.*, 1994). SeqA inhibits initiation of replication from *oriC* *in vitro* by preventing prepriming complex formation (Taghbalout *et al.*, 2000; Torheim & Skarstad, 1999; Wold *et al.*, 1998) and *in vivo* the GATC sequence, number and spacing between the sites in *oriC* yields full sequestration by SeqA (Bach & Skarstad, 2004; Bach & Skarstad, 2005). *In vitro*, SeqA exhibits a higher affinity for hemi-methylated *oriC* than for fully methylated *oriC* (Slater *et al.*, 1995; Taghbalout *et al.*, 2000). SeqA forms a homotetramer composed of two dimers. One monomer of each dimer binds a hemi-methylated GATC site. Thus two nearby located hemi-methylated GATC sites are required for a stable complex formation. Binding of SeqA to hemi-methylated GATC sequences induces a conformational change of the DNA. Two SeqA tetramers bind cooperatively when the spacing between the pairs of hemi-methylated GATC sites is up to 30 bases apart, which induces even longer distance interactions between DNA-bound SeqA molecules and also aggregation of free SeqA protein onto DNA-bound. No cross-linking between SeqA on separate DNAs occurs (Brendler *et al.*, 2000; Han *et al.*, 2003; Han *et al.*, 2004). Electron microscopy studies revealed that SeqA preferentially binds to two sites that each contains 3 GATC sequences, situated on each side of DnaA box R1 in *oriC* (Skarstad *et al.*, 2000; Skarstad *et al.*, 2001). SeqA binds strongly from the AT-rich region to the M DnaA box in *oriC*, especially around DnaA box R1 and M (Taghbalout *et al.*, 2000). DnaA bound to a hemi-methylated fragment containing

DnaA box R1 and M were completely displaced by an equimolar concentration of SeqA. This suggests that SeqA exerts its negative control on replication initiation by out-competing bound DnaA molecules from the region required for strand opening (Taghbalout *et al.*, 2000). What ends sequestration and triggers methylation is not known, but would shed light on the related questions if the sequestration period is invariable or variable with growth rate and if the mechanism ending sequestration acts *in cis* or *in trans*.

SeqA is involved in chromosome organisation and segregation

Besides limiting replication by *oriC* sequestration, binding of SeqA to newly replicated DNA seems to serve another major function. The ability of SeqA to contact other SeqA tetramers bound to hemi-methylated pairs of GATC sites in adjacent regions on the same DNA helix, resulting in looping out of intervening DNA, is proposed to organise and form a nucleoid structure, which can be maintained by other proteins (Brendler *et al.*, 2000; Løbner-Olesen, Skovgaard & Marinus, 2005). SeqA foci, which are dependent on replication and have been observed *in vivo* in microscope studies by immunofluorescence and by a SeqA-GFP construct support this suggestion. The foci probably show how SeqA trails the replication forks, forming clusters bound to the newly replicated and hemi-methylated DNA (Brendler *et al.*, 2000; Hiraga *et al.*, 1998; Hiraga *et al.*, 2000; Onogi *et al.*, 1999). Also, *in vitro*, SeqA binding to DNA affects DNA topology resulting in a restraint of negative supercoils (Klungsoyr & Skarstad, 2004; Torheim & Skarstad, 1999). SeqA is also involved in proper chromosome segregation. The SeqA null mutant phenotype includes abnormal localisation of nucleoids concurrent with initiation asynchrony and over-initiations (Bahloul *et al.*, 1996; Boye *et al.*, 1996; Lu *et al.*, 1994). SeqA overproduction significantly increases the sequestration period of *oriC* and delays nucleoid segregation and cell division (Bach, Krekling & Skarstad, 2003).

Besides SeqA, the MukFEB proteins are essential for correct chromosome partitioning (Hiraga, 1992). MukFEB form a complex *in vitro* (Yamazoe, Onogi & Sunako, 1999) and MukB-GFP is localised in a similar pattern to SeqA in growing cells (Hiraga *et al.*, 1998; Onogi *et al.*, 1999). MukB null mutant cells exhibit abnormally large SeqA clusters at abnormal cellular locations (Hiraga *et al.*, 1998; Onogi *et al.*, 1999). Homologues of Dam, SeqA and MukFEB only exist in *E.coli* and bacteria closely related to *E.coli* (e.g. *Salmonella*). Other gram-negative and gram-positive bacteria do not possess SeqA and MukFEB and most of them lack Dam (e.g. *Bacillus subtilis*) (Hiraga *et al.*, 2000).

Since SeqA is a multi-task protein it is difficult to discriminate the effects on chromosome organisation and segregation, observed in SeqA mutants or at abnormal concentrations of SeqA in the cell, from the effects on replication control. In comparison, to the $\Delta seqA$ strain, a strain where GATC sites in *oriC* had been changed to GTTC, showed only moderate over-initiations (Bach & Skarstad, 2004). Because fast growing cells have overlapping cell cycles and the phase of the cell cycle varies at different growth rates in relation to the division cycle, the guess is that the function of SeqA in replication control (the mechanisms of *oriC* sequestration and its ending) is not coupled to certain steps of the other functions of SeqA in chromosome segregation and localisation prior to cell division.

Control of initiation of chromosome replication

Principally, initiation of replication is regulated so that multiple origins fire synchronously and with a frequency matching the current growth rate leaving each generation of daughter cells to inherit the same chromosome number. Synchrony requires a boost in the initiation potential within a narrow time interval, which remains high until all replication origins have initiated once and only once. A higher affinity of DnaA to DnaA boxes outside *oriC* and a higher density of DnaA binding sites close to *oriC* to ensure that replication of binding sites outside *oriC* does not interfere with a raising initiation potential, should contribute to synchrony. Following initiation no replication of boxes or binding of DnaA to boxes outside *oriC*, must take place to ensure a high initiation potential until all origins have initiated and there must be a period of origin sequestration immediately following initiation to prevent a newly fired origin to reinitiate while the initiation potential is still high.

To maintain a well-defined initiation frequency, initiation synchrony is required. At a given growth rate the control mechanism must be able to adequately respond to deviations in initiation frequency by adjusting the frequency in a way that allows for the maintenance of a stable variation of the *oriC* concentration during each cell cycle. When the growth rate changes, so must the initiation frequency. There exists compelling experimental evidence that the initiation frequency is mainly regulated through the rate of demand and supply of DnaA. The DnaA demand is determined by the frequency of DnaA binding sites outside *oriC* appears during replication which depends on the position and the DnaA binding ability of the boxes on the chromosome and the rate of replication fork movement along the chromosome. The supply is controlled by the *de novo* synthesis of DnaA, where the regulation of *dnaA* expression may be central.

Previous models

Many models of initiation of replication in *E.coli* have been published suggesting different principles for its control. The two most interesting suggestions are the inhibitor dilution model by Pritchard, Barth & Collins (1969) and the initiator titration model by Hansen, Christensen & Atlung (1991), which may be regarded as the same principle.

In the inhibitor dilution model, a fixed number of inhibitors are synthesised at the time of initiation. The inhibitor interacts with *oriC* or the initiator and inhibits *de novo* initiation of replication until it is diluted due to cell growth to half its concentration immediately following initiation. Then, the inhibitor has reached a threshold level allowing a new round of replication to start.

In the initiator titration model, DnaA boxes are distributed either evenly along the chromosome or with higher density close to *oriC*. The main idea is that the binding affinity of the DnaA boxes in *oriC* is lower than for boxes located elsewhere. During the cell cycle the boxes outside *oriC* titrate DnaA and when saturated, DnaA starts to bind to the *oriC* boxes triggering initiation. It is further suggested that synchrony is promoted by a release of DnaA with retained activity followed by rebinding to unfired origins and each origin is refractory to initiation a period after initiation.

The inhibitor dilution model and the initiator titration model are basically the same principle. In the latter model the inhibitor is the DnaA box, which prevents initiation as long as there are unsaturated boxes outside *oriC*. When boxes are assumed to be located with high density around *oriC*, and therefore become replicated shortly after initiation, the analogy between the two models becomes even clearer.

Results and discussion

A stochastic model of the regulation of initiation of replication

Despite extensive studies during decades a consensus of the basic principals behind replication control in *E.coli* is still lacking. Chromosome replication is controlled by a number of molecular mechanisms acting together within a growing and dividing cell. In order to fully understand these coordinated interactions between the regulatory units, they must be integrated into a global description of a cell. Further, a low copy number of discrete molecules call for a stochastic description, where fluctuations of chemical reactions are taken into account (van Kampen, 1997). We have developed a global stochastic model of the initiation control of replication (**I**) based on the initiator titration model. The chromosome model describes the regulation of replication in a single cell, followed during several generations of exponential growth and division. Initiation at individual *oriC*s and elongation of individual forks moving along the chromosome is carefully followed. We assume that a Markov process models the system and realisations are simulated using the Gillespie algorithm (Gillespie, 1976). The time of the next reaction, t_{event} , is exponentially distributed and the inverse of the sum of all reaction rates r_i . The probability of a certain event is then $r_i/\sum r_i$. In the model the chromosome is divided into 1000 segments, with *oriC* in segment 1, the *dnaA* gene in segment 25, the *datA* locus in segment 200 and the *ter* sites in segment 1000 (Fig. 4). In addition to *datA*, about 300 groups of DnaA binding sites, one DnaA box and two DnaA-ATP boxes are equally distributed along the chromosome. DnaA-ADP and DnaA-ATP binds a DnaA box with equal affinity, while only DnaA-ATP binds to a DnaA-ATP box and only if the nearby DnaA box is bound. The *datA* locus is assumed to only bind DnaA-ATP, which is a critical assumption for the proposed regulation of *dnaA* gene expression (see below). Only one of the bi-directionally moving replication forks are modelled and a replication fork replicates one segment at a time with a rate constant corresponding to replication of 25 segments per minute on the average. Thus, the average time for completing one round of replication (C-period) is 40 minutes and the *dnaA* gene and *datA* locus are reached after 1 minute and 8 minutes on the average, respectively. Division occurs 20 minutes after replication termination (D-period) implicating that initiation control regulates the cell size. Replication of a segment results in dissociation of all DNA-bound DnaA molecules on the segment and DnaA-ATP is converted into DnaA-ADP through RIDA. Re-methylation of *oriC* following initiation, is modelled by three different scenarios. In scenario I (S_1) sequestration termination is modelled *ad hoc*, occurring when the *in cis* replication fork replicates segment 350, approximately 14 minutes after initiation. Seven reactions can occur, (*i*) initiation of replication,

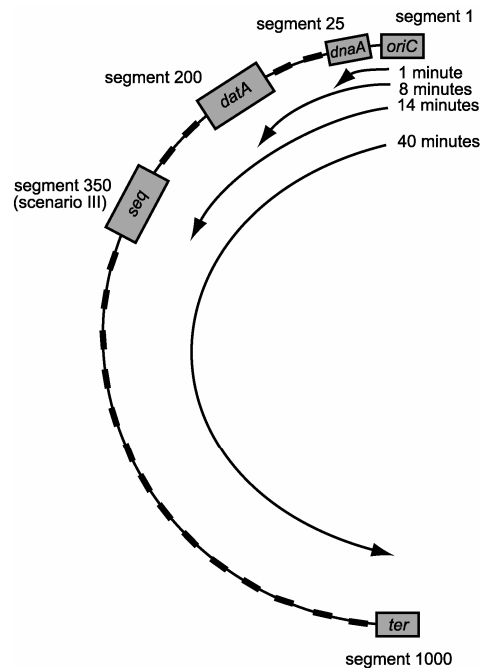


Figure 4. A schematic of the modelled chromosome. Replication initiates at *oriC* and ends at *ter* 40 minutes later, passing the *dnaA* gene and the *datA* locus 1 minute and 8 minutes after initiation, respectively. In scenario III a hypothetical *seq* locus is reached 14 minutes following initiation, which while hemi-methylated can bind a high number of SeqA molecules. In addition to *datA* (which is assumed to only bind DnaA-ATP) approximately 300 groups of DnaA binding sites (one DnaA box and two DnaA-ATP boxes) are evenly distributed along the chromosome.

(ii) replication of a segment, (iii) synthesis of a DnaA molecule in the ATP form, (iv) association of DnaA in either of the nucleotide forms to a DnaA box, (v) dissociation of a DnaA molecule from a DnaA box, (vi) association of a DnaA-ATP molecule to a DnaA-ATP box and (vii) dissociation of a DnaA-ATP molecule from a DnaA-ATP box. In scenario II (S_{II}) the eleven GATC sites are re-methylated in a sequence, either in a specific order or a random order. In scenario III (S_{III}) we have introduced a hypothetical *seq* locus in segment 350 (Fig. 4), which while hemi-methylated, can bind a high number of SeqA molecules, drastically lowering the free concentration of SeqA and largely increasing the probability of *oriC* methylation. In scenario II-III two more reactions can occur (viii) methylation of the GATC sites in *oriC* step-wise (scenario II) or by one rate-limiting step (scenario III) and (ix) methylation of unmethylated GATC sites in segments outside *oriC*. The sequestration period of *oriC* and the *dnaA* promoter start by replication of segment 1 and 25, respectively, and are assumed to end simultaneously in all scenarios. Also, the *dnaA* promoter is either constitutively expressed or *dnaA* expression is regulated by the free concentration of DnaA-ADP in all scenarios.

Factors determining the initiation mass

That initiation takes place at a constant initiation mass has long been a prevailing idea (Donachie, 1968). We investigated what exactly is required to maintain a constant initiation mass under different growth conditions when *dnaA* is constitutively expressed. We then used a simplified version of scenario I; the *datA* locus close to *oriC* provided the dominating number of DnaA binding sites and the sequestration period of the *dnaA* promoter following initiation was disregarded. Also, the constitutive expression per *dnaA* promoter was such that the total synthesis of DnaA increased strictly proportionally to the growth rate, so that the total DnaA concentration was constant, irrespective of the growth medium. This means that the expression per *dnaA* promoter must increase less than proportionally to an increasing growth rate since the fraction of *dnaA* genes increases with decreasing generation times. With these assumptions the initiation mass or initiation volume were kept constant as seen by the expected increase in cell volume by a factor of 4 when decreasing the generation time from 60 minutes to 20 minutes (Fig. 4 in I).

However, whether the initiation mass is constant or not is probably less relevant than how different factors affect the initiation mass (Herrick *et al.*, 1996). We therefore investigated how the positioning of additional DnaA binding sites along the chromosome, besides the *datA* locus, affects the initiation mass as well as the length of the sequestration period of the *dnaA* promoter. Additional evenly distributed DnaA binding sites will lower the initiation mass with increasing growth rate because the number of the additional scattered binding sites will decrease at generation times below 40 minutes with overlapping rounds of replication. Additional DnaA binding sites close to *oriC* do not affect the initiation mass. If the *dnaA* promoter is sequestered a constant fraction of the generation time the initiation mass stays unchanged while a sequestration period a constant number of minutes irrespective the generation time will increase the initiation mass with increasing growth rate. The assumptions above of the constitutive expression of *dnaA* implicates that if instead the expression per promoter is strictly proportional to the growth rate the initiation mass decreases with increasing growth rate.

Regulation of the expression of the dnaA promoter

To maintain regulated and synchronous initiations of replication the total concentration of the activator should be constant, which is generated by a constitutive *dnaA* promoter perfectly proportional to the growth rate. However, it is far from obvious that a neutral expression of the *dnaA* promoter prevails. Many genes are strongly growth regulated (Bremer & Churchward, 1991). One solution to this problem would then be a regulated expression of *dnaA* by the total concentration of DnaA. Usually, it is the free concentration of a repressor that controls the fraction of promoter-controlling operators. Both DnaA-ATP and DnaA-ADP can repress *dnaA* expression (Speck, Weigel & Messer, 1999), but a regulated *dnaA* expression by the free concentration of DnaA-ATP poses two principle problems, if DnaA-ATP is the key-regulator of initiation. The first problem is that an initiator protein, rate limiting for the initiation of replication along with a control locus that binds and sequesters the initiator to control initiation is inconsistent with an auto-regulated gene expression of the initiator

gene. Titration of the initiator by the control locus counteracts adequate regulation of the initiator gene. Binding to the control locus reduces the free concentration of the initiator and relieves the auto-repressed initiator gene to compensate for the reduction. This has been named the auto-regulation-sequestration paradox (Chattoraj, Mason & Wickner, 1988). One solution to this problem has been proposed for plasmid P1, where looping of DNA with DNA-bound initiators can interact with the promoter of the initiator gene so rather the total than the free concentration of the initiator controls initiator gene expression (Chattoraj, Mason & Wickner, 1988; Das *et al.*, 2005). The second problem is that if the free concentration of DnaA-ATP regulates *dnaA* expression it strives to keep the free concentration of DnaA-ATP constant, inconsistent with a rapid increase in the free DnaA-ATP concentration at initiation. Consequently, synchronous initiations are precluded.

Although, *dnaA* expression regulated by the total DnaA concentration principally can control replication initiation, the *datA* locus and RIDA offers another solution where the free concentration of DnaA-ADP regulates *dnaA* expression. The principle of the idea is that with one dominating binding locus (*datA*) which predominately binds DnaA in the ATP form and with RIDA converting the bound DnaA-ATP at the control locus into free DnaA-ADP, the free concentration of DnaA-ADP reflects the flow of DnaA-ATP to DnaA-ADP proportional to the *total* DnaA-ATP concentration and the dilution of DnaA-ADP by cell growth. This means that by a *dnaA* expression controlled by the free concentration of DnaA-ADP, the total concentration of DnaA-ATP in the cell can be regulated. This way the free concentration of DnaA-ADP will also be proportional to the *oriC* concentration, why another way to understand this regulation is by an expression of *dnaA* striving to keep the free concentration of DnaA-ADP constant and thereby a constant concentration of *oriC*. Fig. 5 shows DnaA-ADP regulated *dnaA* expression for a cell growing with a generation time of 20 minutes (scenario I).

Two tentative molecular mechanisms ending oriC sequestration

The time of replication initiation must be well separated from the time of *oriC* methylation to avoid immediate re-initiations or asynchronous initiations. We have modelled two principal mechanisms for the re-methylation of *oriC* following initiation. Either the GATC sites became step-wise methylated in a specific or random order (scenario II) or methylation occurred in one rate-limiting step after replication of a hypothetical *seq* locus downstream of *datA* (scenario III). While hemi-methylated, the *seq* locus can bind a high number of SeqA molecules, drastically lowering the free concentration of SeqA and largely increasing the probability of *oriC* methylation. Fig. 7 in **I** illustrates the principles. Both the suggested mechanisms generated a wild-type regulation of chromosome replication, for the simulated generation times between 60 and 20 minutes either with a constitutively expressed or a DnaA-ADP regulated *dnaA* promoter. The re-methylation pattern of individual GATC sites in *oriC* is presently studied experimentally.

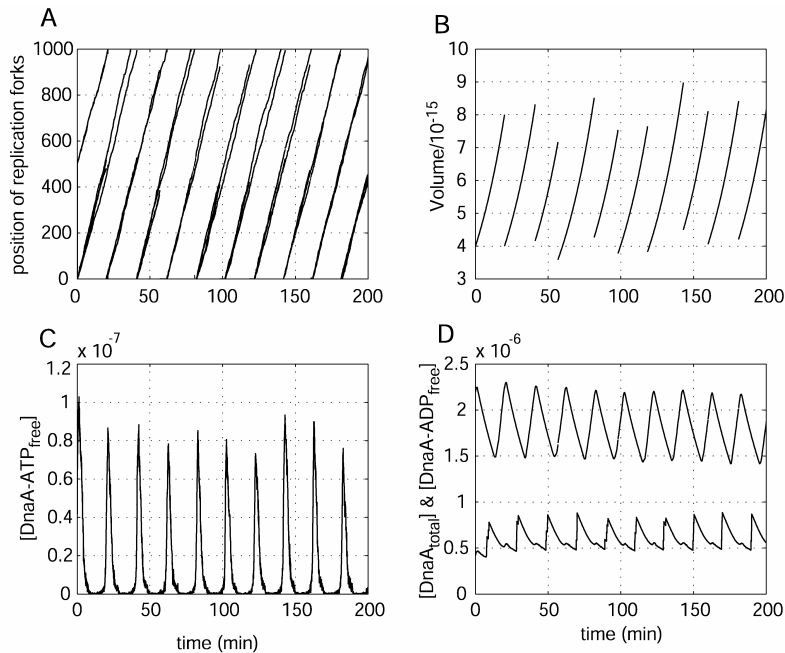


Figure 5. Regulation of *dnaA* expression by DnaA-ADP. The cell is born with two complete chromosome copies. On each copy replication is halfway through (position 500 in A) and another round is about to start. Initiation is triggered (from 4 origins synchronously) as a result of the free DnaA-ATP concentration boosting at 20 minutes intervals (C). The total DnaA concentration declines during the sequestration period of the *dnaA* promoter due to dilution by cell growth but increases back to a maximal value at the time of initiation (D). When the *datA* locus at position 200 (A) is replicated, the free concentration of DnaA-ADP peaks (D). The cell volume varies slightly between generations (B). An early initiation results in a somewhat smaller cell at division, which is corrected back by a somewhat later initiation the next generation and vice versa.

Future modelling

We have performed one first critical testing of the chromosome model. The *datA* locus was deleted resulting in a smaller cell and a partial lost of initiation synchrony, while the initiation frequency and DNA content virtually remained the same (Fig. 5 in I) in accordance with experimental observations from *datA* deletion (Morigen, Molina & Skarstad, 2005). We believe there are three further key tests of the model; the observed compatibility of as many as 30 mini-chromosomes per *oriC* with only minor changes in initiation mass or cell size (Løbner-Olesen, 1999), the introduction of extra *datA* loci on plasmids which delays initiation and increases cell size (Morigen, Løbner-Olesen & Skarstad, 2003) and finally observed responses to a higher or lower total DnaA concentration than wild-type, where a low DnaA concentration generates an increased initiation mass and increased initiation asynchrony and a high DnaA concentration results in a decreased initiation mass and potentially increased initiation asynchrony (Løbner-Olesen *et al.*, 1989; Skarstad *et al.*, 1989; Atlung & Hansen, 1993). We expect the same manipulations within our present model with a DnaA-ADP regulated *dnaA*

expression to generate virtually the same responses (see Discussion in **I**). There also seem to exist an intricate feedback between the replication fork elongation rate dependent on the synthesis of deoxyridonucleotides (dNTPs) by ribonucleotide reductase (RNR) and the replication dependent conversion of DnaA-ATP to DnaA-ADP by RIDA (Gon *et al.*, 2006). The *nrd* operon encodes RNR and both DnaA and DnaA-ATP boxes are found in the promoter region similar to the promoter region of the *dnaA* gene. An important extension of the present model would be to include a DnaA auto-repressed expression of RNR connected to the rate of replication fork elongation, which may reproduce the observed changes of the rate of replication fork movement in the presence of excess DnaA and in the presence of extra *datA* loci on plasmids (Skarstad *et al.*, 1989; Morigen, Løbner-Olesen & Skarstad, 2003).

The principle for an auto-regulated expression of an initiator presented in **I**, may be represented in a more pure form by gram-positives, *e. g.* *Bacillus subtilis*, which contain a DnaA binding locus with many more binding sites than *datA*, next to its origin, suggesting the capacity of titrating a high number of DnaA molecules (Boye, Løbner-Olesen & Skarstad, 2000; Messer, 2002). Also, the *dnaA* promoter region in *B. subtilis* contains more DnaA binding sites than in *E.coli* suggesting DnaA-dependent regulation to more important (Ogura *et al.*, 2001). A model of the regulation of replication initiation applicable to *B. subtilis* is in progress.

Macrolide antibiotics

Introduction

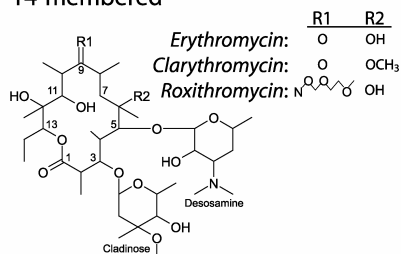
Naturally occurring macrolides are produced by actinomycetes, a group of gram-positive bacteria, which contains the soil-living subgroup *Streptomyces* important in antibiotic production (Lim, 1989). The common structure of all macrolides is a 14-, 15- or 16-membered lactone ring, with one or more sugar residues attached to it (Fig. 6). Biosynthesis of macrolides is carried out by polyketide synthases (PKSs), which is exceptionally large, multifunctional proteins organised into coordinated groups of active sites, modules. Each module is responsible for one cycle of polyketide chain elongation and associated group modifications in a sequence similar to an industrial assembly line. For example, the 6-deoxyerythronolide B synthase synthesises the macrolactone ring precursor of erythromycin antibiotics (Cane, Walsh & Khosla, 1998). The mode of action of macrolide antibiotics is to bind to the large ribosomal subunit (50S) close to the peptidyl-transferase center (ptc) and interfere with protein synthesis, causing growth arrest (Vázquez, 1979). Thus, macrolides belong to bacteriostatic antibiotics, which only inhibit growth but do not kill the bacteria in contrast to bactericidal antibiotics. Macrolides are often classified together with lincosamide and streptogramin B antibiotics (Fig. 6), referred to as MLS_B-antibiotics. The classification is based on observations that resistance to one class often results in resistance to the two other classes (Weisblum, 1995a). Although structurally heterogeneous, the classes have overlapping binding sites on the 50S subunit (Schlünzen *et al.*, 2001; Hansen *et al.*, 2002; Tu *et al.*, 2005), which explains the observed co-resistance within the group. Macrolides are clinically important antibiotics for treating respiratory tract infections caused by gram-positive bacteria such as the pathogens *Staphylococcus aureus* and *Streptococcus pneumoniae*. The drugs are also effective to some gram-negative bacteria and *Mycoplasma* species (Alvarez-Elcoro & Enzler, 1999; Zhong & Shortridge, 2001).

Four generations of macrolides

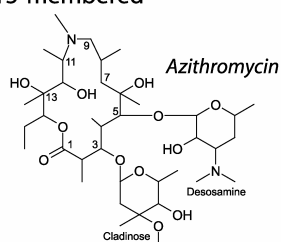
The history of macrolide antibiotics in clinical use started in 1952, when the macrolide erythromycin A was extracted from *Saccharopolyspora erythraea* (formerly *Streptomyces erythreus*), isolated from Philippine soil samples, and its antibiotic activity was discovered (Flynn, Powell & Smith, 1952). One year later, in 1953, erythromycin was introduced into the clinics but soon inducible MLS_B-resistant isolates of *S. aureus* appeared (Weisblum, 1995a). Two other macrolides were introduced, oleandomycin and megalomicin, which showed only slightly improved pharmacokinetics and as in the case of erythromycin exhibited inducible resistance. The first generation of 14-membered ring macrolides was followed by 16-membered ring macrolides such as carbomycin, spiramycin and josamycin in the second generation. Initially inducible erythromycin strains remained susceptible to 16-membered macrolides. However, erythromycin-inducible strains rapidly mutated to a high level resistance of both 14- and 16-membered ring macrolides, as well as of lincosamide and streptogramin B antibiotics. Another

A Macrolides

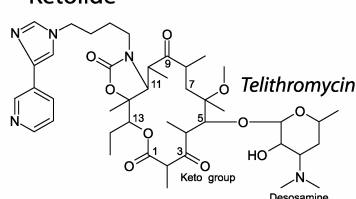
14-membered



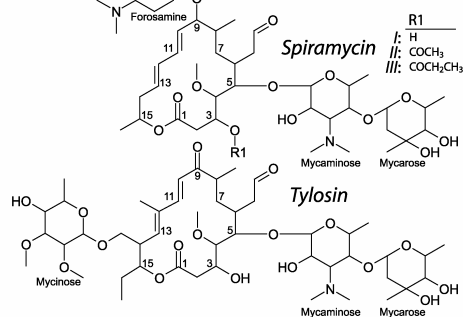
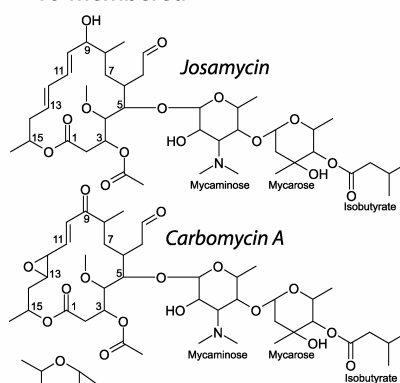
15-membered



Ketolide

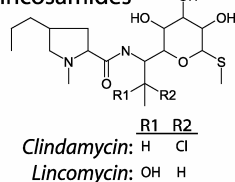


16-membered



B Lincosamides and Streptogramin B

Lincosamides



Streptogramin B

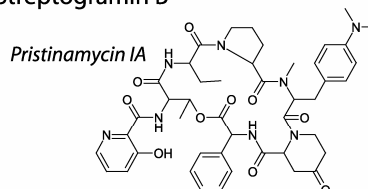


Figure 6. Chemical structures of some MLS_B-antibiotics.

group of resistant strains based on antibiotic efflux also started to spread. The third generation is semi-synthetic, more acid-stable and shows a broader activity spectrum than the originally 14-membered ring macrolides. Examples from this generation of macrolides are clarithromycin, roxithromycin and the 15-membered ring macrolide azithromycin. However, the third generation is as effective as the first generation in inducing resistance. The broader activity spectrum of the third generation, including *Mycobacterium intracellulare* and *Mycobacterium tuberculosis*, selected for intrinsic MLS_B-resistance. The two bacteria only contain

a single copy of the 23S rRNA gene, why mutations in the 23S rRNA gene will dominate the phenotype and change macrolide binding (see below) (Weisblum, 1998). The ketolides constitute the fourth generation of macrolides. Ketolides are 14-membered, semi-synthetic derivatives of erythromycin A (Ackermann & Rodloff, 2003). The cladinose sugar residue at position C3 on the lactone ring is replaced by a keto-group, which may be the reason why this type of drug does not induce MLS_B-resistance (“*erm*” resistance, see below) (Ackermann & Rodloff, 2003; Tenson & Mankin, 2006). Telithromycin is the first developed ketolide and was introduced for clinical use in 2001 (Ackermann & Rodloff, 2003).

Macrolide binding and mode of action

Binding site and binding kinetics

Already in the 1960s it was discovered that erythromycin binds to the large ribosomal subunit (Vázquez, 1979 and references therein). In the past few years, crystal structures of several MLS_B-antibiotics bound to the large ribosomal subunit have been published. The large ribosomal subunit from two different organisms were used, the eubacterium *Deinococcus radiodurans* (Dra) and the archaeobacterium *Haloarcula marismortui* (Hma) (Schlünzen *et al.*, 2001; Hansen *et al.*, 2002; Tu *et al.*, 2005). The published location of the binding sites on the ribosome of the antibiotics for the two species is by and large the same. All macrolides bind in the nascent exit tunnel between the ptc and the constriction of the tunnel exerted by the L4 and L22 proteins (Fig. 7). However, some surprising differences in detail have been pointed out (Hansen *et al.*, 2002; Tu *et al.*, 2005). The exact binding to the ribosome of the very same drug molecule may be different in different organisms (Tenson & Mankin, 2006) and there is one important difference in position 2058 (*E. coli* numbering) in 23S rRNA between the species. Dra, as most eubacteria, has an A at position 2058, while Hma, as most archaeobacteria, carries a G at that position. An A2058G mutation confers resistance to MLS_B-antibiotics why Hma are intrinsically resistant (Vester & Douthwaite, 2001). Further, methylation of this very base is the main resistance mechanism against drugs of the MLS_B-group (see below). However, recently published structures of erythromycin, azithromycin and telithromycin bound to the Hma ribosome containing a G2058A mutation, is consistent with previously published structures of azithromycin, spiramycin and carbomycin A bound to wild-type Hma ribosomes. In all cases, the lactone ring, the central structure of all macrolides, show the same orientation. The ring lies flat against the tunnel wall with the hydrophobic side of the ring facing a hydrophobic part of the wall and the hydrophilic side of the ring faces the lumen of the tunnel. Apart from the lactone ring, the sugar residues, different for different macrolides, also interact with the tunnel wall. In the case of erythromycin and josamycin (exemplified by very structurally similar carbomycin A) their sugar residues are pointing towards the ptc, but the sugar of josamycin reaches further than the sugars of erythromycin because of differences in size (Hansen *et al.*, 2002; Tu *et al.*, 2005). Interestingly, the desoamine sugar of erythromycin makes a single hydrogen bond with base 2058 which may explain why erythromycin binding is so sensitive to mutations or modifications of that base (Tu *et al.*, 2005). In contrast, for example the

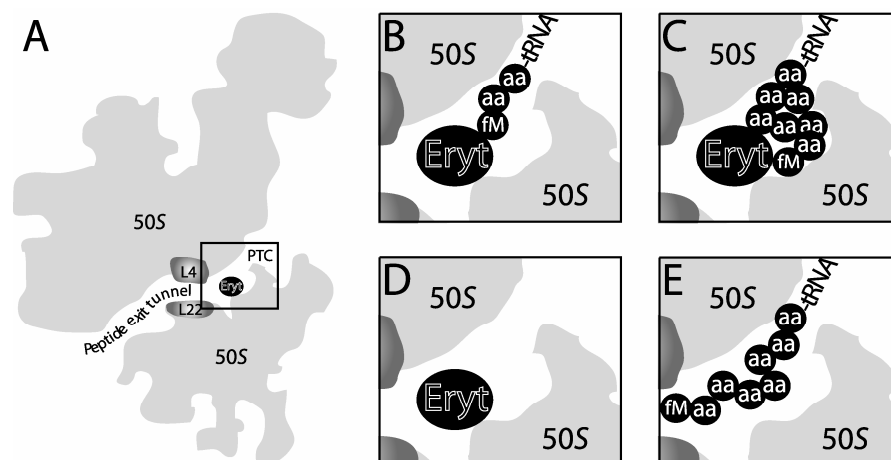


Figure 7. Inhibition of protein synthesis by macrolides, exemplified by erythromycin. (A) shows a cross-section of the large ribosomal subunit along the nascent peptide exit tunnel. A few rounds of peptidyltransferase can be carried out in the presence of a bound macrolide (B). When the peptide reaches the macrolide molecule, protein synthesis stalls (C), followed either by peptidyl-tRNA drop-off ending protein synthesis (D) or spontaneous dissociation of the macrolide resuming protein synthesis (E). The L4 and L22 proteins make up a constriction in the tunnel, PTC = peptidyltransferase center.

hydrophobic side of the lactone ring of 14-membered macrolides are reported to face the hydrophilic lumen of the tunnel in the Dra structure and seven hydrogen bonds mediate the binding of the macrolide to the ribosome. Therefore the published structures of MLS_B-antibiotics bound to Hma seem more reliable than the reported corresponding structures in Dra.

The location of binding and chemical interactions with the 50S subunit is only one side of macrolide binding. To further understand the antibiotics mode of action it is important to know how they interact with the ribosome on a dynamical level described by their kinetic properties. Recent measurements of erythromycin and josamycin binding (the macrolides used in the studies in this thesis) show that the dissociation constant (K_D) of the two antibiotics is fairly similar; K_D is 10.8 nM for erythromycin and 5.5 nM for josamycin (Lovmar, Tenson & Ehrenberg, 2004). However, the rate constants of binding differ considerably. While, the association rate constant (k_a) and the dissociation rate constant (k_d) of erythromycin is $1.0 \mu\text{M}^{-1}\text{s}^{-1}$ and $10.8 \cdot 10^{-3} \text{s}^{-1}$, respectively, the corresponding rate constants of josamycin binding is $k_a = 0.325 \text{mM}^{-1}\text{s}^{-1}$ and $k_d = 0.18 \cdot 10^{-3} \text{s}^{-1}$. The difference in k_d probably explains the observed differences in the amount of formed full-length product in the presence of erythromycin or josamycin (Tenson, Lovmar & Ehrenberg, 2003; Lovmar, Tenson & Ehrenberg, 2004) (see below), and may be the reason behind the different mechanisms of peptide-mediated macrolide resistance for the two drugs (**II**; **III**) (see below).

Peptidyl-tRNA drop-off – the primary effect of macrolide binding

That erythromycin causes an increased drop-off of peptidyl-tRNA has been known since the mid 1970s (see reference within Menninger & Otto, 1982). Peptidyl-tRNA enhanced drop-off was also confirmed for other types of macrolides. Menninger & Otto (1982) conclude that, “It seems likely that stimulated dissociation of peptidyl-tRNA from ribosomes is the major mechanism of action of macrolide antibiotics”. However, they believed that macrolides stimulated peptidyl-tRNA drop-off at any step during translation rather than at a specific step. Later, it was shown *in vivo* that ribosomes are only susceptible to erythromycin during initial stages of translation while polysomes are refractory to the drug (Andersson & Kurland, 1987). The published structures of macrolides bound to the 50S subunit along with biochemical experiments where the length of the synthesised oligopeptides were reported to vary depending on macrolide, suggested a tight relation between macrolide structure and length of dissociated peptidyl-tRNA (Kirillov *et al.*, 1997; Hansen *et al.*, 2002). Tenson, Lovmar & Ehrenberg (2003) further clarified the dependence by using a cell-free translation system with components from *E.coli* and studying peptidyl-tRNA drop-off of MLS_B-antibiotics from ribosomes translating naturally occurring peptide sequences. All the MLS_B-drugs caused dissociation of peptidyl-tRNA. Antibiotics with a structure which reaches the ptc (for example josamycin) caused dissociation of peptidyl-tRNAs containing two, three or four amino acids while antibiotics which do not reach ptc (for example erythromycin) caused dissociation of peptidyl-tRNA containing six, seven or eight amino acids. The data suggest a common mode of action of all MLS_B-antibiotics, which is modulated by the space available between the drug and the ptc. The suggestion is that all antibiotics prevent a nascent peptide entering the ribosomal tunnel by steric hindrance (Tenson, Lovmar & Ehrenberg, 2003). Lovmar, Tenson & Ehrenberg (2004) showed that a bound antibiotic molecule actively stimulates dissociation of peptidyl-tRNA and thus peptidyl-tRNA is not merely an effect of ribosome stalling. It has been suggested that 16-membered macrolides, such as josamycin, inhibit the peptidyltransfer reaction directly (Poulsen, Kofoed & Vester, 2000). However, both di- and tripeptides can be formed in the presence of josamycin depending on the size of the amino acid in the second position (Tenson, Lovmar & Ehrenberg, 2003; Lovmar, Tenson & Ehrenberg, 2004). Further, a considerable amount of full-length products was formed in the presence of the MLS_B-antibiotics except in the presence of 16-membered macrolides (Tenson, Lovmar & Ehrenberg, 2003). This may suggest that the steric hindrance is incomplete for some macrolides (Tu *et al.*, 2005). Structural modelling with erythromycin bound to the 50S subunit proposes that a peptide may pass the bound antibiotic molecule and that an eight amino acid long peptide would have past the drug while dissociated peptidyl-tRNA containing eight amino acids was observed in the presence of erythromycin (Tenson, Lovmar & Ehrenberg, 2003; Tu *et al.*, 2005). The peptide was modelled in an extended conformation, which may not be the case *in vivo* (Fig. 7) (Lovmar, 2005). The seemingly contradiction between read-through and the suggested mode of macrolide action may be explained by the different kinetic properties of erythromycin and josamycin. Erythromycin stays bound on the ribosome during 1.5 minutes on the average while josamycin stays bound 1.5 hours on the average. The

rate constant of peptidyl-tRNA drop-off is approximately the same in the presence of either of the antibiotics, which in turn is approximately the same as the dissociation rate constant of erythromycin. If it is assumed that macrolides when bound completely prevent a nascent peptide to enter the exit tunnel but translation can continue if the macrolide spontaneously dissociates before the peptidyl-tRNA dissociates, the predicted level of read-through correspond well with the measured levels when ribosomes were titrated to saturation by erythromycin or josamycin (Lovmar, Tenson & Ehrenberg, 2004; Lovmar, 2005). Unlike “normal” competitive enzyme inhibitors, macrolides allow the substrate to bind to the enzyme but prevents the product to leave the enzyme (Lovmar, 2005). Only if the peptidyl-tRNA drops off before the macrolide dissociates, translation is inhibited otherwise translation is merely slowed down. The ability of inhibiting protein synthesis may then be a direct consequence of the value of the dissociation rate constant (Lovmar, 2005).

Possible secondary effects of macrolide binding

While the primary effect of macrolide action is straightforward, secondary effects are much more difficult to evaluate. Macrolides may indirectly slow down protein synthesis by a deficiency in peptidyl-tRNA hydrolase (pth), required for recycling of tRNA and amino acids. Even in the absence of macrolide antibiotics, translation is prematurely terminated to some extent by dissociation of peptidyl-tRNA. When the frequency of drop-off exceeds the capacity of pth to release tRNAs sequestered as peptidyl-tRNA, essential tRNA isoacceptors are starved leading to a decreased ribosome elongation rate and finally cell death. Drop-off induced by macrolides may therefore be anticipated to be toxic for bacterial cells because of accumulation of peptidyl-tRNA (Heurgué-Hamard *et al.*, 1996; Tenson *et al.*, 1999; Heurgué-Hamard *et al.*, 2000), which depletes the pools of free tRNA isoacceptors. It has also been shown that a strain with a temperature sensitive pth becomes hypersensitive to erythromycin at the non-permissive temperature (Menninger & Otto, 1982). It is however difficult to thoroughly validate macrolide-induced pth deficiency since manipulations over a wide range of expression levels of pth leads to cell death (Tenson T., unpublished results). It is also claimed that macrolides inhibit 50S subunit assembly since the amount of 50S subunits decrease in the presence of macrolides in comparison to 30S subunits (Usary & Champney, 2001; Champney, 2003). An alternative explanation may be that inhibition of protein synthesis by macrolides, disturbs the balance between ribosomal protein and rRNA synthesis. A ribosome is a multi-nucleo-protein complex and if some important factor is missing it may result in erroneous or incomplete assembly of the subunits. The observed difference between the 30S and 50S subunits may then just as well be an effect of different degradation rates of inactive subunits (Lovmar, 2005). Macrolides further affect stringent response, which co-regulates the synthesis of ribosomal RNA and ribosomal proteins through the regulatory nucleotide guanosine 5', 3'-bis-diphosphate (ppGpp). Erythromycin induces the synthesis of ribosomal proteins and total RNA in response to a decreased concentration of ppGpp (Evers *et al.*, 2001).

Resistance mechanisms

Resistance mechanisms against antibiotics can generally be divided into three categories, (i) enzymatic destruction or modification of the antibiotic, (ii) resistance by efflux pumps lowering the intracellular concentration of the antibiotic and (iii) resistance by replacement or modification of the drug binding site (Walsh, 2003). Examples from all three categories are found among the resistance mechanisms against macrolides. In addition, there is a fourth category, peptide-mediated macrolide resistance. Three forms of macrolide resistance due to antibiotic modification are known, (i) esteratic ring cleavage, (ii) glycosylation and (iii) phosphorylation but are limited to a small number of clinical isolates. Antibiotic efflux and target site modification are much more common (Weisblum, 1998). The clinical relevance of peptide-mediated resistance is not clear.

Post-transcriptional modification of 23S rRNA

The most common resistance mechanism found in pathogens resistant to macrolide antibiotics is a post-transcriptional modification of 23S rRNA by methylation of a specific single adenine base which drastically reduces the affinity of the antibiotics to the ribosome (Walsh, 2003). In retro-perspective the reported resistance against erythromycin shortly after its introduction into clinical practice in the 1950s can be ascribed to this modification of 23S rRNA (Weisblum, 1995a). This resistance,

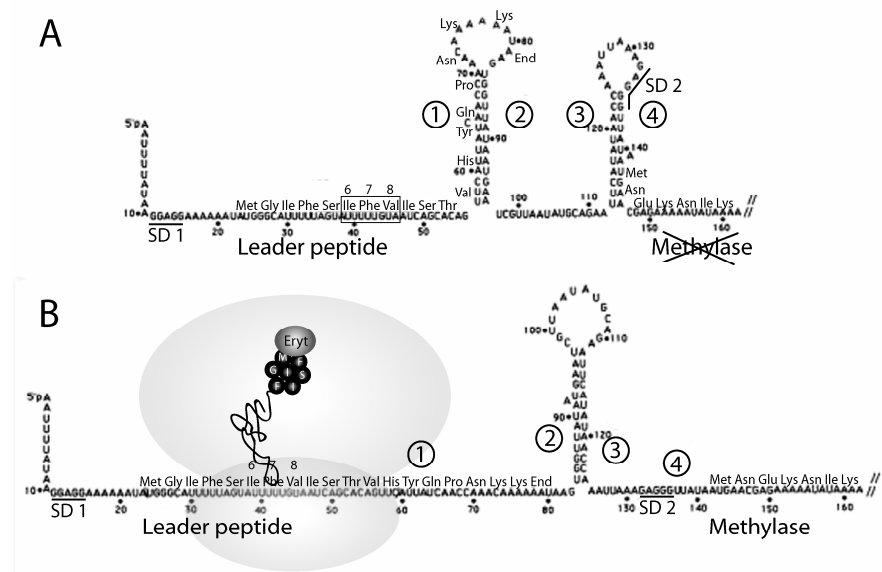


Figure 8. The 5' end of the *ermC* transcript. (A) Secondary structure of the native form of the *ermC* transcript. Translation of the ErmC ORF is inhibited by a hairpin structure (segments 3 and 4) containing the SD2 and the initiation codon. (B) An erythromycin-carrying ribosomes stalls in the leader ORF and opens up the hairpin structure between segments 1 and 2. A new hairpin structure between segments 2 and 3 is formed which un masks the SD2 and the initiation codon in segment 4 and allows translation of the ErmC ORF. Adapted from Mayford & Weisblum (1989b).

first encountered in *S. aureus*, was originally referred to as the MLS_B-resistance phenotype, since it also confers resistance to the other members of the MLS_B-group (Vester & Douthwaite, 2001). Decades later, the molecular mechanism behind the MLS_B-resistance phenotype was unravelled. Resistant strains carry a modified 23S rRNA, where a single base A2058 (according to *E. coli* numbering) located in domain V has been methylated (Lai & Weisblum, 1971; Skinner, Cundliffe & Schmidt, 1983) by an N-methyltransferase (Shivakumar & Dubnau, 1981). Reconstitution of 50S subunits, with 23S rRNA from a resistant strain, showed that the 23S rRNA modification indeed is fully responsible for the observed resistance (Lai *et al.*, 1973). The family of methylases, Erm (erythromycin resistance methylation) enzymes, responsible for the modification of nascent 23S rRNA, transfer methyl groups from S-adenosylmethionine to the N⁶ of adenines, forming a mono- or dimethylated adenine. Approximately 40 members have been isolated and characterised from the homologues *erm* gene family (Leclercq, 2002). The natural erythromycin producer, *S. erythraea*, contains a constitutive production of ErmE, to protect its own ribosomes. ErmE may be a recent progenitor to other Erms found in resistant pathogens (Walsh, 2003). While ErmE is constitutively synthesised, the MLS_B-resistance phenotype is usually inducible by erythromycin. The Erm synthesis is regulated through translational attenuation although one case of transcriptional attenuation (*ermK*) has been reported (Kwak, Choi & Weisblum, 1991; Weisblum, 1995b). The most well studied example of an inducible Erm production is ErmC in *S. aureus* and a model for its induction has been proposed (Weisblum, 1995b). The *ermC* gene contains a 141-nucleotide long leader sequence which makes the mRNA in its native state form a hairpin structure with segments 1 and 2 and another hairpin structure with segments 3 and 4 (Fig. 8). With the *ermC* mRNA in this conformation, translation of the ErmC open reading frame (ORF) is low because its ribosome binding site and two first codons are sequestered by the secondary structure of the mRNA. Only translation of the leader ORF occurs in the absence of erythromycin. Translation of the leader ORF by an erythromycin-carrying ribosome changes the mRNA conformation to the induced state. The erythromycin-carrying ribosome stalls after melting the first hairpin, where a new hairpin structure is formed of segments 2 and 3, leaving the ribosome binding site and the start codon of the ErmC ORF readily accessible for other ribosomes (Weisblum, 1995b) (Fig. 8). The amino acid sequence at which the ribosome with erythromycin stalls in the leader ORF is important, since it must stabilise the ribosome:peptidyl-tRNA complex long enough for efficient induction (Weisblum, 1995b). Usually, macrolide-induced ribosome stalling results in destabilisation and peptidyl-tRNA drop-off. Erythromycin allows formation of 6-8 amino acid long peptides before drop-off (Tenson, Lovmar & Ehrenberg, 2003) consistent with the observations that codons coding for the 5th to the 9th amino acid in the leader ORF of the *ermC* mRNA is critical for induction (Mayford & Weisblum, 1989a). Interestingly, amino acids 6-8, -Ile-Phe-Val-, corresponds well to be consensus sequence of the erythromycin resistance peptide (Tenson, DeBlasio & Mankin, 1996; Tenson *et al.*, 1997) (Fig. 8). The erythromycin resistance peptide destabilises erythromycin binding in the termination step of peptide synthesis presumably by interacting with either erythromycin or the tunnel wall (II). In the absence of a stop codon, a similar interaction in the *ermC* mRNA case may lead to a stabilisation of the ribosome:peptidyl-tRNA complex. The half-life of the *ermC*

mRNA has been reported to increase from 2 minutes to about 40 minutes during induction in *B. subtilis* (Bechhofer & Dubnau, 1987).

Mutations in 23S rRNA and ribosomal proteins

Generally, in pathogens with multiple *rrn* operons, e.g. *Streptococcus* and *Staphylococcus* species, resistance is conferred by Erm methylation of A2058 or by drug efflux, while in pathogens with one or two *rrn* operons, e.g. *Helicobacter pylori* and *Mycobacterium* species, resistance is conferred by mutations at A2058 or neighbouring nucleotides (Vester & Douthwaite, 2001). A low gene copy number of 23S rRNA makes a single mutation more likely to change the phenotype than a single mutated 23S rRNA gene at high copy numbers. The transition A2058G gives the highest level of resistance to 14-membered ring macrolides and is the most frequently clinically isolated mutation (Vester & Douthwaite, 2001).

The first reports of ribosomal structural changes generating resistance in *E. coli* described changes of the ribosomal proteins, especially in proteins L4 and L22 (Wittmann *et al.*, 1973) which supported the idea at that time of the ribosome as a multi-protein complex where the rRNA merely functioned as an inert scaffold (Weisblum, 1995a). L4 and L22 is not in direct contact with a bound macrolide but make up the constriction of the nascent exit tunnel, located below the macrolide binding site in the large ribosomal subunit (Fig. 7). The ribosomes of the strain with a mutated L4 protein showed a decreased affinity for erythromycin while the ribosomes of the L22 mutated strain exhibited an almost unchanged affinity for erythromycin but ribosomes with close to wild-type activity (Wittmann *et al.*, 1973). The genes for the erythromycin-resistant mutations of L4 and L22 have been cloned and sequenced (Chittum & Champney, 1994) and the structural implications of the mutations have been studied by cryo-EM (Gabashvili *et al.*, 2001). In the L4 mutant an A to G transition in codon 63 changes the amino acid from Lys to Glu and creates a substantial narrowing of the tunnel constriction. In the L22 mutant a 9-bp deletion of codons 82-84 removes amino acids Met-Lys-Arg from the protein and creates a widening of the tunnel constriction. If erythromycin only binds through the tunnel, a narrowing or widening of the constriction may result in changed association and dissociation rate constants of erythromycin, changing the inhibitory effect of the macrolide on protein synthesis (Lovmar, 2005). A narrowed constriction may then slow down the association (and dissociation) of erythromycin and make the cells tolerant to an elevated concentration of the antibiotic. A widening of the constriction may instead increase the rate constants of association and dissociation of the macrolide to the same extent, but leave the dissociation constant unchanged (Lovmar, 2005), which could decrease the inhibitory effect on protein synthesis in line with the observations by Wittmann *et al.* (1973).

Antibiotic efflux

Macrolide efflux by transporters located in the membrane is a clinically important category of resistance mechanisms. Four different types of efflux transporters (or efflux pumps) have been described (Weisblum, 1998), (i) M-type, (ii) MS-type, (iii) "actinomycete"-type and (iv) broad-spectrum or multi-drug resistance (mdr) type. The first three types are specialist on a certain group of antibiotics while the

fourth type may transport diverse categories of antibiotics as well as other compounds out of the cell. The M-type was first thoroughly described in 1996 by Suthcliffe, Tait-Kamradt & Wondrack. The transporter is mainly found in *Streptococcus* and is encoded by a *mef* gene (Clancy *et al.*, 1996; Tait-Kamradt *et al.*, 1997; Klaassen & Mouton, 2005). It confers low-level resistance to 14- and 15-membered macrolides but not to the other members of the MLS_B-group of antibiotics. The MS-type has been characterised from studies in *Staphylococcus* and is encoded by an *msr* gene. It confers resistance to 14-membered macrolides and streptogramin B, but resistance to 16-membered macrolides has also been reported (Weisblum, 1998). Ross *et al.* (1990) have suggested that the *msrA*-mediated resistance is regulated by translational attenuation, as for *ermC* described above. The actinomycete-type has been characterised in macrolide-producing *Streptomyces* where the transporters confer resistance to the bacterium that produces the macrolide (Weisblum, 1998). The low permeable outer membrane and the *mdr*-type of transporters are responsible for the intrinsic resistance to antibiotics in gram-negatives. The *E.coli* genome encodes 37 (!) different transporters, but the pump responsible for the dominating part of the efflux is the AcrAB-TolC system. The AcrB is the efflux pump, residing in the inner membrane. AcrB is connected to a membrane fusing protein AcrA, which links or fuses the outer and inner membranes to the channel protein TolC in the outer membrane. The system displays unusually broad substrate diversity, including the majority of clinically important antibiotics and toxicants such as dyes, detergents and organic solvents (Zgurskaya & Nikaido, 1999; Li & Nikaido, 2004). The AcrAB-TolC system is important for peptide-mediated resistance (III, see below).

Peptide-mediated macrolide resistance

The discovery

Tenson, DeBlasio & Mankin, coincidentally discovered peptide-mediated macrolide resistance in 1996. *E.coli* cells expressing random fragments of the *rrnB* operon, in search for fragments that can bind antibiotics, were screened for erythromycin resistant clones (Tenson & Mankin, 2001). All the found erythromycin resistant clones expressed rRNA fragments, which all contained the same sequence of 34 nucleotides ranging between positions 1235 and 1268 of domain II in 23S rRNA. The rRNA fragment comprises the characteristic features of an mRNA; it contains a Shine-Dalgarno sequence, an initiator codon (GUG), a terminator codon (UAA) and the open reading frame codes for the penta-peptide Met-Arg-Met-Leu-Thr. Further analysis showed that indeed expression of this mini-gene is both required and sufficient to confer resistance to low concentrations of erythromycin. In translation experiments *in vitro*, where the peptide or the resistance peptide mRNA (rpmRNA) were supplied, revealed the necessity of active translation of the rpmRNA for protection against erythromycin. It was therefore suggested that the resistance peptide acts *in cis*, on the ribosome (Tenson, DeBlasio & Mankin, 1996).

Correlation between macrolide structure and peptide sequence

In consequent studies, peptides conferring resistance against erythromycin and other macrolides were selected from *in vivo* expressed random peptide libraries

(Tenson *et al.*, 1997, Tripathi, Kloss & Mankin, 1998; Vimberg *et al.*, 2004). Only short peptides, 3-6 amino acids long, induce erythromycin resistance (Tenson *et al.*, 1997). Sequence comparison of the 5-codon resistance peptides revealed a strong preference for leucine or isoleucine as the third amino acid and a hydrophobic amino acid in the C-terminus. Not only did these sequence signatures appear in majority but also corresponded to the resistance peptides with the highest activity against erythromycin. Further, clones grown at a very high erythromycin concentration ($1.4 \cdot 10^{-3}$ M) showed a high tendency to contain a hydrophobic amino acid also in the second and fourth position and the hydrophobic Val in the C-terminus (Tenson *et al.*, 1997). A comparison between the amino acid sequence of the resistance peptides against erythromycin and a ketolide discovered a correspondence between the peptide sequence and the chemical structure of the macrolide. This was corroborated *in vivo* by comparing the resistance patterns of two very similar peptide sequences, one selected against erythromycin and the other selected against the ketolide. Only the resistance peptide against erythromycin rendered cells resistant to erythromycin and vice versa (Tripathi, Kloss & Mankin, 1998). Vimberg *et al.* (2004) also observed a strong correlation between peptide sequence and the structure of the macrolide when they further extended the search of resistance peptides to structurally different macrolides including for instance josamycin. Interestingly, Vimberg *et al.* (2004) found resistance peptides against all the tested macrolides but were unable to find resistance peptides against the lincosamide antibiotic clindamycin or the streptogramin B antibiotic quinupristin. This suggests that although the MLS_B-antibiotics have overlapping binding sites on the ribosome, the way they interact with the ribosome is fundamentally different.

The “bottle-brush” mechanism

Based on the findings that resistance peptides act *in cis* and the correlation between peptide sequence and chemical structure of the macrolide, Tripathi, Kloss & Mankin proposed the “bottle-brush” model of peptide-mediated macrolide resistance in 1998. They suggested that synthesis of a resistance peptide, removes the macrolide from the ribosome by direct interaction between the antibiotic molecule and the resistance peptide. The resistance peptide acts as a “bottle-brush” and “cleans” the ribosome. This restores the protein synthesis capability of the ribosome but the effect should only be temporary since another macrolide molecule may rebind as long as the synthesised peptide has not reached a critical length and passed the macrolide binding site in the nascent peptide exit tunnel.

Results and discussion

Validation of the “bottle-brush” mechanism

The aim in **II** was to test the proposed hypothesis and to study the details of the mechanism of peptide-mediated erythromycin resistance. The mechanism was studied *in vitro* in our cell-free mRNA translation system of *E.coli* components. The dissociation rate of erythromycin was measured by chasing with an excess of josamycin when either a control peptide (fMNAIK) or a resistance peptide

(fMRLFV) was expressed. Since penta-peptides can be synthesised with an erythromycin molecule bound to the ribosome, peptide synthesis continues until erythromycin dissociates and is replaced by josamycin, which only allows di- and tri-peptidyl-tRNAs to be formed before drop-off (Tenson, Lovmar & Ehrenberg, 2003). Erythromycin was found to dissociate faster in the presence of resistance peptide expression while expression of the control peptide did not change the dissociation rate constant but was the same as the spontaneous dissociation rate constant (Lovmar, Tenson & Ehrenberg, 2004). However, the most important finding in this set of experiments was that the resistance peptide ejects the macrolide every time it is expressed, which means that the resistance peptide indeed acts as a “bottle-brush” and “cleans” the ribosome as suggested by the “bottle-brush” hypothesis. In another set of experiment, we used [¹⁴C]-labelled erythromycin to monitor labelled dissociation of erythromycin from the ribosome in conjunction with [³H]-labelled fMet to simultaneously follow [³H]-peptidyl-tRNA or [³H]-peptide release to further examine at what step during resistance peptide synthesis and with what rate, erythromycin is expelled from the ribosome. The macrolide is removed with the highest probability in the termination step when the penta-peptide is released from the peptidyl-tRNA by a class 1 release factor. Synthesis of a hexa- or a hepta-peptide with the same N-terminal as the resistance peptide did not increase the dissociation of erythromycin.

To validate that the rate constant of resistance peptide synthesis by an erythromycin-infected ribosome can account for the resistance observed in cell populations we constructed a mathematical model. We set up a system of differential equations with ribosomes in 7 different states based on the scheme in Fig. 9A along with biochemical data of the resistance peptide action, binding kinetics of erythromycin and rate constants of protein synthesis obtained from our cell-free translation system (II; Lovmar, Tenson & Ehrenberg, 2004). The model also includes differential equations for the change in the total intracellular concentration of the macrolide by the inflow and outflow over the cell membrane as well as synthesis and degradation of mRNAs and rpmRNA. All components are diluted by cell growth. The system was solved numerically by Euler’s method (Heath, 1997), after the introduction of a certain concentration of erythromycin in the medium, and cell growth was recorded as volume expansion during 8 hours following induction. At the time of macrolide introduction the system resided at steady state for a certain synthesis rate of rpmRNA. A detailed description of the model is found in supplementary material online to II. Cell growth after the introduction of varying concentrations of erythromycin in the medium at varying synthesis rates of rpmRNA synthesis was simulated and compared to *in vivo* experiments. In the *in vivo* experiments we used a multi-copy plasmid with a regulated expression of rpmRNA through *tac* promoter control by IPTG. The IPTG and erythromycin concentrations in the growth medium were varied and cell growth was measured as bacterial mass (optical density) after 8 hours of growth following the addition of erythromycin in the medium. We found a good agreement between experimentally observed and modelled growth behaviour (Fig. 9B-C) but the model predicted significant resistance in the presence of resistance peptide expression only if we assumed a rapid equilibration between the erythromycin concentration in the growth medium and the intracellular concentration of the

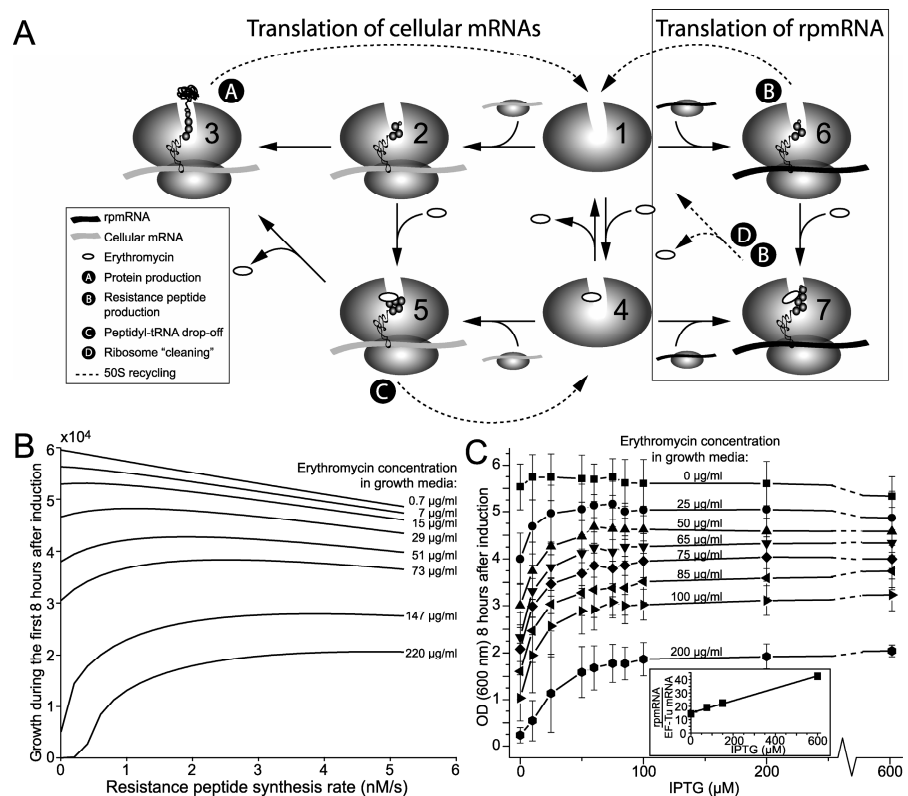


Figure 9. A schematic of the peptide-mediated erythromycin resistance model (A) and cell growth, modelled (B), *in vivo* (C). (A, left) Ribosomes without erythromycin synthesise proteins (state 3) while ribosomes with erythromycin (state 5) leads to peptidyl-tRNA drop-off (and recycling of the 50S subunit (state 4)) or translation resumes (state 3) if the drug spontaneously dissociates before peptidyl-tRNA drop-off. (A, right) Translation of rpmRNA by ribosomes with erythromycin leads to dissociation of the drug (state 7). Calculated (B) and measured (C) cell growth 8 hours after addition of erythromycin for different concentrations of erythromycin in the growth medium and different expression levels of rpmRNA.

macrolide. Since the growth experiments were done using gram-negative *E. coli* cells, which contain an outer membrane expected to generate a low permeability of macrolides, it was not apparent that the net exchange dynamics of the antibiotic over the cell membrane should be fast. A multi-drug efflux pump located in the inner membrane, the AcrAB-TolC system, offered a solution to the problem (see below).

Different mechanism of peptide-mediated josamycin and erythromycin resistance

Previous experiments *in vivo* and *in vitro* suggested that the action of peptide-mediated josamycin resistance is different from the mechanism of erythromycin resistance. The formation of di- and tripeptides is inhibited resulting in synthesised peptidyl-tRNAs containing mainly 2 or 3 amino acids before drop-off in the

presence of josamycin while the length of selected resistance peptides contains 4 or 5 amino acids (Tenson, Lovmar & Ehrenberg, 2003; Lovmar, Tenson & Ehrenberg, 2004; Vimberg *et al.*, 2004). The very low dissociation rate constant for josamycin implicates that the interaction between peptide and drug must be stronger than in the case of erythromycin to destabilize the binding of the drug to the ribosome (Lovmar, Tenson & Ehrenberg, 2004; **II**). The first objective of **III** was to understand the mechanism of peptide-mediated josamycin resistance. The mechanism was studied *in vitro* in our cell-free mRNA translation system of *E. coli* components. Ribosomes translating either an rpmRNA (coding for MFLV) or a control peptide mRNA (coding for MVSN) in the presence of josamycin were chased with erythromycin to reveal whether the dissociation of josamycin increased from rpmRNA expressing ribosomes. No significant increase of the dissociation rate was detected, but interestingly we observed an eight-fold lower drop-off rate of resistance di-peptidyl-tRNA (rate constant $\sim 0.008 \text{ s}^{-1}$) compared to the drop-off rate of the control di-peptidyl-tRNA (rate constant $\sim 0.06 \text{ s}^{-1}$). This difference between the drop-off rates may be the key for understanding peptide-mediated josamycin resistance. The difference in resistance mechanisms was further demonstrated by length dependence of the rpmRNAs for the two drugs. We let *E. coli* cells express peptides of lengths varying between 2 and 10 amino acids. Besides sequence dependence (Tenson *et al.*, 1997), erythromycin resistance peptides also showed length dependence in agreement with previous experiments that removal of erythromycin occurs at termination of penta-peptide synthesis and that shorter or longer peptides either does not reach far enough to interact with or loses the interaction with the bound erythromycin molecule, respectively (**II**). In contrast, josamycin resistance peptides showed no length dependence. All peptides, which contained a phenylalanine as second amino acid, conferred the same degree of josamycin resistance. This is in line with previous experiments which show that josamycin inhibit formation of peptides longer than two (or three) amino acids (Lovmar, Tenson & Ehrenberg, 2004). The only important feature of josamycin rpmRNAs appears to be a sequence coding for phenylalanine or tyrosine in the second position (Vimberg *et al.*, 2004).

We also wanted to see if josamycin resistance *in vivo*, monitored as cell growth in the presence of resistance peptide expression and josamycin could be reproduced within the model previously developed for peptide-mediated erythromycin resistance (**II**) but now adapted for resistance peptide expression against josamycin. A bacterial population containing a plasmid-borne resistance peptide gene, coding for peptide MFLV, and under the control of the *tac* promoter was grown in media with varying IPTG concentrations to regulate the level of resistance peptide expression combined with varying josamycin concentrations. The increase in bacterial mass after 8 hours of growth after induction was monitored by optical density as a function of the IPTG concentration in the medium. The mathematical model was changed to account for josamycin resistance by modelling a delayed di-peptidyl-tRNA drop-off from a josamycin-carrying ribosome expressing the resistance peptide while the antibiotic stays bound to the ribosome. By assuming a low rate of degradation of mRNAs with a stalled ribosome in the 5' end instead of full protection against degradation, we obtained growth curves mimicking the *in vivo* observed growth curves.

The apparent explanation to why a decreased drop-off rate of resistance di-peptidyl-tRNA in comparison to the drop-off rate of other di-peptidyl-tRNAs may confer resistance is that it reduces the demand of a factor required for translation elongation or recycling of ribosomes, which has become limiting. The importance of the modelled mRNA degradation can be understood as follows. The concentration of protein mRNAs in a cell is much lower than the concentration of ribosomes. Thus, only a small fraction of drug-inhibited ribosomes, stalled on an mRNA can potentially severely slow down protein synthesis. When protein mRNAs with a stalled ribosome is slowly degraded as opposed to fully protected from degradation, the free concentration of protein mRNAs on which a ribosome can initiate translation drastically declines. The delay at initiation increases the impact of the macrolide since 50S subunits exist in a josamycin-susceptible state a longer period of time. The result is a larger fraction of free and infected 50S subunits as well as a larger fraction of ribosomes stalled on mRNAs, which contributes to further lowering the concentration of free mRNAs. The feedback between the low concentration of free protein mRNAs and concentration of inactivated 50S subunits makes the growth rate severely reduced within a narrow range of antibiotic concentrations. When rpmRNA is present in the cell, josamycin-infected ribosomes are “absorbed” on the rpmRNA. The free concentration of protein mRNAs remains high and ribosomes can initiate translation at a higher rate and escapes josamycin to a larger extent. The concentration of active, translating ribosomes increases, thereby raising the cell growth rate. The predicted resistance by mRNA limitation in the model critically depends on a low rate constant of resistance peptidyl-tRNA drop-off compared to the rate constant for drop-off of other peptidyl-tRNAs, which absorbs josamycin-carrying ribosomes on rpmRNA and lowers the concentration of josamycin-ribosomes on other mRNAs.

Increased drop-off induced by macrolides may also lead to pth saturation and depletion of free tRNA isoacceptors followed by ribosome stalling at certain codons. This slows down the overall translation rate per ribosome and may in turn lead to a delay at initiation, which leaves 50S subunits in a josamycin-susceptible state a longer period of time. Synthesis of rpmRNA may reduce pth saturation, by decreasing the concentration of josamycin-ribosomes on other mRNAs. It is difficult to manipulate the expression level of pth within a wide range, why there may be a problem of thoroughly validating macrolide induced pth deficiency. An increased or decreased expression level lead to cell death probably because fMet-tRNA is hydrolysed or because pth is not recycled, respectively (Tenson T., unpublished results). It has previously been reported that in *E.coli*, in the absence of translation, binding of a 30S subunit to the 5' region of the lacZ mRNA, does not protect the full-length mRNA against degradation by RNaseE (Joyce & Dreyfus, 1998). The increased degradation of mRNA in the presence of josamycin is presently under investigation in our laboratories. We also plan to measure the drop-off rate of several mRNAs coding for different amino acids in the second position and to further investigate possible unanimous of pth expression levels and sensitivity to josamycin along with modelling of pth saturation.

Peptide-mediated macrolide resistance requires a fast outflow rate of the antibiotic over the cell membrane

The second objective of **III** was to validate the previous model prediction from **II**, that peptide-mediated erythromycin resistance requires a high outflow rate of the drug over the cell membrane. In gram-positive bacteria the cell wall does not offer much resistance to diffusion of small molecules and the rate of exchange of macrolides over the cell membrane is expected to be rapid, but previous *in vivo* experiments were done with gram-negative *E.coli* cells (Tenson, Lovmar & Ehrenberg, 2003; **II**). In gram-negatives the outer membrane confers an efficient barrier of permeation and the entrance rate of antibiotics are expected to be slow, but as described above, gram-negative bacteria also harbour broad-specific multidrug pumps in their inner membrane, which may generate a considerably higher outflow rate of the antibiotics in comparison to the inflow rate by passive diffusion. Since the AcrAB-TolC pump system has been reported to be the major contributor for raising erythromycin tolerance in gram-negatives (Ma *et al.*, 1995), we decided to study peptide-mediated resistance within a TolC mutant. To validate the model prediction we grew wild-type and TolC mutant *E.coli* cells containing either a resistance peptide expressing plasmid or a control plasmid in the presence of varying concentrations of erythromycin or josamycin in the growth medium. Growth was recorded by optical density after 4 hours following addition of the antibiotic and was registered as a function of the macrolide concentration and at an IPTG concentration corresponding to maximal resistance in the wild-type as seen in previous *in vivo* growth experiments (**II**; **III**). The *in vivo* experiments confirmed the model prediction for both antibiotics. No resistance was observed in the TolC mutant, although the resistance mechanism clearly differs for the two drugs. The TolC mutant is as sensitive to macrolides as the AcrB mutant (Tenson T., personal communication), why we modelled the TolC mutant without pumps. The models reproduced the *in vivo* growth curves. The TolC mutant tolerated a lower concentration of macrolide than the wild-type and resistance was substantially reduced for both erythromycin and josamycin. Fig. 10 shows *in vivo* and modelled growth of the wild-type and TolC mutant in the presence of erythromycin. In the case of erythromycin, where expression of a resistance peptide actively removes a bound drug molecule from the ribosome (**II**) resistance is a consequence of an increased dissociation of erythromycin. Such a resistance mechanism is sensitive to the fate of the drug molecule after ejection. It can either leave the cell (by passive diffusion over the membrane or be actively transported by efflux pumps) or it re-associates to a ribosome. The value of the rate constant for leaving the cell in relation to the association rate constant of the antibiotic becomes very important. The requirement of a fast outflow rate for the erythromycin resistance mechanism to work is then rather a requirement of a fast enough rate constant of the antibiotic for leaving the cell compared to the association rate constant for ribosome binding of the drug. We argue that the AcrAB-TolC efflux pump system provide the required high efflux rate. Thus, a macrolide with a lower association rate constant but with the same or lower dissociation rate constant of erythromycin is predicted by the model to confer resistance also in the TolC mutant, if resistance is mediated by active removal of the drug by the same rate as of erythromycin.

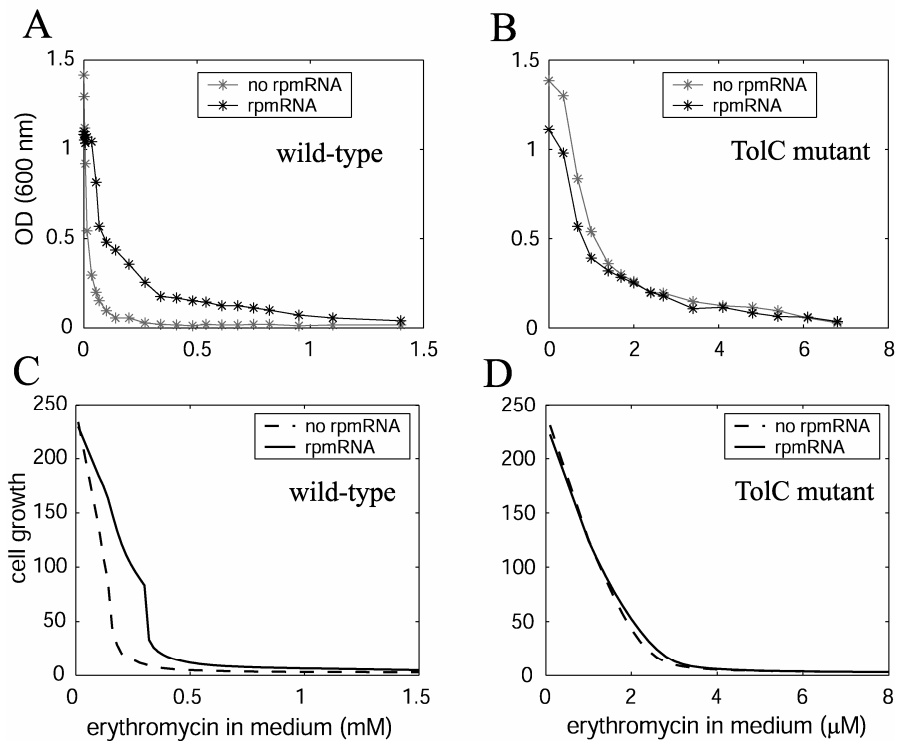


Figure 10. Peptide-mediated resistance in the wild-type but not in a pump mutant. Cell growth 4 hours after induction by erythromycin *in vivo* (A-B) or as modelled (C-D) in the wild-type (A and C) and a TolC mutant (B and D). Adapted from III.

The details of josamycin resistance need to be further clarified by experiments. The absence of modelled peptide-mediated josamycin resistance in the TolC mutant is also a consequence of a too slow efflux rate constant in relation to the association rate constant of the drug, which creates a boost in the intracellular concentration of josamycin followed by a sharp decline in the growth rate within a very narrow range of concentrations of the macrolide in the growth medium and leaves the mechanism of peptide-mediated josamycin resistance ineffective since it can not remove josamycin bound to a ribosome.

Erythromycin-induced methylation of 23S rRNA by ErmC

To study the erythromycin-induced ErmC synthesis by translational attenuation described above we set-up a model. The synthesis of ErmC preceding an increased concentration of ribosomes with a methylated 23S rRNA (methylated ribosomes) and a decreasing concentration of unmodified (unmethylated) ribosomes following induction by erythromycin was modelled by a system of differential equations. Induction of resistance occurs in three consecutive steps in the model; (i) erythromycin binds to free unmethylated ribosomes, (ii) an erythromycin-carrying ribosome stalls in the leader sequence of an *ermC* mRNA and induces synthesis of ErmC and (iii) ErmC methylates nascent ribosomes. Each of these steps of

induction is modelled by a probability. The probability that a ribosome carries erythromycin is a function of the concentration and the dissociation constant of the drug. The probability that an *ermC* mRNA is in an induced state is a function of the concentration of free unmethylated ribosomes with erythromycin and the dissociation constant of erythromycin-ribosomes to the leader region of the *ermC* mRNA at the site of stalling. The probability of methylating a newborn ribosome is a function of the concentration and activity of ErmC. The cell growth rate was modelled as a function of translationally active ribosomes. See the Appendix in **IV** for a detailed description of the model. We studied the time of transformation and the degree of transformation (the fraction of methylated ribosomes) after erythromycin induction as a function of the dissociation constant of a stalled ribosome in the leader region of an *ermC* mRNA (K_Q), the activity of ErmC (K_{QM}) and the intracellular concentration of erythromycin (e), where transformation refers to the conversion from an erythromycin susceptible cell to an MLS_B-resistant cell. The time of transformation decreases and the final fraction of resistant ribosomes increases with a decreasing value of K_Q and an increasing value of K_{QM} . The suggested stabilisation of the *ermC* transcript during induction makes the induction mechanism respond more strongly to the antibiotic, and thus increases the sensitivity of the resistance mechanism to the drug. The transformation time is reduced and the fraction of methylated ribosomes at steady state is raised, compared to when the half-life of the *ermC* mRNA is unaffected. The most conspicuous feature of the induction dynamics is the appearance of an optimal erythromycin concentration at which the induction response rate is maximal as observed by the fastest boost in synthesis of both ErmC and methylated ribosomes (Fig. 3(a) in **IV**). Induction depends critically on the presence of ribosomes both with and without a bound erythromycin molecule. At low concentrations of the antibiotic the concentration of erythromycin-carrying ribosomes are low, why only a low fraction of *ermC* mRNAs are in the induced state. At high concentrations of the antibiotic, on the other hand, the fraction of *ermC* mRNAs in the induced state are high but the concentration of ribosomes without erythromycin is low. The maximal response rate corresponds to an optimal blend of ribosomes with and without erythromycin. However, the optimal inducing concentration of erythromycin may not be of any biological significance. When cell growth was monitored during the transformation phase, instead of the concentration of ErmC and methylated ribosomes, the initial reduction in growth rate and the time of its recovery monotonically decreased with an increasing concentration of erythromycin (Fig. 3(b) in **IV**). The maximal response rate appears to be a consequence of the mechanism of induction but of less relevance for cell growth, the expected parameter genuinely subjected to selection pressure. Therefore, cell growth was also studied during the induction phase as a function of K_Q , K_{QM} and e , and related to selection pressures on the resistance mechanism. For instance may a certain combination of K_Q - and K_{QM} -values generate a higher total cell growth during the transformation phase than another combination of K_Q - and K_{QM} -values but a lower growth rate at steady state after transformation is complete. The time periods and frequency bacteria are exposed to a certain drug concentration should than select for the K_Q - and K_{QM} -values, which gives the highest total cell growth. Also, the model shows how an increased antibiotic concentration although in short-

term is rewarding, creates a high selective advantage to change the K_Q - and K_{QM} - values to generate a yet more competent resistance mechanism.

Bi-stable growth rates generated by antibiotics with low membrane permeability

The use of gram-negative *E.coli* with a low entrance rate of macrolides over the outer membrane in the studies of peptide-mediated resistance gave us the idea of bi-stable growth rates. The principle of how bi-stable growth rates may emerge is described in V. Bi-stable growth rates means that exponentially growing bacteria subjected to a fixed concentration of an antibiotic will show different growth rates in the presence of the drug depending on the bacterial growth rate at the time of introduction of the drug. During fast growth, the intracellular concentration may remain small by rapid cell volume expansion and dilution of the antibiotic why the growth rate remains high. During slow growth, on the other hand, the intracellular concentration may be become high due to a slow volume expansion and slow dilution why the growth rate may drastically decrease. The requirement for bi-stability to emerge is low membrane permeability and a sensitive response of the growth rate to the intracellular concentration of the antibiotic. A relevant group of antibiotics, which may generate bi-stability is drugs with low membrane permeability in gram-negatives.

The future objective is to experimentally validate the existence of bi-stable growth rates in response to antibiotics, supported by modelling. For instance, modelling of josamycin in the TolC mutant predicts bi-stability given that the permeability of the drug is slow enough over the outer membrane.

Personal reflections on modelling

Here follows some personal reflections on modelling put into the context of my experience of modelling during my time as a Ph D student.

A model is a simplification of the system it is describing. There are two types of simplifications, “physical” and “biological” assumptions of the system. Some common physical assumptions are to let the copy number distribution of a molecule be characterised by an average value or assuming reactions to be quickly equilibrated. These assumptions can be justified by mathematical methods to find the limits within the assumptions are valid. Biological assumptions are the features of the system, which is believed to be important for its function while other features, which is believed to be unimportant, are disregarded. Biological assumptions can only be justified by experimental observations, why assumptions not known should be regarded as predictions, which can be validated or falsified by later experimental observations.

To formulate a model of a biological system in terms of mathematics the precise interactions between molecules and values of parameters must be defined. This is the strength of a mathematical model since it creates well-defined predictions based of well-defined assumptions of the system in comparison to a mere verbal description. It pinpoints the critical assumptions for the system to function and at the same time rules out features that do not. A “good” model is a simple and comprehensive model, which still captures the relevant characteristics of the system in a way that it clarifies the function of the system.

Mathematical models can be powerful tools in at least four ways: (i) outline possible principles (*e. g.* bi-stable growth rates in response to antibiotics with a low membrane permeability (**V**)), (ii) make well-defined predictions (*e. g.* peptide-mediated resistance requires a fast outflow rate of the macrolide) (**II**, **III**), (iii) strengthen experimental observations (*e. g.* that the dissociation rate constant of erythromycin by rpmRNA translating ribosomes observed *in vitro* may generate the *in vivo* observed resistance (**II**)) and (iv) separate mechanistic units and study its effect in the global context (*e. g.* to understand the factors determining the initiation mass in **I**).

I hope and believe that the full potential of modelling will be recognized in the future where experimental observations along with modelling mutually stimulate and drive biological knowledge forward.

References

- Ackermann G. & Rodloff A. C. 2003. Drugs of 21st century: telithromycin (HMR 3647) – the first ketolide. *Journal of Antimicrobial Chemotherapy* 51, 497-511.
- Alvarez-Elcoro S. & Enzler M. J. 1999. The macrolides: Erythromycin, Clarithromycin and Azithromycin. *Mayo Clinical Proceedings* 74, 613-634.
- Andersson S. & Kurland C. G. 1987. Elongating ribosomes *in vivo* are refractory to erythromycin. *Biochimie* 69, 901-904.
- Aranovich A., Gdalevsky G. Y. Cohen-Luria R., Fishov I. & Parola A. H. 2006. Membrane-catalyzed nucleotide exchange on DnaA: effect of surface molecular crowding. *The Journal of Biological Chemistry* 281, 12526-12534.
- Atlung T., Clausen E. S. & Hansen F. G. 1985. Autoregulation of the *dnaA* gene of *Escherichia coli* K12. *Molecular & General Genetics* 200, 442-450.
- Atlung T., Løbner-Olesen A. & Hansen F. G. 1987. Overproduction of DnaA protein stimulates initiation of chromosome and minichromosome replication in *Escherichia coli*. *Molecular & General Genetics* 206, 51-59.
- Atlung T. & Hansen F. G. 1993. Three distinct chromosome replication states are induced by increasing concentrations of DnaA protein in *Escherichia coli*. *Journal of Bacteriology* 175, 6537-6545.
- Bach T., Krekling M. A. & Skarstad K. 2003. Excess SeqA prolongs sequestration of *oriC* and delays nucleoid segregation and cell division. *The EMBO Journal* 22, 315-323.
- Bach T. & Skarstad K. 2004. Re-replication from non-sequesterable origins generates three-nucleoid cells which divide asymmetrically. *Molecular Microbiology* 51, 1589-1600.
- Bach T. & Skarstad K. 2005. An *oriC*-like distribution of GATC sites mediates full sequestration of non-origin sequences in *Escherichia coli*. *Journal of Molecular Biology* 350, 7-11.
- Bahloul A., Meury J., Kern R., Garwood J., Guha S. & Kohiyama M. 1996. Co-ordination between membrane *oriC* sequestration factors and a chromosome partitioning protein TolC (MukA). *Molecular Microbiology* 22, 275-282.
- Bechhofer D. H. & Dubnau D. 1987. Induced mRNA stability in *Bacillus subtilis*. *Proceedings of the National Academy of Sciences of the United States of America* 84, 498-502.
- Bochner B. R. & Ames B. N. 1982. Complete analysis of cellular nucleotides by two-dimensional thin layer chromatography. *The Journal of Biological Chemistry* 257, 9759-9769.
- Boye E. & Løbner-Olesen A. 1990. The role of *dam* methyltransferase in the control of DNA replication in *E. coli*. *Cell* 62, 981-989.
- Boye E., Marinus M. G. & Løbner-Olesen A. 1992. Quantification of Dam methyltransferase in *Escherichia coli*. *Journal of Bacteriology* 174, 1682-1685.
- Boye E., Stokke T., Kleckner N. & Skarstad K. 1996. Coordinating DNA replication initiation with cell growth: differential roles for DnaA and SeqA proteins. *Proceedings of the National Academy of Sciences of the United States of America* 93, 12206-12211.
- Boye E., Løbner-Olesen A. & Skarstad K. 2000. Limiting DNA replication to once and only once. *EMBO Reports* 1, 479-483.
- Bremer H. & Churchward G. 1991. Control of cyclic chromosome replication in *Escherichia coli*. *Microbiological Reviews* 55, 459-475.
- Brendler T., Sawitzke J., Sergueev K. & Austin S. 2000. A case for sliding SeqA tracts at anchored replication forks during *Escherichia coli* chromosome replication and segregation. *The EMBO Journal* 19, 6249-6258.
- Camara J. E., Skarstad K. & Crooke E. 2003. Controlled initiation of chromosomal replication in *Escherichia coli* requires functional Hda protein. *Journal of Bacteriology* 185, 3244-3248.
- Camara J. E., Breier A. M., Brendler T., Stuart A., Cozzarelli N. R. & Crooke E. 2005. Hda inactivation of DnaA is the predominant mechanism preventing hyperinitiation of *Escherichia coli* DNA replication. *EMBO Reports* 6, 736-741.

- Campbell J. L. & Kleckner N. 1990. *E.coli oriC* and the *dnaA* gene promoter are sequestered from *dam* methyltransferase following the passage of the chromosomal replication fork. *Cell* 62, 967-979.
- Cane D. E., Walsh C. T. & Khosla C. 1998. Harnessing the biosynthetic code: combinations, permutations, and mutations. *Science* 282, 63-68.
- Cassler M. R., Grimwade J. E. & Leonard A. C. 1995. Cell cycle-specific changes in nucleoprotein complexes at a chromosomal replication origin. *The EMBO Journal* 14, 5833-5841.
- Champney W. S. 2003. Bacterial ribosomal subunit assembly is an antibiotic target. *Current Topics in Medicinal Chemistry* 3, 929-947.
- Chattoraj D. K., Mason R. J. & Wickner S. H. 1988. Mini-P1 plasmid regulation: the auto-regulation-sequestration paradox. *Cell* 52, 551-557.
- Chiaromello A. E. & Zyskind J. W. 1990. Coupling of DNA replication to growth rate in *Escherichia coli*: a possible role for guanosine tetraphosphate. *Journal of Bacteriology* 172, 2013-2019.
- Chittum H. S. & Champney W. S. 1994. Ribosomal protein gene sequence changes in erythromycin-resistant mutants of *Escherichia coli*. *Journal of Bacteriology* 176, 6192-6198.
- Christensen B. B., Atlung T. & Hansen F. G. 1999. DnaA boxes are important elements in setting the initiation mass of *Escherichia coli*. *Journal of Bacteriology* 181, 2683-2688.
- Churchward G., Estiva E. & Bremer H. 1981. Growth rate-dependent control of chromosome replication initiation in *Escherichia coli*. *Journal of Bacteriology* 145, 1232-1238.
- Clancy J., Petitpas J., Dib-Hajj F., Yuan W., Cronan M., Kamath A. V., Bergeron J. & Retsema J. A. 1996. Molecular cloning and functional analysis of a novel macrolide-resistance determinant, *mef(A)*, from *Streptococcus pyogenes*. *Molecular Microbiology* 22, 867-879.
- Cooper S. & Helmstetter C. E. 1968. Chromosome replication and the division cycle of *Escherichia coli* B/r. *Journal of Molecular Biology* 31, 519-540.
- Das N., Valjavec-Gratian M., Basuray A. N., Fekete R. A. Papp P.P., Paulsson J. & Chattoraj D. K. 2005. Multiple homeostatic mechanisms in the control of P1 plasmid replication. *Proceedings of the National Academy of Sciences of the United States of America* 102, 2856-2861.
- Dasgupta S. & Løbner-Olesen A. 2004. Host controlled plasmid replication: *Escherichia coli* minichromosomes. *Plasmid* 52, 151-168.
- Donachie W. D. 1968. Relationship between cell size and time of initiation of DNA replication. *Nature* 219, 1077-1079.
- Evers S., Di Padova, K. Meyer M., Langen H., Fountoulakis M., Keck W. & Gray C. P. 2001. Mechanism-related changes in the gene transcription and protein synthesis patterns of *Haemophilus influenzae* after treatment with transcriptional and translational inhibitors. *Proteomics* 1, 522-544.
- Flynn E. H., Powell H. M. & Smith J. W. 1952. "Ilotycin" a new antibiotic. *Antibiotics and Chemotherapy* 11, 281-283.
- Gabashvili I. S., Gregory S. T., Valle M., Grassucci R., Worbs M., Wahl M. C., Dahlberg A. E. & Frank J. 2001. The polypeptide tunnel system in the ribosome and its gating in erythromycin resistance mutants of L4 and L22. *Molecular Cell* 8, 181-188.
- Gillespie D. T. 1976. A general method for numerically simulating the stochastic time evolution of coupled chemical reactions. *Journal of Computational Physics* 22, 403-434.
- Gon S., Camara J. E., Klungsoyr H. K., Croke E., Skarstad K. & Beckwith J. 2006. A novel regulatory mechanism couples deoxyribonucleotide synthesis and DNA replication in *Escherichia coli*. *The EMBO Journal* 25, 1137-1147.
- Grimwade J. E., Ryan V. T. & Leonard A. C. 2000. IHF redistributes bound initiator protein, DnaA, on supercoiled *oriC* of *Escherichia coli*. *Molecular Microbiology* 35, 835-844.
- Han J. S., Kang S., Lee H., Kim H. K. & Hwang D. S. 2003. Sequential binding of SeqA to paired hemi-methylated GATC sequences mediates formation of higher order complexes. *The Journal of Biological Chemistry* 278, 34983-34989.

- Han J. S., Kang S., Kim S. H., Ko M. J. & Hwang D. S. 2004. Binding of SeqA protein to hemi-methylated GATC sequences enhances their interaction and aggregation properties. *The Journal of Biological Chemistry* 279, 30236-30243.
- Hansen F. G., Hansen E. B. & Atlung T. 1982. The nucleotide sequence of the *dnaA* gene promoter and of the adjacent *rpmH* gene, coding for the ribosomal protein L34, of *Escherichia coli*. *The EMBO Journal* 1, 1043-1048.
- Hansen F. G., Christensen B.B. & Atlung T. 1991. The initiator titration model: computer simulation of chromosome and minichromosome control. *Research in Microbiology* 142, 161-167.
- Hansen J. L., Ippolito J. A., Ban N., Nissen P., Moore P. B. & Steitz T. A. 2002. The structures of four macrolides antibiotics bound to the large ribosomal subunit. *Molecular Cell* 10, 117-128.
- Heath M. T. 1997. Scientific computing. An introductory survey. 1st edition. The McGraw-Hill Companies, INC, New York, The United States of America. 274-275 pp.
- Helmstetter C. E. & Leonard A. C. 1987. Coordinate initiation of chromosome and minichromosome replication in *Escherichia coli*. *Journal of Bacteriology* 169, 3489-3494.
- Herrick J., Kohiyama M. Atlung T. & Hansen F. G. 1996. The initiation mess. *Molecular Microbiology* 19, 659-666.
- Heurgué-Hamard V., Mora L., Guarneros G. & Buckingham R. H. 1996. The growth defect in *Escherichia coli* deficient in peptidyl-tRNA hydrolase is due to starvation for Lys-tRNA^{Lys}. *The EMBO Journal* 15, 2826-2833.
- Heurgué-Hamard V., Dincbas V., Buckingham R. H. & Ehrenberg M. 2000. Origins of minigene-dependent growth inhibition in bacterial cells. *The EMBO Journal* 19, 2701-2709.
- Hill T. M. 1996. Features of the chromosomal terminus region. In *Escherichia coli* and *Salmonella* cellular and molecular biology (Neidhardt F. C., ed.). 2nd edition. ASM Press, Washington D.C., The United States of America. 1602-1614 pp.
- Hiraga S. 1992. Chromosome and plasmid partition in *Escherichia coli*. *Annual Review of Biochemistry* 61, 283-306.
- Hiraga S., Ichinose C., Niki H. & Yamazoe M. 1998. Cell cycle-dependent duplication and bi-directional migration of SeqA-associated DNA-protein complexes in *E.coli*. *Molecular Cell* 1, 381-387.
- Hiraga S., Ichinose C., Onogi T., Niki H. & Yamazoe M. 2000. Bidirectional migration of SeqA-bound hemimethylated DNA clusters and pairing of *oriC* copies in *Escherichia coli*. *Genes to Cells* 5, 327-341.
- Jensen M. R., Løbner-Olesen A. & Rasmussen K. V. 1990. *Escherichia coli* minichromosomes: random segregation and absence of copy number control. *Journal of Molecular Biology* 215, 257-265.
- Joyce S. A. & Dreyfus M. 1998. In the absence of translation, RNase E can bypass 5' mRNA stabilizers in *Escherichia coli*. *Journal of Molecular Biology* 282, 241-254.
- Katayama T., Kubota T., Kurokawa K., Croke E. & Sekimizu K. 1998. The initiator function of DnaA protein is negatively regulated by the sliding clamp of the *E.coli* chromosomal replicase. *Cell* 94, 61-71.
- Kato J. & Katayama T. 2001. Hda, a novel DnaA-related protein, regulates the replication cycle in *Escherichia coli*. *The EMBO Journal* 20, 4253-4262.
- Kirillov S., Porse B. T., Vester B, Wolley P. & Garrett R. A. 1997. Movement of the 3'-end of tRNA through the peptidyl transferase centre and its inhibition by antibiotics. *FEBS Letters* 406, 223-233.
- Kitagawa R., Mitsuki H., Okazaki T. & Ogawa T. 1996. A novel DnaA protein-binding site at 94.7 min on the *Escherichia coli* chromosome. *Molecular Microbiology* 19, 1137-1147.
- Kitagawa R., Ozaki T., Moriya S. & Ogawa T. 1998. Negative control of replication initiation by a novel chromosomal locus exhibiting exceptional affinity for *Escherichia coli* DnaA protein. *Genes & Development* 12, 3032-3043.

- Klaassen C. H. W. & Mouton J. W. 2005. Molecular detection of the macrolide efflux gene: to discriminate or not discriminate between *mef(A)* and *mef(E)*. *Antimicrobial Agents and Chemotherapy* 49, 1271-1278.
- Klungsoyr H. K. & Skarstad K. 2004. Positive supercoiling is generated in the presence of *Escherichia coli* SeqA protein. *Molecular Microbiology* 54, 123-131.
- Kuriyan J. & O'Donnell M. 1993. Sliding clamps of DNA polymerases. *Journal of Molecular Biology* 234, 915-925.
- Kurokawa K., Nishida S., Emoto A., Sekimizu K. & Katayama T. 1999. Replication cycle-coordinated change of the adenine nucleotide-bound forms of DnaA protein in *Escherichia coli*. *The EMBO Journal* 18, 6642-6652.
- Kwak J.-H., Choi E.-C. & Weisblum B. 1991. Transcriptional attenuation control of *ermK*, a macrolide-lincosamide-streptogramin B resistance determinant from *Bacillus licheniformis*. *Journal of Bacteriology* 173, 4725-4735.
- Lai C.-J. & Weisblum B. 1971. Altered methylation of ribosomal RNA in an erythromycin-resistant strain of *Staphylococcus aureus*. *Proceedings of the National Academy of Sciences of the United States of America* 68, 856-860.
- Lai C.-J., Weisblum B., Fahnestock S. R. & Nomura M. 1973. Alteration of 23S ribosomal RNA and erythromycin-induced resistance to lincomycin and spiramycin in *Staphylococcus aureus*. *Journal of Molecular Biology* 74, 67-72.
- Leclercq R. 2002. Mechanisms of resistance to macrolides and lincosamides: nature of the resistance elements and their clinical implications. *Clinical Infectious Diseases* 34, 482-492.
- Leonard A. C. & Grimwade J. E. 2005. Building a bacterial orisome: emergence of new regulatory features for replication origin unwinding. *Molecular Microbiology* 55, 978-985.
- Li X.-Z. & Nikaido H. 2004. Efflux-mediated drug resistance in bacteria. *Drugs* 64, 159-204.
- Li Z., Kitchen J. L., Boeneman K., Anand P. & Crooke E. 2005. Restoration of growth to acidic phospholipid-deficient cells by DnaA(L366K) is independent of its capacity for nucleotide binding and exchange and requires DnaA. *The Journal of Biological Chemistry* 280, 9796-9801.
- Lim D. V. 1989. *Microbiology*. 1st edition. West Publishing Company. St. Paul, The United States of America. 303-306 pp.
- Lovmar M., Tenson T. & Ehrenberg M. 2004. Kinetics of macrolide action. *The Journal of Biological Chemistry* 279, 53506-53515.
- Lovmar M. 2005. Macrolide Antibiotics in Bacterial Protein Synthesis. Uppsala University Press, Uppsala, Sweden. ISBN 91-554-6361-4.
- Løbner-Olesen A., Skarstad K., Hansen F. G., von Meyenburg K. & Boye E. 1989. The DnaA protein determines the initiation mass of *Escherichia coli* K-12. *Cell* 57, 881-889.
- Løbner-Olesen A. 1999. Distribution of minichromosomes in individual *Escherichia coli* cells: implications for replication control. *The EMBO Journal* 18, 1712-1721.
- Løbner-Olesen A., Skovgaard O. & Marinus M. G. 2005. Dam methylation: coordinating cellular processes. *Current Opinion in Microbiology* 8, 154-160.
- Lu M., Campbell J. L., Boye E. & Kleckner N. 1994. SeqA: a negative modulator of replication initiation in *E. coli*. *Cell* 77, 413-426.
- Ma D., Cook D.N., Alberti M., Pon N. G., Nikaido H. & Hearst J. E. 1995. Genes *acrA* and *acrB* encode a stress-induced efflux system of *Escherichia coli*. *Molecular Microbiology* 16, 45-55.
- Mayford M. & Weisblum B. 1989a. *ermC* leader peptide. Amino acid sequence critical for induction by translational attenuation. *Journal of Molecular Biology* 206, 69-79.
- Mayford M. & Weisblum B. 1989b. Conformational alterations in the *ermC* transcript *in vivo* during induction. *The EMBO Journal* 8, 4307-4314.
- Marinus M. G. 1996. Methylation of DNA. In *Escherichia coli* and *Salmonella* cellular and molecular biology (Neidhardt, F. C. ed.). 2nd edition. ASM Press, Washington D. C., The United States of America. 782-791 pp.

- Marsh R. C. & Worcel A. 1977. A DNA fragment containing the origin of replication of the *E. coli* chromosome. *Proceedings of the National Academy of Sciences of the United States of America* 74, 2720-2724.
- McGarry K. C., Ryan V. T., Grimwade J. E. & Leonard A. C. 2004. Two discriminatory binding sites in the *Escherichia coli* replication origin are required for strand opening by initiator DnaA-ATP. *Proceedings of the National Academy of Sciences of the United States of America* 101, 2811-2816.
- Menninger J. R. & Otto D. 1982. Erythromycin, carbomycin, and spiramycin inhibit protein synthesis by stimulating the dissociation of peptidyl-tRNA from ribosomes. *Antimicrobial Agents and Chemotherapy* 21, 811-818.
- Messer W. & Weigel C. 1997. DnaA initiator - also a transcription factor. *Molecular Microbiology* 24, 1-6.
- Messer W. 2002. The bacterial replication initiator DnaA. DnaA and *oriC*, the bacterial mode to initiate DNA replication. *FEMS Microbiology Reviews* 26, 355-374.
- Morigen, Boye E., Skarstad K. & Løbner-Olesen A. 2001. Regulation of chromosomal replication by DnaA protein availability in *Escherichia coli*: effects of the *data* region. *Biochimica et Biophysica Acta* 1521, 73-80.
- Morigen, Løbner-Olesen A. & Skarstad K. 2003. Titration of the *Escherichia coli* DnaA protein to excess *data* sites causes destabilization of replication forks, delayed replication initiation and delayed cell division. *Molecular Microbiology* 50, 349-362.
- Morigen, Molina F. & Skarstad K. 2005. Deletion of the *data* site does not affect once-per-cell-cycle timing but induces rifampin-resistant replication. *Journal of Bacteriology* 187, 3913-3920.
- Ogura Y., Imai Y., Ogasawara N. & Moriya S. 2001. Autoregulation of the *dnaA-dnaN* operon and effects of DnaA protein levels on replication initiation in *Bacillus subtilis*. *Journal of Bacteriology* 183, 3833-3841.
- Onogi T., Niki H., Yamazoe M. & Hiraga S. 1999. The assembly and migration of SeqA-Gfp fusion in living cells of *Escherichia coli*. *Molecular Microbiology* 31, 1775-1782.
- Poulsen S. M., Kofoed C. & Vester B. 2000. Inhibition of the ribosomal peptidyl transferase reaction by the mycarose moiety of the antibiotics carbomycin, spiramycin and tylosin. *Journal of Molecular Biology* 304, 471-481.
- Pritchard R. H., Barth P. T. & Collins J. 1969. Control of DNA synthesis in bacteria. *Symposium of the Society for General Microbiology* 19, 263-297.
- Riber L., Olsson J. A., Jensen R. B., Skovgaard O., Dasgupta S., Marinus M. G. & Løbner-Olesen A. 2006. Hda-mediated inactivation of the DnaA protein and *dnaA* gene autoregulation act in concert to ensure homeostatic maintenance of the *Escherichia coli* chromosome. *Genes & Development* 20, 2121-2134.
- Ross J. I., Eady E. A., Cove J.H., Cunliffe W. J., Baumberg S. & Wootton J. C. 1990. Inducible erythromycin resistance in staphylococci is encoded by a member of the ATP-binding transport super-gene family. *Molecular Microbiology* 4, 1207-1214.
- Roth A. & Messer W. 1998. High-affinity binding sites for the initiator protein DnaA on the chromosome of *Escherichia coli*. *Molecular Microbiology* 28, 395-401.
- Russell D. W. & Zinder N. D. 1987. Hemimethylation prevents DNA replication in *E.coli*. *Cell* 50, 1071-1079.
- Ryan V. T., Grimwade J. E., Nievera C. J. & Leonard A. C. 2002. IHF and HU stimulate assembly of pre-replication complexes at *Escherichia coli oriC* by two different mechanisms. *Molecular Microbiology* 46, 113-124.
- Ryan V. T., Grimwade J. E., Camara J. E., Crooke E. & Leonard A. C. 2004. *Escherichia coli* prereplication complex assembly is regulated by dynamic interplay among Fis, IHF and DnaA. *Molecular Microbiology* 51, 1347-1359.
- Samitt C. E., Hansen F. G., Miller J. F. & Schaechter M. 1989. *In vivo* studies of DnaA binding to the origin of replication of *Escherichia coli*. *The EMBO Journal* 8, 989-993.
- Schaechter M., Maaløe O. & Kjeldgaard N. O. 1958. Dependency on medium and temperature of cell size and chemical composition during balanced growth of *Salmonella typhimurium*. *Journal of General Microbiology* 19, 592-606.
- Schaper S. & Messer W. 1995. Interaction of the initiator protein DnaA of *Escherichia coli* with its DNA target. *The Journal of Biological Chemistry* 270, 17622-17626.

- Schlünzen F., Zarivach R., Harms J., Bashan A., Tocilj A., Albrecht R., Yonath A. & Franceschi F. 2001. Structural basis for the interaction of antibiotics with peptidyl transferase centre in eubacteria. *Nature* 413, 814-821.
- Sekimizu K., Bramhill D. & Kornberg A. 1987. ATP activates *dnaA* protein in initiating replication of plasmids bearing the origin of the *E. coli* chromosome. *Cell* 50, 259-265.
- Sekimizu K. & Kornberg A. 1988. Cardiolipin activation of *dnaA* protein, the initiation protein of replication in *Escherichia coli*. *The Journal of Biological Chemistry* 263, 7131-7135.
- Shivakumar A. G. & Dubnau D. 1981. Characterization of a plasmid-specified ribosome methylase associated with macrolide resistance. *Nucleic Acid Research* 9, 2549-2562.
- Simmons L. A., Breier A. M., Cozzarelli N. R. & Kaguni J. M. 2004. Hyperinitiation of DNA replication in *Escherichia coli* leads to replication fork collapse and inviability. *Molecular Microbiology* 51, 349-358.
- Skarstad K., Boye E. & Steen H. B. 1986. Timing of initiation of chromosome replication in individual *Escherichia coli* cells. *The EMBO Journal* 5, 1711-1717.
- Skarstad K., Løbner-Olesen A., Atlung T., von Meyenburg, K & Boye E. 1989. Initiation of DNA replication in *Escherichia coli* after overproduction of the DnaA protein. *Molecular & General Genetics* 218, 50-56.
- Skarstad K., Lueder G., Lurz R., Speck C. & Messer W. 2000. The *Escherichia coli* SeqA protein binds specifically and co-operatively to two sites in hemimethylated and fully methylated *oriC*. *Molecular Microbiology* 36, 1319-1326.
- Skarstad K., Torheim N., Wold S., Lurz R., Messer W., Fossum S. & Bach T. 2001. The *Escherichia coli* SeqA protein binds specifically to two sites in fully and hemimethylated *oriC* and has the capacity to inhibit DNA replication and affect chromosome topology. *Biochimie* 83, 49-51.
- Skinner R., Cundliffe E. & Schmidt F. J. 1983. Site of action of a ribosomal RNA methylase responsible for resistance to erythromycin and other antibiotics. *The Journal of Biological Chemistry* 258, 12702-12706.
- Slater S., Wold S., Lu M., Boye E., Skarstad K. & Kleckner N. 1995. *E. coli* SeqA protein binds *oriC* in two different methyl-modulated reactions appropriate to its roles in DNA replication initiation and origin sequestration. *Cell* 82, 927-936.
- Speck C., Weigel C. & Messer W. 1999. ATP- and ADP-DnaA protein, a molecular switch in gene regulation. *The EMBO Journal* 18, 6169-6176.
- Su'etsugu M., Takata M., Kubota T., Matsuda Y. & Katayama T. 2004. Molecular mechanism of DNA replication-coupled inactivation of the initiator protein in *Escherichia coli*: interaction of DnaA with the sliding clamp-loaded DNA and the sliding clamp-Hda complex. *Genes to Cells* 9, 509-522.
- Suthcliffe J., Tait-Kamradt A. & Wondrack L. 1996. *Streptococcus pneumoniae* and *Streptococcus pyogenes* resistant to macrolides but sensitive to clindamycin: a common resistance pattern mediated by an efflux system. *Antimicrobial Agents and Chemotherapy* 40, 1817-1824.
- Szyf M., Avraham-Haetzi, Reifman A., Shlomai J., Kaplan F., Oppenheim A. & Razin A. 1984. DNA methylation pattern is determined by the intracellular level of the methylase. *Proceedings of the National Academy of Sciences of the United States of America* 81, 3278-3282.
- Taghbalout A., Landoulsi A., Kern R., Yamazoe M., Hiraga S., Holland B., Kohiyama M. & Malki A. 2000. Competition between the replication initiator DnaA and the sequestration factor SeqA for binding to the hemimethylated chromosomal origin of *E. coli* *in vitro*. *Genes to Cells* 5, 873-884.
- Tait-Kamrat A., Clancy J., Cronan M., Dib-Hajj F., Wondrack L., Yuan W. & Suthcliffe J. 1997. *mef(E)* is necessary for erythromycin-resistant M phenotype in *Streptococcus pneumoniae*. *Antimicrobial Agents and Chemotherapy* 41, 2251-2255.
- Tenson T., DeBlasio A. & Mankin A. 1996. A functional peptide encoded in the *Escherichia coli* 23S rRNA. *Proceedings of the National Academy of Sciences of the United States of America* 93, 5641-5646.

- Tenson T., Xiong L., Kloss P. & Mankin A. S. 1997. Erythromycin resistance peptides selected from random peptide libraries. *The Journal of Biological Chemistry* 272, 17425-17430.
- Tenson T., Vega Herrera J., Kloss P., Guarneros G. & Mankin A. S. 1999. Inhibition of translation and cell growth by minigene expression. *Journal of Bacteriology* 181, 1617-1622.
- Tenson T. & Mankin A. S. 2001. Short peptides conferring resistance to macrolide antibiotics. *Peptides* 22, 1661-1668.
- Tenson T., Lovmar M. & Ehrenberg M. 2003. The mechanism of action of macrolides, lincosamides and streptogramin B reveals the nascent peptide exit path in the ribosome. *Journal of Molecular Biology*, 330, 1005-1014.
- Tenson T. & Mankin A. 2006. Antibiotics and the ribosome. *Molecular Microbiology* 59, 1664-1677.
- Torheim N. K. & Skarstad K. 1999. *Escherichia coli* SeqA protein affects DNA topology and inhibits open complex formation at *oriC*. *The EMBO Journal* 18, 4882-4888.
- Tripathi S., Kloss P. S. & Mankin A. S. 1998. Ketolide resistance conferred by short peptides. *The Journal of Biological Chemistry* 273, 20073-20077.
- Tu D., Blaha G., Moore P. B. & Steitz T. A. 2005. Structures of MLS_BK antibiotics bound to mutated large ribosomal subunits provide structural explanation for resistance. *Cell* 121, 257-270.
- Urig S., Gowher H., Hermann A., Beck C., Fatemi M., Humeny A. & Jeltsch A. 2002. The *Escherichia coli* Dam DNA methyltransferase modifies DNA in a highly processive reaction. *Journal of Molecular Biology* 319, 1085-1096.
- Usary J. & Champney W. S. 2001. Erythromycin unhibition of 50S ribosomal subunit formation in *Escherichia coli* cells. *Molecular Microbiology* 40, 951-962.
- van Kampen N. G. 1997. Stochastic processes in physics and chemistry. 2nd edition. Elsevier, Amsterdam, The Netherlands.
- Vázquez, D. 1979. Inhibitors of protein synthesis. Molecular Biology Biochemistry and Biophysics 30. Springer-Verlag, Berlin-Heidelberg, Germany. 169-175 pp.
- Vester, B & Douthwaite S. 2001. Macrolide resistance conferred by base substitutions in 23S rRNA. *Antimicrobial Agents and Chemotherapy* 45, 1-12.
- Vimberg V., Xiong L., Bailey M., Tenson T. & Mankin A. 2004. Peptide-mediated macrolide resistance reveals possible specific interactions in the nascent peptide exit tunnel. *Molecular Microbiology* 54, 376-385.
- von Freiesleben U., Rasmussen K. V. & Schaechter M. 1994. SeqA limits DnaA activity in replication from *oriC* in *Escherichia coli*. *Molecular Microbiology* 14, 763-772.
- Walsh, C. 2003. Antibiotics. Actions, origins, resistance. 1st edition. ASM Press, Washington, D.C., The United States of America.
- Weisblum, B. 1995a. Erythromycin resistance by ribosome modification. *Antimicrobial Agents and Chemotherapy* 39, 577-585.
- Weisblum, B. 1995b. Insights into erythromycin action from studies of its activity as inducer of resistance. *Antimicrobial Agents and Chemotherapy* 39, 797-805.
- Weisblum B. 1998. Macrolide resistance. *Drug Resistance Updates* 1, 29-41.
- Wittmann H. G., Stoffler G., Apirion D., Rosen L., Tanaka K., Tamaki M., Takata R., Dekio S. & Otaka E. 1973. Biochemical and genetic studies on two different types of erythromycin resistant mutants of *Escherichia coli* with altered ribosomal proteins. *Molecular & General Genetics* 127, 175-189.
- Wold S., Skarstad K., Steen H. B., Stokke T. & Boye E. 1994. The initiation mass for DNA replication in *Escherichia coli* K-12 is dependent on growth rate. *The EMBO Journal* 13, 2097-2102.
- Wold S., Boye E., Slater S., Kleckner N. & Skarstad K. 1998. Effects of purified SeqA protein on *oriC*-dependent DNA replication *in vitro*. *The EMBO Journal* 17, 4158-4165.
- Xia W. & Dowhan W. 1995. *In vivo* evidence for the involvement of anionic phospholipids in initiation of DNA replication in *Escherichia coli*. *Proceedings of the National Academy of Sciences of the United States of America* 92, 783-787.

- Yamazoe M., Onogi T., Sunako Y., Niki H., Yamanaka K., Ichimura T. & Hiraga S. 1999. Complex formation of MukB, MukE and MukF proteins involved in chromosome partitioning in *Escherichia coli*. *The EMBO Journal* 18, 5873-5884.
- Zheng W., Li Z., Skarstad K. & Crooke E. 2001. Mutations in DnaA protein suppress the growth arrest of acidic phospholipid-deficient *Escherichia coli* cells. *The EMBO Journal* 20, 1164-1172.
- Zhong P. & Shortridge V. 2001. The emerging new generation of antibiotic: ketolides. *Current Drug Targets- Infectious Disorders* 1, 125-131.
- Zgurskaya H. I. & Nikaido H. 1999. Bypassing the periplasm: reconstitution of the AcrAB multidrug efflux pump of *Escherichia coli*. *Proceedings of the National Academy of Sciences of the United States of America* 96, 7190-7195.

Acknowledgements

I would like to thank you all the people who have helped me one way or another during my years as a Ph D student.

A deep gratitude goes to **Dietrich** for taking me on as a Ph D student in the first place and for your never-ending moral support, whenever I needed it.

Another (equally) deep gratitude goes to **Måns** for accepting to be my supervisor and for introducing me to some interesting research fields with the intention to combine theory with experiments. I believe we have reached farther with that intention within some projects than others. Most importantly you have shared your passion for science.

I want to thank **Johan** for helping me out in my projects and **Martin** for fruitful discussions within our common projects. I want to give you a special elege, Martin, for helping me out during the finalizing of this thesis.

I want to thank **Tanel** and your group (especially **Vladimir**) for being good collaborators and for your open mind regarding mixing modelling with experiments.

I would also like to thank all the other members of Måns' group and all Ph D students at the Department of Biometry and Engineering (and the former department of Biometry and Informatics) over the years, especially **Razaw**, **Kristi**, **Zhanna**, **Dilip**, **Johannes** and **Anna** for your companionship.

I am finally grateful to the department of Biometry and Engineering for extending my position and providing for me financially when needed so that I could complete my doctoral studies.



I



Stochastic Modelling of Regulation of Initiation of Chromosome Replication in Single *Escherichia coli* Cells

Karin Nilsson^{1, 2}, Johan Elf^{2, 3}, Anna Ringheim², Santanu Dasgupta⁴, Kurt Nordström⁴ and Måns Ehrenberg²

¹ Department of Biometry and Engineering, Swedish University of Agricultural Sciences, Uppsala S-75007, Sweden

² Department of Cell and Molecular Biology, Molecular Biology Program, Uppsala University, Uppsala S-75124, Sweden

³ Present affiliation: Department of Chemistry and Chemical Biology, Harvard University, 02138 Cambridge, MA, U.S.A.

⁴ Department of Cell and Molecular Biology, Microbiology Program, Uppsala University, Uppsala S-75124, Sweden

Correspondence to: Måns Ehrenberg

Dept. of Cell and Molecular Biology,
Molecular Biology Program,
BMC, Box 596, Uppsala University,
S-75124 Uppsala, Sweden
E-mail: ehrenberg@xray.bmc.uu.se
Tel: +46 18 471 42 13
Fax: +49 18 471 42 62

ABSTRACT

We have developed a stochastic model of the regulation of initiation of chromosome replication in *Escherichia coli*, which automatically generates the correct initiation frequency and chromosome number, synchronous initiation at multiple origins and varying cell size as functions of the growth rate. Expression of the *dnaA* gene for the activator, DnaA, of chromosome replication is more strongly auto-repressed by DnaA-ATP than by DnaA-ADP. However, we demonstrate that repression of *dnaA* by free DnaA-ATP is inconsistent with adequate regulation of *dnaA* gene expression and propose that DnaA-ADP is the main regulator of *dnaA* expression, while DnaA-ATP is the key-activator of replication initiation. This suggests that the conversion of DnaA-ATP to DnaA-ADP by RIDA is essential for chromosome copy number control. We also clarify what is required for an invariant cell volume at initiation for exponentially growing cells in different growth media and propose two alternative molecular mechanisms that define the sequestration period of the *oriC* following initiation. Experimental observations in relation to the model and future experiments are discussed.

INTRODUCTION

The *E. coli* genome consists of a single circular chromosome and replication starts from the unique *oriC* site (Marsh and Worcel, 1977). The DnaA protein binds *oriC* and builds up a nucleoprotein complex promoting DNA strand opening and thereby initiation of replication (Messer, 2002). The chromosome is replicated bi-directionally by two replisomes proceeding from the *oriC* to the *ter* sites in the terminus region (Hill, 1996). One round of replication, completed after the C-period of about 40 minutes, is followed by cell division after the D-period of about 20 minutes. The C- and D-periods are approximately constant for generation times between 20 and 60 minutes (Cooper and Helmstetter, 1968), implying that it takes about 60 minutes (C+D) for a cell to replicate its genome and divide. When the generation time, which can vary from about 20 minutes to infinity, is less than 60 minutes, replication is initiated in the mother, grandmother or grand-grandmother generation and the cells are born with 2, 4 or 8 origins, respectively (Fig. 1). When the generation time is longer than 60 minutes, there is also a B-period between cell birth and initiation of replication (Cooper and Helmstetter, 1968). Initiation occurs only once per generation and cells with multiple *oriCs* initiate synchronously (Skarstad *et al.*, 1986; Boye *et al.*, 2000). Irrespective of growth rate, initiation takes place at an approximately constant cell mass (or cell volume) per origin, which has been named the “initiation mass” (Donachie, 1968). Just after initiation of replication the *oriCs* are hemi-methylated and they become fully methylated after a delay time corresponding to about 30% of the generation time (Campbell and Kleckner, 1990).

DnaA initiates replication at fully methylated, but not hemi-methylated *oriC* (Russell and Zinder, 1987). The methylation status of *oriC* is regulated by the SeqA protein (Lu *et al.*, 1994) and the Dam methyltransferase (Løbner-Olesen *et al.*, 2005). The SeqA protein binds and sequesters *oriC* thereby preventing immediate methylation by Dam (Lu *et al.*, 1994; von Freiesleben *et al.*, 1994). About eight minutes after initiation of replication the replication forks duplicate the *datA* locus, which can bind a large number of DnaA molecules, thereby lowering the free concentration of DnaA (Kitagawa *et al.*, 1996; Kitagawa *et al.*, 1998). DnaA exists in two forms, DnaA-ATP and DnaA-ADP, and DnaA-ATP is active at initiation (Messer, 2002; McGarry *et al.*, 2004). Conversion of the active form into DnaA-ADP is stimulated by the replication fork and is called RIDA (regulatory inactivation of DnaA) (Katayama *et al.*, 1998; Katayama and Sekimizu, 1999). Fig. 2 shows the molecules involved in the control of replication initiation.

Although initiation of chromosome replication in *E. coli* has been extensively studied during decades, the basic principles by which the bacterium coordinates initiation of replication with the cell cycle and synchronizes initiation at multiple origins is still debated. One reason for this is that chromosome replication is controlled by a number of molecular mechanisms that act together in the global context of growing and dividing cells. In order to assess the function of these mechanistic units they must be integrated in a global description of the living cell, and such descriptions have been scarce as well as incomplete in the past. Here, we have used stochastic modeling of the replication process in growing *E. coli* cells as a tool to test hypotheses regarding regulation of initiation of chromosome replication. The regulation problem is conveniently partitioned in two parts. The first relates to the control of the number of chromosome copies per cell of *E. coli* populations growing under different conditions and the second to the synchronization of initiation of replication at different origins. Our analysis shows that DnaA carries out copy number

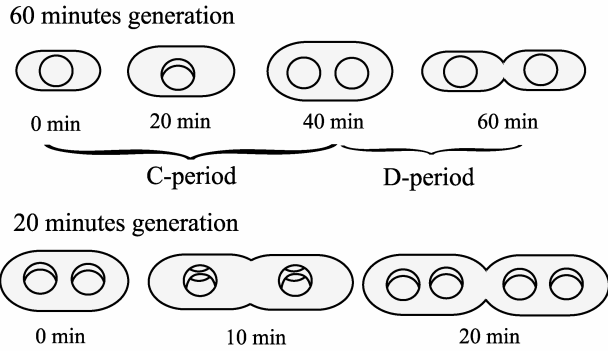


Figure 1. Cell growth and division for a cell with a generation time of 60 or 20 minutes. The time for completing one round of replication is 40 minutes and cell division occurs 20 minutes after each round is terminated for both generation times. The 20 minutes generation cell is therefore born with two complete chromosome copies which replication was initiated in the beginning of the grandmother generation.

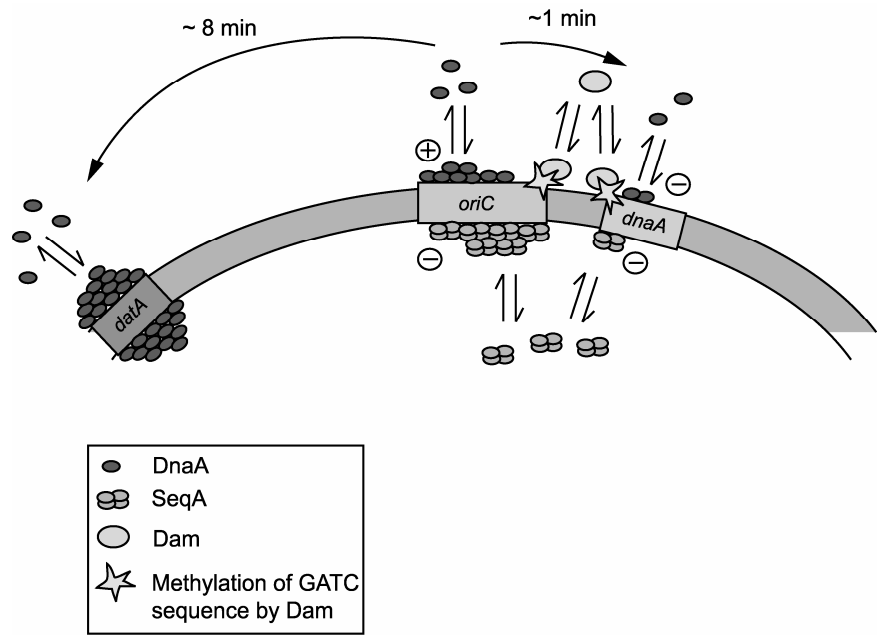


Figure 2. The regulation of replication initiation. The DnaA protein binds to boxes in *oriC* and DnaA-ATP triggers initiation. Following initiation the GATC sites in *oriC* become hemi-methylated and sequestered by the SeqA protein thereby preventing immediate re-methylation of *oriC* by the Dam methylase and re-initiation by DnaA. The replication fork reaches the *dnaA* gene after one minute and the *datA* locus after 8 minutes, when replication takes 40 minutes to complete. SeqA sequesters the *dnaA* promoters following initiation and both DnaA-ADP and DnaA-ATP can bind the promoters and repress *dnaA* expression. The *datA* locus can bind a high number of DnaA molecules, approximately 370 *in vitro*.

control and, accordingly, that regulation of the *total* concentration of DnaA is crucial for the proper working of the mechanism. We will suggest that control of the total concentration of DnaA is likely to be carried out by DnaA-ADP acting as an auto-repressor of expression from the *dnaA* gene, which may shed new light on the functional meaning of the conversion of DnaA from its ATP to its ADP form by RIDA. It seems clear that binding of DnaA to boxes along the chromosome and the relatively long sequestration period of newly fired *oriCs* contribute to synchronization of chromosome replication (Boye *et al.*, 2000). At the same time, the molecular mechanism that determines the sequestration period has remained unclear. Therefore we discuss three different molecular mechanisms, and show that each one of these can account for synchronization of initiation of replication. We also discuss future experiments to subject the theory to further experimental testing, and outline extensions of the theory to include (i) regulation of synthesis of deoxyribonucleotides by DnaA, affecting the rate of replication fork elongation and (ii) further model testing of critical experimental observations.

THE MOLECULAR BASIS OF THE MODEL

Regulation of *dnaA* expression

In the cell, DnaA exists either in the DnaA-ATP or DnaA-ADP form, and the former is essential for initiation of chromosome replication (Messer, 2002). The *dnaA* gene is expressed from two promoters, *dnaAp1* and *dnaAp2*, with the majority of transcripts coming from *dnaAp2* (Hansen *et al.*, 1982; Chiaramello and Zyskind, 1990; Hansen *et al.*, 1991). The sequence between the promoters contains both 9-mer DnaA boxes and 6-mer DnaA-ATP boxes (Speck *et al.*, 1999; Messer, 2002). The 9-mer, “strong”, DnaA boxes bind the ATP and ADP forms of DnaA with equal affinity, while the 6-mer boxes preferentially bind DnaA-ATP, conditional on occupation of an adjacent strong box with either form of DnaA (Messer, 2002). Expression of *dnaA* is strongly and intermediately auto-repressed by DnaA-ATP and DnaA-ADP, respectively (Atlung *et al.*, 1985; Speck *et al.*, 1999). As *oriC*, the *dnaA* promoter region also contains GATC sites with a delayed remethylation (Campbell and Kleckner, 1990), implying that *dnaA* expression is temporarily shut-off after initiation of replication (Theisen *et al.*, 1993). The functional meaning of this intermittent shutdown of DnaA synthesis has remained unclear.

For performance comparison, we have modeled *dnaA* expression constitutive as well as regulated by the free concentration of either DnaA-ATP or DnaA-ADP. The constitutive scenario is motivated by the previous suggestion that the free concentration of DnaA-ATP is normally too small to inhibit *dnaA* expression (Bremer and Churchward, 1991), although more recent experiments suggest that DnaA is, indeed, an auto-repressor (Hansen *et al.*, 1987; Christensen *et al.*, 1999; Morigen *et al.*, 2001; Morigen *et al.*, 2003). To simplify, we have assumed a *dnaA* gene per chromosome with a single promoter (*dnaAp*) modeled after *dnaAp2*, with two strong DnaA and three weak DnaA-ATP boxes (Speck *et al.*, 1999). We define *dnaA* expression as constitutive when *dnaAp* is always free from repressor and when the rate constants for initiation of transcription by RNA polymerase do not change (Bremer *et al.*, 2003). This definition excludes stringent control of *dnaA* (Chiaramello and Zyskind, 1990), but allows for variation of promoter activity due to varying concentration of free RNA polymerase (Dennis *et al.*, 2004). The number of DnaA molecules produced per cell volume under different conditions will always be

determined by the outcome of a competition between *dnaA* expression and the expression from all other genes in the chromosome. This means, for instance, that as long as the competition remains neutral with respect to varying growth conditions, constitutive *dnaA* expression per cell volume will be proportional to the current growth rate μ . In our modeling we have also taken into account that the dosage of *dnaA* compared to all other genes may vary with growth conditions, since *dnaA* is located close to *oriC* (Fig. 2). It should, however, be kept in mind that such competition neutrality may be hard or even impossible to come by (Bremer and Churchward, 1991). In addition to the constitutive aspect of *dnaAp*, the promoter may also be regulated by DnaA-ATP or DnaA-ADP, since both forms of DnaA are known to inhibit initiation of *dnaA* transcription *in vitro*, with DnaA-ATP as the stronger auto-repressor (Speck *et al.*, 1999). A newly formed DnaA molecule *in vivo* is assumed to rapidly bind ATP (Speck *et al.*, 1999) and normally stay in the ATP form (Messer, 2002) until converted to DnaA-ADP by RIDA-induced ATP hydrolysis (see below).

Experimental data suggest that the population averaged total concentration of DnaA is constant over a wide range of growth rates for *E. coli* K-12 strains, but increases with growth rate for an *E. coli* B/r strain (Churchward *et al.*, 1981; Wold *et al.*, 1994; Herrick *et al.*, 1996). Whether the total concentration of DnaA changes during the cell cycle is not known, but constitutive expression of *dnaA* on a plasmid can complement a *dnaA*(Ts) mutation at non-permissive temperatures (Løbner-Olesen *et al.*, 1989).

Initiation of replication and sequestering of DnaA in DNA boxes

The strong 9-mer DnaA and the weak 6-mer DnaA-ATP boxes are scattered along the chromosome (Roth and Messer, 1998; Messer, 2002) and both types of boxes are found within the *oriC* (Messer, 2002; Leonard and Grimwade, 2005) along with the recently discovered type I-sites, which are 9-mer sequences with weak binding affinity to DnaA-ATP (McGarry *et al.*, 2004). At initiation of chromosome replication, two of the I-sites occupied by DnaA-ATP are required for DNA strand opening (McGarry *et al.*, 2004) and in total 20-30 DnaA molecules are cooperatively bound to the *oriC* (Messer, 2002).

We have modeled the rate of initiation of replication at *oriC*, the “initiation potential”, by, firstly, neglecting the binding of DnaA-ADP to *oriC* and, secondly, introducing a simplified scheme in which initiation requires a number of DnaA-ATP molecules cooperatively bound to *oriC*. The current rate of initiation per *oriC* is computed from the condition that *oriC* must be fully methylated (Russell and Zinder, 1987), the rate constant when *oriC* is saturated by DnaA-ATP and the probability of saturation as determined by the concentration of free DnaA-ATP (Appendix).

The *datA* locus, reached by the replication fork around eight minutes after initiation, sequesters about 370 DnaA-ATP molecules *in vitro* (Kitagawa *et al.*, 1996), but the exact number *in vivo* is uncertain and may be somewhat lower. The *datA* locus has been suggested to synchronize initiation of replication at different *oriC*s by regulating the fraction free DnaA-ATP during the cell cycle. While deletion of *datA* confers asynchronous and excessive initiations, simultaneous disruption of seven other major DnaA binding sites appears to preserve the synchrony of initiation of replication (Kitagawa *et al.*, 1998; Ogawa *et al.*, 2002). However, recently Morigen *et al.* (2005) demonstrated that the previously reported extensive initiation asynchrony observed by *datA* deletion is caused by rifampin-resistant initiations. Addition of a

high concentration of rifampin in replication run-out experiments largely decreases initiation asynchrony.

In the model, we have used 370 (*in vitro* estimate) (Kitagawa *et al.*, 1996) independent, strong binding sites for DnaA-ATP in *dataA*. In addition, we have positioned approximately 300 binding clusters, consisting of one strong DnaA box together with two weak DnaA-ATP boxes along the chromosome. To simplify, we have assumed that the boxes are equally spaced (Appendix).

Conversion of DnaA-ATP to DnaA-ADP by RIDA

A newly synthesized DnaA molecule is assumed to rapidly bind ATP and then stay in the ATP form until ATP hydrolysis is stimulated on chromosome bound DnaA-ATP by Regulatory Inactivation of DnaA (RIDA), *i.e.* by the “sliding clamp” β -subunit of DNA polymerase III in complex with the Hda protein (Katayama *et al.*, 1998; Su’etsugu *et al.*, 2004). Interestingly, in spite of the great excess of ATP in the cytoplasm (Bochner and Ames, 1982) there is a slow nucleotide exchange on DnaA (Messer, 2002). The experimental data supporting the suggestion that acidic phospholipids may interact with DnaA-ADP and regenerate the ATP-form of the protein (Sekimizu and Kornberg, 1988) are unclear (Aranovich *et al.*, 2006).

In the model we have therefore assumed that DnaA is synthesized in the ATP form, where it remains until ATP is hydrolyzed by RIDA, and that the ADP form of DnaA is stable (Appendix). If assumed that DnaA-ATP is the main auto-repressor of *dnaA*, then the system will strive to keep the *free* concentration of DnaA-ATP constant during the major part of the cell cycle when *oriC* is not sequestered, which would make synchronous initiation of replication at different *oriC*s problematic. However, ATP hydrolysis by RIDA and DnaA-ADP as the main repressor of *dnaA* may solve this problem, by effectively controlling the total, rather than the free, concentration of DnaA-ATP in *E. coli* and other bacteria.

Sequestration and methylation of *oriC*

The chromosome is dispersed with GATC sequences (Urig *et al.*, 2002), in which the adenine is methylated by the Dam methyltransferase (Løbner-Olesen *et al.*, 2005), and there are eleven GATC sites within the *oriC* (Messer, 2002). During chromosome replication, unmethylated adenine nucleotides are incorporated resulting in hemi-methylated DNA with one (old) methylated and one (new) unmethylated strand (Løbner-Olesen *et al.*, 2005). Most GATC sites are methylated by Dam within a few minutes after their synthesis, but GATC sites within *oriC* and the *dnaA* promoter region remain hemi-methylated much longer (Campbell and Kleckner, 1990; Lu *et al.*, 1994). This methylation delay depends on the presence of the SeqA protein (Lu *et al.*, 1994; von Freiesleben *et al.*, 1994), which binds with high affinity to hemi-methylated GATC sites in *oriC* (Slater *et al.*, 1995; Messer, 2002). Initial binding of SeqA to two sites in *oriC*, one on each side of the DnaA box R1, leads to cooperative binding of SeqA to adjacent sites (Skarstad *et al.*, 2000; Skarstad *et al.*, 2001). This results in a multi-SeqA complex, in which one SeqA tetramer is associated with two hemi-methylated GATC sequences (Han *et al.*, 2003; Han *et al.*, 2004), which effectively inhibits the binding of DnaA to *oriC* (Skarstad *et al.*, 2000; Taghbalout *et al.*, 2000; Skarstad *et al.*, 2001). What triggers re-methylation and ends sequestration of *oriC* has remained obscure.

In the model we have therefore used three, functionally equivalent, scenarios for the sequestration period of *oriC* after its replication. In the first scenario (S_1), we have inserted experimental observations for the sequestration period in the model

without providing a molecular mechanism. In the second scenario (S_{II}), we have postulated sequential re-methylation of the GATC sites in *oriC*, which also leads to resolution of the multi-SeqA complex at a well-defined time when the concentration of free DnaA-ATP is small. Scenario S_{II} is presently studied experimentally in our laboratories. In the third scenario (S_{III}), we have postulated the existence of a *seq* locus, situated downstream from the *data* locus, which greatly reduces the concentration of free SeqA molecules and thereby resolves the multi-SeqA complex in *oriC* at a time point when there is little free DNA-ATP in the cell (Appendix).

Simulation of the whole chromosome replication cycle and the timing of cell division

The number of *oriC*s in a single *E. coli* cell ranges between one and eight depending on growth condition and time point in the cell cycle (Cooper and Helmstetter, 1968) and the per cell numbers of molecules involved in replication control are small. This motivates a stochastic description (van Kampen, 1997) of chromosome replication and timing of cell division, which accounts for the random nature of these processes. The time (t_{event}) of any event changing the replication state of the cell is statistically sampled and followed by sampling of which event that has occurred according to the Gillespie algorithm (Gillespie, 1976). We have divided the chromosome into 1000 segments, starting with *oriC*, with the *data* locus in segment 200 and one DnaA box combined with two DnaA-ATP boxes in approximately every third segment (Fig. 3). Replication starts at *oriC*, ends at *ter* and the replication fork jumps from one segment to the next with a first order rate constant (k_R) set at 25 min^{-1} , so that the average chromosome replication time (C-period) is equal to 40 minutes ($C=1000/k_R$) and the *data* box is reached on the average 8 minutes after initiation. At a fixed time of 20 minutes after termination of replication (D-period) the cell divides, implicating that the timing of cell division and thus the cell size are regulated by the control of initiation of replication. Whenever a chromosome segment containing DnaA-ATP is replicated, the ATP is hydrolyzed by RIDA and DnaA in the ADP form dissociates to the free state from which it may rebind to any unoccupied DnaA box. There are 7 events in the model that change the replication state of the cell. These are (i) initiation of replication with rate r_1 (ii) movement of the replication fork one step with rate r_2 (iii) synthesis of one molecule of DnaA (rapidly turned into DnaA-ATP) with rate r_3 (iv) association of DnaA-ADP or DnaA-ATP to DnaA boxes with rate r_4 (v) dissociation of DnaA-ADP or DnaA-ATP from DnaA boxes with rate r_5 (vi) association of DnaA-ATP to DnaA-ATP boxes with rate r_6 (vii) dissociation of DnaA-ATP from DnaA-ATP boxes with rate r_7 . The exponentially distributed t_{event} is the inverse of the sum of all rates r_i and the probability of an event “i” is r_i multiplied by t_{event} .

In scenario S_I, *oriC* and the *dnaA* promoter are sequestered from the time of replication until the replication fork reaches segment 350, which takes 14 minutes on the average. In this scenario, we have studied control of initiation of replication both when *dnaA* is constitutively expressed and when it is auto-regulated by DnaA-ADP and DnaA-ATP (Appendix).

In scenario S_{II}, the sequestration of *oriC* after replication is over when the eleven GATC sites in *oriC* have been methylated either in a specific or a random order. Scenario S_{II} has two state changing events, in addition to those in scenario S_I, i.e. (viii) methylation of an unmethylated GATC site in *oriC* with rate r_8 and (ix) methylation of unmethylated GATC sites in other chromosomal segments with rate r_9 .

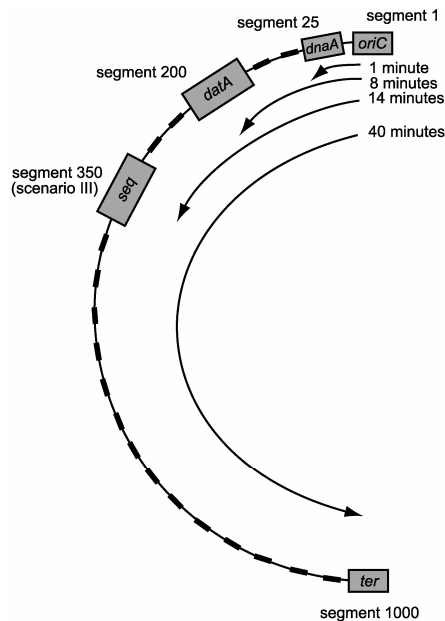


Figure 3. A schematic of the modelled chromosome. Only one replication fork is followed. Replication initiates at *oriC* (segment 1) and ends at *ter* (segment 1000), on the average 40 minutes later. The replication fork reaches the *dnaA* gene and the *dataA* locus 1 minute (segment 25) and 8 minutes (segment 200) on the average after initiation at *oriC*, respectively. In addition to *dataA*, the chromosome contains 307 evenly distributed groups of DnaA binding sites (illustrated as black boxes), each group consisting of one DnaA box which binds DnaA-ADP and DnaA-ATP with equal affinity, and two DnaA-ATP boxes which only binds DnaA-ATP. The *dataA* locus only binds DnaA-ATP. In scenario III the replication fork passes a hypothetical *seq* locus, at segment 350, reached by the fork 14 minutes on the average after leaving *oriC*. The *seq* locus has a high affinity of the SeqA protein when hemimethylated.

In scenario S_{III} , sequestration of *oriC* after replication depends on a putative *seq* locus in segment 350 of the chromosome (Fig. 3). Upon replication of the *seq* locus the concentration of free SeqA decreases strongly, which activates the rate of Dam-methylation of GATC sites in *oriC* and other chromosomal segments. In this scenario, additional state changing events are (viii) methylation of hemimethylated *oriC* with rate r_8 and (ix) methylation of unmethylated GATC sites in other chromosomal segments with rate r_9 . In scenario S_{II-III} *dnaA* expression is either constitutive or regulated by DnaA and *dnaA* sequestration ends when *oriC* methylation is complete. See Appendix for details of the model.

RESULTS

Regulation of chromosome replication under different growth conditions

The size of the *E. coli* cell increases with increasing growth rate (Donachie and Robinson, 1987), but the cell volume or cell mass per *oriC* at which replication starts (“initiation volume” or “initiation mass”) remains virtually (Wold *et al.*, 1994) or approximately (Churchward *et al.*, 1981) constant. In this section, we study regulation of chromosome replication under different growth conditions with a simplified version of S_I .

To illustrate principles, we will initially assume that the *dataA* locus close to *oriC* provides the dominating number of binding sites for DnaA-ATP on the chromosome. Second, DnaA-ATP is constitutively expressed with a rate that is strictly proportional to the growth rate μ , so that the *total* DnaA concentration is constant, irrespective of the growth medium and the increasing fraction of *dnaA* to all chromosomal genes with increasing growth rate. Third, the sequestering of the *dnaA*

gene after replication of *oriC* is disregarded. We will also disregard the conversion of DnaA-ATP to DnaA-ADP by RIDA, which under the above assumptions has no effect on the initiation mass. Just after replication of the *datA* loci in the cell, the concentration of *datA* binding sites for DnaA-ATP supersedes the number of DnaA-ATP molecules by a factor of two so that the free concentration of DnaA-ATP is very low. As the cell volume grows, the concentration of *datA* sites is diluted, the concentration of total DnaA molecules remains unaltered, and the fraction of filled *datA* sites increases while the concentration of free DnaA-ATP remains low. Just when all *datA* sites have become occupied, the total concentrations of *datA* sites and DnaA-ATP molecules are almost equal. Thereafter, the free concentration of DnaA-ATP increases sharply, rapidly leading to a new round of replication. Accordingly, initiation of chromosome replication is triggered at a time point in the cell cycle when the concentrations of DnaA-ATP molecules and *datA* sites are approximately equal, irrespective of the value of the growth rate μ . Since, by assumption, the total number of DnaA-ATP molecules per cell is proportional to the cell volume and, since the concentrations of *datA* and *oriC* are the same at the initiation event, this simplified version of S_1 leads to synchronous initiation once and only once per generation time at a constant initiation mass and initiation volume at varying growth rates.

To further illustrate these properties of the model we have simulated a series of up-shifts leading to step-wise increases in the growth rate. The model accounts for the well-known increase in cell volume with increasing growth rate for generation times between 20 and 60 minutes by, first, fixing the time to complete one round of replication (C-period = 40 minutes) and, second, by fixing the minimal time between termination of replication and cell division (D-period = 20 minutes). When a cyclic steady state with synchronous initiations has been established, then the initiation age a_i , that separates cell division of a mother cell from the first initiation round in the daughter cell is given by $a_i = n - (C + D) / \tau_G$, where τ_G is the generation time and n is the next largest integer of $(C + D) / \tau_G$ (Cooper and Helmstetter, 1968; Bremer and Churchward, 1991). In the basic form of the model, initiations of chromosome replication occur when $[DnaA]V = [DnaA]V_0 2^{n - (C+D)/\tau_G} = n_{ori} N_{dat} = 2^n N_{dat}$. Here, V is the volume at which initiation occurs, V_0 is the volume of a newly born cell, n_{ori} is the number of *oriC*s per cell, equal to the number of *datA* loci, and N_{dat} is the number of DnaA binding sites per *datA*. From this follows that, in our model, V_0 is determined by the generation time τ_G through $V_0 = N_{dat} 2^{(C+D)/\tau_G} / [DnaA]$, and that the initiation volume $V_I = V / n_{ori} = N_{dat} / [DnaA]$ is determined by the total DnaA concentration, so far assumed to be constant.

In Fig. 4 the cells initially grow in a medium associated with a generation time of 60 minutes. Chromosome replication starts at *oriC* (position 1 in Fig. 4A) in the newly born cell and reaches *ter* (position 1000) after an average time of 40 minutes. Cell division is modelled to occur 20 minutes after termination of replication, and the varying cell volume is shown in Fig. 4B. The model generates a cyclic steady state, where the free concentration of DnaA-ATP sharply rises in 60 minutes intervals, stays large until it drops to a small value when the *datA* locus is duplicated 8 minutes after initiation (Fig. 4C). In the beginning of fourth division cycle, there is an up-shift so that the generation time decreases from 60 to 40 minutes, which by assumption, results in a 50% increase of the total *dnaA* expression. After the up-shift, *oriC* is as before duplicated in the newly born cell, but due to the increased

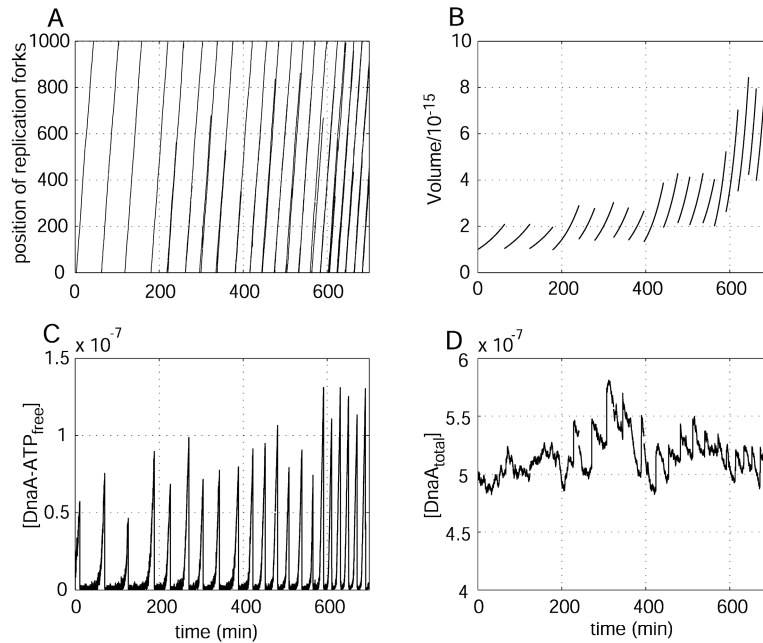


Figure 4. Cell size increases with increasing growth rate. At time 0 the cell is growing at a rate corresponding to a 60 minutes generation time. After 3, 8 and 13 generations the growth rate increases, corresponding to a generation time of 40 minutes, 30 minutes and 20 minutes, respectively. (A) Position of replication forks, *oriC* is located in segment 1 and the *datA* locus is positioned in segment 200. (B) Normalised cell volume. (C) The free concentration of DnaA-ATP, which peaks at initiation. (D) The total concentration of DnaA (both bound and free). Simplified version of scenario I with no RIDA, no DnaA binding sites besides *datA*, constitutive expression of *dnaA* and no sequestration of the *dnaA* promoter are assumed. Total expression of *dnaA* is strictly proportional to the growth rate.

rate of synthesis of DnaA, so that the *datA* locus is more rapidly filled, the two *oriCs* in the cell are now replicated after 40 minutes and soon the free DnaA-ATP concentration peaks at 40 minutes, rather than 60 minutes, intervals (Fig. 4C) and the cell volume is approximately 50% larger than before (Fig. 4B). In the beginning of the 9th generation and in the beginning of the 14th generation there are further up-shifts leading to a generation time of 30 minutes and 20 minutes, respectively. The total *dnaA* expression is further increased by 33% and 50% percent, respectively. The increased expression of DnaA, to keep the total DnaA concentration constant during the division cycle, makes the *datA* loci saturated faster, at a rate generating an initiation frequency of 30 and 20 minutes, respectively. Since the C and D periods are fixed, the next cell division lags behind initially after each up-shift, resulting in a further increased cell volume by a factor of 2 and 4, respectively, compared to the cell volume at the initial 60 minutes generation time. Thus, by allowing one round of replication to take 40 minutes and cell division to occur 20 minutes later the proposed regulation of replication initiation generates a well-defined cell size for a certain generation time.

Both the conversion of DnaA-ATP to DnaA-ADP by RIDA and sequestration of *dnaA* after replication of *oriC* decrease the total concentration DnaA-ATP in the

cell. It has therefore been suggested that RIDA and *dnaA* sequestration (Boye *et al.*, 2000) contribute to synchronous initiation of replication by decreasing the initiation potential after *oriC* replication. Our modelling shows, in contrast, that neither RIDA nor *dnaA* sequestration contributes to synchrony by this type of effect. Given that *oriC* is sequestered by SeqA, DnaA titration by binding sites, *e.g.* *datA*, is enough to sustain synchronous initiations. Thus, by introducing RIDA or *dnaA* sequestration during 14 minutes in the model and increasing the constitutive rate of synthesis of DnaA-ATP per promoter virtually the same synchronous replication pattern as before is obtained at all studied growth rates. It is, however, still possible that RIDA or *dnaA* sequestration could facilitate rapid sequestration of *oriC* after its replication but, as will be argued below, the main function of RIDA is to allow for DnaA as an activator of chromosome replication to function also as a repressor of its own synthesis.

As we have seen, the basic version of S_1 generates a constant initiation mass when the chromosomal sites that titrate the free concentration of DnaA-ATP are positioned close to *oriC*, as in the *datA* locus. However, when there are DnaA binding sites evenly scattered around the chromosome, in addition to those in *datA*, then the initiation mass decreases with increasing growth rate at generation times smaller than 40 minutes. The reason is that at such short generation times the number of scattered DnaA binding sites will decrease in relation to the number of *datA* loci and *oriCs* per cell due to overlapping rounds of replication as the growth rate increases. For a constant total DnaA concentration this will then decrease the initiation mass. If, however, the extra chromosomal binding sites are positioned sufficiently close to *oriC*, then the initiation mass will remain unaltered as the growth rate changes. The sequestration period of the *dnaA* promoter also affect the initiation mass, which is neutral or increases as the growth rate increases if the sequestration period is a fixed fraction or a fixed number of minutes of the generation time, respectively.

When the *datA* locus is removed from a chromosome with additional DnaA binding sites (S_1), a period of adjustment follows where the cell decreases in size (Fig. 5). Then the cell is smaller than before but initiates with the same frequency and harbors the same amount of DNA as before (*i.e.* a higher concentration of DNA). The initiation mass will increase considerably and synchronisation of replication will be partially lost, as observed experimentally (Morigen *et al.*, 2005). Increased asynchrony is a result of less distinct peaks of the free concentration of DnaA-ATP at the time of initiation. The total concentration of DnaA is approximately the same as before *datA* deletion while the free concentration of DnaA-ADP has decreased.

Regulation of *dnaA* expression

As we have seen in the previous section, constitutive expression of *dnaA*, such that the fraction of total protein synthesis devoted to DnaA is always the same, leads to a constant concentration of total DnaA, allowing for precise control of *oriC* replication at constant initiation mass under different growth conditions (Fig. 4). It is, however, not obvious how such neutral expression of *dnaA* can prevail, since it will depend on a competition with the expression of all other genes in the cell, many of which are strongly regulated up or down depending on the current growth habitat (Bremer and Churchward, 1991). It is, furthermore, known that DnaA can function as an auto-repressor of *dnaA*; more strongly as DnaA-ATP but also as DnaA-ADP (Speck *et al.*, 1999). It has therefore been suggested that DnaA-ATP represses the synthesis of DnaA by direct binding to the *dnaA* promoters (Nordström and Dasgupta, 2006). If, as we propose here, DnaA-ATP is the key-regulator of initiation of replication at *oriC*,

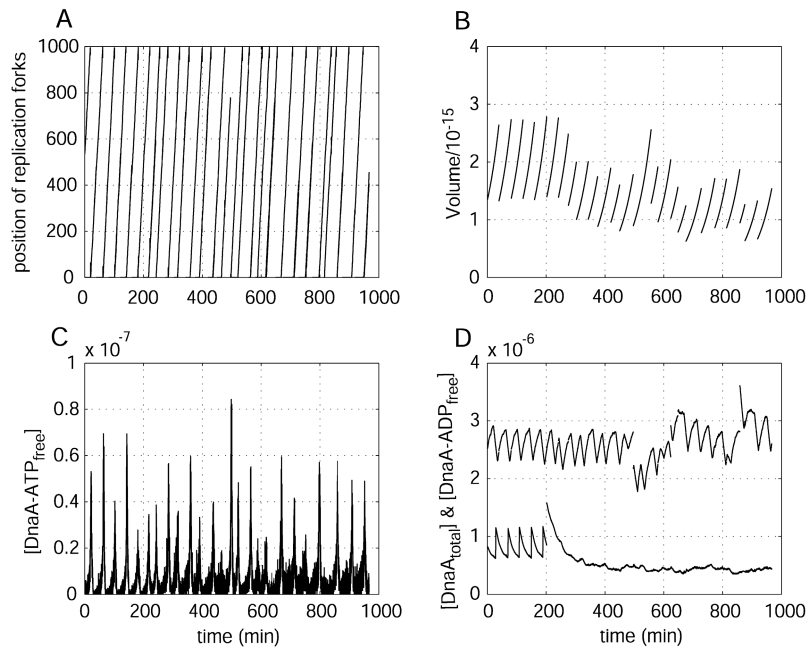


Figure 5. Adjustment after deletion of the *data* locus. The *data* locus is deleted after the 5th division cycle for a cell growing with a generation time of 40 minutes (scenario I, see text). (A) Position of the replication forks. (B) Normalised cell volume. (C) The free concentration of DnaA-ATP. (D) The total concentration of DnaA and the free concentration of DnaA-ADP.

the proposal that DnaA-ATP inhibits its own synthesis leads to a principal problem (Bremer and Churchward, 1991), later named the auto-regulation-sequestration paradox in the context of P1 plasmid copy number control (Chattoraj *et al.*, 1988). The problem arises since normally it is the free, rather than the total, concentration of an active repressor that determines the occupied fraction of a promoter-controlling operator. Ideally, this would mean that the free concentration of DnaA-ATP is always constant, which would lead to a constant initiation potential, except when *dnaA* is sequestered. Accordingly, synchronous initiation of multiple *oriCs* in a cell would be precluded and, furthermore, chromosome copy number would fail, since the sequestration of free DnaA-ATP by *data* and other DnaA binding boxes on the chromosome would be over-ruled by the condition of a constant free concentration of DnaA-ATP. If the resulting constant initiation potential would, on the average, lead to more than, less than or exactly one initiation per generation time there would be, respectively, run-away, dwindling or randomized chromosome copy numbers in the cell. A less precise and perhaps more realistic version of this type of control system will have features intermediate to those of constitutive *dnaA* expression and precise control of the free concentration of DnaA-ATP. Stochastic modelling of such a mechanism shows expression of *dnaA* to be maximal until *data* is saturated. Subsequently, when the free DnaA-ATP concentration starts to rise, expression of *dnaA* is attenuated, leading to large variation in initiation time and loss of initiation synchrony (not shown).

These considerations and the results of the previous section show that regulation of the gene for an activator of initiation of replication should be based on the total, rather than the free, concentration of the activator. One solution to this principal problem has been suggested for the iteron-controlled plasmid P1, where the activator for plasmid duplication represses its synthesis. The proposal here is that iteron-bound activators can interact with the promoter for the activator by DNA-looping, which effectively controls the total, rather than the free, activator concentration (Chattoraj *et al.*, 1988; Das *et al.*, 2005). In principle, a similar mechanism for bacterial chromosome copy number control is conceivable, but we propose instead that the ATP to ADP conversion on DnaA by RIDA is the key to chromosome copy number control in *E. coli*.

When the replication fork passes *datA* and other DnaA boxes along the chromosome, DNA-bound DnaA-ATP is converted to DnaA-ADP by the Hda protein in PolIII (Su’etsugu *et al.*, 2004) by RIDA, resulting in an increased concentration of free DnaA-ADP in the cell. To illustrate principles, we assume that *datA* dominates DnaA-ATP binding to the chromosome and note that the number of converted DnaA-ATPs in *datA* loci approximates the total number of DnaA-ATP molecules in the cell. Accordingly, the free concentration of DnaA-ADP in the cell will reflect the flow of DnaA-ATP to DnaA-ADP, proportional to the *total* DnaA-ATP concentration, and the dilution of DnaA-ADP by volume growth. This implies that if *dnaA* expression is regulated with DnaA-ADP, rather than DnaA-ATP, as the auto-repressor, the total concentration of DnaA-ATP in the cell can be regulated. Note the critical assumption that DnaA-ADP has a lower affinity to the *datA* locus than DnaA-ATP, to generate a free concentration of DnaA-ADP, which in the case of only one dominating DnaA binding site on the chromosome will approximately always be proportional to the *oriC* concentration. Deviations in the initiation mass is corrected by a slightly slower or higher expression level from the *dnaA* promoter, since the free DnaA-ADP concentration reflects the *oriC* concentration. If, by such a feed-back system, the free concentration DnaA-ADP is adjusted to the value K_R and the DNA-bound fraction of DnaA-ADP is neglected, initiation of chromosome replication will occur virtually as in the previous section with K_R replacing the total concentration of DnaA in the expressions for the volume V_0 of a newly born cell and for the initiation volume V_I . The important difference between the two cases is that the control of initiation of replication is expected to be much more robust against internal parameter changes and varying growth conditions when the total DnaA concentration is regulated than when it is determined by constitutive expression of *dnaA*. Note that even if DnaA-ATP is an intrinsically stronger repressor of *dnaA* than DnaA-ADP, its free concentration will be so small that its effect on *dnaA* expression can be neglected.

Apart from the *datA* locus, the modelled chromosome contains uniformly positioned groups of DnaA binding sites along the chromosome (Fig. 3). Each group contains one DnaA box, which can bind both forms of DnaA with equal affinity and two DnaA-ATP boxes, which only bind DnaA-ATP. When a segment becomes replicated, bound DnaA dissociates from the DNA and DnaA-ATP is simultaneously converted to DnaA-ADP through RIDA. While newly replicated DnaA boxes are quickly rebound by DnaA-ADP, the DnaA-ATP boxes are filled with the rate of DnaA-ATP synthesis, implying that a large fraction of the DnaA-ADP in the cell will be free while the free concentration of DnaA-ATP is practically zero until all DnaA-

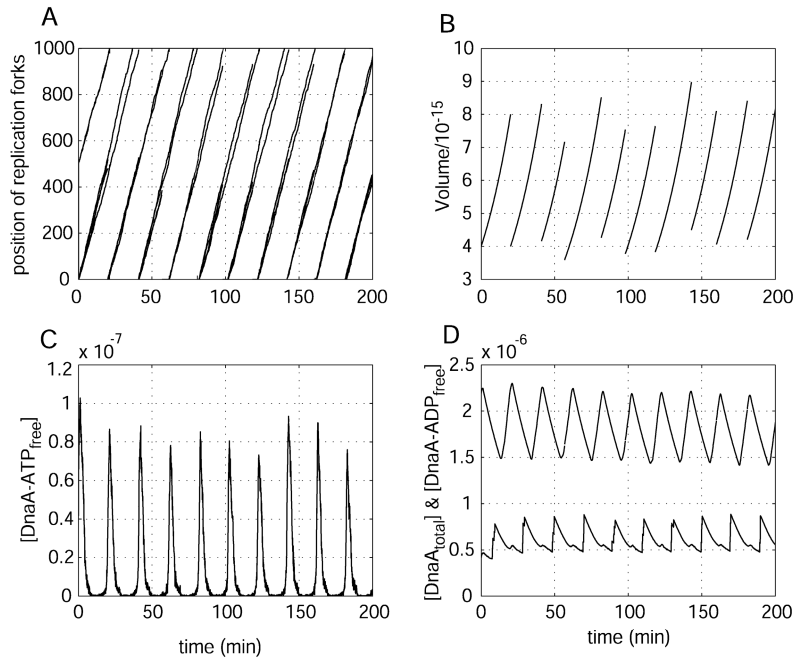


Figure 6. Regulation of *dnaA* expression by DnaA-ADP. (A) Position of replication forks. The generation time is 20 minutes and the cell is born with two complete chromosome copies. On each copy one round of replication is halfway through (position 500) and another round is about to start. (B) Normalised cell volume. (C) The free concentration of DnaA-ATP. (D) The total concentration of DnaA and the free concentration of DnaA-ADP. The total concentration of DnaA is reduced during the sequestration period of the *dnaA* promoter. The free concentration of DnaA-ADP peaks when the forks replicate the *datA* locus and bound DnaA-ATP is converted to DnaA-ADP through RIDA (scenario I, see text).

ATP boxes are saturated. With only the uniformly located groups of DnaA binding sites (and no *datA* locus), replication will generate a free concentration of DnaA-ADP in the cell, which reflects the flow of DnaA-ATP to DnaA-ADP proportional to the synthesis of DNA and the dilution of DnaA-ADP by cell growth.

Fig. 6 depicts a cell growing with a generation time of 20 minutes. Initiation is triggered from 4 origins synchronously (A) as a result of the free DnaA-ATP concentration rising from virtually zero to a high initiation potential every 20 minutes (C). The free concentration of DnaA-ADP, which regulates *dnaA* expression, varies much less during the division cycle and peaks (D) when the *datA* locus at position 200 (A) is replicated. The total concentration of DnaA changes during the division cycle as a result of the period of *dnaA* promoter sequestration following initiation (D). The cell volume varies slightly between generations. An early initiation results in a somewhat smaller cell at division, which is corrected back by the copy number control mechanism the next generation and vice versa (B). The sharp peak in the free concentration of DnaA-ATP occurs when the number of DnaA-ATP boxes outside *oriC* are saturated. The *datA* locus can be removed without completely disrupting the regulation of replication. As for constitutive expression of DnaA, the cell size decreases and initiation synchrony is partially lost. Distinct from constitutive

expression of DnaA the free concentration of DnaA-ADP stays approximately the same after *data* deletion while the total DnaA concentration increases.

Sequestration and methylation of *oriC*

So far we have used an *ad hoc* description of the sequestration period (S_I) after replication of *oriC*, during which *oriC* in its hemi-methylated form cannot be replicated and *dnaA* cannot be expressed. Without DnaA boxes close to *oriC* and *dnaA* promoter sequestration, the hemi-methylated state of *oriC* must prevail longer than the time of about 8 minutes for the replication fork to reach and duplicate *data*, so that when sequestration ends, the concentration of free DnaA-ATP is low enough to prevent pre-mature re-initiation of *oriC*. At the same time, *oriC* must be fully methylated and ready for a new round of replication in a window significantly shorter than a generation time. For cells with a generation time of 20 minutes the methylation time window is then only 12 minutes, but with *dnaA* promoter sequestration and DnaA boxes close to *oriC*, besides *data*, the initiation potential is reduced earlier, increasing the methylation time window to about maximally 20 minutes. Experiments (Campbell and Kleckner, 1990) have shown that the average re-methylation time for two of the GATC sites in *oriC* is about 13 minutes in a synchronised cell culture, almost exactly as required to maximally separate the initiation event from the re-methylation event of *oriC* in time. The SeqA protein has high affinity to the 11 hemi-methylated GATC sites in *oriC* and strongly inhibits their methylation by Dam (Slater *et al.*, 1995). Although the molecular basis for the sequestration period of *oriC* has remained obscure, we will here model two tentative molecular mechanisms, each of which could lead to a sequestration time sufficiently well-defined to result in one and only one initiation of *oriC* per generation time. The first molecular mechanism (S_{II}) is based on the testable hypothesis that the 11 hemi-methylated GATC sites in *oriC* are Dam-methylated step-wise in a specific or random order. The second mechanism is based on the hypothesis that there exists a “*seq*” locus for SeqA binding downstream from but near *data*, leading to sequestration of SeqA and rapid GATC methylation when the free DnaA-ATP concentration is small. A third possibility is that the activity of Dam itself increases with time after replication of *oriC*, *e.g.* due to a gene dosage effect. Although this third option, which requires rapid turnover of Dam or another unknown regulation of Dam-activity, will not be modelled here, it may be kept in mind and explored at a time when other hypotheses have failed.

The time at which all 11 GATC sites have been sequentially methylated in a unique order is gamma distributed whereas the time has the distribution of the largest value of 11 independent, exponentially distributed methylation events when methylation occurs in a random sequence (Appendix). Our modelling shows that methylation of the 11 GATC sites both in a specific and a random order in conjunction either with a constant or a DnaA-ADP regulated total concentration of DnaA lead to wild-type regulation of chromosome replication for all generation times between 60 and 20 minutes. However, to generate wild-type regulation for cells with a generation time of 20 minutes the probability of an unbound GATC site (p_{free}) had to be large (0.9) and thereby insensitive to changes in the concentration of free SeqA (Appendix). Changes of the free concentration of SeqA created by the stochastic variation in initiation mass threatens to counteract proper regulation of replication initiation by slowing down *oriC* methylation when initiation takes place at a time later than average (increased free concentration of SeqA) instead of speeding up methylation for a slightly earlier initiation the next generation and vice versa. Fig. 7

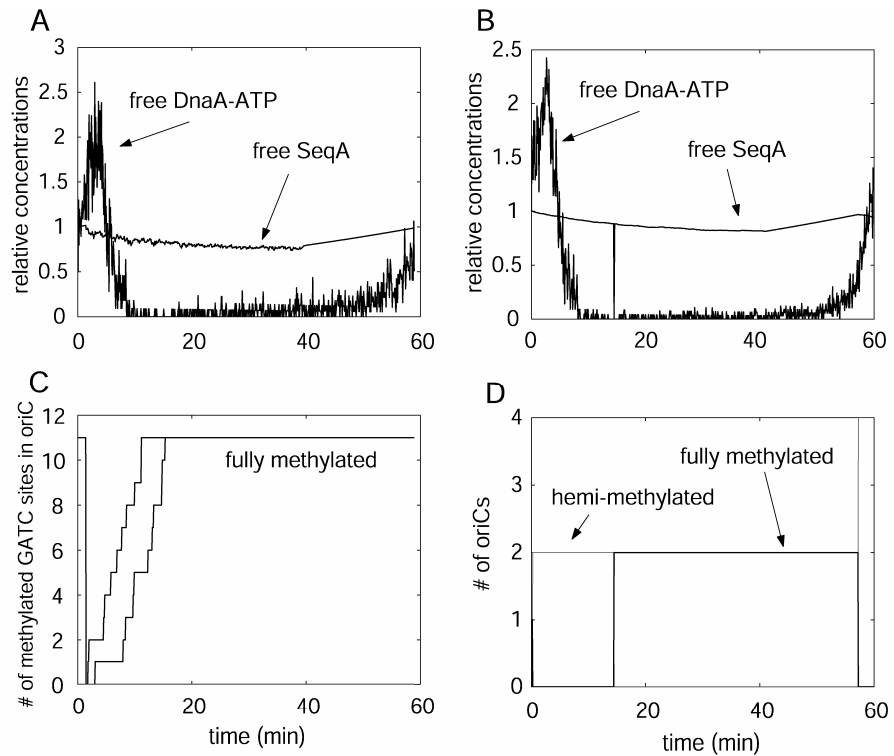


Figure 7. Putative mechanisms of *oriC* methylation. (A) and (C) Methylation occurs by a step-wise methylation in an specific or random sequence (scenario II, see text) After the free concentration of DnaA-ATP is diminished following initiation (A), methylation of the *oriC* GATC sites is completed (C). (B) and (D) Methylation occurs when a hypothetical *seq* locus, downstream of *data*, becomes hemi-methylated by passage of the replication fork (scenario III, see text). When hemi-methylated the *seq* locus binds a high number of SeqA molecules, lowering the free concentration of SeqA (B) and triggering re-methylation of *oriC* (D).

(A) and (C) illustrates the principle of a step-wise methylation of the *oriC* GATC sites.

As the replication forks proceed from *oriC* to *ter*, hemi-methylated GATC sites are created along the chromosome, and these may in principle serve to reduce the concentration of free SeqA and thus stimulate re-methylation of *oriC* with a suitable time-delay after initiation of replication. In spite of an extensive modeling search we have failed to identify conditions under which this type of mechanism with scattered SeqA sites around the chromosome can lead to synchronous initiation at multiple *oriCs* for all growth rates. To illustrate principles, we have therefore introduced a putative SeqA sequestration locus (*seq*) at 14 minutes from *oriC* (S_{III}, Fig. 3 and Fig. 7 (B) and (D)). When the replication fork reaches *seq*, the concentration of free SeqA decreases sharply, which by hypothesis activates rapid re-methylation of *oriC*. Also this mechanism (S_{III}), which requires a constant total concentration of SeqA in the cell, leads to synchronous initiation of replication at all growth rates, as for the above described S_I.

DISCUSSION

We have developed a stochastic model with all known major features of the regulation of initiation of chromosome replication in *E.coli*. The model automatically generates the correct initiation frequency and chromosome number, synchronous initiation of multiple origins and changing cell size when the cell growth rate is changed (Fig. 4 and 6).

Factors determining the initiation mass

Donachie (1968) combined the findings of a constant C- and D-period for cells with generation times between 60 and 20 minutes (Cooper and Helmstetter, 1968) with cell mass measurements of *Salmonella typhimurium* grown in different media (Schaechter *et al.*, 1958) to introduce the concept of a constant initiation mass, defined as cell mass/#chromosome origins, at the onset one round of replication. Later measurements of the initiation mass in different strains of *E.coli* indicate that the initiation mass may be constant (K-12) or increasing with increasing growth rate (B/r) (Churchward *et al.*, 1981; Wold *et al.*, 1994; Herrick *et al.*, 1996). Therefore, whether the initiation mass is constant or not is probably not crucial for a proper initiation control. Instead one should focus on what the factors are that determine the initiation mass (Herrick *et al.*, 1996). Our modelling presented here shows what is required for the initiation mass to stay constant under varying growth conditions, given a constitutive expression of the *dnaA* promoter. The fraction of total protein synthesis devoted to DnaA must always be constant (which leads to a constant total concentration of DnaA), all DnaA binding sites must be located close to *oriC* and the sequestration period of the *dnaA* promoter must be a constant fraction of the generation time as the growth rate μ changes. Boxes located further away from *oriC* than half the way to the *ter* region will lead to a decreased initiation mass when the growth rate increases beyond 40 minutes while a sequestration period of the *dnaA* promoter a fixed number of minutes generates an increased initiation mass with increasing growth rate. The net outcome on the initiation mass of many boxes located far away from *oriC* and of sequestration of *dnaA* expression a constant time is therefore not obvious.

Regulation of *dnaA* expression

Although, a modelled constitutive expression of the *dnaA* promoter proportional to the growth rate can sustain a proper regulation of initiation it may be difficult to achieve *in vivo*. Adequate regulation of *dnaA* expression on the other hand is expected to generate a much more robust control of initiation. The *dnaA* promoter contains both DnaA boxes and DnaA-ATP boxes and *dnaA* expression is repressed by both DnaA-ADP and DnaA-ATP *in vitro* (Speck *et al.*, 1999). A number of experimental observations also suggest that the *dnaA* promoter become derepressed when additional DnaA binding sites located on plasmids are introduced in a cell (Hansen *et al.*, 1987; Christensen *et al.*, 1999; Morigen *et al.*, 2001; Morigen *et al.*, 2003). As emphasised, there are principal problems facing DnaA-ATP of both being the key-regulator of replication initiation and repressor of its own synthesis. Sequestration of synthesised DnaA-ATP to binding sites along the chromosome generates an inadequate *dnaA* expression denoted the auto-regulation-sequestration paradox, and *dnaA* repression by free DnaA-ATP is inconsistent with a rapid boost of the free DnaA-ATP concentration to generate a high initiation potential at the time of initiation.

Our solution to the problem is that the two forms of DnaA perform each of the two tasks. DnaA-ATP triggers strand opening while DnaA-ADP regulates *dnaA*

expression. Two key factors are required for generating a free DnaA-ADP concentration, which adequately regulates *dnaA* expression. One is RIDA, which couples replication to *dnaA* expression. Therefore we propose that RIDA is a central process for producing DnaA-ADP and an adequate auto-regulation of *dnaA* expression rather than for preventing immediate re-initiations by lowering the concentration of DnaA-ATP. Two, binding of DnaA-ADP to binding sites along the chromosome must be such that the free concentration of DnaA-ADP still reflects the DNA concentration in the cell. Specifically, it requires that DnaA-ADP possess a much lower binding affinity to *data* than DnaA-ATP. In the most pure form of this principle, the chromosome only contains one DnaA binding locus outside *oriC*, which is located close to the origin. Passage of the replication fork converts all bound DnaA-ATP to the binding locus to DnaA-ADP, which cannot rebind. This way the free concentration of DnaA-ADP will always be proportional to the *oriC* concentration. Thus, when the *oriC* concentration becomes lower than normal the *dnaA* expression will increase and DnaA-ATP synthesis boosts and vice versa, correcting the initiation mass back to its ideal value. Gram-positives, e.g. *Bacillus subtilis*, may be a better representative for this proposed principle of how to adequately auto-regulate an initiator. *Bacillus subtilis* contain a binding locus with many more binding sites than *data*, next to its origin, suggesting the capacity of sequestering a high number of DnaA molecules (Boye *et al.*, 2000; Messer, 2002). To demonstrate that control of initiation can be maintained even when *data* is deleted for the suggested regulation of *dnaA* expression, we also included groups consisting of one DnaA box and two DnaA-ATP boxes equally scattered along the chromosome. As in the case of a constitutive expression of *dnaA*, the cell size decreased and initiation synchrony was partially lost (Fig. 5) in line with experimental findings (Morigen *et al.*, 2005).

Sequestration of *oriC* and the *dnaA* promoter

The molecular details behind the initiation and termination of the prolonged sequestration period of *oriC* and the *dnaA* promoter following initiation of replication is yet to be discovered. Sequestration is terminated by a process either acting *in trans* or *in cis*. We have modelled two tentative molecular mechanisms of methylation of *oriC*. One, sequential methylation of the eleven GATC sites in *oriC* ending sequestration *in cis* or two, methylation takes place when a hypothetical *seq* locus positioned downstream of *data* is replicated, lowering the free concentration of the SeqA protein and ending *oriC* sequestration *in trans*. Both processes are plausible as suggested by modelling. However, one may argue that both the processive activity of Dam, where 55 GATC sites on λ -DNA have been estimated to become methylated at each binding event of the enzyme (Urig *et al.*, 2002) and the co-operative binding of SeqA protein (Skarstad *et al.*, 2000; Han *et al.*, 2004) suggest that all GATC sites are quickly methylated after SeqA has quickly left *oriC* as in the case of a *seq* locus abruptly lowering the free concentration of SeqA. Whether methylation occurs in a sequence or not can be found out experimentally (see below). Of principle interest is also the length of the sequestration period, whether it is a constant fraction of the generation time or a constant time independent of the growth rate. It is often stated that the sequestration period is one third of a generation time referring to calculations based on average values of two hemi-methylated GATC sites in *oriC* for asynchronous cell cultures growing in two different growth media (Campbell and Kleckner, 1990). We argue, that it is far from validated that *oriC* sequestration makes up a constant fraction of the generation time. The sequestration period is not exactly one third of the generation time in any of the two cases and while the sequestration

period of the two GATC sites in *oriC* and the GATC site in the *dnaA* promoter studied coincide in a synchronised culture, the period is very different as calculated from the asynchronous cultures.

Previous models

The most well-known, previous stochastic model is the initiator titration model presented by Hansen *et al.* in 1991. The model is based on four main assumptions; (i) the initiator (DnaA) has a higher affinity for binding sites outside *oriC* than (ii) for binding sites located within *oriC*, (iii) each *oriC* is refractory to further initiation for some time period following initiation and (iv) bound DnaA protein is released from *oriC* after initiation, keeping its activity and promoting initiation by binding at not yet initiated *oriCs*. With DnaA boxes clustered around *oriC* the model generates synchronous initiation while evenly distributed boxes gives asynchronous initiation. However, by including the methylation of ten GATC sites, the model generates synchronous initiations even for uniformly distributed DnaA boxes along the chromosome. Our model share the first three assumptions of the initiator titration model, while we question the fourth since RIDA is expected to inactivate DnaA-ATP to DnaA-ADP upon initiation, which was not known at the time Hansen *et al.* published their model. However, further comparisons are difficult to make since the initiator titration model never was published along with the mathematics it is based on. Hansen *et al.* did not clarify the connection between the location of DnaA boxes on the chromosome or how the length of the sequestration period of the *dnaA* promoter affect the initiation mass. Neither did they clarify the fundamental problems behind an initiator with auto-regulated synthesis merely note that auto-repression of the *dnaA* promoter confer a problem.

Bremer and Churchward (1991) are in doubt about DnaA as the protein regulating replication initiation while Donachie and Blakely (2003) question the DnaA concentration as controlling initiation. The most serious objections against DnaA models according to Bremer and Churchward are the observations that initiation continuous synchronously in excess DnaA and that oversupply of DnaA only stimulates a single round of replication. However, although it was known that initiation required methylation of *oriC* GATC sites at that time the SeqA protein was not yet discovered. As long as SeqA sequestering of *oriC* after each initiation stays unaffected, we do not see why prevention of immediate re-initiations and initiation synchrony should not prevail. Also, the observation regarding initiation synchrony in DnaA over-expressing strains, diverge in the literature (Løbner-Olesen *et al.*, 1989; Skarstad *et al.*, 1989; Atlung and Hansen, 1993). The arguments against the accumulation of an initiation potential, through an elevating concentration of free DnaA-ATP, triggering initiation are that initiation requires *de novo* synthesis or cell growth, that a five-fold increase of the total DnaA concentration shows minor effects on the time of initiation and that extra *oriC* copies on plasmids, mini-chromosomes, exhibit synchronous initiations with the chromosome at a normal cell size (Donachie and Blakely, 2003). We believe that all these experimental observations can be explained within the idea of a high enough free DnaA-ATP concentration triggering initiation. *De novo* protein synthesis is required to saturate DnaA binding to DnaA boxes along the chromosome, *e.g.* the *datA* locus, which become duplicated following the movement of the replication fork. It is also required for building up a high concentration of DnaA-ATP, since DNA-bound DnaA-ATP is converted to DnaA-ADP by RIDA during replication. The second argument originates from a paper by Atlung *et al.* (1987). However, what Atlung *et al.* report are an increased copy

number of mini-chromosomes as well as an increase in chromosomal gene dosage of *oriC* proximal DNA. Both these observations are in line with an initiation frequency stimulated by an elevated concentration of DnaA. The increased gene dosage around *oriC*, observed in other reports as well (Skarstad *et al.*, 1989; Atlung and Hansen, 1993), rather indicate a slowed down movement or premature abortion of replication forks following over-initiations. The third argument about the minor effect of mini-chromosomes is probably explained by the low number of DnaA molecules over the total number of DnaA molecules synthesised each cell cycle, which is required to bind to *oriC*, in order to promote strand opening. There is definitely a correlation between the number of extra binding sites and the number of DnaA molecules that bind to each site a cell can handle. Many more *oriC* sites can be introduced than *datA* loci (Kitagawa *et al.*, 1996; Messer, 2002). The *datA* locus binds approximately ten times more DnaA than *oriC* (Løbner-Olesen, 1999; Morigen *et al.*, 2003).

As an alternative to free DnaA-ATP concentration controlled initiation Donachie and Blakely suggest control through the DnaA-ATP/DnaA-ADP ratio in cell. They describe in broad outline how this ratio may vary during each cell cycle through RIDA and *de novo* synthesis of DnaA in the ATP form, but they lack a detailed description for how a certain ratio can trigger initiation. Many different concentrations of DnaA-ATP and DnaA-ADP give the same DnaA-ATP/DnaA-ADP ratio. Although, the DnaA-ATP over total DnaA does indeed vary during the cell cycle in the model (not shown), which is supported by experimental observations (Kurokawa *et al.*, 1999; Katayama *et al.*, 2001) the ratio *per se* does not decide when initiation occurs in the model but a high enough free concentration of DnaA-ATP.

We would also like to pinpoint that the principle for how an initiator (DnaA) at the same time can auto-regulate its own synthesis presented here is distinct from the Sompayrac-Maaløe auto-repressor model (Sompayrac and Maaløe, 1973). The auto-repressor model couples the initiator gene with a gene encoding an auto-repressor regulating the expression of the operon, which corresponds to regulation of the *dnaA* promoters by the total DnaA concentration. What we suggest is that the auto-repressor (DnaA-ADP) is produced during another process, replication, in a way that allows the free concentration of auto-repressor to adequately regulate and correct deviations of the synthesis of the initiator (DnaA-ATP).

Future testing of the model

The stochastic model presented here meets the basic demands of any model claiming to describe the regulation of replication initiation in *E.coli*. In addition, we suggest an elegant solution to a difficult problem; how an initiator of replication can at the same time regulate its own synthesis, which positions RIDA as central for replication control rather than merely contributing to prevent immediate re-initiations. We have performed one first critical test of the model, deletion of the *datA* locus, with constitutive or DnaA-ADP regulated *dnaA* expression and compared the model predictions with experimental observations. Experimental manipulations performed on the molecular set-up involved in initiation control are vast and further testing of the model wait. We believe there are three key tests of the model; the observed compatibility of mini-chromosomes where as many as 30 mini-chromosomes per *oriC* can co-exist with the chromosome without drastically changing cell size or the initiation mass (Løbner-Olesen, 1999), the introduction of extra *datA* locus on plasmids which delays initiation and increases cell size (Morigen *et al.*, 2003) and finally observed responses to a lower than wild-type concentration of DnaA (increased initiation mass and increased initiation asynchrony) or higher than wild-

type concentration of DnaA (decreased initiation mass and potential increased initiation asynchrony) (Løbner-Olesen *et al.*, 1989; Skarstad *et al.*, 1989; Atlung and Hansen, 1993). We believe all these observations can be explained within the present model especially if *dnaA* expression is regulated. The increased initiation mass at a DnaA concentration below wild-type is expected to result from a longer time to fill the DnaA binding sites on the chromosome and asynchrony arise because a slowly, less distinct rise in the free concentration of DnaA-ATP. We expect a higher than wild-type concentration of total DnaA to fill *data* and other binding sites more quickly, decreasing the initiation mass. Asynchrony may arise if the sequestration period of *oriC* is affected but initiation is otherwise expected to remain synchronous. Extra *data* loci is expected to increase cell size because of a higher number DnaA binding sites to fill, and delays initiation until all *data* loci are saturated with DnaA. Mini-chromosomes may co-exist with the chromosome in a high number and only increase cell size slightly if the extra *oriC* copies do not increase the free concentration of DnaA-ADP in the cell leaving the *dnaA* promoter slightly depressed. The only experimental observation, which it is difficult to predict the model response to, is the increased total DnaA concentration after introduction of additional *data* copies on plasmids (Morigen *et al.*, 2003).

Chain elongation of DNA requires a sufficient supply of deoxyribonucleotides (dNTPs), which are produced by ribonucleotide reductase (RNR). The *nrd* operon encodes the two RNR subunits and the promoter contains both DnaA boxes and DnaA-ATP boxes just as the *dnaA* promoter. Recently Gon *et al.* (2006) presented evidence that the replication dependent conversion of DnaA-ATP to DnaA-ADP (RIDA) is critical for coordinating DNA replication with dNTPs synthesis. This feedback probably explains the reported decrease of elongation fork movement in the presence of excess DnaA and the increased fork elongation rate in the presence of extra *data* locus on plasmids (Atlung *et al.*, 1987; Morigen *et al.*, 2003; Skarstad *et al.*, 1989). An important development of our present model would be to incorporate the connection between dNTPs supply by DnaA regulated synthesis of RNR and replication fork movement, which regulates the rate of DnaA-ATP conversion.

Future experiments

The time and fraction of cells hemi-methylated at individual GATC sites can be studied in experiments with synchronised cell cultures (Campbell and Kleckner, 1990). The anticipated pattern of hemi-methylation for individual GATC sites in *oriC* following initiation of replication is then different for the different proposed principles of *oriC* methylation. The longer a particular GATC site stays hemi-methylated, the higher is the fraction of cells in a hemi-methylated state and the longer is the average time of hemi-methylation. Thus, if methylation occurs in a specific order, the fraction of cells and the time of hemi-methylation increase with the position of the site in the methylation order. The first sites stay hemi-methylated a short time and the fraction of hemi-methylated cells at these sites is low, while the last sites in the methylation order are hemi-methylated a long time and the fraction of cells hemi-methylated at these sites may be close to one. If methylation occurs in a random order the pattern of hemi-methylation is the same for all sites. If re-methylation starts directly after initiation the fraction of cells hemi-methylated at any site will be far below one. If re-methylation is delayed the same time for all sites and then quickly methylated (as in the case of a *seq* locus) the re-methylation pattern is also the same for all GATC sites but the fraction hemi-methylated cells is expected to reach close to one before methylation occurs. To settle the question of whether re-methylation of

oriC GATC sites is sequential or occurs simultaneously at a certain time point following initiation, a systematic study of the re-methylation rate of a majority of the eleven GATC sites in *oriC* is in progress (S. Dasgupta, in preparation).

Whether the *dnaA* promoters during exponential growth are constitutively expressed or regulated is another major question to answer, although a feasible experiment which can settle the question if DnaA-ADP regulates *dnaA* expression seems hard to find. Both DnaA-ADP and DnaA-ATP can repress *dnaA* expression (Speck *et al.*, 1999). If the *dnaA* promoters are constitutively expressed it suggests that the free concentration of both forms of DnaA is far below their regulatory concentration in the cell. One way to discriminate between constitutive and regulated *dnaA* expression may be through a moderate manipulation of the number of *datA* locus, by introducing another *datA* site close to the already existing one on the chromosome. If *dnaA* expression is constitutive the total concentration of DnaA is predicted to be approximately constant while in the case *dnaA* expression is regulated by the free concentration of DnaA-ADP, the total concentration of DnaA is predicted to decrease while the free concentration of DnaA-ADP stays approximately the same (not shown).

REFERENCES

- Aranovich A., G. Y. Gdalevsky, R. Cohen-Luria, I. Fishov and A. H. Parola. 2006. Membrane-catalyzed nucleotide exchange on DnaA: Effect of surface molecular crowding. *J. Biol. Chem.* 281:12526-12534.
- Atlung T., E. S. Clausen and F. G. Hansen. 1985. Autoregulation of the *dnaA* gene of *Escherichia coli* K12. *Mol. Gen. Genet.* 200:442-450.
- Atlung T., A. Løbner-Olesen and F. G. Hansen. 1987. Overproduction of DnaA protein stimulates initiation of chromosome and minichromosome replication in *Escherichia coli*. *Mol. Gen. Genet.* 206:51-59.
- Atlung T. and F. G. Hansen. 1993. Three distinct chromosome replication states are induced by increasing concentrations of DnaA protein in *Escherichia coli*. *J. Bacteriol.* 175:6537-6545.
- Bochner B. R. and B. N. Ames. 1982. Complete analysis of cellular nucleotides by two-dimensional thin layer chromatography. *J Biol. Chem.* 257:9759-9769.
- Boye E., A. Løbner-Olesen and K. Skarstad. 2000. Limiting DNA replication to once and only once. *EMBO Reports.* 1:479-483.
- Bremer H. and G. Churchward. 1991. Control of cyclic chromosome replication in *Escherichia coli*. *Microbiol. Rev.* 55:459-475.
- Bremer H., P. Dennis and M. Ehrenberg. 2003. Free RNA polymerase and modeling global transcription in *Escherichia coli*. *Biochimie.* 85:597-609.

- Campbell J. L. and N. Kleckner. 1990. *E. coli oriC* and the *dnaA* gene promoter are sequestered from *dam* methyltransferase following the passage of the chromosomal replication fork. *Cell*. 62:967-979.
- Chattoraj D. K., R. J. Mason and S. H. Wickner. 1988. Mini-P1 plasmid regulation: the autoregulation-sequestration paradox. *Cell*. 52:551-557.
- Chiaranello A. E. and J. W. Zyskind. 1990. Coupling of DNA replication to growth rate in *Escherichia coli*: a possible role for guanosine tetraphosphate. *J. Bacteriol.* 172:2013-2019.
- Christensen B. B., T. Atlung and F. G. Hansen. 1999. DnaA boxes are important elements in setting the initiation mass of *Escherichia coli*. *J. Bacteriol.* 181:2683-2688.
- Churchward G., E. Estiva and H. Bremer. 1981. Growth rate-dependent control of chromosome replication initiation in *Escherichia coli*. *J. Bacteriol.* 145:1232-1238.
- Cooper S. and C. E. Helmstetter. 1968. Chromosome replication and the division cycle of *Escherichia coli* B/r. *J. Mol. Biol.* 31:519-540.
- Das N., M. Valjavec-Gratian, A. N. Basuray, R. A. Fekete, P. P. Papp, J. Paulsson, and D. K. Chattoraj. 2005. Multiple homeostatic mechanisms in the control of P1 plasmid replication. *Proc. Natl. Acad. Sci. USA*. 102: 2856-2861.
- Dennis P. P., M. Ehrenberg and H. Bremer. 2004. Control of rRNA synthesis in *Escherichia coli*: a systems biology approach. *Microbiol. Mol. Biol. Rev.* 68:639-668.
- Donachie W.D. 1968. Relationship between cell size and time of initiation of DNA replication. *Nature*. 219:1077-1079.
- Donachie W. D. and A. C. Robinson. 1987. Cell division: parameter values and the process. In *Escherichia coli* and *Salmonella* Cellular and Molecular Biology (Neidhardt, F. C., ed.), pp. 1578-1592, American Society for Microbiology, Washington, D.C.
- Donachie W. D. and G. W. Blakely. 2003. Coupling the initiation of chromosome replication to cell size in *Escherichia coli*. *Curr Opin Microbiol.* 6:146:150.
- Gillespie D.T. 1976. A general method for numerically simulating the stochastic time evolution of coupled chemical reactions. *J. Comput. Phys.* 22:403-434.
- Gon S., J. E. Camara, H. K. Klungsøyr, E. Crooke, K. Skarstad and J. Beckwith. 2006. A novel regulatory mechanism couples deoxyribonucleotide synthesis and DNA replication in *Escherichia coli*. *EMBO J.* 25:1137-1147.
- Han J. S., S. Kang, H. Lee, H.K. Kim and D. S. Hwang. 2003. Sequential binding of SeqA to paired hemi-methylated GATC sequences mediates formation of higher order complexes. *J. Biol. Chem.* 278:34983-34989.

- Han J. S., S. Kang, S. H. Kim, M. J. Ko and D. S. Hwang. 2004. Binding of SeqA protein to hemi-methylated GATC sequences enhances their interaction and aggregation properties. *J. Biol. Chem.* 279:30236-30243.
- Hansen F- G., E. B. Hansen and T. Atlung. 1982. The nucleotide sequence of the *dnaA* gene promoter and of adjacent *rpmH* gene, coding for the ribosomal protein L34, of *Escherichia coli*. *EMBO J.* 1:1043-1048.
- Hansen F. G., S. Koefoed, L. Sørensen and T. Atlung. 1987. Titration of DnaA protein by *oriC* DnaA-boxes increases *dnaA* gene expression in *Escherichia coli*. *EMBO J.* 6:255-258.
- Hansen F. G., B. B. Christensen and T. Atlung. 1991. The initiator titration model: computer simulation of chromosome and minichromosome control. *Res. Microbiol.* 142:161-167.
- Herrick J., M. Kohiyama, T. Atlung and F. G. Hansen. 1996. The initiation mess. *Mol. Microbiol.* 19:659-666.
- Hill T. M. 1996. Features of the chromosomal terminus region. In *Escherichia coli* and *Salmonella* Cellular and Molecular Biology (Neidhardt, F. C., ed.), pp. 1602-1614, ASM Press, Washington, D.C.
- Katayama T., T. Kubota, K. Kurokawa, E. Crooke and K. Sekimizu. 1998. The initiator function of DnaA protein is negatively regulated by the sliding clamp of the *E. coli* chromosomal replicase. *Cell.* 94:61-71.
- Katayama T. and K. Sekimizu. 1999. Inactivation of *Escherichia coli* DnaA protein by DNA polymerase III and negative regulations for initiation of chromosomal replication. *Biochimie.* 81:835-840.
- Katayama T., K. Fujimitsu and T. Ogawa. 2001. Multiple pathways regulating DnaA function in *Escherichia coli*: distinct roles for DnaA titration by the *datA* locus and the regulatory inactivation of DnaA. *Biochimie.* 83:13-17.
- Kitagawa R., H. Mitsuki, T. Okazaki and T. Ogawa. 1996. A novel DnaA protein-binding site at 94.7 min on the *Escherichia coli* chromosome. *Mol. Microbiol.* 19:1137-1147.
- Kitagawa R., T. Ozaki, S. Moriya and T. Ogawa. 1998. Negative control of replication initiation by a novel chromosome locus exhibiting exceptional affinity for *Escherichia coli* DnaA protein. *Gen. & develop.* 12:3032-3043.
- Kurokawa K., S. Nishida, A. Emoto, K. Sekimizu and T. Katayama. 1999. Replication cycle-coordinated change of the adenine nucleotide-bound forms of DnaA protein in *Escherichia coli*. *EMBO J.* 18:6642-6652.
- Leonard A. C. and J. E. Grimwade. 2005. Building a bacterial orisome: emergence of new regulatory features for replication origin unwinding. *Mol. Microbiol.* 55:978-985.

- Løbner-Olesen A., K. Skarstad, F. G. Hansen, K. von Meyenburg and E. Boye. 1989. The DnaA protein determines the initiation mass of *Escherichia coli* K-12. *Cell*. 57:881-889.
- Løbner-Olesen A. 1999. Distribution of minichromosomes in individual *Escherichia coli* cells: implications for replication control. *EMBO J.* 18:1712-1721.
- Løbner-Olesen A., O. Skovgaard and M. G. Marinus. 2005. Dam methylation: coordinating cellular processes. *Curr Opin Microbiol.* 8:154:160.
- Lu M., J. L. Campbell, E., Boye and N. Kleckner. 1994. SeqA: A negative modulator of replication initiation in *E.coli*. *Cell*. 77:413-426.
- Marsh R. C. and A. Worcel. 1977. A DNA fragment containing the origin of replication of the *E.coli* chromosome. *Proc. Natl. Acad. Sci. USA*. 74:2720-2724.
- McGarry K. C., V. T. Ryan, J. E. Grimwade and A. C. Leonard. 2004. Two discriminatory binding sites in the *Escherichia coli* replication origin are required for DNA strand opening by initiator DnaA-ATP. *Proc. Natl. Acad. Sci. USA*. 101:2811-2816.
- Messer W. 2002. The bacterial replication initiator DnaA. DnaA and *oriC*, the bacterial mode to initiate DNA replication. *FEMS Microbiol. Rev.* 26:355-374.
- Morigen E. Boye, K. Skarstad and A. Løbner-Olesen. 2001. Regulation of chromosomal replication by DnaA protein availability in *Escherichia coli*: effects of the *datA* region. *Biochim. Biophys. Acta*. 1521:73-80.
- Morigen A. Løbner-Olesen and K. Skarstad. 2003. Titration of the *Escherichia coli* DnaA protein to excess *datA* sites causes destabilization of replication forks, delayed initiation and delayed cell division. *Mol. Microbiol.* 50:349-362.
- Morigen F. Molina and K. Skarstad. 2005. Deletion of the *datA* site does not affect once-per-cell-cycle timing but induces rifampin-resistant replication. *J. Bacteriol.* 187:3913-3920.
- Nordström K. and S. Dasgupta. 2006. Copy-number control of the *Escherichia coli* chromosome: a plasmidologist's view. *EMBO Reports*. 7:484-488.
- Ogawa T., Y. Yamada, T. Kuroda, T. Kishi and S. Moriya. 2002. The *datA* locus predominately contributes to the initiator titration mechanism in the control of replication initiation in *Escherichia coli*. *Mol. Microbiol.* 44:1367-1375.
- Roth A. and W. Messer. 1998. High-affinity binding sites for the initiator protein DnaA on the chromosome of *Escherichia coli*. *Mol. Microbiol.* 28:395-401.
- Russell D. W. and N. D. Zinder. 1987. Hemimethylation prevents DNA replication in *E. coli*. *Cell*. 50:1071-1079.

- Schaechter M., O. Maaløe and N. O. Kjeldgaard. 1958. Dependency on medium and temperature of cell size and chemical composition during balanced growth of *Salmonella typhimurium*. *J Gen. Microbiol.* 19:592-606.
- Sekimizu K. and A. Kornberg. 1988. Cardiolipin activation of *dnaA* protein, the initiation protein of replication in *Escherichia coli*. *J. Biol. Chem.* 263:7131-7135.
- Skarstad K., E. Boye and H. B. Steen. 1986. Timing of initiation of chromosome replication in individual *Escherichia coli* cells. *EMBO J.* 5:1711-1717.
- Skarstad K., A. Løbner-Olesen, T. Atlung, K. von Meyenburg and E. Boye. 1989. Initiation of DNA replication in *Escherichia coli* after overproduction of the DnaA protein. *Mol. Gen. Genet.* 218:50-56.
- Skarstad K., G. Lueder, R. Lurz, C. Speck and W. Messer. 2000. The *Escherichia coli* SeqA protein binds specifically and co-operatively to two sites in hemimethylated and fully methylated *oriC*. *Mol. Microbiol.* 36:1319-1326.
- Skarstad K., N. Torheim, S. Wold, R. Lurz, W. Messer, S. Fossum and T. Bach. 2001. The *Escherichia coli* SeqA protein binds specifically to two sites in fully and hemimethylated *oriC* and has the capacity to inhibit DNA replication and affect chromosome topology. *Biochimie.* 83:49-51.
- Slater S., S. Wold, M. Lu, E. Boye, K. Skarstad and N. Kleckner. 1995. *E. coli* SeqA protein binds *oriC* in two different methyl-modulated reactions appropriate to its roles on DNA replication initiation and origin sequestration. *Cell.* 82:927-936.
- Sompayrac L. and O. Maaløe. 1973. Autorepressor model for control of DNA replication. *Nature New Biol.* 241:133-135.
- Speck C., C. Weigel and W. Messer. 1999. ATP- and ADP-DnaA protein, a molecular switch in gene regulation. *EMBO J.* 18:6169-6176.
- Su'etsugu M., M. Takata, T. Kubota, Y. Matsuda and T. Katayama. 2004. Molecular mechanism of DNA replication coupled inactivation of the initiator protein in *Escherichia coli*: interaction of DnaA with the sliding clamp-loaded DNA and the sliding clamp-Hda complex. *Genes to Cells.* 9:509-522.
- Taghbalout A., A. Landoulsi, R. Kern, M. Yamazoe, S. Hiraga, B. Holland, M. Kohiyama and A. Malki. 2000. Competition between the replication initiator DnaA and the sequestration factor SeqA for binding to hemimethylated chromosomal origin of *E.coli in vitro*. *Genes to Cells.* 5:873-884.
- Theisen P. W., J. E. Grimwade, A. C. Leonard, J. A. Bogan and C. E. Helmstetter. 1993. Correlation of gene transcription with the time of initiation of chromosome replication in *Escherichia coli*. *Mol. Microbiol.* 10:575-584.
- Urig S., H. Gowher, A. Hermann, C. Beck, M. Fatemi, A. Humeny and A. Jeltsch. 2002. The *Escherichia coli* Dam DNA Methyltransferase Modifies DNA in a highly processive reaction. *J. Mol. Biol.* 319:1085-1096.

van Kampen N. G. 1997. Stochastic processes in physics and chemistry (second edition). Elsevier, Amsterdam.

von Freiesleben U., K. V. Rasmussen and M. Schaechter. 1994. SeqA limits DnaA activity in replication from *oriC* in *Escherichia coli*. *Mol. Microbiol.* 14:763-772.

Wold S., K. Skarstad, H. B. Steen, T. Stokke and E. Boye. 1994. The initiation mass for DNA replication in *Escherichia coli* K-12 is dependent on growth rate. *EMBO J.* 13:2097-2102

APPENDIX

Stochastic chromosome model

Discrete molecules at a low copy number motivate a stochastic description, which takes fluctuations of chemical reactions into account (van Kampen, 1997). We assume that a Markov process can describe the system and realisations are simulated using the Monte Carlo method presented by Gillespie (1976). The stochastic chromosome model describes the regulation of replication in a single cell, monitored during several cell generations of continuous growth and division. Initiation of replication at individual *oriCs* and the movement of individual replication forks along the chromosome are followed. The time, t_{event} , of the next reaction in the cell cycle is drawn from the exponential distribution $t_{event} \in [1/k_{event}]$, where k_{event} is the sum of all reaction rates. The probability for a certain reaction to occur during t_{event} is the fraction its reaction rate makes up of the sum of all reaction rates. In scenario I (S_I), 7 reactions can occur, ¹⁾ initiation of replication (r_1), ²⁾ replication of a chromosome segment (r_2), ³⁾ synthesis of DnaA-ATP (r_3), ⁴⁾ association of DnaA-ADP or DnaA-ATP to DnaA boxes (r_4), ⁵⁾ dissociation of DnaA-ADP or DnaA-ATP from DnaA boxes (r_5), ⁶⁾ association of DnaA-ATP to DnaA-ATP boxes (including the *data* locus) (r_6), ⁷⁾ dissociation of DnaA-ATP from DnaA-ATP boxes (including the *data* locus) (r_7). In scenario II-III (S_{II-III}) two more reactions can occur, methylation of *oriC* GATC sites step-wise or by one rate-limiting step (r_8) and methylation of unmethylated GATC sites in a segment outside *oriC* (r_9).

$$\begin{aligned}
 r_1 &= k_I \cdot (\# \text{ of methylated } oriCs), \\
 r_2 &= k_R \cdot (\# \text{ of replication forks}), \\
 r_3 &= k_s \cdot \mu \cdot N_A \cdot V_{cell} \cdot \frac{(\# \text{ of methylated dnaA promoters})}{(\# \text{ of total genes})}, \\
 r_4 &= k_{a1} \cdot [DnaA_{free}] \cdot (\# \text{ of free DnaA binding sites}), \\
 r_5 &= k_{d1} \cdot (\# \text{ of bound DnaA to DnaA binding sites}), \\
 r_6 &= k_{a2} \cdot [DnaA-ATP_{free}] \cdot (\# \text{ of free DnaA-ATP binding sites}), \\
 r_7 &= k_{d2} \cdot (\# \text{ of bound DnaA-ATP to DnaA-ATP binding sites}), \\
 r_8 &= k_{met} \cdot (\# \text{ of hemi-methylated } oriCs) \text{ (S}_{II}\text{, specific sequence)}, \\
 &\text{or} \\
 r_8 &= k_{met} \cdot (\# \text{ of hemi-methylated GATC } oriCs) \cdot (\# \text{ of unmethylated GATC sites}), \\
 &\text{(S}_{II}\text{, random sequence)} \\
 &\text{or} \\
 r_8 &= k_{m,oriC} \cdot (\# \text{ of hemi-methylated } oriCs) \text{ (S}_{III}\text{)}, \\
 r_9 &= k_{m,GATC} \cdot (\# \text{ of hemi-methylated segments}) \text{ (S}_{II-III}\text{)}.
 \end{aligned}$$

(A1)

Replication. The chromosome is divided into 1000 segments. The current position of a replication fork is kept track of by the segment number and each fork is moving at a

constant average rate, k_R . At replication one copy of a fully methylated segment becomes two hemi-methylated segments. Replication starts from *oriC* and a segment can only be replicated if the upstream segment next to it has already been replicated. Instead of two replication forks moving bi-directionally along the chromosome only one fork is taken into account. It takes 40 minutes to complete one round of replication and any ongoing replications on a fully replicated chromosome at cell division is carefully followed to the next generation. Approximately every 3rd segment of the chromosome contains one DnaA box and two DnaA-ATP boxes binding one DnaA molecule each, in all 307 groups of boxes starting from segment 76. The DnaA-ATP boxes are only accessible for DnaA-ATP binding if the adjacent DnaA box is bound, and dissociation of DnaA from the DnaA box results in simultaneous dissociation of bound DnaA-ATP molecules from the adjacent DnaA-ATP boxes. A *data* locus, titrating DnaA-ATP molecules, is located in segment 200 (8 minutes from *oriC*). When methylation of *oriC* follows a change in the free concentration of SeqA, the model also includes a hypothetical sequestration (*seq*) locus (a cluster of GATC sites in segment 350) downstream of *data* with the ability to bind a large number of SeqA molecules while hemi-methylated.

Initiation of replication. The rate of initiation of replication is a function of the free concentration of DnaA-ATP,

$$k_I = \frac{k_{I,\max}}{1 + \left(\frac{K_{D,\text{oriC}}}{[DnaA-ATP_{\text{free}}]} \right)^{n_D}}. \quad (\text{A2})$$

The number of free DnaA-ATP molecules is followed by DnaA-ATP synthesis and association to/dissociation from DnaA-ATP binding sites along the chromosome except at *oriC*, which we do not explicitly model. During the cell cycle the concentration of free DnaA-ATP varies and reaches a peak at the time of initiation. A high concentration corresponds to a high rate of initiation and vice versa, given that *oriC* is fully methylated. At *oriC*, DnaA-ATP molecules bind cooperatively but we disregard the different types of DnaA binding sites.

Regulation of dnaA transcription. The *dnaA* promoter is located in segment 25 (one minute from *oriC*). Only one promoter is assumed for simplicity, motivated by one dominating promoter and that both promoters show similar expression patterns (Hansen *et al.*, 1991; Speck *et al.*, 1999). The promoter is auto-repressed by both DnaA-ADP and DnaA-ATP, when modelled regulated. We assume that the promoter contains two DnaA boxes which both forms of DnaA binds with equal affinity and cooperatively and three DnaA-ATP boxes which cooperatively is bound by DnaA-ATP only. The number of free DnaA-ADP molecules, generated by conversion of bound DnaA-ATP molecules through RIDA and association to/dissociation from the DnaA binding sites is followed explicitly as well as the number of free DnaA-ATP molecules through synthesis and association to/dissociation from the DnaA-ATP binding sites. Only DnaA in ATP-form is synthesised with rate,

$$k_s = \frac{k_{s,\max}}{1 + \left(\frac{[DnaA - ADP_{free}] + [DnaA - ATP_{free}]}{K_{D1}} \right)^{n_A} + \left(\frac{[DnaA - ATP_{free}]}{K_{D2}} \right)^{n_{AT}} \cdot \left(\frac{[DnaA - ADP_{free}] + [DnaA - ATP_{free}]}{K_{D1}} \right)^{n_A}}.$$

(A3)

When *dnaA* expression was modelled constitutively, k_s is constant. Sequestration is induced by passage of the replication fork and ends simultaneously when the *in cis oriC* becomes methylated.

Methylation of GATC sites in a chromosomal segment and in oriC. When replication of a *seq* locus ends *oriC* sequestration (S_{III}), both rates of methylation are a function of the free concentration of SeqA,

$$k_{m,DNA} = \frac{k_{m,GATC\max}}{1 + \frac{[SeqA_{free}]}{K_{s,hm}}}, \quad (A4)$$

$$k_{m,oriC} = \frac{k_{m,oriC\max}}{1 + \left(\frac{[SeqA_{free}]}{K_{s,oriC}} \right)^{n_s}}.$$

Free SeqA is calculated in a similar way as free DnaA. SeqA can bind to two different binding sites, base pairs in general with dissociation constant $K_{s,bp}$ and hemi-methylated GATC sites with dissociation constant $K_{s,hm}$ in our hypothetical *seq* locus. Bound SeqA to other GATC sites than in the *seq* locus is disregarded. The concentration of free SeqA was calculated from the following system

$$\begin{aligned} [seqlocus_{free}] + [SeqA_{free}] &\xrightleftharpoons{K_{s,hm}} [C_1], \\ [bp_{free}] + [SeqA_{free}] &\xrightleftharpoons{K_{s,bp}} [C_2], \\ [seqlocus_{free}] + [C_1] &= N_{GATC} \cdot [seqlocus_{tot}], \\ [bp_{free}] + [C_2] &= N_{bp} \cdot [bp_{tot}], \\ [SeqA_{free}] + [C_1] + [C_2] &= [SeqA_{tot}]. \end{aligned} \quad (A5)$$

The free concentration of SeqA is high during the cell cycle, except a short period of time directly after replication of the *seq* locus when the GATC binding sites are hemi-methylated. A low concentration of free SeqA greatly increases the rate of methylation of hemi-methylated GATC sites, while a high concentration decreases the rate of methylation. When methylation of individual GATC sites in *oriC* was modelled (S_{II}), the chromosome contained 19000 (Urig *et al.*, 2002) evenly distributed GATC sites instead of the *seq* locus and the concentration of *seq* loci was replaced by the concentration of hemi-methylated chromosomal segments in eq. A5. The rate

constant of methylation, k_{met} , is described for the Markov processes in the section below.

Probability of completed *oriC* methylation within the methylation time window for a specific or random methylation order of individual GATC sites

Methylation of *oriC* can be treated as an independent stochastic process, detached from the rest of the initiation control by DnaA. The maximum probability that methylation of an individual *oriC* is completed within the methylation time window of each cell cycle can be calculated and compared for methylation of the eleven GATC sites in a specific or random sequence. Given that binding by SeqA to the GATC sites equilibrates much faster than the rate of methylation of a site by Dam, each site is unbound and free for methylation with probability $p_{free} = 1/(1 + [SeqA_{free}]/K_{Dmet})$ where K_{Dmet} is the dissociation constant of SeqA binding to a GATC site in *oriC*. If we further assume that the free concentration of SeqA and of Dam is approximately constant, then a GATC site becomes methylated with average rate or intensity $k_{met} = k \cdot [Dam_{total}] \cdot p_{free}$, where k is the maximum rate of methylation. The sequential methylation of eleven GATC sites in a specific order can then be described by a Markov process, formulated by the Master equations and initial conditions

$$\begin{aligned} \frac{dP(11,t)}{dt} &= -k_{met} \cdot P(11,t), \\ \frac{dP(i,t)}{dt} &= k_{met} \cdot P(i+1,t) - k_{met} \cdot P(i,t), \\ \frac{dP(0,t)}{dt} &= k_{met} \cdot P(1,t), \\ P(11,0) &= 1, P(i,0) = P(0,0) = 0, \end{aligned} \tag{A11}$$

where $i=10,9,\dots,1$. The time of completing methylation of *oriC* is gamma distributed, $\Gamma(11, 1/k_{met})$, and the probability density function is $f(t) = \frac{(k_{met} \cdot t)^{10}}{10!} \cdot k_{met} \cdot e^{-k_{met} \cdot t}$. The maximal probability mass that can be fitted within a methylation time window of 14 or 20 minutes is 0.87 and ~ 1 , respectively. Methylation of eleven GATC sites in a random sequence can similarly be described by

$$\begin{aligned} \frac{dP(11,t)}{dt} &= -11 \cdot k_{met} \cdot P(11,t), \\ \frac{dP(i,t)}{dt} &= (i+1) \cdot k_{met} \cdot P(i+1,t) - i \cdot k_{met} \cdot P(i,t), \\ \frac{dP(0,t)}{dt} &= k_{met} \cdot P(1,t), \\ P(11,0) &= 0, P(i,0) = P(0,0) = 0, \end{aligned} \tag{A12}$$

where $i=10,9,\dots,1$. The time of completing methylation of *oriC* has the distribution of the largest value of eleven independent, exponentially distributed stochastic variables each with distribution $\text{Exp}(1/k_{met})$. The probability density function is

$f(t) = 11 \cdot (1 - e^{-k_{met} \cdot t})^{10} \cdot k_{met} \cdot e^{-k_{met} \cdot t}$, and maximally 0.75 or ~ 1 of the probability mass can be placed within a methylation time window of 14 and 20 minutes, respectively.

Table A1. Parameters used in the chromosome model.

Parameter	Symbol	Value
# of chromosome segments	N	1000
# of base-pairs in the <i>E.coli</i> genome	N _{bp}	4*10 ⁶
Cooperativity factor of DnaA binding to <i>oriC</i>	n _D	4
Cooperativity factor of DnaA-ADP binding to the <i>dnaA</i> promoter	n _A	2
Cooperativity factor of DnaA-ATP binding to the <i>dnaA</i> promoter	n _{AT}	3
Cooperativity factor of SeqA binding to <i>oriC</i>	n _S	4
# of DnaA binding sites in <i>datA</i> locus	N _{datA}	370 ; 300 ^{I)}
# of SeqA binding sites in <i>seq</i> locus	N _{GATC}	5000 ^{II)}
Total concentration of SeqA	[SeqA _{tot}]	1.1 μM
Dissociation constant of DnaA to <i>oriC</i>	K _{D,oriC}	80 nM
Dissociation constant of DnaA-ADP binding to the <i>dnaA</i> promoter	K _{D1}	0.2 μM
Dissociation constant of DnaA-ATP binding to the <i>dnaA</i> promoter	K _{D2}	0.1 μM
Dissociation constant of SeqA binding to <i>oriC</i>	K _{S,oriC}	1.0 nM
Dissociation constant of SeqA binding to GATC sites	K _{S,hm}	3.0 nM
Dissociation constant of SeqA binding to base-pairs	K _{S,bp}	0.5 mM
Maximum initiation rate constant	k _{I,max}	1 s ⁻¹
Association rate constant of DnaA-ADP binding to DnaA boxes	k _{a1}	10 ⁸ (Ms) ⁻¹
Dissociation rate constant of DnaA-ADP dissociation from DnaA boxes	k _{d1}	0.03 s ⁻¹
Association rate constant of DnaA-ATP binding DnaA-ATP boxes	k _{a2}	10 ⁸ (Ms) ⁻¹
Dissociation rate constant of DnaA-ATP dissociation from DnaA-ATP boxes	k _{d2}	0.003 s ⁻¹
Maximum synthesis rate of DnaA-ATP	k _{s,max}	3.5·10 ⁻³ III); 3.5·10 ⁻² IV)
Maximum methylation rate constant of <i>oriC</i>	k _{m,oriC}	100 s ⁻¹ V)
Methylation rate constant of individual GATC sites in <i>oriC</i>	k _{met}	0.018 s ⁻¹ VI); 0.005 s ⁻¹ VII)
Dissociation constant of SeqA binding to <i>oriC</i> GATC sites	K _{DGATC}	3 nM; 40.5 μM (τ=20 min)
Maximum methylation rate constant of GATC sites outside <i>oriC</i>	k _{m,GATC}	1 s ⁻¹
Replication rate constant	k _R	1/(40*60/N) s ⁻¹
Generation time	τ	60-20 min
Growth rate constant	μ	ln2/τ*60 s ⁻¹
Cell volume at initiation when τ = 60 minutes	V _{cell}	10 ⁻¹⁵ l
Avogadro's constant	N _A	6·10 ²³

I) Simplified version of scenario I

II) When methylation of individual GATC sites in *oriC* was modeled, the *seq* locus was replaced by 19000 evenly distributed GATC sites along the chromosome

III) With constitutive expression of *dnaA*

IV) With regulated expression of *dnaA*

- V) With seq locus
- VI) Specific sequence
- VII) Random sequence



II



The Molecular Mechanism of Peptide-mediated Erythromycin Resistance*[§]

Received for publication, November 4, 2005, and in revised form, December 21, 2005. Published, JBC Papers in Press, January 12, 2006, DOI 10.1074/jbc.M511918200

Martin Lovmar^{‡1}, Karin Nilsson^{‡§1}, Vladimir Vimberg[¶], Tanel Tenson[¶], Martin Nervall^{||}, and Måns Ehrenberg^{‡2}

From the [‡]Department of Cell and Molecular Biology, Molecular Biology Program, Uppsala University, Uppsala S-75124, Sweden

[§]Department of Biometry and Engineering, Swedish University of Agricultural Sciences, S-75007 Uppsala, Sweden, [¶]Institute of Technology, Tartu University, 51010 Tartu, Estonia, and ^{||}Department of Cell and Molecular Biology, Structural Biology Program, Uppsala University, S-75124 Uppsala, Sweden

The macrolide antibiotic erythromycin binds at the entrance of the nascent peptide exit tunnel of the large ribosomal subunit and blocks synthesis of peptides longer than between six and eight amino acids. Expression of a short open reading frame in 23 S rRNA encoding five amino acids confers resistance to erythromycin by a mechanism that depends strongly on both the sequence and the length of the peptide. In this work we have used a cell-free system for protein synthesis with components of high purity to clarify the molecular basis of the mechanism. We have found that the nascent resistance peptide interacts with erythromycin and destabilizes its interaction with 23 S rRNA. It is, however, in the termination step when the pentapeptide is removed from the peptidyl-tRNA by a class 1 release factor that erythromycin is ejected from the ribosome with high probability. Synthesis of a hexa- or heptapeptide with the same five N-terminal amino acids neither leads to ejection of erythromycin nor to drug resistance. We propose a structural model for the resistance mechanism, which is supported by docking studies. The rate constants obtained from our biochemical experiments are also used to predict the degree of erythromycin resistance conferred by varying levels of resistance peptide expression in living *Escherichia coli* cells subjected to varying concentrations of erythromycin. These model predictions are compared with experimental observations from growing bacterial cultures, and excellent agreement is found between theoretical prediction and experimental observation.

Erythromycin is a clinically important broad-spectrum antibiotic that belongs to the macrolide class. It binds to a site in 23 S rRNA on the large ribosomal subunit (50 S)³ close to the peptidyl transferase center, near the entrance to the nascent peptide exit tunnel (1). Erythromycin-bound ribosomes can synthesize peptides with lengths between six and eight amino acids, but further peptide elongation is inhibited, and peptidyl-tRNA dissociates prematurely from the ribosome in the drop-off pathway (2). Different macrolides allow formation of peptides with different lengths depending on the space available between the macrolide

and the peptidyl transferase center. This suggests that macrolides act by preventing the nascent peptide from entering the peptide exit tunnel in the 50 S subunit (2). Once a nascent peptide has passed the erythromycin binding site and entered the peptide exit tunnel of a drug-free ribosome, erythromycin cannot bind to the 50 S subunit, which makes the ribosome refractory to the drug until peptide elongation is terminated by a class 1 release factor (3).

The way nascent peptides interact with the exit tunnel is important both for regulation of messenger RNA (mRNA) translation and protein export (4). For example, expression of the ErmC methyltransferase, which causes erythromycin resistance by methylating base A2058 (*Escherichia coli* numbering) at the erythromycin binding site in 23 S rRNA, is regulated by nascent peptide-erythromycin interactions in the peptide exit tunnel. That is, when there is erythromycin in a cell carrying the *ermC* gene, ribosomes are stalled during translation of an open reading frame present in the leader of the *ermC* mRNA. This causes rearrangements of the secondary structure of the leader mRNA, which make the ribosome binding site available for initiation of translation of the ErmC encoding the open reading frame of the *ermC* mRNA. This regulation requires a special sequence of the leader-encoded peptide, suggesting the existence of specific interactions between the peptide, the peptide exit tunnel, and erythromycin (5).

Another example of such specific interactions is the mechanism by which expression of a small open reading frame buried in the *E. coli* 23 S rRNA and encoding a pentapeptide causes low level resistance to erythromycin. This pentapeptide can only work in *cis*, meaning that resistance is conferred only to a ribosome on which the peptide is synthesized (6). Random libraries have been used to determine a consensus sequence for peptides that cause erythromycin resistance, *i.e.* fMet-(bulky/hydrophobic)-(Leu/Ile)-(hydrophobic)-Val (7). The random library approach has also been used to select resistance peptides to macrolides other than erythromycin. These studies have established correlations between macrolide structures and resistance peptide sequences, suggesting a unique peptide-drug interaction in the ribosomal tunnel for each tested macrolide (8–10). It has been suggested that synthesis of the *cis*-acting peptide that confers resistance to erythromycin removes the drug from the ribosome in an unknown manner (8). However, there has been no direct experimental evidence to support this proposal, and the molecular mechanism by which peptide synthesis could putatively remove erythromycin from the ribosome has remained obscure.

We have used a cell-free translation system with purified components from *E. coli* (11) to study the mechanism of peptide-mediated erythromycin resistance. We have found that, indeed, translation of the resistance peptide mRNA ejects the peptide, and we have identified the very step where this occurs. Based on our biochemical data and with support from docking simulations, we propose a structural model for

Downloaded from www.jbc.org at ULUNA BIBLIOTEKET on August 29, 2006

* This work was supported by the Swedish Research Council, the Wellcome Trust International Senior Fellowship (070210/z/03/z), and the Estonian Science Foundation (5311). The costs of publication of this article were defrayed in part by the payment of page charges. This article must therefore be hereby marked "advertisement" in accordance with 18 U.S.C. Section 1734 solely to indicate this fact.

[§] The on-line version of this article (available at <http://www.jbc.org>) contains supplemental material.

¹ These authors are equal contributors.

² To whom correspondence should be addressed: Dept. of Cell and Molecular Biology, Molecular Biology Program, BMC, Box 596, Uppsala University, S-75124 Uppsala, Sweden. Tel: 46-18-471-42-13; Fax: 46-18-471-42-62; E-mail: ehrenberg@xray.bmc.uu.se.

³ The abbreviations used are: 50 S, large ribosomal subunit; IF, initiation factor; RF, release factor; IPTG, isopropyl- β -D-thiogalactopyranoside; EF, elongation factor; rpmRNA, resistance peptide mRNA; HPLC, high performance liquid chromatography.

Erythromycin Resistance Peptides

mix with 20 μ l of the elongation mix, reactions were quenched by the addition of 1 ml of ice-cold polymix and applied to nitrocellulose filters. The filters were washed twice with 1 ml of polymix, and both the ^3H and ^{14}C activity were counted for both the flow-through and the filters.

Formic Acid Precipitation Assay—After mixing 20 μ l of the initiation mix with 20 μ l of the elongation mix, reactions were quenched by the addition of 150 μ l of 20% formic acid, and the precipitates were pelleted by centrifugation. The ^3H activities in the supernatants, containing released peptides were counted directly, whereas 160 μ l of 0.5 mM KOH was added to the pellets. After 10 min of incubation at room temperature, 10 μ l of 100% formic acid was added, and the precipitates were pelleted again. The ^3H activities in the supernatants at this second step correspond to the peptides that were still bound to tRNA at the time point when the reaction was quenched.

Data Evaluation—The dissociation rate constants for erythromycin leaving the ribosome were estimated by fitting the data to a single exponential model. The corresponding peptide- and peptidyl-tRNA dissociation rate constants were also estimated by fitting to a single exponential because the peptide synthesis was much faster than the dissociation (data not shown), and thus, the dissociation could be approximated with a single step reaction. The fitting was performed using the Marquardt algorithm (16) implemented in Origin 7 (OriginLab Corp.).

Docking of the Peptides to the Ribosome

Computational modeling was done to investigate the possible modes of interaction between peptides and erythromycin in different stages of peptide elongation. We used docking of the resistance peptide, fMet-Arg-Leu-Phe-Val-Stop (fMRLFV), to find a specific pattern of interaction with erythromycin. Furthermore, we used the peptide fMet-Asn-Ala-Ile-Lys-Stop (fMNAIK) as the negative control, in line with the experimental work (9). For this purpose we used GOLD 3.0 (CCDC, Cambridge, UK) in combination with the crystal structure 1YI2 (1), which contains the ribosome in complex with erythromycin. The docked peptide was covalently constrained to tRNA in either the A (acceptor) or the P (peptidyl) site. The position of the tRNA was taken from the crystal structure 1QVG (17). The docking study was carried out using 2,000,000 operations per docking. Atom c21 in erythromycin was defined as the floodfill center, and a radius of 10 Å was used in the floodfill. Thus an "active site" was defined around the erythromycin facing the A and P sites. The two peptides were docked as tri-, tetra-, penta- and hexapeptides (extended with Ala). Each peptide was docked 20 times, and the 15 best solutions were saved. We used the Chemscore option in GOLD for scoring the generated binding poses (18).

Simulations of Peptide-mediated Resistance in the Living Cell

Based on our model for erythromycin ejection from the ribosome and biochemical data, we set up a system of differential equations of ribosomes in different states (see Fig. 3A). The model accounts for changes in the total concentration of intracellular erythromycin by the inflow and outflow of the macrolide over the membrane and the change of resistance peptide mRNA and protein mRNA through synthesis and degradation. All components are also diluted by cell growth. The system was solved numerically by Euler's method (26), after the introduction of a certain macrolide concentration in the medium. Cell growth was registered as volume expansion during the first 8 h after induction. Before macrolide exposure, the system resided at steady state for a certain synthesis rate of resistance peptide mRNA (rpmRNA). The used program software was MATLAB 6.5 (The MathWorks, Inc., Natick, MA). A detailed description of the model and the parameters used is presented in the supplemental material.

Measurements on Cell Cultures

Strains—*E. coli* DH5 α strain (F' ϕ 80dlacZ Δ (lacZYA-argF)U169 *recA1 endA1 hsdR17* (rk $^-$, mk $^+$) *phoA supE44 λ -thi-1 gyrA96 relA1/F' proAB+ lacIqZ Δ M15 Tn10(tetr)*) was used in all experiments.

Effects of Mini-gene Expression on Macrolide Resistance—Overnight cultures of cells expressing resistance peptide (9) were grown at 37 °C in LB medium containing 100 μ g/ml ampicillin. Cultures were diluted into 96-well plates with fresh LB medium containing erythromycin and IPTG at different concentrations to final densities of $A_{600} = 0.01$. The cell cultures were grown in the shaker at 37 °C for 8 h, and the optical densities at A_{600} were recorded using the TECAN SUNRISE instrument.

RNA Copy Number—Cells expressing the resistance peptide were grown overnight in LB medium containing 100 μ g/ml ampicillin at 37 °C. Cultures were diluted with fresh LB medium containing IPTG and erythromycin at the concentrations as indicated. The cultures were grown for 2 h before 1-ml cultures were taken for total RNA isolation. Total RNA was purified with NucleoSpin RNA II kit (Macherey-Nagel). Concentrations of the resistance peptide and EF-Tu mRNAs were measured by reverse transcription PCR using the TaqMan Gold reverse transcription PCR kit (Applied Biosystems). The reverse transcription real-time PCR program was as follows; 1) annealing of the forward primer to mRNA (75 °C for 2 min, 65 °C for 5 min, and 53 °C for 5 min); 2) reverse transcription reaction, started by adding TaqMan reverse transcription buffer, dNTPs, RNase inhibitor, and reverse transcriptase followed by incubation at 45 °C for 10 min, 48 °C for 30 min, and 95 °C for 30 min; 3) real-time PCR, started by the addition of PCR buffer, dNTP, AmpliTaq Gold DNA polymerase, and the respective reverse primers and Taqman probes followed by PCR steps (prePCR (50 °C for 2 min and 95 °C for 10 min) and 40 PCR cycles (95 °C for 15 s, 50 °C for 30 s, and 60 °C for 15 s). The final reaction volume was 25 μ l. The concentrations of forward and reverse primers were 900 nM each, and the probe concentration was 100 nM. Annealing and reverse transcription steps were done in GeneAmp PCR System 2700 (Applied Biosystems). Real-time PCR was run and monitored in Rotor-Gene 5.0.47.

Primers—Specific primers for resistance peptide encoding mRNA were: forward, d(AAAAGCCCGCTCATTAGG), reverse, d(TGCTAGTCT-TAAGGAGGTCACAT), and Taqman probe, d(CTAGAGAATTCAGCTAGTTAAACAACAAAACCA). Specific primers for EF-Tu mRNA were: forward, d(GAGATGGAGAATACGCTCTCGA), reverse, d(AC-CAGAGCGTGCATTG), and Taqman probe, d(CGGCAGCAG-GAACGGCTT). Taqman probes had the 5' end modified with a FAM fluorophore and the 3' end modified with a TAMRA fluorophore.

RESULTS

Stoichiometric Removal of Erythromycin by Resistance Peptide Synthesis—To study the effects of resistance peptide synthesis on the rate of dissociation of erythromycin from the 50 S subunit, we took advantage of a cell-free translation system with purified components from *E. coli* (11). The resistance pentapeptide fMRLFV and a control pentapeptide, fMNAIK, were synthesized (9) on ribosomes in recycling mode (19). Erythromycin insignificantly affected the rate of synthesis of resistance and control peptide, whereas their synthesis was shut down by the presence of josamycin (Fig. 1). We took advantage of this by chasing the erythromycin, originally on the recycling ribosomes, with josamycin (Fig. 1). Because the two drugs have overlapping ribosomal binding sites (1, 20, 21), josamycin cannot bind and shut down peptide synthesis until after dissociation of erythromycin from the 50 S subunit. The josamycin concentration used in the chase (83 μ M) leads to an association rate of 2.7 s $^{-1}$ (21). Thus, the rate-limiting step in the josa-

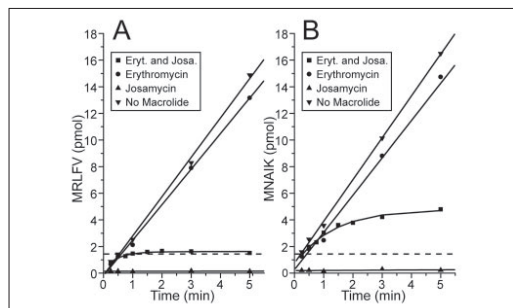


FIGURE 1. Erythromycin chased with josamycin in a recycling experiment. The amounts of resistance peptide (MRLFV, *panel A*) and control peptide (MNAIK, *panel B*) are plotted against time. Erythromycin (Eryt., ●) allows formation of both pentapeptides almost as well as without any antibiotic (○), whereas josamycin (Josa., ▲) does not allow any pentapeptide formation. When erythromycin dissociates in the chase experiment (■) it is replaced by josamycin, and further pentapeptide formation is inhibited. The dashed lines correspond to the amount of active ribosomes in the experiments (1.7 pmol). Translation of the resistance peptide (MRLFV, *panel A*) is inhibited already after a single round of translation, which means that all erythromycin has dissociated and been replaced by josamycin before the next round of translation initiates. This is in contrast to the several rounds of recycling that is allowed when expressing the control peptide (MNAIK, *panel B*). The pentapeptide synthesis rate per ribosome in the absence of josamycin (k_1) is 0.03 s^{-1} ($3 \text{ pmol min}^{-1}/1.7 \text{ pmol of ribosomes} = 1.8 \text{ min}^{-1} = 0.03 \text{ s}^{-1}$). The erythromycin dissociation rate (k_2) can be estimated from the value of k_1 and the plateau level in the josamycin chase experiments (see "Experimental Procedures").

mycin-induced inhibition of peptide formation is the erythromycin dissociation. The value of the rate constant for dissociation of erythromycin from ribosomes synthesizing the control peptide was estimated as 0.01 s^{-1} (Fig. 1B), which corresponds to the rate constant for spontaneous dissociation of erythromycin from empty ribosomes (21). In contrast, the value of the rate constant for dissociation of erythromycin from ribosomes synthesizing the resistance peptide was estimated as 0.03 s^{-1} , a value coinciding with the rate (s^{-1}) of pentapeptide synthesis per ribosome in the absence of josamycin (Fig. 1A). From these results follows that erythromycin was removed with high probability from the ribosome during each cycle of resistance, but not control peptide synthesis. Identification of the step at which drug dissociation was induced by the *cis*-acting peptide required further experiments, to be described in the next paragraph.

Dissociation of Erythromycin during Different Stages of Resistance Peptide Synthesis—To estimate the rate constants for dissociation of erythromycin at different stages of resistance peptide synthesis, we used nitrocellulose filtration techniques.

Ribosomes were initiated for synthesis of resistance (fMRLFV) or control (fMNAIK) peptides. By selective exclusion of amino acids and aminoacyl-tRNA synthetases in the peptide elongation assays, ribosomes carrying fMR, fMRL, fMRLF, or fMRLFV as well as fMN, fMNA, fMNAI, or fMNAIK peptides ester-bonded to the P-site tRNA were produced. Subsequently, [^{14}C]erythromycin was chased from each one of these ribosome complexes by the addition of unlabeled erythromycin in excess, and the fraction of [^{14}C]erythromycin-containing ribosomes was monitored by nitrocellulose filtration at different incubation times. From these data, rate constants for the dissociation of erythromycin were estimated, and the results are summarized in Table 1. The rate constant for dissociation of erythromycin increased from its smallest value (0.011 s^{-1}) in the initiation complex with every amino acid that was added, in accordance with the resistance peptide sequence to its largest value of 0.068 s^{-1} when the pentapeptide was completed (Fig. 2A and Table 1). There was at the same time little effect on the rate of

TABLE 1
Erythromycin dissociation rate constants

Translated peptide	Erythromycin dissociation rate constant
Initial complex	0.011 ± 0.001
MR	0.017 ± 0.005
MRL	0.025 ± 0.004
MRLF	0.051 ± 0.004
MRLFV	0.068 ± 0.006
MRLFVA	0.014 ± 0.001
MRLFVAN	0.014 ± 0.001
MN	0.011 ± 0.001
MNA	0.015 ± 0.001
MNAI	0.016 ± 0.001
MNAIK	0.017 ± 0.001

erythromycin dissociation by amino acid addition, in accordance with the control peptide sequence (Fig. 2B and Table 1).

It has been shown that active resistance peptides must have lengths between four and six amino acids (7). To clarify why this is so, we prepared mRNAs encoding the hexapeptide fMet-Arg-Leu-Phe-Val-Ala-Stop, which is the resistance peptide with a C-terminal addition of Ala, and the heptapeptide fMet-Arg-Leu-Phe-Val-Ala-Asn-Stop, which is the resistance peptide with a C-terminal addition of Ala-Asn. Both these C-terminal additions reduced the rate constant for erythromycin dissociation from 0.068 s^{-1} (in the presence of the authentic resistance peptide) to 0.014 s^{-1} (in the presence of the C-terminal extension) (Table 1).

These results show that when the resistance peptide grew from two to five amino acids, this led to successively faster dissociation of erythromycin. Because, however, synthesis of the resistance peptide was considerably faster than the largest rate of erythromycin dissociation, these data cannot explain why every round of resistance peptide synthesis resulted in near-stoichiometric removal of the 50 S-bound erythromycin (Fig. 1). This pointed at class 1 release factor-induced peptide release from the ribosome as the critical step for resistance peptide action. Experiments addressing this question follow.

Termination of Resistance Peptide Synthesis Drives Dissociation of Erythromycin—The largest rate constant for erythromycin dissociation (0.14 s^{-1}) was obtained when either one of the class 1 release factors was also present to terminate the synthesis of the resistance peptide at the UAA codon of its mRNA (Fig. 2C, Table 2). At the same time, there was no effect on the rate of erythromycin dissociation by release factor addition in the case of the control peptide (Fig. 2C, Table 2). To further investigate class 1 release factor action, we used nitrocellulose binding to monitor the release of different peptides from the ribosome and formic acid precipitation followed by peptide identification by HPLC to directly monitor hydrolysis of the ester bond connecting peptide and P-site tRNA. The rate of dissociation from the ribosome and the rate of ester bond hydrolysis were similar in the cases described below in this section of text, suggesting fast dissociation of peptides from the ribosome after the rate-limiting ester bond hydrolysis.

The rate of resistance peptide release from the ribosome, as induced by either one of the class 1 release factors (0.073 s^{-1}) as monitored by the ribosome-bound ^3H -labeled fMet, was significantly smaller than the rate constant for dissociation of erythromycin (0.14 s^{-1}). At the same time, the rate of control peptide release as induced by RF2 (0.22 s^{-1}) was almost 30 times larger than the rate constant for erythromycin dissociation (Fig. 2E). These results in conjunction with the observation (Fig. 1) that every cycle of resistance peptide synthesis removed the ribosome-bound erythromycin with high probability suggest, first, that binding of a class 1 release factor to an erythromycin-containing ribosome carrying a resistance pentapeptide further destabilized the binding of the

Erythromycin Resistance Peptides

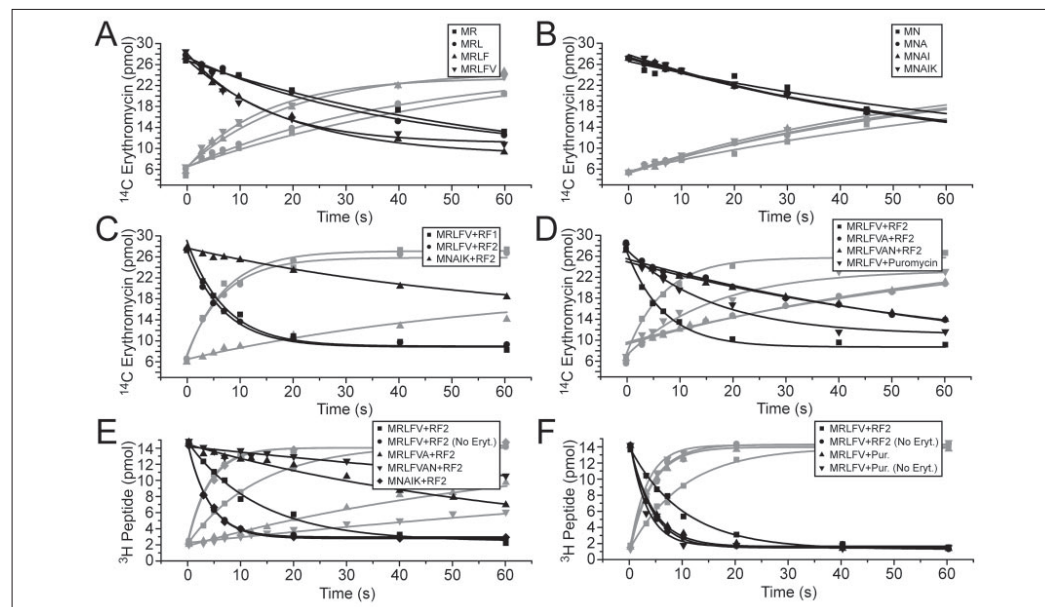


FIGURE 2. Erythromycin and peptide dissociation rates. Panels A–D show the amount of ribosome bound (or released) [^{14}C]erythromycin as a function of time. Essentially all ribosomes contain [^{14}C]erythromycin at time 0, and a 75-fold excess of cold erythromycin was added to the pre-initiated ribosome complexes together with the elongation mix to prevent re-binding of [^{14}C]erythromycin. Panel E shows dissociation of the peptide labeled with [^3H]Met as a function of time. The black symbols in panels A–E show the amount that is bound to ribosomes and thereby stick to the nitrocellulose filters, whereas the gray symbols show the amount that have gone through the filters. Panel F shows the release factor-mediated hydrolysis of the peptidyl-tRNA and the puromycin reaction as a function of time. The black symbols show the peptides that are still bound to tRNA and thereby precipitable with formic acid, whereas the gray symbols show the peptides in the supernatant. All lines are obtained by simultaneously fitting the data shown by black and gray symbols to single exponentials using least square fits. The estimated rate constants are collected in Tables 1 and 2.

TABLE 2
Erythromycin and peptide dissociation rate constants

Translated peptide	Releasing agent	Erythromycin dissociation rate constant ^a	Peptide dissociation rate constant ^a	Peptidyl-tRNA hydrolysis rate constant ^b
		s^{-1}	s^{-1}	s^{-1}
MRLFV	RF1	0.14 ± 0.02	0.073 ± 0.007	
MRLFV	RF1	No erythromycin	0.22 ± 0.02	
MRLFV	RF2	0.13 ± 0.01	0.074 ± 0.01	0.10 ± 0.01
MRLFV	RF2	No erythromycin	0.25 ± 0.01	0.26 ± 0.03
MRLFV	Puromycin	0.067 ± 0.009	Not determined ^c	0.23 ± 0.02
MRLFV	Puromycin	No erythromycin	Not determined ^c	0.31 ± 0.03
MRLFVA	RF2	0.014 ± 0.001	0.015 ± 0.002	0.015 ± 0.001
MRLFVA	RF2	No erythromycin	0.29 ± 0.03	0.32 ± 0.03
MRLFVAN	RF2	0.014 ± 0.001	0.006 ± 0.0004	0.004 ± 0.0004
MRLFVAN	RF2	No erythromycin	0.27 ± 0.03	0.44 ± 0.03
MNAIK	RF2	0.015 ± 0.001	0.26 ± 0.03	0.28 ± 0.02
MNAIK	RF2	No erythromycin	0.25 ± 0.02	0.27 ± 0.02

^a Measured by nitrocellulose filter binding.

^b Measured by formic acid precipitation.

^c Could not be determined because fMRLFV-puromycin bind to NC-filters.

drug to the ribosome and, second, that termination was slow enough to allow dissociation of erythromycin from the ribosome with a probability close to one, in accordance with the results in Fig. 1. It cannot be excluded that dissociation of erythromycin was strictly required for termination to occur, in which case the probability for drug rejection would be exactly 100%. The reason for the ambiguity relates to the experimental design in which [^{14}C]erythromycin was chased with unlabeled erythromycin at a high concentration (75 μM), which could allow for rapid rebinding of an unlabeled erythromycin after dissociation of the labeled one (21), before significant termination could occur. In this latter scenario, which leads to the simplest interpretation of the peptide

release data, termination in our *in vitro* experiments occurred in the presence of erythromycin.

The addition of RF2 to ribosomes carrying the resistance peptide with a C-terminal addition of one amino acid (the hexapeptide) led to peptide release with a rate constant of 0.015 s^{-1} , virtually identical with the rate constant of 0.014 s^{-1} for dissociation of erythromycin (Figs. 2, D and E and Table 2). The addition of RF2 to the resistance peptide with a C-terminal addition of two amino acids (the heptapeptide) led to peptide release with a considerably smaller rate constant of 0.006 s^{-1} but to a similar rate constant of 0.014 s^{-1} for dissociation of erythromycin (Figs. 2, D and E, and Table 2). This rate constant for dissociation of erythro-

mycin is similar to the corresponding rate constant for the peptide-lacking initiation complex. These experiments show that release of the extended peptides did not accelerate dissociation of erythromycin, in line with the previous observation of a strong sequence length dependence of resistance activity (7).

Treatment of ribosomes carrying full-length resistance peptides with puromycin, an antibiotic mimicking the aminoacylated 3'-adenosine of an aminoacylated tRNA (17), did not alter the rate of dissociation of erythromycin (Fig. 2D and Table 2). It was not possible to monitor release of the resistance peptide-puromycin complex from the ribosome, since it remained filter-bound in free as well as ribosome-bound configuration. We could, however, monitor peptidyl transfer to puromycin using HPLC after formic acid precipitation. We found that the rate constant for transfer of the resistance peptide to puromycin (0.23 s^{-1}) was much larger than the rate constant for dissociation of erythromycin (0.067 s^{-1}) (Figs. 2, D and F). This means that transfer of the resistance peptide to puromycin was unhindered by the presence of erythromycin, in contrast to the hydrolytic reaction induced by a class 1 release factor (Fig. 2C and Table 2). It is normally assumed that when a small peptide is transferred to puromycin, it rapidly leaves the ribosome. However, if this were the case, one would expect that the rate constant for erythromycin release would be reduced from its value of 0.068 s^{-1} in the absence of puromycin to its value of 0.011 s^{-1} in the absence of peptide. The experiments show, in contrast, that in response to puromycin treatment dissociation of erythromycin remained unaltered at 0.067 s^{-1} . This suggests that the resistance peptide-puromycin complex remained ribosome-bound long enough to allow for dissociation of the radio-labeled erythromycin.

Docking of the Resistance Peptide to the Ribosome—Previous genetic studies (7) and the biochemical data in this work suggest the existence of specific interactions between the resistance peptide and ribosome-bound erythromycin. To test this, we performed docking simulations with a resistance or a control peptide anchored to an A-site- or a P-site-bound tRNA of a ribosome in complex with erythromycin. In 8 of the top 15 simulations for the resistance pentapeptide anchored to the P-site tRNA, the leucine in fMRLFV was bound to a small hydrophobic cavity on the surface of erythromycin, between the cladinose and desosamine residues (see Fig. 4, E and F), and a similar result was obtained for the tetrapeptide fMRLF. Similar, but less pronounced leucine binding patterns were observed also for fMRLEFV and fMRLF anchored to the A-site tRNA. At the same time, no distinct binding patterns were observed for amino acids other than leucine in the resistance peptide or for any of the amino acids in the control peptide fMNAIK. In the case of the resistance tripeptide, the leucine did not reach into the erythromycin cavity, and in the case of the resistance hexapeptide, the leucine binding pattern was gone, possibly due to steric hindrance.

Validation of the Model for Resistance Peptide Action by Cell Population Experiments—From the biochemical experiments described above, kinetic constants for resistance peptide action were obtained (Table 2). We constructed a model for erythromycin resistance in bacterial populations (Fig. 3A) based on these and other parameters (listed in the supplemental material) for protein synthesis obtained from our cell-free mRNA translation system (21). The model (detailed description in the supplemental material) contains seven different states of the large ribosomal subunit (50 S) (Fig. 3A); it accounts for dilution of all compounds due to cell volume growth and for a finite rate of diffusion across the cell membrane, which reduces the intracellular concentration in relation to the outer concentration of erythromycin. Furthermore, the model takes into account the efflux pumps used by *E. coli* to actively transport eryth-

Erythromycin Resistance Peptides

romycin and other antibiotic drugs from the membrane and cytoplasm to the growth medium (22).

To validate the model, we varied the expression of rpmRNA under *tac* promoter control from a multicopy plasmid by varying the concentration of IPTG in an erythromycin-containing growth medium (6, 9). Cell growth at different IPTG and erythromycin concentrations was monitored along with reverse transcription real-time PCR analysis of the intracellular concentration of rpmRNA relative to the concentration of EF-Tu mRNA (Fig. 3C, inset). The *tac* promoter was leaky, and the response in rpmRNA synthesis to the external IPTG level was linear. At the highest IPTG concentration ($600 \mu\text{M}$) in the medium, the mRNA level was 3-fold higher than in the absence of IPTG (Fig. 3C, inset). Increasing IPTG concentrations led to increasing erythromycin resistance until a plateau, specific for each concentration of erythromycin, was reached (Fig. 3C). The increase in bacterial mass (optical density) during 8 h of growth at varying concentrations of erythromycin and IPTG in the medium were monitored, and there was excellent agreement between the experimentally observed and model-simulated growth behavior in which the measured, relative rpmRNA levels had been taken into account (Fig. 3B).

DISCUSSION

Erythromycin binds in the nascent peptide exit tunnel close to the peptidyl transferase center (1, 23) (Fig. 4A) and prevents synthesis of peptides longer than eight amino acids (2). Expression of a mini-gene buried in the 23 S rRNA causes low level resistance to erythromycin (6), and it has been suggested that synthesis of this resistance peptide on an erythromycin-containing ribosome can clean it from the drug, thereby making an erythromycin-free 50 S subunit available for a new round of initiation of protein synthesis with another mRNA (8). When the nascent peptide is longer than six to eight amino acids, it covers the erythromycin binding site, which makes the ribosome refractory to further inhibition by erythromycin, allowing for synthesis of full-length proteins (3, 21).

The present experiments directly demonstrate that synthesis of a resistance peptide can, indeed, remove erythromycin from the 50 S subunit. During every cycle of resistance peptide synthesis erythromycin dissociates with close to 100% probability, whereas the synthesis of a control peptide does not induce dissociation of the drug (Fig. 1). As the resistance peptide grows by successive amino acid additions, the rate constant for dissociation of erythromycin increases in a stepwise manner (Table 1). It is, however, not until class 1 release factor induced termination of the full-length resistance pentapeptide, that erythromycin is removed from the ribosome with high probability. Termination is, in other words, the crucial kinetic step for erythromycin dissociation and, therefore, the point at which resistance is conferred.

To validate the mechanism for resistance peptide action, we modeled it in the context of the cytoplasm of a living cell (Fig. 3A and supplemental material) using kinetic data from the present (Table 2) and earlier (21) work. We describe in particular the degree to which inhibition of the growth rate of a bacterial population due to the presence of varying concentrations of erythromycin in the cytoplasm is expected to be relieved by the expression of the resistance peptide at varying levels (Fig. 3B).

These simulations were compared with experimental observations from a bacterial population containing the resistance peptide gene under *tac* promoter control on a multicopy plasmid. The cells were grown in media containing varying concentrations of erythromycin as well as IPTG to control the level of resistance peptide expression. The increase in bacterial mass during 8 h of growth was monitored by optical

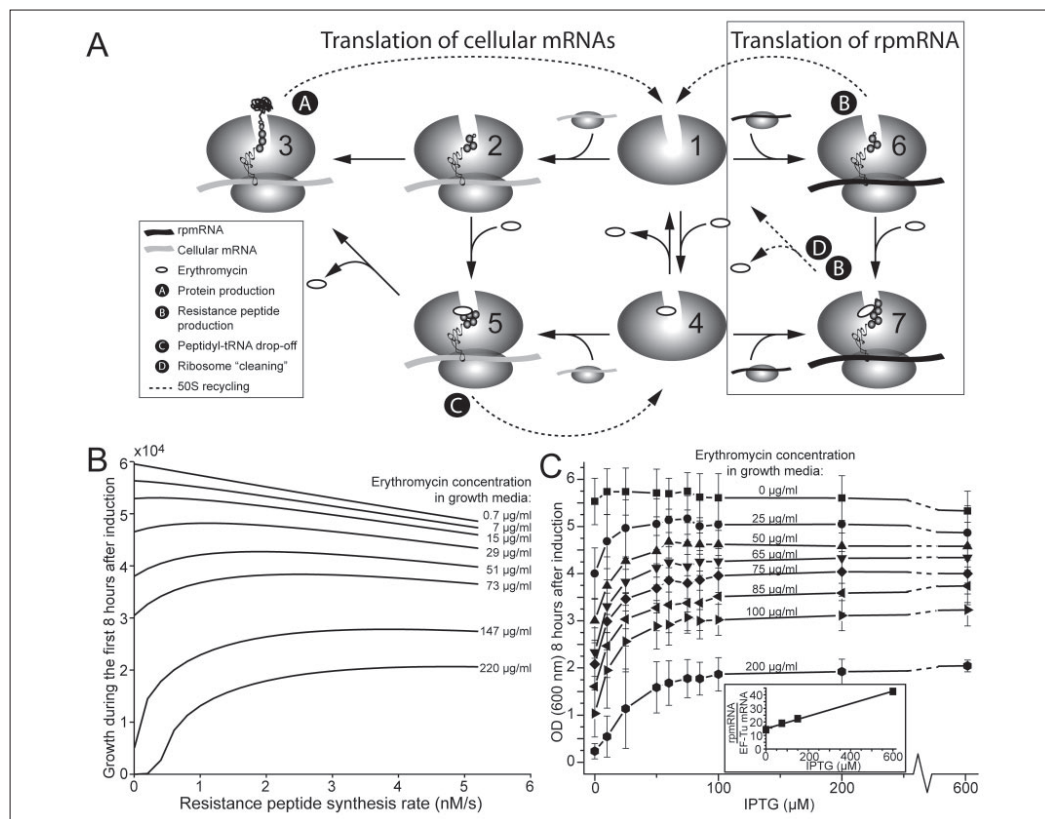


FIGURE 3. The model, simulation data, and data from cell culture experiments. Panel A shows a schematic of the model we have developed for simulating translation in the presence of erythromycin and the effect of translating a resistance peptide in the context of a growing *E. coli* cell. The 50 S subunits are in seven different states in the model. Free 50 S subunit (state 1) is susceptible to erythromycin binding and likewise is the newly initiated ribosomes (state 2 and state 6), whereas elongating ribosomes with a longer protein become refractory to macrolide binding (state 3) and, thus, this state always results in full-length product. If erythromycin is bound to the 50 S subunit (state 4) it can still initiate and translate the first codons before protein synthesis is inhibited (state 5). The ribosome is stuck in state 5 until either the peptidyl-tRNA drops off and the ribosome is recycled to state 4, or erythromycin dissociates and protein synthesis is resumed in state 3 and thus refractory to rebinding of erythromycin. If a ribosome with erythromycin (state 4) initiates on a resistance peptide mRNA (rpmRNA) (state 7) it will be "cleaned" and recycled as an erythromycin free 50 S (state 1). The model also contains the cell membrane and erythromycin efflux pumps present in *E. coli* that change the intracellular concentration in comparison to erythromycin concentration in the growth media. For further details about the model, see the supplemental material. Panel B, simulated growth (defined as how many times the cell volume has increased) during the first 8 h after the addition of erythromycin plotted against the rate of rpmRNA synthesis for different concentrations of erythromycin. Panel C, optical density (600 nm) measured 8 h after the addition of erythromycin plotted against the concentration of IPTG. Inset, level of expression of rpmRNA in relation to EF-Tu mRNA plotted against the IPTG concentration.

density (Fig. 3C) along with the level of resistance peptide mRNA normalized to the level of EF-Tu mRNA (Fig. 3C, inset), as measured by reverse transcription real-time PCR. The simulated growth rates in Fig. 3B, where the experimentally measured resistance peptide mRNAs are taken into account, are in excellent agreement with the measured growth rates in Fig. 3C. This shows that the mechanism we propose for peptide-mediated low level resistance against erythromycin (Fig. 3A) and the rate constants obtained from our cell-free *in vitro* translation system (Table 2 and Ref. 21) are sufficient to fully account for the *in vivo* induced resistance in a large interval of erythromycin concentrations and peptide expression levels (Figs. 3, B and C (and inset)).

The structural basis of resistance peptide action is of considerable interest, not the least because it is one special case of the general and poorly understood phenomenon of peptide-specific interactions with the ribosomal peptide exit tunnel (4, 24). Our data show that when the

control peptide grows from a di- to a pentapeptide, there is little change in the rate constant for erythromycin dissociation. When, furthermore, RF2 is added to terminate peptide synthesis, hydrolysis of the ester bond in the peptidyl-tRNA proceeds with the same rate as in the absence of erythromycin (Tables 1 and 2). For the resistance peptide, in contrast, our data show that the rate constant for erythromycin dissociation increases gradually by a factor of six as the peptide grows from just the fMet to di- and then to pentapeptide. In addition, when RF2 is added, the rate constant for erythromycin release is further enhanced by a factor of two, and the rate of ester bond hydrolysis is much smaller than in the absence of erythromycin (Tables 1 and 2). We know from data obtained from open reading frame libraries that the consensus sequence for peptide-mediated erythromycin resistance has two outstanding features; there is a leucine or isoleucine in the third position and a valine in the fifth, C-terminal position (7, 9). Resistance peptides for different

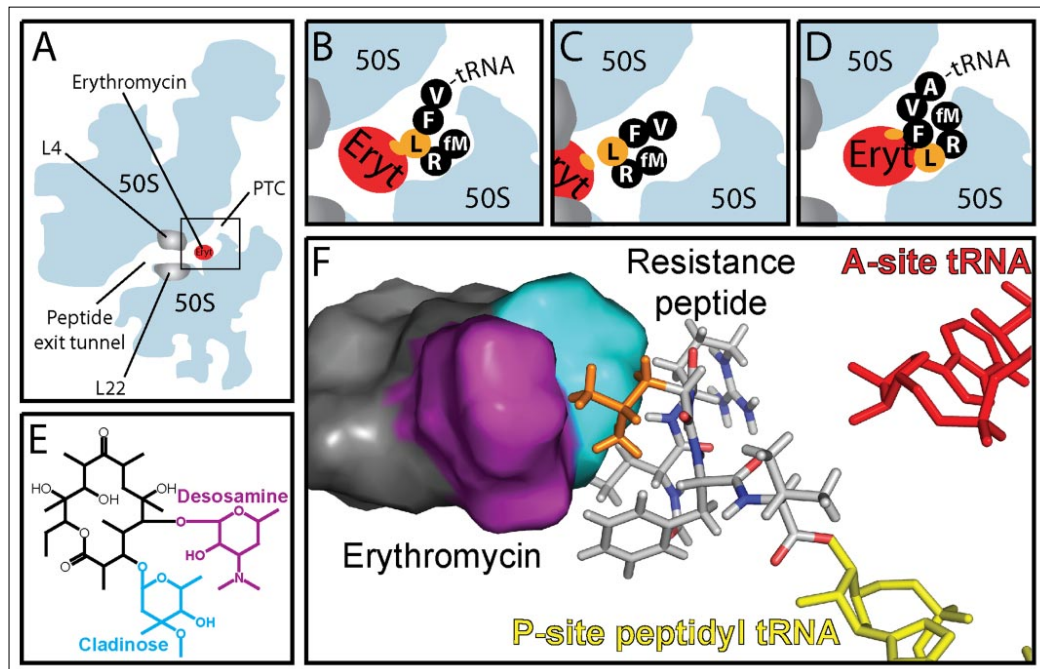


FIGURE 4. **A structural model for the mechanism of resistance peptide action.** Panel A shows a schematic of the large ribosomal subunit cut along the nascent peptide exit tunnel with an erythromycin molecule bound (red). The peptidyl transferase center (PTC) and the two ribosomal proteins (L4 and L22) constituting the constriction in the tunnel are indicated. The black rectangle indicates the section shown in panels B–D where our hypothesis about the mechanism of the resistance peptide action is shown. Panel B shows the pentapeptidyl-tRNA that interacts with erythromycin (Eryt). Panel C shows the resistance peptide during termination of protein synthesis has removed erythromycin. Panel D shows the hexapeptidyl-tRNA which has lost its contact with erythromycin and is trapped in a dead end that eventually leads to peptidyl-tRNA drop-off. Panel E shows the chemical structure of erythromycin. Panel F presents the interaction between the conserved leucine residue (orange) in the resistance peptide and erythromycin as indicated by the docking studies.

types of macrolides have different consensus sequences, suggesting specific and perhaps direct interactions between the conserved residues and each type of ribosome bound macrolide (9, 10). From the present kinetic data (Tables 1 and 2) and docking simulations (Fig. 4F) along with previous open reading frame library data (7), we propose a structural model for peptide-mediated erythromycin resistance (Figs. 4, A–D).

Our docking studies based on the crystal structure of a *Haloarcula marismortui* 50 S subunit in complex with erythromycin (1) suggest that the side chain of leucine in the resistance peptide binds to the hydrophobic cleft between the two sugar moieties of erythromycin (Figs. 4, E and F). To date, there is no crystal structure of an *E. coli* 50 S subunit in complex with erythromycin, but the similarity of the 50 S subunits from the two organisms near the erythromycin binding site (1, 25) suggests that our docking data are relevant also for the erythromycin-bound *E. coli* ribosome. Leucine binding to erythromycin is observed both for resistance tetra- and pentapeptides, and the binding pattern is more distinct for resistance peptides anchored to the P-site than to the A-site tRNA. By hypothesis, the observed interaction between the resistance tetrapeptide and the drug weakens the affinity of erythromycin for the ribosome, which accounts for the fact that a leucine (or an isoleucine) is critical for resistance peptide action. Completion of the resistance pentapeptide by the addition of valine further increases the erythromycin dissociation rate constant, probably because the force by which the resistance

peptide pushes erythromycin out from its binding site increases (Fig. 4B). When a class 1 release factor binds to the pre-termination ribosome containing a resistance pentapeptide ester-bonded to the P-site tRNA, the rate constant for erythromycin dissociation increases by another factor of two. At the same time, the rate constant for ester bond hydrolysis of the peptidyl-tRNA decreases very significantly (Table 2), which partially accounts for the fact that every cycle of peptide synthesis led to erythromycin dissociation with near 100% probability (Fig. 1). It is, furthermore, possible that the resistance peptide forms a specific hydrophobic structure that prevents it from leaving the ribosome through the peptidyl transferase center after its release from the P-site tRNA. The peptide is then forced to leave the ribosome through the peptide exit tunnel, where its hydrophobic C terminus could interfere with the hydrophobic interactions between erythromycin and the exit tunnel wall and chase the drug out through the L4/L22 constriction in the tunnel (Fig. 4C). This would lead to 100% probability of drug ejection per cycle of resistance peptide synthesis. When instead of termination, an additional amino acid is added to the resistance pentapeptide, our simulations suggest that the leucine interaction with erythromycin becomes lost and that, accordingly, the hexa-peptide is expected to behave like any other peptide. It will fill up the space available between drug and peptidyl transfer center until further protein synthesis is inhibited by crowding (Fig. 4D).

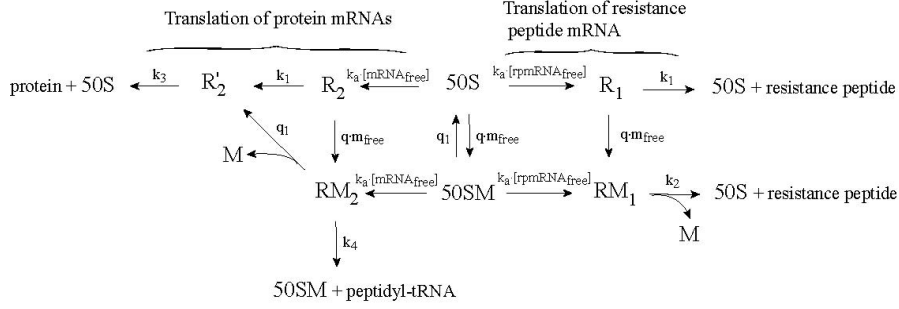
Erythromycin Resistance Peptides

REFERENCES

1. Tu, D., Blaha, G., Moore, P. B., and Steitz, T. A. (2005) *Cell* **121**, 257–270
2. Tenson, T., Lovmar, M., and Ehrenberg, M. (2003) *J. Mol. Biol.* **330**, 1005–1014
3. Andersson, S., and Kurland, C. G. (1987) *Biochimie (Paris)* **69**, 901–904
4. Tenson, T., and Ehrenberg, M. (2002) *Cell* **108**, 591–594
5. Mayford, M., and Weisblum, B. (1990) *J. Bacteriol.* **172**, 3772–3779
6. Tenson, T., DeBlasio, A., and Mankin, A. (1996) *Proc. Natl. Acad. Sci. U. S. A.* **93**, 5641–5646
7. Tenson, T., Xiong, L., Kloss, P., and Mankin, A. S. (1997) *J. Biol. Chem.* **272**, 17425–17430
8. Tripathi, S., Kloss, P. S., and Mankin, A. S. (1998) *J. Biol. Chem.* **273**, 20073–20077
9. Vimberg, V., Xiong, L., Bailey, M., Tenson, T., and Mankin, A. (2004) *Mol. Microbiol.* **54**, 376–385
10. Tenson, T., and Mankin, A. S. (2001) *Peptides* **22**, 1661–1668
11. Freistoffer, D. V., Pavlov, M. Y., MacDougall, J., Buckingham, R. H., and Ehrenberg, M. (1997) *EMBO J.* **16**, 4126–4133
12. Jelenc, P. C., and Kurland, C. G. (1979) *Proc. Natl. Acad. Sci. U. S. A.* **76**, 3174–3178
13. Pavlov, M. Y., and Ehrenberg, M. (1996) *Arch. Biochem. Biophys.* **328**, 9–16
14. MacDougall, J., Holst-Hansen, P., Mortensen, K. K., Freistoffer, D. V., Pavlov, M. Y., Ehrenberg, M., and Buckingham, R. H. (1997) *Biochimie (Paris)* **79**, 243–246
15. Ehrenberg, M., Bilgin, N., and Kurland, C. G. (1990) *Design and Use of a Fast and Accurate in Vitro Translation System*, pp. 101–129, IRL Press at Oxford University Press, Oxford
16. Marquardt, D. W. (1963) *J. Soc. Ind. Appl. Math.* **11**, 431–441
17. Schmeing, T. M., Moore, P. B., and Steitz, T. A. (2003) *RNA* **9**, 1345–1352
18. Verdonk, M. L., Cole, J. C., Hartshorn, M. J., Murray, C. W., and Taylor, R. D. (2003) *Proteins* **52**, 609–623
19. Pavlov, M. Y., Freistoffer, D. V., MacDougall, J., Buckingham, R. H., and Ehrenberg, M. (1997) *EMBO J.* **16**, 4134–4141
20. Hansen, J. L., Ippolito, J. A., Ban, N., Nissen, P., Moore, P. B., and Steitz, T. A. (2002) *Mol. Cell* **10**, 117–128
21. Lovmar, M., Tenson, T., and Ehrenberg, M. (2004) *J. Biol. Chem.* **279**, 53506–53515
22. Zgurskaya, H. I., and Nikaïdo, H. (1999) *Proc. Natl. Acad. Sci. U. S. A.* **96**, 7190–7195
23. Schlunzen, F., Zarivach, R., Harms, J., Bashan, A., Tocilj, A., Albrecht, R., Yonath, A., and Franceschi, F. (2001) *Nature* **413**, 814–821
24. Cruz-Vera, L. R., Rajagopal, S., Squires, C., and Yanofsky, C. (2005) *Mol. Cell* **19**, 333–343
25. Schuwirth, B. S., Borovinskaya, M. A., Hau, C. W., Zhang, W., Vila-Sanjurjo, A., Holton, J. M., and Cate, J. H. (2005) *Science* **310**, 827–834
26. Heath, M. T. (1997) *Scientific Computing: An Introductory Survey*, pp. 274–275, The McGraw-Hill Inc., New York

SUPPLEMENTARY MATERIAL

Model of peptide mediated erythromycin resistance or the “bottlebrush” model



The model above is described by the following system of differential equations,

$$\begin{aligned}
 \frac{d[50SM]}{dt} &= q \cdot [m_{free}] \cdot [50S] + k_4 \cdot [R_2M] - (k_a \cdot ([mRNA_{free}] + [rpmRNA_{free}]) + q_1 + \mu) \cdot [50SM], \\
 \frac{d[R_1]}{dt} &= k_a \cdot [rpmRNA_{free}] \cdot [50S] - (k_1 + q \cdot [m_{free}] + \mu) \cdot [R_1], \\
 \frac{d[R_1M]}{dt} &= k_a \cdot [rpmRNA_{free}] \cdot [50SM] + q \cdot [m_{free}] \cdot [R_1] - (k_2 + \mu) \cdot [R_1M], \\
 \frac{d[R_2]}{dt} &= k_a \cdot [mRNA_{free}] \cdot [50S] - (k_1 + q \cdot [m_{free}] + \mu) \cdot [R_2], \\
 \frac{d[R_2M]}{dt} &= k_a \cdot [mRNA_{free}] \cdot [50SM] + q \cdot [m_{free}] \cdot [R_2] - (q_1 + k_4 + \mu) \cdot [R_2M], \\
 \frac{d[R_2']}{dt} &= k_1 \cdot [R_2] + q_1 \cdot [R_2M] - (k_3 + \mu) \cdot [R_2'], \\
 \frac{d[m_{tot}]}{dt} &= r_{in} \cdot [m_m] - r_{out} \cdot [m_{free}] - \mu \cdot [m_{tot}], \\
 \frac{d[rpmRNA_{tot}]}{dt} &= k_{s1} - k_{d1} \cdot [rpmRNA_{free}] - \mu \cdot [rpmRNA_{tot}], \\
 \frac{d[mRNA_{tot}]}{dt} &= k_{s2} - k_{d2} \cdot [mRNA_{free}] - k_{d3} \cdot [R_2M] - \mu \cdot [mRNA_{tot}].
 \end{aligned} \tag{1}$$

A large ribosomal subunit can exist in seven different states. The 50S subunit may be free without ([50S]) or with ([50SM]) a bound macrolide. It may be a part of a ribosome ready to translate the first codons of a protein mRNA without ([R₂]) or with ([R₂M]) a bound macrolide or it may have translated the first codons and become temporarily immune to the drug ([R₂']). The subunit may also be a part of a ribosome ready to translate a resistance peptide mRNA (rpmRNA) without ([R₁]) or with ([R₁M]) a bound antibiotic molecule. The rate constant of association and spontaneous dissociation of the antibiotic is q and q_1 , respectively. Association of the ribosomal subunits occurs with rate constant k_a times the free concentration of protein mRNAs ([mRNA_{free}]) and free rpmRNA ([rpmRNA_{free}]). The first rounds of translation when the antibiotic can attack a ribosome (which is approximately the length of a resistance

peptide) occur with rate k_1 . The rate for completing synthesis of a protein beyond translation of the first codons is k_3 , the drop-off rate of an antibiotic-carrying, stalled ribosome on a protein mRNA is k_4 and a resistance peptide is synthesised with rate k_2 when the ribosome carries a macrolide. The system of equations also contains differential equations describing the change of the total concentration of the macrolide in the cell ($[m_{tot}]$) and of the total concentration of protein mRNAs ($[mRNA_{tot}]$) and rpmRNA ($[rpmRNA_{tot}]$), respectively. The inflow rate of the macrolide is r_{in} and the outflow rate is denoted r_{out} . The free intracellular concentration of the macrolide is defined by $[m_{free}] = [m_{tot}] - [50SM] - [R_1M] - [R_2M]$. The synthesis rate of rpmRNA is k_{s1} and active degradation of free rpmRNA occurs with rate constant k_{d1} . The corresponding rates of synthesis and degradation of protein mRNAs are denoted k_{s2} and k_{d2} , respectively. It is also assumed that a stalled, macrolide-carrying ribosome on the 5' end of an mRNA does not fully protect the mRNA from degradation, but it is degraded by a low rate constant, k_{d3} . The free concentration of rpmRNA and protein mRNAs is defined by $[rpmRNA_{free}] = [rpmRNA_{tot}] - [R_1] - [R_1M]$ and $[mRNA_{free}] = [mRNA_{tot}] - [R_2] - [R_2M]$, respectively. The system expands by exponential growth with cell growth rate μ , defined by

$$\mu = \frac{v_e \cdot [R_2']}{\rho_0}, \quad [2]$$

where v_e is the average elongation rate of an uninhibited ribosome and ρ_0 is the concentration of amino acids incorporated in proteins. The total concentration of 50S subunits ($[50S_{tot}]$) is kept constant and new 50S subunits are thus synthesised by rate $\mu \cdot [50S_{tot}]$ and the free concentration of 50S subunits varies according to $[50S] = [50S_{tot}] - [50SM] - [R_1] - [R_1M] - [R_2] - [R_2'] - [R_2M]$.

The system was solved numerically by Euler's method. Cell growth was calculated for the first 8 hours after introduction of a certain macrolide concentration the growth medium, $[m_m]$ by

$$V_t = V_{t-dt} \cdot e^{\mu \cdot dt}, \quad [3]$$

where dt is a small time-step and V_{t-dt} and V_t is the volume prior and after time-step dt . Prior to macrolide exposure, the system resided at steady state for a certain synthesis rate of resistance peptide mRNA. The used program software was MATLAB 6.5 (The MathWorks, Inc., Natick, Massachusetts, U.S.A.).

The effect of the erythromycin ejection mechanism in relation to the exchange dynamics of erythromycin over the cell membrane

For the *in vivo* experiments presented in the paper, the Gram-negative bacterium *Escherichia coli* was used. The entrance rate of macrolide antibiotics is expected to be slow in Gram-negatives because the outer membrane confers an efficient barrier of permeation. If the inflow rate is low, a high outflow rate is required to make the "bottlebrush" mechanism function for a macrolide with the kinetic properties of erythromycin (Nilsson *et al.*, manuscript in preparation). Broad-specific efflux pumps in the inner membrane, mainly the AcrAB-TolC pump system, may provide the required high outflow rate (Li and Nikaido, (2004) *Drugs* **64**(2), 159-204). We adjusted the influx rate constant (r_{in}) and the efflux rate constant (r_{out}) to reconstitute the pattern of the growth curves from the *in vivo* experiments in Fig. 3C. The efflux rate constant determines the general form of the curves and width of the antibiotic interval within which the "bottlebrush" confers resistance. The influx rate constant determines which erythromycin concentrations that lie within the interval of antibiotic concentrations that confer resistance (Nilsson *et al.*, manuscript in preparation). See Supplement table 1 for used parameter values in the model.

Supplement table 1. Definitions and values of used parameters.

	Description	Value	Reference
k_a	association rate constant of ribosomal subunits at initiation of translation	$2 \cdot 10^6 \text{ M}^{-1} \text{ s}^{-1}$	(1)
k_1	rate constant for translation of the first codons when the ribosome is susceptible for the antibiotic or for translation of a resistance peptide by a drug-free ribosome	1 s^{-1}	(2)
k_2	rate constant for translation of a resistance peptide by an erythromycin-infected ribosome	0.1 s^{-1}	Present study
k_3	rate constant for translation beyond the first codons of a protein mRNA and translation termination	0.03 s^{-1}	(2)
k_4	drop-off rate constant of peptidyl-tRNA from a stalled ribosome on a protein mRNA	0.06 s^{-1}	Lovmar, unpublished results
q	association rate constant of erythromycin	$10^6 \text{ M}^{-1} \text{ s}^{-1}$	(4)
q_1	dissociation rate constant of erythromycin	0.01 s^{-1}	(4)
k_{s1}	synthesis rate of resistance peptide mRNA (rpmRNA)	$0.06 \cdot 10^{-8} \text{ Ms}^{-1}$	
k_{d1}	degradation rate constant of free rpmRNA	$8.33 \cdot 10^{-3} \text{ s}^{-1}$	
k_{s2}	synthesis rate of protein mRNAs	$8.33 \cdot 10^{-9} - 0.05 \cdot k_{s1} \text{ Ms}^{-1}$	(5)
k_{d2}	degradation rate constant of free protein mRNAs	$8.33 \cdot 10^{-3} \text{ s}^{-1}$	(3)
k_{d3}	degradation rate constant of protein mRNAs with a drug-inhibited, stalled ribosome	$8.33 \cdot 10^{-4} \text{ s}^{-1}$	
r_{in}	rate constant of influx over cell membrane (membrane permeability constant)	$3 \cdot 10^{-5} \text{ s}^{-1}$	
r_{out}	rate constant of efflux over cell membrane (membrane permeability or pump capacity)	0.18 s^{-1}	*
v_e	elongation rate of an uninhibited ribosome	20 s^{-1}	(2)
ρ_0	concentration of amino acids in proteins	2 M	(2)
$[50S_{tot}]$	total concentration of 50S ribosomal subunits	$4 \cdot 10^{-5} \text{ M}$	(2)
$[m_m]$	concentration of macrolide in the growth medium	$0.7 - 220 \text{ } \mu\text{g/ml}$	(see Fig. 3B)

1. Antoun, A., Pavlov, M., Andersson, A., Tenson, T. & Ehrenberg M. (2003) *EMBO J.* **22**, 5593-5601.
2. Bremer, H. & Dennis, P. (1996) in *Escherichia coli and Salmonella typhimurium Cellular and Molecular Biology*, ed. Neidhardt, F. C. (ASM Press, Washington, DC.), pp. 1553-1569.
3. Kushner, S. R. (1996) in *Escherichia coli and Salmonella typhimurium Cellular and Molecular Biology*, ed. Neidhardt, F. C. (ASM Press, Washington, DC.), pp. 849-860.
4. Lovmar, M., Tenson T. & Ehrenberg, M. (2004) *J. Biol. Chem.* **279**, 53506-53515.
5. Neidhardt, F. C. & Umbarfer, H. E. (1996) in *Escherichia coli and Salmonella typhimurium Cellular and Molecular Biology*, ed. Neidhardt, F. C. (ASM Press, Washington, DC.), pp. 13-16.

* If the inflow rate is low as expected in Gram-negative bacteria such as *Escherichia coli*, which was used in the *in vivo* experiments presented in the paper, a high outflow rate is required to make the “bottlebrush” mechanism function for a macrolide with the kinetic properties of erythromycin. Broad-specific efflux pumps in the inner membrane, mainly the AcrAB-TolC pump system, may provide the high outflow rate (Nilsson *et al.*, manuscript in preparation).



III



Mechanisms and Requirements of Peptide-Mediated Macrolide Resistance

Karin Nilsson^{1,2*}, Martin Lovmar^{2*}, Vladimir Vimberg³, Tanel Tenson³ and Måns Ehrenberg²

¹ Department of Biometry and Engineering, Swedish University of Agricultural Sciences, Uppsala S-75007, Sweden

² Department of Cell and Molecular Biology, Molecular Biology Program, Uppsala University, Uppsala S-75124, Sweden

³ Institute of Technology, Tartu University, 51010 Tartu, Estonia

* Equal contribution.

Correspondence to: Måns Ehrenberg
Dept. of Cell and Molecular Biology,
Molecular Biology Program,
BMC, Box 596, Uppsala University,
S-75124 Uppsala, Sweden
E-mail: ehrenberg@xray.bmc.uu.se
Tel: +46 18 471 42 13
Fax: +46 18 471 42 62

ABSTRACT

Macrolide antibiotics bind at the entrance of the nascent peptide exit tunnel of the large ribosomal subunit, inducing premature termination of translation by drop-off of peptidyl-tRNA. Expression of specific *cis*-acting peptides confers resistance to macrolides. Recently the molecular mechanism behind erythromycin resistance was revealed. The resistance peptide works like a “bottle-brush” and expels erythromycin from the ribosome upon termination of translation. Here, we have used a cell-free translation system to study the mechanism of peptide-mediated josamycin resistance. Distinct from erythromycin resistance peptides, expression of a josamycin resistance peptide did not lead to an increased dissociation of the drug. Instead, the rate of resistance di-peptidyl-tRNA drop-off is decreased by an order of magnitude compared to the control peptide. Further, the level of resistance is independent of the length of the josamycin resistance peptide mRNAs while erythromycin resistance peptides show strict length dependence. We propose therefore that josamycin resistance peptides work by “quarantining” the josamycin bound ribosomes. A quantitative model of the josamycin resistance was constructed and it mimics the degree of resistance in *Escherichia coli* cells expressing a resistance peptide and subjected to varying concentrations of josamycin. Both this model and the previous model for erythromycin resistance predict that an active efflux pump system is required for the resistance peptide mechanism to function. This prediction was tested using an *E. coli* mutant lacking a functional AcrAB-TolC efflux pump system and, indeed, no peptide mediated resistance was detected in the mutant.

INTRODUCTION

Since the 1950s macrolide antibiotics have been used in the treatment of infections (Weisblum, 1995). Macrolides consist of several neutral or amino sugars attached to a 14-, 15- or 16-membered lactone ring (Leclercq, 2002). The first generation contains naturally occurring 14-membered ring macrolides, and includes erythromycin, currently the best-known macrolide. Josamycin belongs to the second generation, with a 16-membered lactone ring (Weisblum, 1998). Macrolides bind to the large ribosomal subunit, in the vicinity of the peptidyl transferase centre (Hansen *et al.*, 2002; Schlunzen *et al.*, 2001) and most likely inhibit protein synthesis by blocking the entrance to the tunnel through which nascent peptides exit the ribosome (Lovmar *et al.*, 2004; Tenson *et al.*, 2003). Resistance mechanisms to macrolide antibiotics include modifications of the drug-binding site, inactivation of the drug by degradation or modification and cellular efflux by specialized transporter proteins (Weisblum, 1998). However, in the focus in this study is a unique resistance mechanism conferred by expression of specific *cis*-acting peptides (Tenson and Mankin, 2001).

Peptides mediating macrolide resistance was first encountered in experiments where *E. coli* cells expressed random rRNA fragments of the *rrnB* operon (Tenson *et al.*, 1996). Biochemical and genetic studies revealed the presence of a 34 nucleotides long mini-gene ranging between positions 1235 and 1268 in domain II of the 23S rRNA in all resistant clones. Additional *in vitro* experiments, where resistance peptides or resistance peptide mRNA (rpmRNA^{eryt}) were supplied, showed the necessity of active translation of the rpmRNA^{eryt} for protection against erythromycin. Using selection

from random libraries it became clear that the resistance peptides require both specific length and sequence (Tenson *et al.*, 1997). Tripathi *et al.* (1998) proposed a “bottlebrush” model based on these experiments and further library studies selecting resistance peptides against a ketolide. The “bottlebrush” model suggests that synthesis of a resistance peptide removes the drug molecule, by direct interaction between macrolide and resistance peptide, thus restoring the protein synthesis capability of the ribosome. The resistance peptide acts as a “bottlebrush” and “cleans” the ribosome. Recently, Lovmar *et al.* (2006) showed that synthesis of a *cis*-acting peptide indeed accelerates the rate of erythromycin dissociation by destabilizing the binding of the drug to the ribosome. In addition, it was shown that erythromycin was most probably always expelled from the ribosome during release factor mediated translation termination. The biochemical data was also used within the framework of a mathematical model to predict resistance and finally the predictions of the model could be validated by growth experiments *in vivo*.

It has been suggested that the “bottlebrush” mechanism is general and work for all classes of macrolides with modulated specific sequences (Tenson and Mankin, 2001; Tripathi *et al.*, 1998; Vimberg *et al.*, 2004). However, in the case of josamycin there are at least two major features suggesting a closer examination of the effects of $\text{rpmRNA}^{\text{josa}}$ expression. First, peptidyl transfer is inhibited already after 2 or 3 amino acids in the presence of josamycin (Lovmar *et al.*, 2004; Tenson *et al.*, 2003), and the selected resistance peptides, containing 4 or 5 amino acids (Vimberg *et al.*, 2004), will therefore never reach the stop codon and thus never reach the termination step which seems to be crucial for the “bottlebrush” mechanism. Secondly, josamycin is bound to the ribosome 1.5 h on the average (Lovmar *et al.*, 2004). This means that a dissociation rate increase of josamycin by a factor of 10 as measured for $\text{rpmRNA}^{\text{eryt}}$ will still not render resistance since the peptidyl-tRNA drop-off rate would still be much higher (Lovmar *et al.*, 2006).

We begin this study with a biochemical characterization of the peptide mediated josamycin resistance. In combination with an examination of how the activities of $\text{rpmRNA}^{\text{josa}}$ and $\text{rpmRNA}^{\text{eryt}}$ depend on the length of the encoded peptides it enables us to conclude that they work through different mechanisms. Using the rate constants from the biochemistry in a mathematical model, similar to the previously published one (Lovmar *et al.*, 2006), we propose that the effect of $\text{rpmRNA}^{\text{josa}}$ is to “quarantine” a fraction of the josamycin containing ribosomes from the active pool of ribosomes. How expression of $\text{rpmRNA}^{\text{josa}}$ can be connected to the growth and survival of cells at different concentrations of josamycin is examined in the model, and the result is compared to *in vivo* growth curves.

Previous modeling of peptide-mediated erythromycin resistance resulted in one clear predicted requirement for the resistance mechanism to function; the intracellular concentration of erythromycin has to rapidly equilibrate with the surrounding media (Lovmar *et al.*, 2006). However, all *in vivo* experiments were performed with gram-negative *Escherichia coli* cells where the outer membrane offers an efficient barrier of permeation (Lovmar *et al.*, 2006; Tenson and Mankin, 2001). It seemed therefore that either the prediction, and thus also the model, has to be wrong or there had to be more to the story than appreciated at first. In the previous paper we argued that broad-specific multi-drug pumps located in the inner membrane, especially the AcrAB-TolC system (Zgurskaya and Nikaido, 1999), may account for the rapid antibiotic

equilibration required to confer peptide-mediated resistance (Lovmar *et al.*, 2006). This prediction is tested in this study using a mutant without a working AcrAB-TolC system and both the resulting increase in sensitivity and the loss of peptide mediated resistance of the mutant corresponds well with the model predictions.

EXPERIMENTAL PROCEDURES

Chemicals and buffers

GTP, ATP and [³H]Met were from GE Biosciences (Uppsala, Sweden). Putrescine, spermidine, phosphoenolpyruvate (PEP), myokinase (MK), inorganic pyrophosphatase (PPiase), erythromycin and non-radioactive amino acids were from Sigma-Aldrich (St. Louis, MO, USA). Pyruvate kinase (PK) was from Boehringer-Mannheim (Mannheim, Germany). Josamycin was from Alexis Biochemicals (Lausen, Switzerland).

All experiments were performed in polymix buffer, at working strength containing 5 mM magnesium acetate, 5 mM ammonium chloride, 95 mM potassium chloride, 0.5 mM calcium chloride, 8 mM putrescine, 1 mM spermidine, 5 mM potassium phosphate and 1 mM dithioerythritol (DTE) (Jelenc and Kurland, 1979).

In vitro transcribed mRNA for the cell-free translation system

The template DNAs for *in vitro* transcription were prepared by annealing the following oligonucleotides at the complementary sequences (underlined) and filling the gaps by PCR.

Forward oligo: CTCTCTGGTACCGAAATTAATACGACTCACTATAGGGAATT
CGGGCCCTTGTTAACAATTAAGGAGG.

Reverse oligo for MFLV: TTTTTTTTTTTTTTTTTTTTTTTATACTAGGAACATAG
TATACCTCCTAATTGTTAACAAGGGCCCG

Reverse oligo for MVSN: TTTTTTTTTTTTTTTTTTTTTTTAGTTAGAAACCATAG
TATACCTCCTAATTGTTAACAAGGGCCCG

In vitro transcription and purification of mRNAs containing a poly(A) tail were as described in (Pavlov and Ehrenberg, 1996).

DNA oligos used to create plasmids expressing peptides of variable lengths

DNA sequences of different length, designed were amplified by annealing the following oligonucleotides and fill the gaps with PCR. The PCR products were subsequently cut with *Eco*RI and *Afl*II restriction enzymes and cloned into a pPOT1AE vector (Tenson *et al.*, 1996).

Forward oligo for rpmRNA^{josa}: ATACAATTGCTAGTCTTAAGGAGGTCACAT
ATGTTC

Reverse oligo for rpmRNA^{josa+LLA}: CTAGAGAATTCAGCTAGTTACGCCAG
AAGTACTAGGAACATATGTGACCTC

Reverse oligo for rpmRNA^{josa+LLASGS}: CTAGAGAATTCAGCTAGTTAGCTGCC
TGACGCCAGAAGTACTAGGAACATATGTGACCTC

Reverse oligo for rpmRNA^{josaMF}: CTAGAGAATTCAGCTAGTTAGAAACAT
ATGTGACCTC)

Forward oligo for rpmRNA^{eryt}: ATACAATTGCTAGTCTTAAGGAGGTCACAT
ATGGTT

Reverse oligo for rpmRNA^{eryt+LL}: CTAGAGAATTCAGCTAGTTACAGAAGAAC
AAACAAAACCATATGTGACCTC

Reverse oligo for rpmRNA^{eryt+LLASG}: CTAGAGAATTCAGCTAGTTAGCCTGAC
GCCAGAAGAACAAAACAAAACCATATGTGACCTC

Reverse oligo for rpmRNA^{erytMV}: CTAGAGAATTCAGCTAGTTAAACCAT
ATGTGACCTC

Procedures

The components of the purified translation system

Components of the translation system were purified as described in (Tenson *et al.*, 2003), except for RF1, RF2 and RF3 which were purified as described in (Freistoffer *et al.*, 1997), RRF as described in (MacDougall *et al.*, 1997) and peptidyl-tRNA hydrolase (PTH) as described in (Dincbas *et al.*, 1999). All experiments were performed at 37 °C in polymix buffer with addition of ATP (1 mM), GTP (1 mM) and PEP (10 mM).

Recycling experiments

The initiation mixture contained ribosomes (0.2 μM, ~50% active), [³H]fMet-tRNA^{fMet} (5 μM), mRNA (0.5 μM), IF2 (0.5 μM), IF1 (1 μM), IF3 (1 μM) and josamycin (2.5 μMn). The recycling mixture contained EF-G (2 μM), EF-Tu (30 μM), EF-Ts (1 μM), RF2 (2 μM), RF3 (2 μM), RRF (2μM), tRNA^{bulk} (~0.18 mM), PPIase (5 μg/ml), MK (3 μg/ml), PK (50 μg/ml), the relevant aminoacyl-tRNA synthetases (aaRS) (0.15 Units/μl) (defined in (Ehrenberg *et al.*, 1990)) and amino acids (aa) (leucine 300 μM and 100 μM each of the others). Erythromycin (100 μM) was also added to the recycling mixture when relevant.

Both initiation mixture and recycling mixture were pre-incubated for 8 minutes at 37 °C to allow for formation of ribosomal initiation complexes and ternary complexes, respectively. At time zero, the initiation mixture (10 μl) and the recycling mixture (10 μl) were mixed and at the specified time points the reactions were quenched by adding 155 μl 20% formic acid, and peptide formation were analyzed using RP-HPLC as described in (Tenson *et al.*, 2003). Peptidyl-tRNA hydrolase (~250 Units (hydrolysed tRNA/s)) was added to the reaction mixture 15 s prior to quenching to allow detection of the drop-off products on the HPLC in parallel to the full-length peptide.

Measuring the length dependence for josamycin- and erythromycin resistance peptides

Overnight cultures of cells expressing peptides of different length were grown in medium containing 100 μg/ml ampicillin. Cultures were diluted with fresh medium containing 100 μg/ml ampicillin, 1 mM IPTG, 75 μg/ml erythromycin or 200 μg/ml josamycin and in parallel with medium containing 100 μg/ml ampicillin, 1 mM IPTG to the final density of A₆₀₀ = 0.01. Cells were grown until the optical densities of cultures grown in the absence of macrolide reached A₆₀₀ of c.1. At this point the absorbance of the corresponding macrolide containing culture was measured, which is equal to the relative resistance because the absorbance of the culture grown without macrolide is one.

Measuring growth with varying josamycin concentration and rpmRNA^{jos} expression levels

Overnight cultures of cells expressing rpmRNA^{jos} (MFLV-peptide) were grown in medium containing 100 µg/ml ampicillin. Cultures were diluted to A₆₀₀ = 0.01 into 96-well plates with fresh medium containing josamycin and IPTG at different concentrations. IPTG concentrations for rpmRNA^{jos} expressing cells were 0 µM; 50 µM; 75 µM; 100 µM; 125 µM; 150 µM; 175 µM; 200 µM; 500 µM; 1000 µM. Josamycin concentrations were 0 µg/ml; 100 µg/ml; 150 µg/ml; 200 µg/ml; 250 µg/ml; 300 µg/ml; 500 µg/ml; 1000 µg/ml. The cell cultures were grown 8 hours and the absorbance at 600 nm were measured using a TECAN Sunrise instrument.

Measuring the effect of efflux pump mutants on josamycin sensitivity and resistance

MG1655 cells and MG1655 TolC mutant cells, expressing rpmRNA^{eryt} (MVLV-peptide) or rpmRNA^{jos} (MFLVLLA-peptide), or possessing empty vector pPOT1 (Tenson *et al.*, 1996) were grown overnight in 2*YT medium in the presence of ampicillin (100 µg/ml) at 37 °C. Overnight cultures were diluted to A₆₀₀ = 0.01 with fresh 2*YT medium containing 100 µg/ml ampicillin, 100 µM IPTG and different concentrations of erythromycin and josamycin respectively. Cultures were grown in the microtiter plate for 4 hours at 37 °C and A₆₀₀ was measured using a TECAN Sunrise instrument. Expression of rpmRNA^{jos} encoding MFLVLLA-peptide was used instead of the classical MFLV-peptide, because MFVLLA expression does not inhibit bacterial growth.

RESULTS

Biochemical characterization of expression of josamycin resistance peptide

Using a cell-free translation system with purified components from *E. coli* (Pavlov and Ehrenberg, 1996) we translated the rpmRNA^{jos} encoding fMet-Phe-Leu-Val (Vimberg *et al.*, 2004) and a control mRNA encoding fMet-Val-Ser-Asn. The ribosomes were pre-incubated with either josamycin or erythromycin and used in recycling mode (Pavlov *et al.*, 1997), *i.e.* each ribosome produced several copies of the encoded peptide. In order to probe the dissociation of josamycin we chased it with an excess of erythromycin, which competes with josamycin binding but allows formation of tetrapeptides (Lovmar *et al.*, 2006; Lovmar *et al.*, 2004). The amounts of resistance- and control tetrapeptides produced at different time points are shown in Figs. 1A and 1B, respectively. As expected from the previous studies, josamycin blocked formation of both tetrapeptides, while erythromycin allowed tetrapeptide formation. From the chase experiments it is clear that translation of the rpmRNA^{jos} does not significantly increase the josamycin dissociation rate over translation of the control peptide. From these chase experiments the josamycin dissociation rate constant could be estimated to 0.01 min⁻¹ which is similar to the previously estimated spontaneous dissociation rate constant (Lovmar *et al.*, 2004).

In parallel to the measurements of tetrapeptide formation we also studied the drop-off products formed during translation of rpmRNA^{jos} (Fig. 1C) or control mRNA (Fig. 1D). Interestingly, josamycin-containing ribosomes produced much less dipeptidyl-tRNA when translating the rpmRNA^{jos} rather than the control peptide. The “production” of drop-off products occurs at 0.28 min⁻¹ when josamycin containing ribosomes are translating rpmRNA^{jos}, compared to 2.1 min⁻¹ when translating the control mRNA. The reason for this difference is that josamycin inhibits the peptidyl transfer to the phenylalanine acceptor much more efficiently than to the valine

acceptor (Lovmar *et al.*, 2004). This causes the $\text{rpmRNA}^{\text{josa}}$ to block josamycin containing ribosomes as stable initiation complexes, while peptidyl transfer and subsequent josamycin induced peptidyl-tRNA drop-off is much faster for the control mRNA.

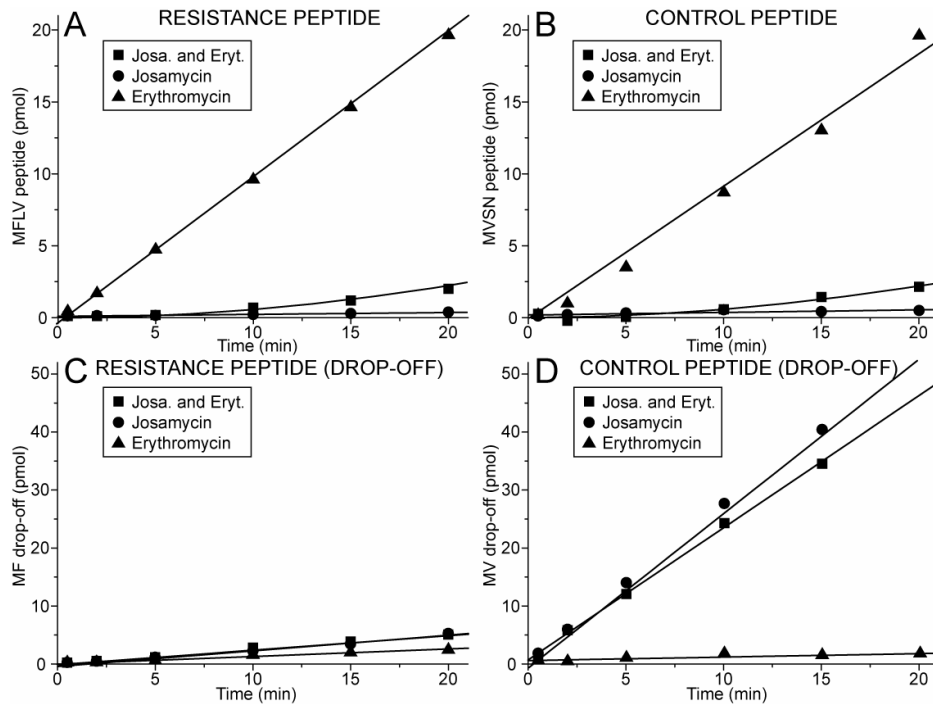


FIGURE 1. Biochemical characterization of peptide mediated josamycin resistance. The amounts of produced resistance peptide (MFLV, panel A) and control peptide (MVSN, panel B) are plotted against time. Erythromycin (▲) allows formation of both tetra-peptides, while josamycin (●) does not allow any tetra-peptide formation. When josamycin dissociates in the chase experiment (■) it is replaced by erythromycin which enables tetra-peptide formation. In panels C and D the accumulation of dipeptidyl-tRNA drop-off products are plotted against time. The symbols in panels C and D is the same as the corresponding experiment in panels A and B. All experiments contain 1 pmol of active ribosomes.

Erythromycin resistance is strictly dependent on the length of the encoded peptide while josamycin resistance is not

The biochemical data propose that the mechanism of $\text{rpmRNA}^{\text{josa}}$ is different to the previously described “bottle-brush” mechanism, and that it instead depends on the reduced rate of peptidyl tRNA-drop-off. The prediction is therefore that $\text{rpmRNA}^{\text{josa}}$, in contrast to $\text{rpmRNA}^{\text{eryt}}$, is insensitive to the length of the encoded peptide. This prediction was tested by measuring the resistance activity *in vivo* of both $\text{rpmRNA}^{\text{josa}}$ and $\text{rpmRNA}^{\text{eryt}}$ encoding peptides with varying lengths (Fig. 2).

The length of the open reading frames of both rpmRNAs were decreased to two codons and increased to seven or ten codons. Bacteria expressing the natural or the modified variants of rpmRNA^{eryt} and rpmRNA^{josa} were grown in the presence and in the absence of the corresponding macrolide. The ratios of the optical densities with or without the respective macrolide are plotted for these strains in figure 2. The length of rpmRNA^{eryt} is crucial for resistance against erythromycin (Fig. 2A), while josamycin resistance by rpmRNA^{josa} is solely dependent on the nature of the second codon and independent of the length in accordance with the prediction (Fig. 2B).

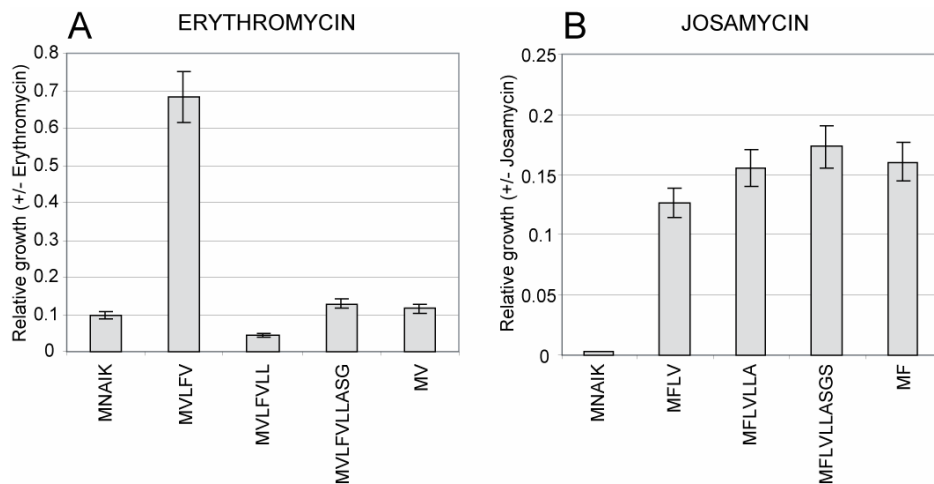


FIGURE 2. The degree of erythromycin resistance is strictly dependent on resistance peptide length but not peptide-mediated josamycin resistance. Resistance is given as the ratio of bacterial growth as measured by optical density of resistance peptide expressing cells in the presence of (A) erythromycin (75 $\mu\text{g/ml}$) or (B) josamycin (200 $\mu\text{g/ml}$), respectively, and bacterial growth in the absence of the macrolide for the indicated peptide sequences.

Expression of rpmRNA^{josa} “quarantines” ribosomes with josamycin and reduces peptidyl-tRNA drop-off

The biochemical experiments described above in combination with previous studies provide kinetic constants that allow modeling of the direct effects of expression of rpmRNA^{josa} (Table 1 in Appendix). We adapted our previously developed model of peptide-mediated erythromycin resistance to josamycin as illustrated in Fig. 3A (see Appendix for details), but because expression of rpmRNA^{josa} does not promote dissociation of josamycin it can not increase protein synthesis directly.

Instead, expression of rpmRNA^{josa} “quarantines” josamycin containing ribosomes in form of initiation complexes encoded with rpmRNA^{josa}. The direct effect of this “quarantine” is that the amount of peptidyl-tRNA drop-off is reduced (Fig. 3B), and thereby there is a reduced risk of peptidyl-tRNA hydrolase (Pth) saturation leading to depletion of tRNA pools. The selectivity of the “quarantine” mechanism allows a large fraction of the josamycin-free ribosomes to continue translating cellular mRNAs, despite the competition with high concentration of rpmRNA^{josa}.

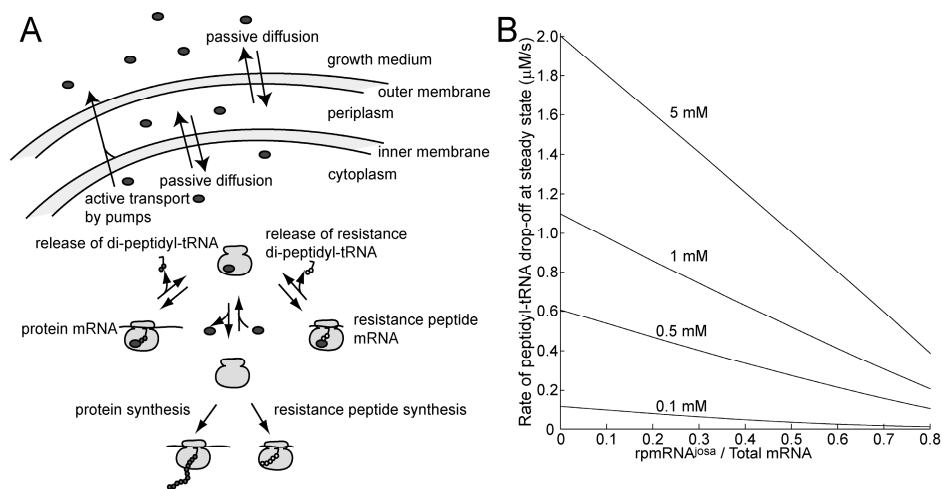


FIGURE 3. Modeling the “quarantine” mechanism. Panel A show a schematic of the model. A josamycin-carrying ribosome stalls on a $\text{rpmRNA}^{\text{josa}}$ (right) or on a protein mRNA (left) which results in drop-off of di-peptidyl-tRNA while josamycin stays bound on the ribosome. A drug-free ribosome completes both protein and resistance peptides synthesis (bottom). The uppermost part illustrates influx and efflux of josamycin in the cell (gram-negative bacterium). Panel B shows how the amount of peptidyl-tRNA drop-off is decreased by expression of $\text{rpmRNA}^{\text{josa}}$.

mRNA limitation might account for the observed resistance peptide action *in vivo*

In addition to the “quarantine” effects described above will expression of $\text{rpmRNA}^{\text{josa}}$ lead to an increase in the total number of ribosome binding sites (RBS) because of the small size of $\text{rpmRNA}^{\text{josa}}$ (assuming a fixed capacity of the RNA polymerases). This increase may be important because josamycin-containing ribosomes block RBS, eventually leading to mRNA depletion. Further, an increased concentration of RBS may lead to more rapid initiation and thus josamycin will have a smaller time window for binding the josamycin-free ribosomes. It is therefore possible that expression of $\text{rpmRNA}^{\text{josa}}$ indirectly can decrease the fraction of ribosomes that contains josamycin.

We modeled the quantitative effects of $\text{rpmRNA}^{\text{josa}}$ expression by focusing on mRNA supply. Especially, the degradation of a protein mRNA with a stalled josamycin-ribosome in the 5' end was modeled in detail. As previously, the model also described both synthesis and degradation of both mRNA and $\text{rpmRNA}^{\text{josa}}$ as well as dynamics of the antibiotic exchange over the inner and outer cell membranes. In addition, the model accounts for the dilution of all compounds due to cell growth. Using this model we predicted the growth at 8 hours after expression of $\text{rpmRNA}^{\text{josa}}$ at different levels in the presence of different concentrations of josamycin (Fig. 4A). It should be pointed out that modeled resistance by mRNA limitation crucially depends on a much slower drop-off rate of the resistance di-peptidyl-tRNA than of other dipeptidyl-tRNAs.

Peptide-mediated josamycin resistance demonstrated by cell population growth

The expression of resistance peptide mRNA coding for peptide MFLV was under *tac* promoter control on a multi-copy plasmid and the expression level could therefore be varied by varying the concentration of IPTG. Cell growth at different IPTG and josamycin concentrations was detected by optical density at 600 nm after 8 hours following the addition of josamycin to the growth medium (Fig. 4B). The results correspond well with the predicted behavior from the mRNA depletion model (Fig. 4A).

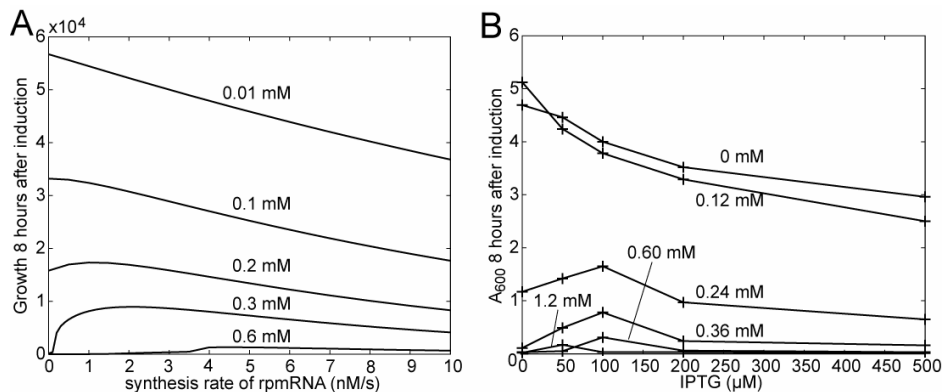


FIGURE 4. Comparison between modeled and *in vivo* peptide-mediated josamycin resistance. A. Simulated growth (defined as how many times the cell volume has increased during the first 8 hours after the addition of josamycin) plotted against the rate of resistance peptide mRNA synthesis for different concentrations of josamycin. B. Optical density (600 nm) measured 8 hours after the addition of josamycin plotted against the concentration of IPTG.

Peptides mediate macrolide resistance in wild-type *E. coli* cells but not in a pump mutant

It has previously been predicted that the resistance peptide mechanism requires rapid equilibration between the intracellular macrolide concentration and the concentration in the surrounding media. It was further proposed that this could be accomplished by a naturally occurring drug-efflux system (Lovmar *et al.*, 2006). Therefore, the resistance models for josamycin and erythromycin were used with the more detailed description of the flows of the antibiotic over the cell membranes described here to study resistance with and without antibiotic efflux pumps (see Appendix). As expected, removal of the antibiotic efflux pump system makes the cells hypersensitive to both erythromycin and josamycin, but in addition the model predicts that the peptide mediated resistance disappears (Fig. 5).

To validate these results we studied growth in bacterial populations of both wild-type *E. coli* cells and *E. coli* cells (TolC) with a mutated efflux pump system, containing a multi-copy vector expressing rpmRNA or containing a control vector. Expression of rpmRNA was under the control of a *tac* promoter induced by 100 μ M of IPTG which corresponds to maximal resistance as observed in Fig. 4B for josamycin and as

previously reported for erythromycin (Fig. 3C in (Lovmar *et al.*, 2006)). Bacterial mass was monitored as absorbance at 600 nm 4 hours after addition of varying concentrations of erythromycin or josamycin to the growth medium. Both the increased sensitivity and the loss of resistance were observed in the TolC mutant (Fig. 6).

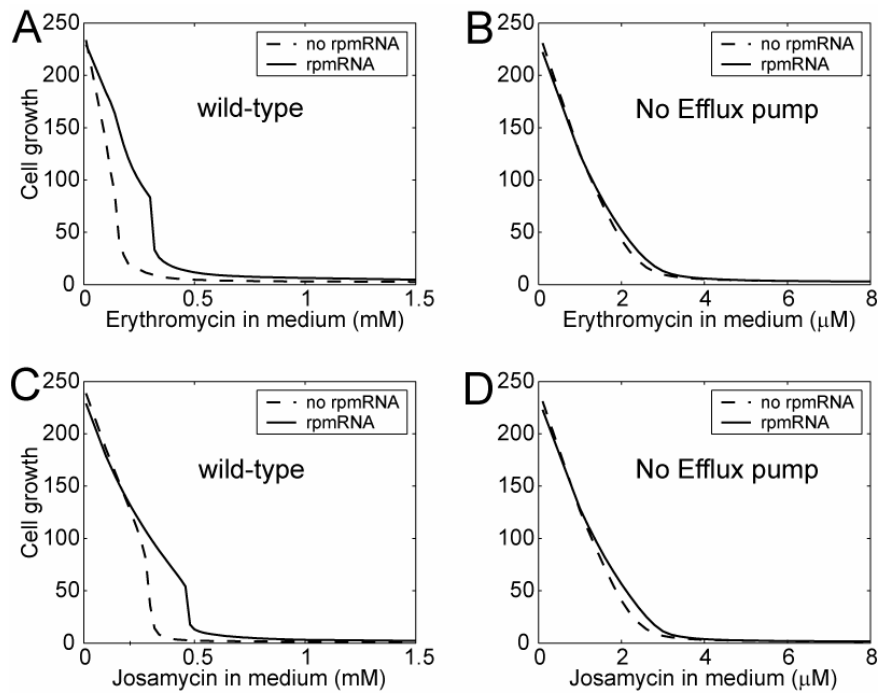


FIGURE 5. Modeled peptide-mediated resistance with but not without pumps. Cell growth is given as volume expansion (defined as how many times the cell volume has increased) 4 hours following the introduction of the indicated macrolide concentrations in the growth medium in the model, with resistance peptide mRNA (rpmRNA) expression (solid line), without rpmRNA expression (broken line). The wild-type (A and C) is modelled with pumps in the inner membrane but not the TolC mutant (B and D). The rate constant of rpmRNA synthesis was 2 nMs^{-1} .

DISCUSSION

Although the clinical relevance of peptide mediated resistance is not clear, it is still an interesting phenomenon that reveals more information about the mechanisms by which macrolide antibiotics inhibit cell growth. It was previously shown that rpmRNA^{eryI} works through a “bottle-brush” mechanism, *i.e.* expression of a resistance peptide “cleans” the nascent peptide exit tunnel from erythromycin (Lovmar *et al.*, 2006). Both the amino acid sequence and the length of the encoded peptide are essential parameters for the “bottle-brush” mechanism to work (Tenson *et al.*, 1997) and, at least in the erythromycin case, the drug seems to be stoichiometrically expelled at the termination step (Lovmar *et al.*, 2006). The “bottle-brush” mechanism has been proposed to be general for all classes of macrolides, albeit with modulated

sequence specificity (Vimberg *et al.*, 2004). The 16-membered macrolide josamycin has been shown to in most cases only allow a single peptidyl transfer reaction to occur before the peptidyl-tRNA dissociates (Tenson *et al.*, 2003) and it was therefore surprising that $\text{rpmRNA}^{\text{josa}}$ expressing tetra- or pentameric peptides could be selected (Vimberg *et al.*, 2004). The present study clearly shows that the “bottle-brush” mechanism is not responsible for the peptide-mediated resistance against josamycin; instead we propose a “quarantine” mechanism to be responsible for the observed resistance.

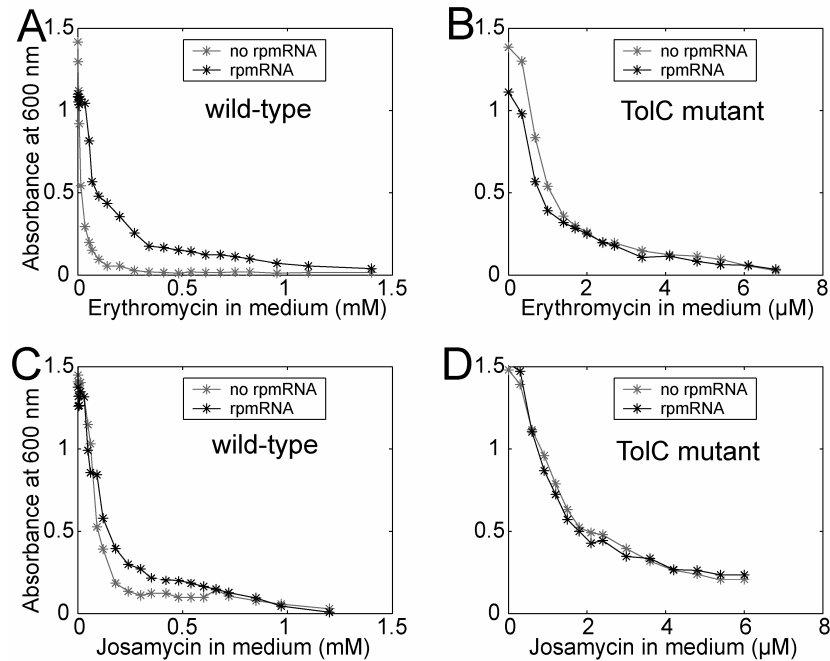


FIGURE 6. Peptide-mediated resistance *in vivo* in the wild-type but not in a pump mutant. Absorbance (600 nm) of wild-type (A and C) and TolC (pump) mutant (B and D) *Escherichia coli* cells with a resistance peptide expressing vector (rpmRNA) or a control vector (no rpmRNA) after 4 hours of growth following addition of the indicated macrolide concentrations.

Comparison between $\text{rpmRNA}^{\text{josa}}$ and $\text{rpmRNA}^{\text{eryt}}$

Expression of $\text{rpmRNA}^{\text{eryt}}$ increase the erythromycin dissociation rate constant by an order of magnitude in concordance with the suggested “bottle-brush” mechanism (Lovmar *et al.*, 2006). In contrast, expression of $\text{rpmRNA}^{\text{josa}}$ did not change the dissociation rate constant of josamycin (Figs. 1A and 1B), but instead it slowed down the rate of peptidyl-tRNA drop-off by an order of magnitude (Fig. 1C) compared to the control mRNA (Fig. 1D). Peptidyl-tRNA drop-off is not an issue during $\text{rpmRNA}^{\text{eryt}}$ expression, because erythromycin leaves enough space in the tunnel to allow translation of the complete penta-peptide (Tenson *et al.*, 2003). The present results on $\text{rpmRNA}^{\text{josa}}$ suggest that it is never completely translated and thus the resistance mechanism for josamycin should be independent of the length of the encoded peptide. This is in contrast to the results on erythromycin resistance where

the peptide length was shown to be crucial for erythromycin resistance both in living cells (Tenson *et al.*, 1997) and in a cell-free translation system (Lovmar *et al.*, 2006).

The prediction on the length dependence was tested by expressing peptides with lengths varying between 2 and 10 amino acids with sequences according to the consensus for rpmRNA^{eryt} and rpmRNA^{josa} respectively (Vimberg *et al.*, 2004). The resistance activity of rpmRNA^{eryt} was shown to be strongly peptide length dependent in agreement with previous experiments (Fig. 2A). In contrast to rpmRNA^{eryt}, but in agreement with the prediction, is the activity of rpmRNA^{josa} not sensitive to the length of the expressed peptides (Fig. 2B). The reason that most of the selected rpmRNA^{josa} encoded pentamers was simply that the mini-gene library encoded pentamers with randomized sequences (Vimberg *et al.*, 2004). In conclusion, it seems that the only important feature of rpmRNA^{josa} appears to be that it encodes a phenylalanine or tyrosine in the second position (Vimberg *et al.*, 2004).

Josamycin resistance through “quarantining” josamycin containing ribosomes

At first it might be hard to imagine how expression of an mRNA encoding phenylalanine or tyrosine in the second position can render resistance to josamycin. The key to understand the mechanism can be found in the slow peptidyl-tRNA drop-off rate when expressing rpmRNA^{josa} compared to other mRNAs. Because rpmRNA^{josa} can not expel josamycin from the ribosomes, it instead works by minimizing the negative effects of josamycin bound ribosomes through “quarantining” them on rpmRNA^{josa}. The “quarantine” can be understood as follows; ribosomes containing josamycin will be stuck on the rpmRNA^{josa} ten times longer than on other mRNAs, while ribosomes without josamycin recycles much faster on the short rpmRNA^{josa} than on other mRNAs. These combined effects lead to an enrichment of josamycin containing ribosomes on rpmRNA^{josa}, while the ribosomes without josamycin are enriched on protein mRNAs where they continue synthesizing proteins with less interference from ribosomes containing josamycin. A requirement for the “quarantine” to work is a very slow exchange of josamycin between different ribosomes, so that most of the ribosomes keep their identity as “josamycin-containing” or “josamycin-free” at least within the time range of ribosome recycling. The average recycling time for josamycin containing ribosomes on rpmRNA^{josa} is 4 minutes, and josamycin stays bound to a ribosome for an average time of 1.5 hours (Lovmar *et al.*, 2004) which clearly fulfils this requirement. It should further be noted that only very few natural mRNAs encodes phenylalanine or tyrosine in the second position, thus over-expression of rpmRNA^{josa} will have a strong impact on the fraction of mRNAs encoding these amino acids in the second position resulting in the “quarantine” effect.

The apparent explanation to why “quarantining” josamycin containing ribosomes on rpmRNA^{josa} confer resistance is that it reduces the demand of a component necessary for translation or recycling of ribosomes, thus allowing the josamycin-free ribosomes to continue translation at a close to normal rate. For example, the josamycin induced peptidyl-tRNA drop-off may accumulate peptidyl-tRNA in the cells, thus the pools of free tRNA isoacceptors will be depleted when the capacity of peptidyl-tRNA hydrolase (Pth) is saturated (Heurgue-Hamard *et al.*, 2000; Heurgue-Hamard *et al.*, 1996; Tenson *et al.*, 1999). There are also some unpublished results indicating that depletion of tRNA pools contributes to the josamycin toxicity, *i.e.* suppression of Pth expression makes cells hyper-sensitive to josamycin, while a slight over-expression of

Pth leads to low-level resistance (Tenson T, unpublished results). However, a fraction of ribosomes containing josamycin might deplete other components of the translation machinery before the pools of tRNAs, and therefore the “quarantine” mechanism might render resistance also without saturated Pth.

Resistance can occur through avoiding depletion of mRNA pools by “quarantining” the josamycin containing ribosomes

A bacterial population containing a plasmid-borne $\text{rpmRNA}^{\text{josa}}$ under control of the *tac* promoter was grown in media with varying IPTG concentrations to regulate the level of resistance peptide expression combined with varying josamycin concentrations. The increase in bacterial mass after 8 hours of growth after induction was monitored by absorbance as a function of the IPTG concentration in the medium. To test whether it is possible to reproduce the *in vivo* effects of $\text{rpmRNA}^{\text{josa}}$ expression without considering the tRNA pools we adapted the model previously developed for peptide-mediated erythromycin resistance (Lovmar *et al.*, 2006) to the parameter values for josamycin. The mathematical model was changed to account for josamycin resistance by modeling a delayed di-peptidyl-tRNA drop-off from a josamycin-carrying ribosome expressing the resistance peptide while the antibiotic stays bound to the ribosome. By assuming a low rate of degradation of mRNAs with a stalled ribosome in the 5' end (Joyce and Dreyfus, 1998), we obtained growth curves mimicking the *in vivo* observed growth curves (Fig. 4).

The importance of the modeled mRNA degradation can be understood as follows. The concentration of protein mRNAs in a cell is much lower than the concentration of ribosomes. Thus, only a small fraction of drug-inhibited ribosomes, stalled on mRNA can potentially severely slow down protein synthesis. When protein mRNAs with a stalled ribosome is slowly degraded, the free concentration of protein mRNAs on which a ribosome can initiate translation drastically declines (not shown). The delay at initiation increases the impact of josamycin since 50S subunits exist in a josamycin-susceptible state a longer period of time. The result is a larger fraction of non-translating and josamycin bound 50S subunits as well as a larger fraction of ribosomes stalled on mRNAs (not shown), which contributes to further lowering the concentration of free mRNAs. The feedback between the low concentration of free protein mRNAs and increased concentration of inactivated 50S subunits makes the growth rate severely reduced at a certain antibiotic concentration. When $\text{rpmRNA}^{\text{josa}}$ is present in the cell, josamycin-infected ribosomes are “quarantined” on the $\text{rpmRNA}^{\text{josa}}$. The free concentration of protein mRNAs boosts and ribosomes can initiate translation at a higher rate and escapes josamycin to a larger extent. The concentration of josamycin-free translating ribosomes increases, thereby raising the cell growth rate.

Peptide-mediated macrolide resistance requires a fast outflow rate of the antibiotic over the cell membrane

Previous modeling of peptide-mediated erythromycin resistance predicted the requirement of a fast outflow rate of the drug over the cell membrane to confer resistance against a macrolide with the binding kinetics of erythromycin. In gram-positive bacteria the cell wall does not offer much resistance to diffusion of small molecules and the rate of exchange of macrolides over the cell membrane is expected to be rapid, but previous *in vivo* experiments were done with gram-negative *E. coli*

cells (Lovmar *et al.*, 2006; Tenson and Mankin, 2001). In gram-negatives the outer membrane confers an efficient barrier of permeation and the entrance rate of antibiotics are expected to be slow. Gram-negative bacteria also harbor broad-specific multidrug pumps in their inner membrane, which together with the outer membrane may explain the “intrinsic” resistance that gram-negatives exhibit (Li and Nikaido, 2004). The AcrAB-TolC pump system is the major contributor of erythromycin resistance (Ma *et al.*, 1995). The efflux pump, AcrB, resides in the inner membrane and seems to form a complex with a periplasmic protein, AcrA, which links or fuses the inner and outer membrane. Then, the channel, TolC, most likely provides the exit path back to the medium for drugs, solvents, detergents etc. (Zgurskaya and Nikaido, 1999). Very little is known about the capacity of the AcrAB-TolC pump system in general and for erythromycin and josamycin in particular.

To validate the model prediction we grew wild-type and TolC mutant *E.coli* cells containing either a resistance peptide expressing plasmid or a control plasmid in the presence of varying concentrations of erythromycin in the growth medium. Corresponding experiments were done with varying concentrations of josamycin in the growth medium. Growth was recorded by absorbance after 4 hours following induction and was registered as a function of the macrolide concentration and at an IPTG concentration corresponding to maximal resistance in the wild-type as seen in previous *in vivo* growth experiments. The *in vivo* experiments confirmed the model prediction for erythromycin. No resistance was observed in the TolC mutant (Fig. 6B). The *in vivo* experiments also showed no josamycin resistance in the TolC mutant (Fig. 6D), which resistance mechanism clearly differs from that of erythromycin.

The TolC mutant is as sensitive to macrolides as the AcrB mutant, why we do not expect the pump to function in the TolC mutant. The TolC mutant was therefore modeled without pumps. The models reproduced the *in vivo* growth curves. Resistance was substantially reduced in the TolC mutant for both erythromycin and josamycin (Fig. 5B and D). In the case of erythromycin, where expression of a resistance peptide actively removes a bound drug molecule from the ribosome (Lovmar *et al.*, 2006) resistance is a consequence of an increased dissociation of erythromycin. Such a resistance mechanism is sensitive to the fate of the drug molecule after ejection. It can either leave the cell (by passive diffusion over the membrane or be actively transported by efflux pumps) or it re-associates to another ribosome. The value of the rate constant for leaving the cell in relation to the association rate constant of the antibiotic becomes very important. The requirement of a fast outflow rate for erythromycin resistance mechanism to work is then rather a requirement of a fast enough rate constant of leaving the cell once inside compared to the association rate constant to a ribosome of the antibiotic. We argue that the AcrAB-TolC efflux pump system provide the required high efflux rate. Thus, a macrolide with a lower association rate constant but with the same or lower dissociation rate constant of erythromycin is predicted by the model to confer resistance also in the TolC mutant, if resistance is mediated by active removal of the drug by the same rate as of erythromycin. For instance, a macrolide with an association rate constant of josamycin but with a dissociation rate constant of erythromycin confer resistance in the simulated TolC mutant (not shown), while a macrolide with an 100 times higher association rate constant than erythromycin gives almost no resistance in the wild-type (not shown).

In the case of josamycin, the absence of resistance in the modelled TolC mutant is also a consequence of a too high association rate constant compared to the rate constant of efflux of the drug. This creates a sharp boost of the intracellular concentration of josamycin within a very narrow interval of concentrations of the antibiotic in the medium accompanied by a dramatic reduction of the growth rate and leaves the resistance mechanism ineffective since it cannot remove josamycin once bound to the ribosomes. For example, if the association rate constant is increased 100 times, resistance is greatly reduced even in the wild-type.

REFERENCES

- Bremer, H., and Dennis, P. P. (1996). Modulation of Chemical Composition and Other Parameters of the Cell by Growth Rate, In *Escherichia coli and Salmonella: cellular and molecular biology*, F. C. Neidhardt, ed. (Washington: ASM Press), pp. 1553-1569.
- Dincbas, V., Heurgue-Hamard, V., Buckingham, R. H., Karimi, R., and Ehrenberg, M. (1999). Shutdown in protein synthesis due to the expression of mini-genes in bacteria. *J Mol Biol* *291*, 745-759.
- Ehrenberg, M., Bilgin, N., and Kurland, C. G. (1990). Design and use of a fast and accurate *in vitro* translation system., In *Ribosomes and protein synthesis: a practical approach*, G. Spedding, ed. (Oxford: IRL Press), pp. 101-128.
- Freistroffer, D. V., Pavlov, M. Y., MacDougall, J., Buckingham, R. H., and Ehrenberg, M. (1997). Release factor RF3 in E.coli accelerates the dissociation of release factors RF1 and RF2 from the ribosome in a GTP-dependent manner. *Embo J* *16*, 4126-4133.
- Hansen, J. L., Ippolito, J. A., Ban, N., Nissen, P., Moore, P. B., and Steitz, T. A. (2002). The structures of four macrolide antibiotics bound to the large ribosomal subunit. *Mol Cell* *10*, 117-128.
- Heath, M. T. (1997). *Scientific computing: an introductory survey* (New York: McGraw-Hill).
- Heurgue-Hamard, V., Dincbas, V., Buckingham, R. H., and Ehrenberg, M. (2000). Origins of minigene-dependent growth inhibition in bacterial cells. *Embo J* *19*, 2701-2709.
- Heurgue-Hamard, V., Mora, L., Guarneros, G., and Buckingham, R. H. (1996). The growth defect in *Escherichia coli* deficient in peptidyl-tRNA hydrolase is due to starvation for Lys-tRNA(Lys). *Embo J* *15*, 2826-2833.
- Jelenc, P. C., and Kurland, C. G. (1979). Nucleoside triphosphate regeneration decreases the frequency of translation errors. *Proc Natl Acad Sci U S A* *76*, 3174-3178.

- Joyce, S. A., and Dreyfus, M. (1998). In the absence of translation, RNase E can bypass 5' mRNA stabilizers in *Escherichia coli*. *J Mol Biol* 282, 241-254.
- Leclercq, R. (2002). Mechanisms of resistance to macrolides and lincosamides: nature of the resistance elements and their clinical implications. *Clin Infect Dis* 34, 482-492.
- Li, X. Z., and Nikaido, H. (2004). Efflux-mediated drug resistance in bacteria. *Drugs* 64, 159-204.
- Lovmar, M., Nilsson, K., Vimberg, V., Tenson, T., Nervall, M., and Ehrenberg, M. (2006). The Molecular Mechanism of Peptide-mediated Erythromycin Resistance. *J Biol Chem* 281, 6742-6750.
- Lovmar, M., Tenson, T., and Ehrenberg, M. (2004). Kinetics of macrolide action: the josamycin and erythromycin cases. *J Biol Chem* 279, 53506-53515.
- Ma, D., Cook, D. N., Alberti, M., Pon, N. G., Nikaido, H., and Hearst, J. E. (1995). Genes *acrA* and *acrB* encode a stress-induced efflux system of *Escherichia coli*. *Mol Microbiol* 16, 45-55.
- MacDougall, J., Holst-Hansen, P., Mortensen, K. K., Freistroffer, D. V., Pavlov, M. Y., Ehrenberg, M., and Buckingham, R. H. (1997). Purification of active *Escherichia coli* ribosome recycling factor (RRF) from an osmo-regulated expression system. *Biochimie* 79, 243-246.
- Neidhardt, F. C., and Umbarger, H. E. (1996). Chemical compositions of *Escherichia coli*, In *Escherichia coli and Salmonella: cellular and molecular biology*, F. C. Neidhardt, ed. (Washington: ASM Press), pp. 13-16.
- Pavlov, M. Y., and Ehrenberg, M. (1996). Rate of translation of natural mRNAs in an optimized in vitro system. *Arch Biochem Biophys* 328, 9-16.
- Pavlov, M. Y., Freistroffer, D. V., MacDougall, J., Buckingham, R. H., and Ehrenberg, M. (1997). Fast recycling of *Escherichia coli* ribosomes requires both ribosome recycling factor (RRF) and release factor RF3. *Embo J* 16, 4134-4141.
- Schlunzen, F., Zarivach, R., Harms, J., Bashan, A., Tocilj, A., Albrecht, R., Yonath, A., and Franceschi, F. (2001). Structural basis for the interaction of antibiotics with the peptidyl transferase centre in eubacteria. *Nature* 413, 814-821.
- Tenson, T., DeBlasio, A., and Mankin, A. (1996). A functional peptide encoded in the *Escherichia coli* 23S rRNA. *Proc Natl Acad Sci U S A* 93, 5641-5646.
- Tenson, T., Herrera, J. V., Kloss, P., Guarneros, G., and Mankin, A. S. (1999). Inhibition of translation and cell growth by minigene expression. *J Bacteriol* 181, 1617-1622.

Tenson, T., Lovmar, M., and Ehrenberg, M. (2003). The mechanism of action of macrolides, lincosamides and streptogramin B reveals the nascent Peptide exit path in the ribosome. *J Mol Biol* 330, 1005-1014.

Tenson, T., and Mankin, A. S. (2001). Short peptides conferring resistance to macrolide antibiotics. *Peptides* 22, 1661-1668.

Tenson, T., Xiong, L., Kloss, P., and Mankin, A. S. (1997). Erythromycin resistance peptides selected from random peptide libraries. *J Biol Chem* 272, 17425-17430.

Tripathi, S., Kloss, P. S., and Mankin, A. S. (1998). Ketolide resistance conferred by short peptides. *J Biol Chem* 273, 20073-20077.

Weisblum, B. (1995). Erythromycin resistance by ribosome modification. *Antimicrob Agents Chemother* 39, 577-585.

Weisblum, B. (1998). Macrolide resistance. *Drug Res Updates* 1, 29-41.

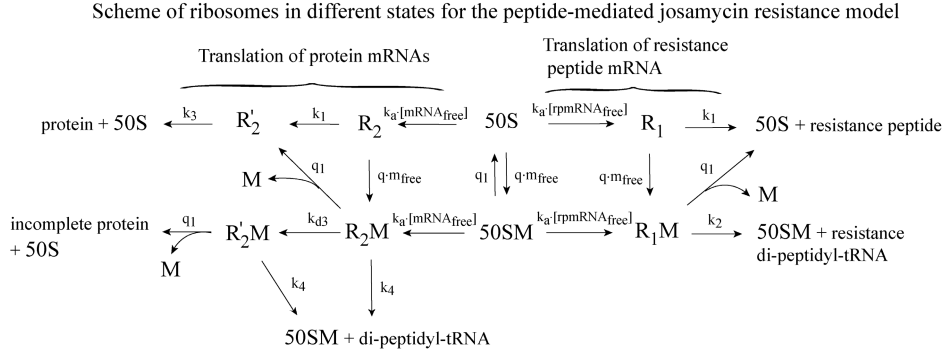
Vimberg, V., Xiong, L., Bailey, M., Tenson, T., and Mankin, A. (2004). Peptide-mediated macrolide resistance reveals possible specific interactions in the nascent peptide exit tunnel. *Mol Microbiol* 54, 376-385.

Zgurskaya, H. I., and Nikaido, H. (1999). Bypassing the periplasm: reconstitution of the AcrAB multidrug efflux pump of *Escherichia coli*. *Proc Natl Acad Sci U S A* 96, 7190-7195.

APPENDIX

Model of peptide-mediated resistance against josamycin

Below is a detailed description of the different states of ribosomes in the model.



The model is described by the following system of differential equations,

$$\begin{aligned}
 \frac{d[50SM]}{dt} &= q \cdot [m_{free}] \cdot [50S] + k_4 \cdot ([R_2M] + [R_2'M]) + k_2 \cdot [R_1M] - (k_a \cdot ([mRNA_{free}] + [rpmRNA_{free}]) + q_1 + \mu) \cdot [50SM], \\
 \frac{d[R_1]}{dt} &= k_a \cdot [rpmRNA_{free}] \cdot [50S] - (k_1 + q \cdot [m_{free}] + \mu) \cdot [R_1], \\
 \frac{d[R_1M]}{dt} &= k_a \cdot [rpmRNA_{free}] \cdot [50SM] + q \cdot [m_{free}] \cdot [R_1] - (k_2 + q_1 + \mu) \cdot [R_1M], \\
 \frac{d[R_2]}{dt} &= k_a \cdot [mRNA_{free}] \cdot [50S] - (k_1 + q \cdot [m_{free}] + \mu) \cdot [R_2], \\
 \frac{d[R_2M]}{dt} &= k_a \cdot [mRNA_{free}] \cdot [50SM] + q \cdot [m_{free}] \cdot [R_2] - (k_4 + q_1 + k_{d3} + \mu) \cdot [R_2M], \\
 \frac{d[R_2']}{dt} &= k_1 \cdot [R_2] + q_1 \cdot [R_2M] - (k_3 + \mu) \cdot [R_2'], \\
 \frac{d[R_2'M]}{dt} &= k_{d3} \cdot [R_2M] - (k_4 + q_1 + \mu) \cdot [R_2'M], \\
 \frac{d[rpmRNA_{tot}]}{dt} &= k_{s1} - k_{d1} \cdot [rpmRNA_{free}] - \mu \cdot [rpmRNA_{tot}], \\
 \frac{d[mRNA_{tot}]}{dt} &= k_{s2} - k_{d2} \cdot [mRNA_{free}] - (k_4 + q_1) \cdot [R_2'M] - \mu \cdot [mRNA_{tot}].
 \end{aligned} \tag{A1}$$

with pumps (wild-type)

$$\frac{d[m_{tot}]}{dt} = c_{II} \cdot \frac{(c_I \cdot [m_m] + c_{II} \cdot [m_{free}])}{c_I + c_{II} + c_{III} + \mu} - (c_{II} + c_{III}) \cdot [m_{free}] - \mu \cdot [m_{tot}],$$

or without pumps (TolC mutant)

$$\frac{d[m_{tot}]}{dt} = c_{II} \cdot \frac{(c_I \cdot [m_m] + c_{II} \cdot [m_{free}])}{c_I + c_{II} + \mu} - c_{II} \cdot [m_{free}] - \mu \cdot [m_{tot}].$$

A large ribosomal subunit can exist in eight different states. The 50S subunit may be free without ($[50S]$) or with ($[50SM]$) a bound macrolide. It may be a part of a ribosome ready to translate the first codons of a protein mRNA without ($[R_2]$) or with ($[R_2M]$) a bound macrolide or it may have translated the first codons and become temporarily immune to the drug ($[R'_2]$). If the mRNA starts to degrade before di-peptidyl-tRNA drop-off or spontaneous dissociation of the macrolide it ends up in state ($[R'_2M]$). State $[R'_2M]$ provides a more detailed description of the fate of ribosomes with a degrading mRNA but was not included in the erythromycin model (Lovmar *et al.*, 2006), where $q_1 \gg k_{d3}$. However, the same approximations as in the erythromycin model are also valid in the josamycin model although they are less intuitive. The subunit may also be a part of a ribosome ready to translate a resistance peptide mRNA (rpmRNA) without ($[R_1]$) or with ($[R_1M]$) a bound antibiotic molecule. The rate constant of association and spontaneous dissociation of the antibiotic is q and q_1 , respectively. Association of the ribosomal subunits occurs with rate constant k_a times the free concentration of protein mRNAs ($[mRNA_{free}]$) and free rpmRNA ($[rpmRNA_{free}]$). The first rounds of translation when the antibiotic can attack a ribosome (which is approximately the length of a resistance peptide) occur with rate k_1 . The rate for completing synthesis of a protein beyond translation of the first codons is k_3 , the drop-off rate of an antibiotic-carrying, stalled ribosome on a protein mRNA is k_4 and the rate of drop-off of resistance di-peptidyl-tRNA is k_2 . The system of equations also contains differential equations describing the change of the total concentration of the macrolide in the cell ($[m_{tot}]$) and of the total concentration of protein mRNAs ($[mRNA_{tot}]$) and rpmRNA ($[rpmRNA_{tot}]$), respectively. The macrolide passively diffuses over the outer membrane with rate constant c_I and over the inner membrane with rate constant c_{II} . The antibiotic is actively transported out of the cell by pumps (either from the cytoplasm or the periplasm) with rate constant c_{III} . The free intracellular (cytoplasmic) concentration of the macrolide is defined by $[m_{free}] = [m_{tot}] - [50SM] - [R_1M] - [R_2M] - [R'_2M]$. The macrolide concentration in the periplasm is assumed to be quickly equilibrated. The synthesis rate of rpmRNA is k_{s1} and active degradation of free rpmRNA occurs with rate constant k_{d1} . The corresponding rates of synthesis and degradation of protein mRNAs are denoted k_{s2} and k_{d2} , respectively. It is also assumed that a stalled, macrolide-carrying ribosome on the 5' end of an mRNA does not fully protect the mRNA from degradation, but it is degraded by a low rate constant, k_{d3} . The free concentration of rpmRNA and protein mRNAs is defined by $[rpmRNA_{free}] = [rpmRNA_{tot}] - [R_1] - [R_1M]$ and $[mRNA_{free}] = [mRNA_{tot}] - [R_2] - [R_2M] - [R'_2M]$, respectively. The system expands by exponential growth with cell growth rate μ , defined by

$$\mu = \frac{v_e \cdot [R'_2]}{\rho_0}, \quad [A2]$$

where v_e is the average elongation rate of an uninhibited ribosome and ρ_0 is the concentration of amino acids incorporated in proteins. The total concentration of 50S subunits ($[50S_{tot}]$) is kept constant and new 50S subunits are thus synthesised by rate $\mu \cdot [50S_{tot}]$ and the free concentration of 50S subunits varies according to $[50S] = [50S_{tot}] - [50SM] - [R_1] - [R_1M] - [R_2] - [R'_2] - [R_2M] - [R'_2M]$.

The system was solved numerically by Euler's method (Heath, 1997). Cell growth was calculated for the first 4 (Fig. 5) or 8 (Fig. 3A) hours after introduction of a certain macrolide concentration in the growth medium, $[m_m]$ by

$$V_t = V_{t-dt} \cdot e^{\mu \cdot dt}, \quad [\text{A3}]$$

where dt is a small time-step and V_{t-dt} and V_t is the volume prior and after time-step dt , respectively. Prior to macrolide exposure, the system resided at steady state for a certain synthesis rate of resistance peptide mRNA. The used program software was MATLAB 6.5 (The MathWorks, Inc., Natick, Massachusetts, U.S.A.).

Peptide-mediated resistance against erythromycin

The previously developed model for peptide-mediated erythromycin resistance was used for Fig. 5 (A and B) (see Supplementary material online of (Lovmar *et al.*, 2006)) but with the more detailed description of the flows over the inner membrane described in the differential equation for m_{tot} in eq. [A1]. The extension of the model account for the difference in macrolide concentrations where cell growth are affected in the wild-type and in the TolC mutant.

Appendix table 1. Definitions and values of used parameters.

	Description	Value	Reference
k_a	association rate constant of ribosomal subunits at initiation of translation	$2 \cdot 10^6 \text{ M}^{-1} \text{ s}^{-1}$	(1)
k_1	rate constant for translation of the first codons when the ribosome is susceptible for the antibiotic or for translation of a resistance peptide by a drug-free ribosome	1 s^{-1}	(2)
k_2	rate constant for translation of a resistance peptide by an erythromycin-infected ribosome	0.008 s^{-1} (josa) 0.1 s^{-1} (eryt)	Present study and (3)
k_3	rate constant for translation beyond the first codons of a protein mRNA and translation termination	0.03 s^{-1}	(2)
k_4	drop-off rate constant of peptidyl-tRNA from a stalled ribosome on a protein mRNA	0.06 s^{-1}	Lovmar, unpublished results
q	association rate constant of erythromycin	$3.3 \cdot 10^4 \text{ M}^{-1} \text{ s}^{-1}$ (josa) $10^6 \text{ M}^{-1} \text{ s}^{-1}$ (eryt)	(4)
q_1	dissociation rate constant of erythromycin	$1.8 \cdot 10^{-4} \text{ s}^{-1}$ (josa) 0.01 s^{-1} (eryt)	(4)
k_{s1}	synthesis rate of resistance peptide mRNA (rpmRNA)	0 - 10 nMs ⁻¹ in Fig. 3A 2 nMs ⁻¹ in Figs. 5-6	
k_{d1}	degradation rate constant of free rpmRNA	$8.3 \cdot 10^{-3} \text{ s}^{-1}$	
$k_{s2\text{max}}$	maximal synthesis rate of protein mRNAs (in the absence of rpmRNA)	$8.3 \cdot 10^{-9} \text{ Ms}^{-1}$	(5)
k_{s2}	synthesis rate of protein mRNAs	$k_{s2\text{max}} - 0.05 k_{s1} \text{ Ms}^{-1}$	
k_{d2}	degradation rate constant of free protein mRNAs	$8.3 \cdot 10^{-3} \text{ s}^{-1}$	(6)
k_{d3}	degradation rate constant of protein mRNAs with a drug-inhibited, stalled ribosome	$4.2 \cdot 10^{-4} \text{ s}^{-1}$	
c_1	rate constant of passive diffusion over outer cell membrane	$2 \cdot 10^{-3} \text{ s}^{-1}$	
c_{11}	rate constant of passive diffusion over inner cell membrane	0.1 s^{-1}	(7)
c_{111}	rate constant of active transport by pump	0.9 s^{-1}	
v_e	elongation rate of an uninhibited ribosome	20 s^{-1}	(2)
ρ_0	concentration of amino acids in proteins	2 M	(2)
$[50S_{\text{tot}}]$	total concentration of 50S ribosomal subunits	$4 \cdot 10^{-5} \text{ M}$	(2)
$[m_m]$	concentration of macrolide in the growth medium	$10^{-7} - 1.5 \cdot 10^{-3} \text{ M}$ (see figures)	

1. Antoun, A., Pavlov, M., Andersson, A., Tenson, T. & Ehrenberg M. (2003) *EMBO J.* **22**, 5593-5601.
2. Bremer, H. & Dennis, P. (1996) in *Escherichia coli and Salmonella typhimurium Cellular and Molecular Biology*, ed. Neidhardt, F. C. (ASM Press, Washington, DC.), pp. 1553-1569.
3. Lovmar, M., Nilsson, K., Vimberg, V., Tenson T., Nervall, M., & Ehrenberg, M. (2006) *J. Biol. Chem.* **281**, 6742-6750.
4. Lovmar, M., Tenson T. & Ehrenberg, M. (2004) *J. Biol. Chem.* **279**, 53506-53515.
5. Neidhardt, F. C. & Umbarger, H. E. (1996) in *Escherichia coli and Salmonella typhimurium Cellular and Molecular Biology*, ed. Neidhardt, F. C. (ASM Press, Washington, DC.), pp. 13-16.
6. Kushner, S. R. (1996) in *Escherichia coli and Salmonella typhimurium Cellular and Molecular Biology*, ed. Neidhardt, F. C. (ASM Press, Washington, DC.), pp. 849-860.
7. Zgurskaya, H. I. & Nikaido, H. (1999) *PNAS* **96**, 7190-7195



IV



Traits of Erythromycin-induced Resistance by Methylation of 23S rRNA

Karin Nilsson^{1,2}, Tanel Tenson³ and Måns Ehrenberg²

¹ Department of Biometry and Engineering, Swedish University of Agricultural Sciences, Uppsala S-75007, Sweden

² Department of Cell and Molecular Biology, Molecular Biology Program, Uppsala University, Uppsala S-75124, Sweden

³ Institute of Technology, Tartu University, 51010 Tartu, Estonia

ABSTRACT

Macrolide antibiotics bind to the large ribosomal subunit. They inhibit protein synthesis, probably by physically blocking the egress of nascent polypeptide chains on the ribosome thereby causing premature termination of translation.

The most widespread resistance mechanism to macrolide antibiotics is methylation of a specific nucleotide residue in the 23S rRNA that substantially lowers the affinity of the drug to its binding site. Methylation is carried out by methyl transferases encoded by *erm* genes. Induction of *ermC* by erythromycin is the most extensively studied *erm* gene-macrolide interaction. The *ermC* mRNA contains a short open reading frame coding for a peptide, followed by the coding sequence of the methyl transferase. In the absence of erythromycin, only the peptide is synthesised. In the presence of erythromycin, a ribosome carrying the macrolide stalls, during translation of the small open reading frame. This leads to a conformational change of the secondary structure of the *ermC* transcript, which allows a ribosome to bind and start translation of the ErmC open reading frame.

We have modelled the *ermC* resistance mechanism mathematically with particular attention to the binding affinity of a stalled ribosome in the short open reading frame of an *ermC* transcript, the specific activity of the methylase enzyme and the intracellular concentration of erythromycin. To maximise the induction response rate and to attain a high fraction of ribosomes with a modified 23S rRNA, a high binding affinity of the stalled ribosome and a highly active methylase are required. Stabilisation of the *ermC* transcript has been suggested to be a second effect of the stalled ribosome. Our analysis shows that a prolonged half-life can greatly reduce the time it takes to convert the pool of susceptible ribosomes to resistant ribosomes and can further enhance the final fraction of immune ribosomes. The most conspicuous feature of the induction dynamics is the existence of an optimal macrolide concentration at which induction of *ermC* occurs most rapidly. We also relate parameters of resistance and the antibiotic concentration to cell growth and to selective pressures on the resistance mechanism.

INTRODUCTION

The macrolides form a clinically important group of antibiotics, frequently used in the treatment of infectious diseases^{1,2}. The core structure of a macrolide is a lactone ring with 14-16 carbon atoms with sugar moieties^{1,2}. Macrolides probably inhibit protein synthesis by preventing the nascent peptide from entering the peptide exit tunnel in

the large ribosomal subunit. Crystal structures of the large ribosomal subunit in complex with different macrolides reveal that the antibiotics bind at the entrance to the exit tunnel^{3,4}, close to the peptidyl transferase centre^{5,6}. In accordance with that, an increased dissociation of peptidyl-tRNA has been reported in the presence of the drugs^{7,8,9,10}. Furthermore, there is a correlation between macrolide structure and the length of the aborted peptide chains¹⁰ and polysomes are immune to the antibiotics¹¹.

Erythromycin is the most extensively characterised macrolide and is produced in nature by the soil actinomycete *Saccharopolyspora erythraea* (formerly *Streptomyces erythraeus*)¹². *S. erythraea* protects its own ribosomes from erythromycin by dimethylating a specific adenine residue located in the drug binding site in 23S rRNA (position 2058, *Escherichia coli* numbering)^{13,14,15}. Methylation is carried out by a methyl transferase encoded by the *ermE* gene and considerably lowers the binding affinity of erythromycin and of other macrolide, lincosamide and streptogramin B (MLS_B) antibiotics^{15,16,17}. There are approximately 40 *erm* (erythromycin ribosome methylation) genes known in pathogenic bacteria and methylation of 23S rRNA is the most widespread resistance mechanism to macrolides^{2,18}. The second most important resistance mechanism is enhanced antibiotic efflux mediated by transporter proteins, while enzymatic modification of the drugs seems to be less significant^{2,18,19}. A fourth proposed mechanism is the expression of short specific *cis*-acting peptides, which confers low-level resistance to macrolides but its existence remains to be proven in clinical isolates^{20,21,22}.

The most well studied *erm* gene is *ermC* from *Staphylococcus aureus* and ErmC synthesis is induced by erythromycin²³. The *ermC* mRNA contains a small open reading frame (ORF) in the *ermC* leader region encoding a 19 amino acids long peptide, followed by the ORF of the methyl transferase. In the absence of erythromycin, the transcript assumes a translationally inactive conformation. The small ORF in the leader region is translated while synthesis of ErmC is initiated at a very low frequency since the ribosome-binding site and the start codon of the ErmC ORF are sequestered in a hairpin structure (Fig. 1(a)). In the presence of erythromycin, in contrast, a ribosome carrying the macrolide and translating the small ORF stalls when the first nine codons have been read. This causes a conformational change of the secondary structure of the *ermC* transcript, which allows for ErmC synthesis (Fig. 1(b))^{23,24}. Stabilisation of the *ermC* transcript is a second effect of the stalled ribosome^{25,26} and prolongs the mRNA half-life about twenty-fold in *Bacillus subtilis*²⁶.

In order to induce and sustain ErmC synthesis, both erythromycin-carrying ribosomes and erythromycin-free ribosomes are required. This suggests the existence of an optimal erythromycin concentration at which the induction rate is the fastest^{27,28}; at low drug concentrations the number of translationally active *ermC* transcripts is low and at high drug concentrations the number of translationally active ribosomes is low. Another question is how the putative *ermC* transcript stabilisation contributes to induce resistance. Here, we model mathematically the induction dynamics of ErmC synthesis and the subsequent transformation of the bacterium into an MLS_B-resistant cell. We discuss the effect of the binding affinity of a stalled ribosome to the leader sequence of the *ermC* mRNA, of the activity of the methyl transferase and of the concentration of erythromycin. We predict that an erythromycin concentration of the order of 10⁻⁷ M maximises the induction response rate as reflected in the most rapid boost of the concentrations of methylase and resistant ribosomes. This is in good

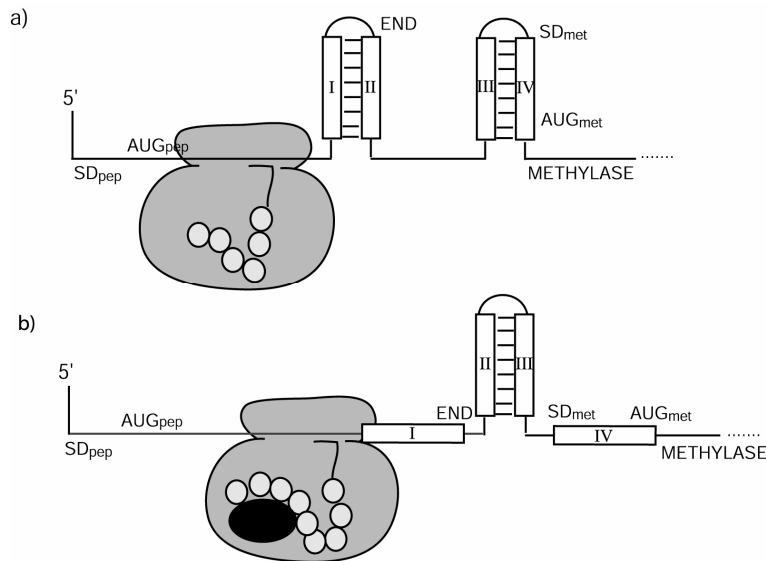


Figure 1. Suggested conformations of the 5' end of *ermC* mRNA transcript. a) Translationally “inactive” conformation of the transcript. The hairpin structure of segments I-II is temporarily disrupted when the peptide, encoded upstream of the open reading frame of the methylase, is synthesised. The downstream hairpin structure (segments III-IV) stays intact. Methylase synthesis is initiated at a low frequency since both the Shine-Dalgarno sequence (SD_{met}) and the initiation codon (AUG_{met}) are sequestered. b) Translationally “active” conformation of the transcript. A ribosome with erythromycin stalls when the first nine codons of the peptide have been translated and segments II and III form a hairpin structure. The Shine-Dalgarno sequence and the initiation codon of the methylase in segment IV are uncovered. Adapted from Weisblum, 1995²³.

agreement with previously reported optimal inducing concentrations between 10^{-8} and 10^{-7} M of erythromycin in *Staphylococcus aureus*²⁷. However, we question the biological significance of the maximal induction rate since it is not accompanied by a maximal cell growth. Further, the highest gain of *ermC* transcript stabilisation is expected for bacteria with a low-active methyl transferase and where the stalled ribosome is tightly bound to the mRNA in the *ermC* leader region and at a high intracellular concentration of erythromycin. The time it takes to change the pool of susceptible ribosomes into a pool of resistant ribosomes is greatly reduced as seen by the increase in cell growth and the growth rate reaches a higher value after resistance is attained. We also relate parameters of induction and antibiotic concentration to selective pressures on the resistance mechanism.

METHODS

The present model describes how the concentration of methyl transferase increases and is followed by the appearance of a large fraction of methylated ribosomes with time after induction by erythromycin. Throughout the paper “transformation” refers to the conversion a bacterium undergoes from an erythromycin susceptible cell to an MLS_B-resistant cell when exposed to the antibiotic, and not to the introduction of DNA into a cell.

Induction of resistance occurs in three consecutive steps. Firstly, erythromycin binds to free unmethylated ribosomes. Secondly, synthesis of the methylase enzyme is induced by a stalled erythromycin-carrying ribosome in the leader sequence of the

ermC mRNA. Thirdly, ErmC methylates a specific nucleotide residue of nascent 23S rRNA molecules and methylated ribosomes assemble. Binding of erythromycin to susceptible ribosomes is assumed to equilibrate rapidly. The probability that a free unmethylated ribosome carries the macrolide is then a function of the dissociation constant for the drug binding to the ribosome and the intracellular concentration of free erythromycin. The dissociation constant has been measured *in vivo* and estimated to be 10^{-7} M in *S. aureus*²⁹. More recent measurements *in vitro* estimate the dissociation constant to 10^{-8} M in an *E. coli* translation system³⁰. Further, binding to the leader sequence of an *ermC* mRNA by a drug-containing ribosome is assumed to quickly equilibrate. The dissociation constant, K_D , for the stalled ribosome has to our knowledge not been determined. We varied the probability that an *ermC* mRNA is open for ErmC synthesis by changing the dissociation constant. Since experiments indicate that the substrate of the methylase enzyme is nascent 23S rRNA rather than mature 50S subunits^{15, 31, 32}, there should exist a time window when methylation is possible. The time window is opened up when the recognition and binding sites for the enzyme on 23S rRNA have formed and is closed once the methylase no longer has access to the binding site, maybe after a conformational change during the first steps of assembly. The probability that a 23S rRNA becomes modified depends on the length of the time window during which methylation is possible, the specific activity of ErmC and the present concentration of the methylase in the cell. We varied the probability for a 23S rRNA to become methylated (modelled as the probability of a nascent ribosome to be methylated) by changing the K_{QM} -value, the normalised k_{cat}/K_m -parameter defined in the Appendix, which is reflecting the activity of the methylase.

Stabilisation of the *ermC* transcript has been proposed as a second effect of a stalled ribosome in the leader region. Bechhofer and Dubnau (1987)²⁶ isolated RNA from *B. subtilis* carrying the wild-type *ermC* gene in the presence and in the absence of erythromycin. The physical half-life of an *ermC* transcript was estimated to increase roughly from 2 to 40 minutes with 27 nM of the drug. By measuring the ability of induced cells to synthesise ErmC, Shivakumar *et al.* (1980)²⁵, suggested a corresponding prolongation of the functional half-life of the mRNA, which should be difficult to discriminate from the increased translation frequency per *ermC* mRNA. Further, a post-transcriptional induction of ErmC, when the stability of the transcript was unaffected, has been demonstrated *in vitro*²⁸, which was comparable to the induction *in vivo*. It is therefore unclear to what extent an increased physical half-life is accompanied with a prolonged functional half-life of the *ermC* mRNA³³. If there is a stabilisation of the *ermC* transcript, it may be a rather intricate function of the concentration of erythromycin and concentration of unmethylated and methylated ribosomes in the cell. To model the suggested mRNA stabilisation we simply increased the half-life approximately 20 times, from 2 to 45 minutes, for *ermC* transcripts with a stalled ribosome in the leader ORF. See Appendix for further details of the model and Table A1 for parameter values.

Two more properties relevant for the *ermC* induction mechanism have been proposed but are omitted in the present model. Accumulation of intermediate particles of 50S subunits and increased degradation of 23S rRNA has been reported in presence of erythromycin^{34, 35, 36, 37}. Therefore, erythromycin seems to interfere with ribosome assembly³⁶. An alternative explanation might be the existence of a quality control mechanism of newborn ribosomes during their first round of translation^{37, 38} or a disturbed balance of the synthesis of ribosomal protein and rRNA resulting in erroneous or incomplete assembly of the subunits. Moreover, experiments indicate

that ErmC binds to its own mRNA, thus repressing its synthesis³⁹. However, the footprint bound ErmC would leave on the transcript has not yet been demonstrated experimentally²³.

RESULTS

How the binding affinity of a stalled ribosome to the leader region of the *ermC* mRNA and the activity of ErmC influence induction of resistance

Intuitively, the binding affinity by an erythromycin-carrying ribosome to the leader sequence and the rate by which ErmC attaches methyl groups to 23S rRNA should be of vital importance for the efficiency of the resistance mechanism. Fig. 2(a)-(b) show what happens after the introduction of erythromycin into bacterial cells with different dissociation constants of the stalled ribosome and with different activities of the methylase enzyme, respectively. The two parameters affect both the rate of transformation and the degree of transformation reached at steady state. The slower the induction response is, the lower is the final fraction of methylated ribosomes and vice versa. As the value of K_Q decreases (stronger binding), the probability of active mRNAs increases and synthesis of the methylase and methylated ribosomes accelerate. The binding affinity of a stalled ribosome also influences the steady state concentration of the methylase, and thus indirectly controls the fraction of methylated ribosomes. With rising K_{QM} -value the probability of methylation for a nascent 23S rRNA increases and the rate by which resistant ribosomes are formed boosts. At steady state the fraction of methylated ribosomes equals the probability for a 23S rRNA to become metylated, which in turn is a direct function of the K_{QM} -parameter of the methylase. Stabilisation of the *ermC* transcript by a stalled ribosome reduces the transformation time and raises the fraction of methylated ribosomes at steady state beyond the limit when the half-life for the mRNA is unaffected (compare Fig. 2(c)-(d)). With the prolonged half-life an increased concentration of *ermC* mRNA follows, which further helps to speed up ErmC synthesis during transformation. The largest effect of a stabilised transcript is seen for bacteria with a low dissociation constant for the stalled ribosome ($K_Q \leq 10^{-5}$ M) and a methylase with a low to moderate activity ($K_{QM} = 10^{-4}$ - 10^{-6} M⁻¹) in Fig. 2(d).

Impact of erythromycin concentration on induction response rate and cell growth rate

With increasing intracellular concentration of free erythromycin, its impact on the translation machinery increases. Fig. 3(a) shows the induction response when the concentration of the macrolide is varied. The most salient feature is the appearance of an optimal erythromycin concentration at 10^{-7} M where methylase synthesis and synthesis of methylated ribosomes increase with maximal rate. Induction depends critically on the presence of ribosomes both with and without a bound macrolide. The fastest inducing concentration of the drug reflects the existence of an optimal blend of both sorts of ribosomes in the cell. Beyond the optimal inducing drug concentration the induction response rate decreases monotonically while the final fraction of resistant ribosomes at steady state only increases slightly. Clearly, the antibiotic concentration sets the final degree of transformation and is unaffected by the transformation time.

Fig. 3(b) shows how the growth rate of the cell is affected by different concentrations of erythromycin during the transformation phase. Our model

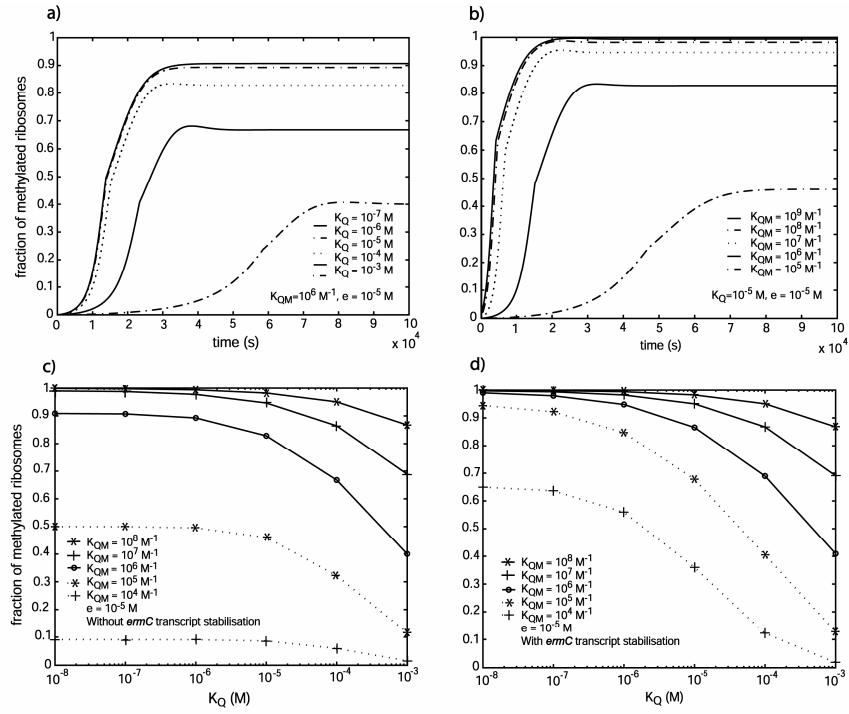


Figure 2. (a)-(b) Fraction of methylated ribosomes as a function of time after induction by erythromycin. (a) The dissociation constant of a stalled ribosome in the *ermC* mRNA leader region (K_Q) is varied while the activity of the methylase is kept constant ($K_{QM} = 10^6 \text{ M}^{-1}$). (b) The normalised Michaelis-Menten parameter of the methylase is varied (K_{QM}) while the binding affinity to the *ermC* mRNA leader sequence is kept constant ($K_Q = 10^5 \text{ M}$). (c)-(d) Fraction of methylated ribosomes attained at steady state as a function of K_Q and K_{QM} . The concentration of erythromycin is 10^{-5} M . (c) Without *ermC* transcript stabilisation. (d) With *ermC* transcript stabilisation. The half-life of the mRNA is prolonged from 2 to 45 minutes when a ribosome is stalled in the leader sequence. The intracellular concentration of free macrolide, e , is 10^{-5} M . (10^5 seconds \sim 28 hours).

demonstrates that as erythromycin is introduced into the cell, the previous pools of non-elongating (free) and elongating ribosomes start to alter, shrinking the pool of elongating ribosomes while the pool of non-elongating ribosomes expands as more and more ribosomes become inhibited by the macrolide. The higher the intracellular concentration of erythromycin becomes, the more the cell is initially drained away functional ribosomes capable of protein synthesis which is reflected in a reduced growth rate. High concentrations of free erythromycin ($[e] \geq 10^{-6} \text{ M}$ in Fig. 3(b)), makes the cell virtually stop growing for a period of time. A high macrolide concentration confers an extensive trauma to the bacterial cell, which prolongs the transformation phase. The apparent optimal concentration (10^{-7} M) of free erythromycin, where the methylase concentration and fraction of methylated ribosomes increase at maximal rate, has no counterpart in the cell growth rate. Also, the growth rate at steady state is slightly reduced as the concentration of free erythromycin increases, in contrast to the fraction of resistant ribosomes, which increases slightly (compare Fig. 3(a)-(b)). The amount of methylase and the fraction of methylated ribosomes in some sense reflect how well the resistance mechanism

works. However, the parameter genuinely subjected to selective pressure should be the growth rate of the cell, which motivates a closer study of cell growth and growth rate at steady state as a function of the three factors discussed above.

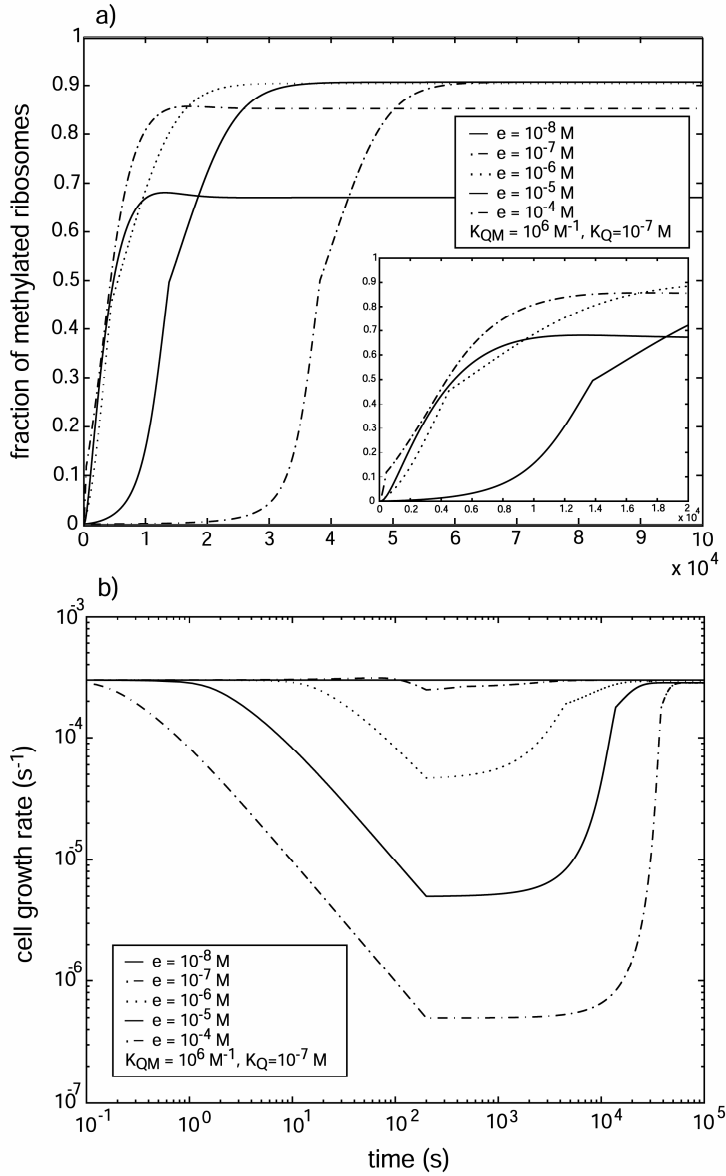


Figure 3. (a) Fraction of methylated ribosomes as a function of time after induction by erythromycin. The free concentration of the macrolide is changed whereas the dissociation constant of a stalled ribosome in the leader region of an *ermC* transcript (K_Q) and the normalised k_{cat}/K_m -parameter of ErmC (K_{QM}) are kept constant. The close up shows the first 20 000 seconds (~ 5.5 hours). (b) The growth rate of the cell in log-log scale for the same parameter values and time interval as in (a). (10^5 seconds ~ 28 hours).

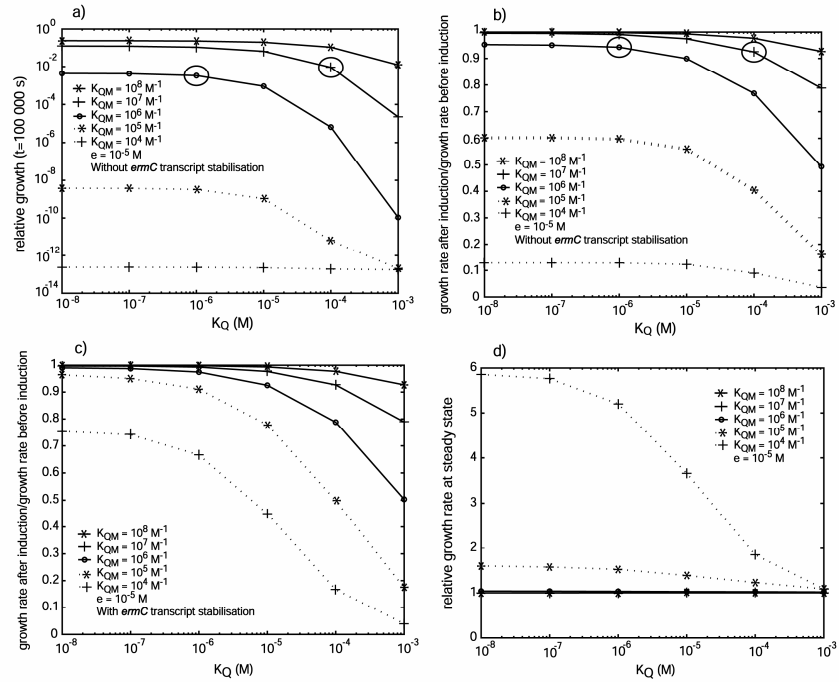


Figure 4. (a)-(c) Relative cell growth after 100 000 seconds (~ 28 hours) and the ratio between the growth rate at steady state before and after induction for the same parameter values as in Fig. 2(c)-(d). Relative cell growth is the number of cells a single cell gives rise to in the presence of erythromycin divided by the corresponding number of cells in the absence of the antibiotic. (a)-(b) Without *ermC* transcript stabilisation. (c) With *ermC* transcript stabilisation. (d) Gain with *ermC* transcript stabilisation. Relative growth rate at steady state says how many times faster the growth rate with *ermC* transcript stabilisation is compared to the growth rate without the stabilisation in Fig. 4(b)-(c).

Correlation between cell growth and parameters of the resistance mechanism

Cell growth and the growth rate of the cell constitute a direct measure of the selective advantage of a certain combination of parameter values of the underlying resistance mechanism. From our definition of the cell growth rate as the rate amino acids are incorporated into proteins normalised to the current amount of amino acids in polypeptides, we calculated cell growth up till a given time (Appendix). Fig. 4(a)-(b) depict cell growth after 100 000 seconds (~ 28 hours) and the growth rate at steady state, respectively for the same parameter values as in Fig. 2(c). Relative growth in Fig. 4(a) is the number of cells a single bacterium would generate in the presence of erythromycin divided by the number of cells a bacterium would generate when grown in the absence of the antibiotic. To maximise the induction response rate both a high binding affinity of a stalled ribosome in the leader region of the *ermC* mRNA and a highly active methylase are required. As a consequence, cell growth increases and the post-transformation growth rate approaches the pre-induction growth rate. Stabilisation of the *ermC* transcript can further promote cell growth. Fig. 4(c)-(d) shows the impact of the prolonged half-life on the growth rate at steady state.

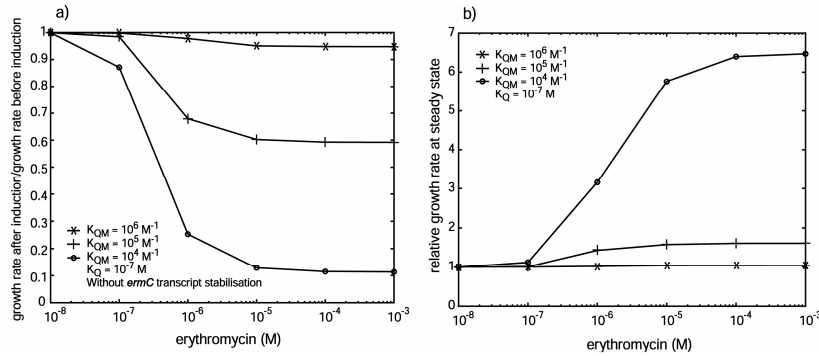


Figure 5. (a) Growth rate at steady state before induction divided by the corresponding growth rate after induction as a function of the concentration of free erythromycin. The dissociation constant of a stalled ribosome in the *ermC* mRNA leader region (K_Q) is 10^{-7} M. The normalised Michaelis-Menten parameter of the methylase (K_{QM}) ranges between 10^3 - 10^6 M^{-1} . (b) Gain with *ermC* transcript stabilisation. Relative growth rate at steady state is defined as in Fig. 4(d).

Correlation between cell growth, drug dose and time periods of drug exposure

Cell growth after a given period of time is the combined effect of how much the bacterium grows during the transformation phase when the cell growth rate can vary considerably as indicated by Fig. 3(b), plus the growth after the new steady state has been attained when the growth rate is approximately constant. A certain combination of K_Q and K_{QM} can give a faster growth during the transformation phase but a lower growth rate at steady state than compared to another K_Q - K_{QM} combination where the growth during transformation is somewhat lower but follows by a slightly higher growth rate at steady state. The encircled points in Fig. 4(a)-(b) provides an example. The time two bacteria have to be exposed to erythromycin before a larger cell growth during induction is out-competed by a higher growth rate at steady state is a function of the transformation time, cell growth during transformation and the growth rate at steady state of the two bacteria (Appendix).

Fig. 5(a) depicts how the growth rate at steady state is affected by different concentrations of erythromycin. As anticipated, the higher the intracellular concentration of the antibiotic, the more the growth rate is reduced after transformation compared to the growth rate before induction. The advantage of a stabilised *ermC* transcript is expected to increase with increasing concentration of erythromycin as seen in Fig. 5(b).

DISCUSSION

Factors determining *ermC* induction dynamics

We have modelled the *ermC* resistance mechanism as a function of the binding affinity of a stalled ribosome in the leader region of an *ermC* mRNA, the activity of the methyl transferase and the intracellular concentration of free erythromycin. The macrolide induces a course of events that converts a bacterium from a susceptible ribosome-producing cell into a cell synthesising ribosomes immune to MLS_B -antibiotics. Both the time of this transformation and the degree of transformation, as seen by the fraction of methylated ribosomes (ribosomes with a methylated 23S rRNA), have been studied. To maximise the induction response rate and to attain a high fraction of methylated ribosomes at steady state, a high binding affinity of a stalled ribosome (a low dissociation constant, K_Q) and a high activity of the methylase

(a high normalised k_{cat}/K_m -value, K_{QM}) are required (Fig. 2(a)-(d)). A tightly bound ribosome to the ORF in the *ermC* leader region increases the time the mRNA is in a translationally active conformation and rapidly boosts the methylase concentration. A highly active methylase increases the portion of nascent methylated 23S rRNA before methylation becomes unfeasible during assembly.

The most conspicuous feature of the induction dynamics, when changing the concentration of erythromycin, is the appearance of an optimal macrolide concentration at 10^{-7} M generating a maximal response rate as shown by the fastest boost of both the ErmC concentration and the fraction of methylated ribosomes (Fig. 3(a)). This is in good agreement with previous experiments by Weisblum *et al.* (1971)²⁷. They added erythromycin at concentrations between 10^{-9} and 10^{-6} M to growing cultures of *S. aureus*. After 60 minutes of incubation, portions were withdrawn and plated on agar plates with $5 \cdot 10^{-5}$ M of erythromycin. The largest number of resistant cells was found in the range 10^{-8} and 10^{-7} M of erythromycin. As previously pointed out by Narayanan and Dubnau (1987)²⁸, the optimal inducing concentration of erythromycin is explained by the requirement of ribosomes both with and without the macrolide to induce ErmC synthesis. The cell “senses” the presence of the drug through the concentration of erythromycin-carrying ribosomes. At low concentrations of the antibiotic many ribosomes are unaffected by the macrolide and there are not enough erythromycin-carrying ribosomes to substantially open up the pool of *ermC* mRNAs for translation. On the other hand, with the cell saturated with erythromycin there is a high probability that an *ermC* transcript is in a translationally active conformation but there are hardly any active ribosomes left to synthesise ErmC. However, the optimal inducing concentration of erythromycin may not be biologically significant. When the cell growth rate is monitored during the transformation phase, instead of the concentration of the methylase and the fraction of methylated ribosomes, another pattern emerges (Fig. 3(b)). With increasing concentration of erythromycin the trauma experienced by a cell is monotonically increased which is shown by a larger initial reduction of the growth rate and a longer time for its recovery. Therefore, the apparent maximal response rate may only be a consequence of the induction mechanism, and may be of no relevance for cell growth, the parameter genuinely subjected to selection pressures.

To test the potential effect of *ermC* mRNA stabilisation we increased the physical and functional half-life approximately 20 times from 2 to 45 minutes for transcripts with a stalled ribosome in the ORF in the leader region. Stabilisation makes the induction mechanism respond more strongly to erythromycin, and thus increases the sensitivity of the resistance mechanism to the drug. The transformation time is reduced and the fraction of methylated ribosomes at steady state is raised, compared to when the half-life of the mRNA is unaffected by the macrolide (Fig. 2(c)-(d)). Bacteria with ribosomes binding with high affinity to the *ermC* leader region of the mRNA (a low K_Q -value), a low active methylase (a low K_{QM} -value) and subjected to a high concentration of the antibiotic are expected to experience the largest gain. An *ermC* mRNA receives a prolonged protection from degradation when the stalled ribosome is tightly bound and the time spent in the transformation phase increases with a low-active enzyme since the production rate of methylated ribosomes is slow. The probability for an *ermC* mRNA to be protected by a stalled ribosome increases as well as the transformation time by a raised initial concentration of erythromycin-carrying ribosomes at high intracellular concentrations of the drug. All three properties contribute to build-up a high pool of *ermC* mRNA. The end result is

promoted cell growth by a reduced transformation time and by a raised growth rate at steady state (Fig. 4(b)-(d) and Fig. 5(b)).

Selective pressures on the *ermC* resistance mechanism

Development of new improved antibiotics with a broader spectrum of action and the emergence of pathogenic bacteria resistant to the drugs seems to be an everlasting armed race. Inducible MLS_B-resistant isolates of *S. aureus* appeared shortly after the introduction of erythromycin into the clinics in the early 1950s. Later, constitutively resistant mutants of the inducible strain emerged when the second generation of macrolides was launched into clinical practice. The extended range of effectiveness of the third generation of macrolides selected bacteria from *Mycobacterium* spp., which confer intrinsic MLS_B-resistance¹⁸. The present analysis of bacteria carrying the inducible *ermC* gene connects cell growth to parameters of the resistance mechanism. Cell growth in turn is an important parameter on which natural selection acts. The model shows that a high cell growth during induction requires a high binding affinity of the stalled ribosome in the *ermC* leader region of the mRNA and a highly active methylase. The expected scenario is therefore that the resistance mechanism evolves towards an increasing normalised k_{cat}/K_m -value for ErmC (K_{QM} -value) and a decreasing value of the dissociation constant of the stalled ribosome (K_Q -value). This is under the assumption that the mutations involved do not reduce the fitness in an erythromycin-free environment. Imagine a bacterium with $K_Q = 10^{-4}$ M and $K_{QM} = 10^5$ M⁻¹ in Fig. 4(a)-(b). At first a mutation causing the dissociation constant to decrease or the k_{cat}/K_m -value of the methylase to increase, 10 times, is expected to significantly boost cell growth and the growth rate at steady state resulting in a high selective advantage compared to other bacteria in the population. As the bacterial population as a whole evolves a smaller and smaller K_Q -value and higher and higher K_{QM} -value, the selective pressure to further increase growth is anticipated to decrease along with a declining selective advantage (Fig. 4(a)-(b)). Our analysis also indicates the huge selective advantage *ermC* transcript stabilisation potentially can give. When a bound ribosome in the *ermC* leader region of the mRNA only makes the transcript accessible for methylase synthesis, the dissociation constant K_Q , soon reaches a value beyond which further selective advantages are negligible as reflected by a minor increase in growth rate at steady state. For a low to moderately active enzyme ($K_{QM} = 10^4$ - 10^5 M⁻¹) an increase of K_{QM} 10 times will not only give a vast selective advantage but is also necessary for improved adaptation to the antibiotic environment (Fig. 4(b)). When a stalled ribosome also protects the *ermC* mRNA from degradation, it is much more rewarding to continue to decrease the dissociation constant, K_Q , even for a bacterium with a low-active methylase as shown in Fig. 4(c).

Selective pressures connected to drug dose and time periods of drug exposure

Both the dose and the length of the time periods bacteria are exposed to the drugs modulate the traits of the resistance mechanism. Short time periods favour bacteria with a low binding affinity of the stalled ribosome and a high methylase activity whereas bacteria with a higher binding affinity to the leader region of the *ermC* mRNA and a less active enzyme is encouraged when exposed to longer periods of the antibiotic because of their slightly higher growth rate at steady state. An example is given in Fig. 4(a)-(b) by the encircled points. Bacterial cells with $K_Q = 10^{-6}$ M and $K_{QM} = 10^6$ M⁻¹ will eventually outgrow bacterial cells with $K_Q = 10^{-4}$ M and $K_{QM} = 10^7$ M⁻¹ since they have the highest growth rate at steady state (Fig. 4(b) and Appendix). If, however, the bacterial population is repeatedly exposed to the antibiotic only

during a short period of time as in Fig. 4(a), cells with $K_Q = 10^{-4}$ M and $K_{QM} = 10^7$ M⁻¹ will instead have a selective advantage. A bacterium with $K_Q = 10^{-6}$ M and $K_{QM} = 10^6$ M⁻¹ needs approximately 3 days to catch up with a bacterium with $K_Q = 10^{-4}$ M and $K_{QM} = 10^7$ M⁻¹. Fig. 5(a) and 3(b) indicate how the selective pressure should change if a bacterial population suddenly experiences, for example, a 10 times higher antibiotic concentration than never subjected to before. The growth rate at steady state is decreased and the prolonged transformation time reduces cell growth further. The bacteria would then be less well adapted to the new situation and the selective advantage of increasing the normalised k_{cat}/K_m -value as well as the binding affinity of a ribosome bound to the leader region of the *ermC* mRNA would rise, which exposes a principle problem. The effect of increasing the dose of an antibiotic in clinical practice when dealing with bacteria resistant to lower levels of the drug is double-edged. At short-term it may be rewarding. Cell growth is suppressed a longer period of time and gives for instance the macrophages of the immune system time to trace and engulf pathogenic bacteria. The prise, however, may be an improved and more competent resistance mechanism in the long run.

REFERENCES

1. Alvarez-Elcoro, S. & Enzler M. J. (1999). The macrolides: erythromycin, clarithromycin, and azithromycin. *Mayo Clin. Proc.* **74**, 613-634.
2. Leclercq, R. (2002). Mechanisms of resistance to macrolides and lincosamides: nature of the resistance elements and their clinical implications. *Clin. Infect. Dis.* **34**, 482-492.
3. Nissen, P., Hansen, J., Ban, N., Moore, P. B. & Steitz, T. A. (2000). The structural basis of ribosome activity in peptide bond synthesis. *Science* **289**, 920-930.
4. Tenson, T. & Ehrenberg, M. (2002). Regulatory nascent peptides in the ribosomal tunnel. *Cell* **108**, 591-594.
5. Hansen, J. L., Ippolito, J. A., Ban, N., Nissen, P., Moore, P. B. & Steitz, T. A. (2002). The structures of four macrolide antibiotics bound to the large ribosomal subunit. *Mol. Cell* **10**, 117-128.
6. Schlünzen, F., Zarivach R., Harms, J., Bashan, A., Tocilj, A., Albrecht, R., Yonath, A., & Franceschi, F. (2001). Structural basis for the interaction of antibiotics with the peptidyl transferase centre in eubacteria. *Nature* **413**, 814-821.
7. Menninger, J. R. & Otto, D. P. (1982). Erythromycin, carbomycin, and spiramycin inhibit protein synthesis by stimulating the dissociation of peptidyl-tRNA from ribosomes. *Antimicrob. Agents Chemother.* **21**, 811-818.
8. Menninger, J. R. & Coleman, R. A. (1993). Lincosamide antibiotics stimulate dissociation of peptidyl-tRNA from ribosomes. *Antimicrob. Agents Chemother.* **37**, 2027-2029.
9. Otaka, T. & Kaji, A. (1975). Release of (oligo) peptidyl-tRNA from ribosomes by erythromycin A. *Proc. Natl. Acad. Sci. USA* **72**, 2649-2652.
10. Tenson, T., Lovmar, M. & Ehrenberg, M. (2003). The mechanism of action of macrolides, lincosamides and streptogramin B reveals the nascent peptide exit path in the ribosome. *J. Mol. Biol.* **330**, 1005-1014.
11. Andersson, S. & Kurland, C. G. (1987). Elongating ribosomes *in vivo* are refractory to erythromycin. *Biochimie* **69**, 901-904.

12. McGuire, J. M., Bunch, R. L., Andersson, R. C., Boaz, H. E., Flynn, E. H., Powell, H. M. & Smith, J. W. (1952). "Ilotycin", a new antibiotic. *Antibiotics and Chemotherapy* **2**, 281-283.
13. Thompson, C. J., Skinner R. H., Thompson, J., Ward, J. M., Hopwood, D. A. & Cundliffe, E. (1982). Biochemical characterisation of resistance determinants cloned from antibiotic-producing streptomycetes. *J. Bacteriol.* **151**, 678-685.
14. Skinner, R. H. & Cundliffe E. (1982). Dimethylation of adenine and the resistance of *Streptomyces erythraeus* to erythromycin. *J. Gen. Microbiol.* **128**, 2411-2416.
15. Weisblum, B. (1995). Erythromycin resistance by ribosome modification. *Antimicrob. Agents Chemother.* **39**, 577-585.
16. Uchiyama, H. & Weisblum, B. (1985). *N*-methyltransferase of *Streptomyces erythraeus* that confers resistance to the macrolide-lincosamide-streptogramin B antibiotics: amino acid sequence and its homology to cognate R-factor enzymes from pathogenic bacilli and cocci. *Gene* **38**, 103-110.
17. Weisblum, B. & Demohn, V. (1969). Erythromycin-inducible resistance in *Staphylococcus aureus*: Survey of antibiotic classes involved. *J. Bacteriol.* **98**, 447-452.
18. Weisblum, B. (1998). Macrolide resistance. *Drug Resist. Updates* **1**, 29-41.
19. Nakajima, Y. (1999). Mechanisms of bacterial resistance to macrolide antibiotics. *J. Infect. Chemother.* **5**, 61-74.
20. Tenson, T., DeBlasio, A. & Mankin, A. (1996). A functional peptide encoded in the *Escherichia coli* 23S rRNA. *Proc. Natl. Acad. Sci. USA* **93**, 5641-5646.
21. Tripathi, S., Kloss P. S. & Mankin A.S. (1998). Ketolide resistance conferred by short peptides. *J. Biol. Chem.* **273**, 20073-20077.
22. Tenson, T. & Mankin, A. S. (2001). Short peptides conferring resistance to macrolide antibiotics. *Peptides*. **22**, 1661-1668.
23. Weisblum, B. (1995). Insights into erythromycin action from studies of its activity as inducer of resistance. *Antimicrob. Agents Chemother.* **39**, 797-805.
24. Mayford, M. & Weisblum B. (1989). Conformational alterations in the *ermC* transcript *in vivo* during induction. *EMBO J.* **8**, 4307-4314.
25. Shivakumar, A. G., Hahn, J., Grandi, G., Kozlov, Y. & Dubnau, D. (1980). Posttranscriptional regulation of an erythromycin resistance protein specified by plasmid pE194. *Proc. Natl. Acad. Sci. USA* **77**, 3903-3907.
26. Bechhofer, D. H. & Dubnau, D. (1987). Induced mRNA stability in *Bacillus subtilis*. *Proc. Natl. Acad. Sci. USA* **84**, 498-502.
27. Weisblum, B., Siddhikol, C., Lai, C. J. & Demohn V. (1971). Erythromycin-inducible resistance in *Staphylococcus aureus*: requirements for induction. *J. Bacteriol.* **106**, 835-847.
28. Narayanan, C. S. & Dubnau, D. (1987). An *in vitro* study of the translational attenuation model of *ermC* regulation. *J. Mol. Chem.* **262**, 1756-1765.
29. Fournet, M. P., Barre, J., Zini, R., Deforges, L., Duval, J. & Tillement, J.P. (1987). Binding parameters and microbiological activity of macrolides, lincosamides and streptogramins against *Staphylococcus aureus*. *J. Pharm. Pharmacol.* **39**, 319-322.
30. Lovmar M, Tenson T. & Ehrenberg M. (2004). Kinetics of macrolide action. *J. Biol. Chem.* **279**, 53506-53515.

31. Villsen, I. D., Vester, B. & Douthwaite, S. (1998). ErmE methyltransferase recognizes features of the primary and secondary structure in a motif within domain V of 23S rRNA. *J. Mol. Biol.* **286**, 365-374.
32. Nielsen, A. K., Douthwaite, S. & Vester, B. (1999). Negative *in vitro* selection identifies the rRNA recognition motif for ErmE methyltransferase. *RNA* **5**, 1034-1041.
33. Sandler, P. & Weisblum, B. (1988). Erythromycin-induced stabilization of ermA messenger RNA in *Staphylococcus aureus* and *Bacillus subtilis*. *J. Mol. Biol.* **203**, 905-915.
34. Chittum, H. S. & Champney, W. S. (1995). Erythromycin inhibits the assembly of the large ribosomal subunit in growing *Escherichia coli* cells. *Curr. Microbiol.* **30**, 273-279.
35. Champney, W. S. & Burdine, R. (1996). 50S ribosomal subunit synthesis and translation are equivalent targets for erythromycin inhibition in *Staphylococcus aureus*. *Antimicrob. Agents Chemother.* **40**, 1301-1303.
36. Usary, J. & Champney, W. S. (2001). Erythromycin inhibition of 50S ribosomal subunit formation in *Escherichia coli* cells. *Mol. Microbiol.* **40**, 951-962.
37. Vester, B. & Garrett, R. A. (1987). A plasmid-coded and site-directed mutation in *Escherichia coli* 23S RNA that confers resistance to erythromycin: implications for the mechanism of action of erythromycin. *Biochimie* **69**, 891-900.
38. Mangiarotti, G., Chiaberge, S. & Bulfone, S. (1997). rRNA maturation as a "quality" control step in ribosomal subunit assembly in *Dictyostelium discoideum*. *J. Biol. Chem.* **272**, 27818-27822.
39. Denoya, C. D., Bechhofer, D. H. & Dubnau, D. (1986). Translational autoregulation of ermC 23S rRNA methyltransferase expression in *Bacillus subtilis*. *J. Bacteriol.* **168**, 1133-1141.
40. Bremer, H. & Dennis, P. (1996). Modulation of chemical composition and other parameters of the cell by growth rate. In *Escherichia coli* and *Salmonella typhimurium* Cellular and Molecular Biology (Neidhardt, F. C., ed.), pp. 1553-1569, ASM Press, Washington, D.C.
41. Heath, M. T. (1997). Scientific computing: an introductory survey. pp.156-158. The McGraw-Hill Companies, Inc., New York.
42. Antoun, A., Pavlov M., Andersson K., Tenson T. & Ehrenberg M. (2003). The roles of initiation factor 2 and guanosine triphosphate in initiation of protein synthesis. *EMBO J.* **22**, 5593-5601.
43. Neidhardt, F. C. & Umbarfer, H. E. (1996). Chemical composition of *Escherichia coli*. In *Escherichia coli* and *Salmonella typhimurium* Cellular and Molecular Biology (Neidhardt, F. C., ed.), pp. 13-16, ASM Press, Washington, D.C.

APPENDIX

Basic equations

Our model describes how the concentration of methylated (r_{met}) and unmethylated (r_{unmet}) ribosomes, proteins (p) and methyl transferase (m) change in time (t) at the introduction of erythromycin into a cell. Here we define proteins as all proteins in the cell, lumped together as one entity, except for ribosomal proteins and the methyl transferase. Ribosomes are synthesised in one step as a protein, *i.e.* we disregard ribosome assembly. Methylated/unmethylated ribosomes refer to ribosomes containing a methylated/unmethylated 23S rRNA. The model is implicitly defined by the following equations

$$\frac{dr_{met}}{dt} = Q_M(m, t) \cdot IT(V_{IT}, Q_E, r_{met}^f, r_{unmet}^f, t) \cdot [\text{mRNA}_{ribprot}] - \mu(v_e, r_{unmet}^e, r_{met}^e, t) \cdot r_{met},$$

$$\frac{dr_{unmet}}{dt} = (1 - Q_M(m, t)) \cdot IT(V_{IT}, Q_E, r_{met}^f, r_{unmet}^f, t) \cdot [\text{mRNA}_{ribprot}] - \mu(v_e, r_{met}^e, r_{unmet}^e, t) \cdot r_{unmet},$$

(A1)

$$\frac{dp}{dt} = IT(V_{IT}, Q_E, r_{met}^f, r_{unmet}^f, t) \cdot [\text{mRNA}_{prot}] - \mu(v_e, r_{met}^e, r_{unmet}^e, t) \cdot p,$$

$$\frac{dm}{dt} = Q(Q_E, r_{unmet}^f, t) \cdot IT(V_{IT}, Q_E, r_{met}^f, r_{unmet}^f, t) \cdot [\text{mRNA}_{met}] - \mu(v_e, r_{met}^e, r_{unmet}^e, t) \cdot m,$$

where $[\text{mRNA}_x]$ is the concentration of mRNA coding for ribosomal protein ($x = ribprot$), proteins ($x = prot$) and methylase ($x = met$), respectively. The mRNA concentrations are assumed to be constant. Stabilisation of the *ermC* transcript is an exception. The *ermC* mRNA concentration is then changing over time and is therefore modelled by a separate equation

$$\frac{d[\text{mRNA}_{met}]}{dt} = k_s - k_{d1} \cdot (1 - Q(Q_E, r_{unmet}^f, t)) \cdot [\text{mRNA}_{met}] - k_{d2} \cdot Q(Q_E, r_{unmet}^f, t) \cdot [\text{mRNA}_{met}].$$

(A2)

IT is the rate of translation initiation per mRNA molecule and μ is the growth rate of the cell. Q_E , Q and Q_M are three probabilities essential in this model, describing the resistance mechanism through induction of methylation of 23S rRNA. Below follows a more detailed description of the parameters of the model.

Parameters of the *ermC* resistance mechanism

Erythromycin bound to a ribosome causes dissociation of peptidyl-tRNA containing only six to eight amino acids which is less than the number of codons a translating ribosome must move before another ribosome can access the site of initiation. If translation initiation includes all steps a ribosome must pass before the next ribosome can start initiation, a ribosome susceptible to erythromycin is always free. If we further assume that association and dissociation of erythromycin always is quickly equilibrated, then the probability that a free unmethylated ribosome carries erythromycin can be described by

$$Q_E(e, t) = \frac{e}{e + K_E}, \quad (\text{A3})$$

where e is the intracellular concentration of free erythromycin and K_E is the corresponding dissociation constant. Unmethylated elongating ribosomes are regarded as temporarily immune to erythromycin, as shown by experiments¹¹.

The association and dissociation of a free unmethylated ribosome, with erythromycin, to the leader sequence of an *ermC* transcript is also supposed to quickly equilibrate and the probability of an *ermC* mRNA to be open for methylase synthesis, is approximated by

$$Q(Q_E, r_{unmet}^f, t) = \frac{Q_E \cdot r_{unmet}^f}{K_Q + Q_E \cdot r_{unmet}^f}, \quad (\text{A4})$$

where r_{unmet}^f denotes the concentration of unmethylated ribosomes free to initiate translation and K_Q is the dissociation constant of the stalled ribosome. Methylation and start of assembly are considered to occur during transcription of 23S rRNA. If methylation/escape of methylation of a nascent 23S rRNA are assumed to each take place with one rate-limiting step, the probability that a 23S rRNA becomes methylated can be calculated as

$$Q_M(m, t) = \frac{m \cdot K_{QM}}{1 + m \cdot K_{QM}}, \quad (\text{A5})$$

where m is the concentration of methylase and $K_{QM} = (k_{cat}/K_m)/k_{escape}$ is a normalised Michaelis-Menten parameter of ErmC. Equation (A4) assumes that the enzyme is normally not saturated by its substrate.

Translation

The rate of initiation of translation of an mRNA molecule, IT , is given by

$$IT(V_{IT}, Q_E, r_{met}^f, r_{unmet}^f, t) = \frac{V_{IT} \cdot (r_{met}^f + (1 - Q_E) \cdot r_{unmet}^f)}{K + r_{met}^f + r_{unmet}^f}, \quad (\text{A6})$$

where r_{met}^f and r_{unmet}^f are the concentration of methylated and unmethylated ribosomes, respectively, free to initiate translation. The probability that a free and unmethylated ribosome is not carrying erythromycin is $1 - Q_E$. The maximal rate that a ribosome may initiate translation of an mRNA is denoted V_{IT} and $K = V_{IT}/10^6$ is the corresponding K_m -parameter. V_{IT} is given by

$$V_{IT}(v_e, t) = \frac{k \cdot v_e}{N_c \cdot k + v_e}, \quad (\text{A7})$$

where k is a constant for a rate-limiting step during initiation of translation, v_e is the elongation rate of a ribosome and N_c is the number of codons a ribosome must move before the next ribosome may initiate translation on the same mRNA.

The protein density or the concentration of amino acids bound in proteins in a cell is close to constant⁴⁰ and

$$\frac{v_e \cdot (r_{met}^e + r_{unmet}^e)}{\bar{N}} = IT \cdot \sum_i [\text{mRNA}_i] \quad (\text{A8})$$

follows. The expression on the left-hand side denotes the total rate of translation termination in the cell. The average number of codons in an mRNA is \bar{N} and $\left(\frac{\bar{N}}{v_e}\right)$ is the expected time for translating an mRNA. The total rate of termination may then be written as a rate constant for termination times the total concentration of elongating ribosomes, *i.e.* $k_{term} \cdot (r_{met}^e + r_{unmet}^e)$, where $k_{term} = \frac{v_e}{\bar{N}}$. The expression on the right-hand side denotes the total rate of initiation of translation, which is simply the rate of initiation of translation per mRNA, IT , times the total concentration of mRNAs, $\sum_i [\text{mRNA}_i]$, in the cell. After reshuffling of factors, eq. A8 can be written as

$$(r_{met}^e + r_{unmet}^e) = \frac{\bar{N}}{v_e} \cdot IT \cdot \sum_i [\text{mRNA}_i], \quad (\text{A9})$$

which gives a relation between free and elongating ribosomes.

Cellular growth rate

The growth rate of the cell, μ , is defined as the rate by which amino acids become bound in proteins divided by the total concentration of amino acids already bound in proteins,

$$\mu(v_e, r_{met}^e, r_{unmet}^e) = \frac{v_e \cdot (r_{met}^e + r_{unmet}^e)}{\rho_0}. \quad (\text{A10})$$

The average elongation rate of a ribosome is v_e , the concentrations of elongating methylated and unmethylated ribosomes are r_{met}^e and r_{unmet}^e , respectively, and ρ_0 is the protein density or concentration of amino acids bound in proteins.

Regulation of translation

To give stability to the model and at the same time introduce a global control of translation in a bacterial cell, translation shifts between synthesising ribosomes and proteins according to the present concentration of amino acids in elongating ribosomes, ρ_r^e , and proteins, ρ_p . The ribosome elongation rate is changed accordingly. In the model, translation regulation strives to keep $\rho_p = 4 \cdot \rho_r^e$, *i.e.* to keep the ribosomes elongating at maximal rate. When $\rho_p > 4 \cdot \rho_r^e$ holds there is an excess of

synthetases and translation factors etc to support translation, only new ribosomes are synthesised and the ribosomes are elongating at maximal rate v_e^{\max} . When $\rho_p < 4 \cdot \rho_r^e$ holds there is an excess of ribosomes and not enough synthetases and factors etc to support a maximal translation rate. Then only proteins are synthesised and the ribosome elongation rate v_e is calculated according to

$$v_e(\rho_p, \rho_r^e, t) = \frac{v_e^{\max} \cdot \rho_p}{4\rho_r^e}. \quad (\text{A11})$$

Computer analysis

All programs, which were used in the simulations, were written in MATLAB 6.1 (The MathWorks, Inc., Natick, Massachusetts, U.S.A.). The system of rate equations was solved using ode45, one of MATLAB's built-in functions for solving ordinary differential equations numerically. The ode45 solver is based on an explicit Runge-Kutta formula. In between every time-step, when solving the system of rate equations, we used Newton's method⁴¹ to solve r_{met}^f , r_{ummet}^f and v_e from eq. A9 and eq. A11. To be able to solve the system after the introduction of erythromycin even at high erythromycin concentrations, the final intracellular concentration of the macrolide was reached after 200 seconds.

Cell growth

The volume of cells, $V(t)$, at time t , after the introduction of erythromycin, is

$$V(t) = V_0 \cdot e^{\int_0^T \mu(u) du + \mu^{ss} \cdot (t-T)}, \quad t > T. \quad (\text{A12})$$

T is the transformation time, μ^{ss} is the post-transformation growth rate at steady state and V_0 is the volume of cells when erythromycin was added. The number of cells at time t is the value of the exponential function since

$$e^{\int_0^T \mu(u) du + \mu^{ss} \cdot (t-T)} = 2^{(\ln 2)^{-1} \cdot \left(\int_0^T \mu(u) du + \mu^{ss} \cdot (t-T) \right)}. \quad (\text{A13})$$

The exponent, $(\ln 2)^{-1} \cdot \left(\int_0^T \mu(u) du + \mu^{ss} \cdot (t-T) \right)$, is the number of cell generations up till time t . To compare cell growth between two bacteria, bacterium A and bacterium B, with different growth during transformation and different growth rate at steady state, we studied the volume ratio

$$\frac{V_A(t)}{V_B(t)} = e^{\int_0^{T_A} \mu_A(u) du - \int_0^{T_B} \mu_B(u) du + \mu_B^{ss} \cdot T_B - \mu_A^{ss} \cdot T_A + (\mu_A^{ss} - \mu_B^{ss}) \cdot t}. \quad (\text{A14})$$

Two outcomes are possible over time. Either bacterium B outgrows bacterium A eventually or bacterium A outgrows bacterium B. Eq. A14 shows that the value of the

growth rates at steady state, μ_A^{ss} and μ_B^{ss} , decide the outcome. If $\mu_B^{ss} > \mu_A^{ss}$, bacterium B will finally outgrow bacterium A and vice versa in agreement with intuition. Suppose bacterium A grows more than bacterium B during the transformation time ($\int_0^{T_A} \mu_A(u) du > \int_0^{T_B} \mu_B(u) du$) but bacterium B has the highest growth rate at steady state ($\mu_B^{ss} > \mu_A^{ss}$). Assume further that the transformation time for bacterium B is longer than for bacterium A ($T_B > T_A$). The time, $t_{\text{catch up}}$, it takes B to catch up with A is given by

$$t_{\text{catch up}} = \frac{\mu_B^{ss} \cdot T_B - \mu_A^{ss} \cdot T_A - \left(\int_0^{T_B} \mu_B(u) du - \int_0^{T_A} \mu_A(u) du \right)}{\mu_B^{ss} - \mu_A^{ss}}. \quad (\text{A15})$$

If $T_B < T_A$ the time it takes bacterium B to catch up with bacterium A may still be given by eq. A15 if the numerator is a positive number. Otherwise bacterium B outgrows bacterium A already during the transformation phase of bacterium A. In the special case when $\mu_A^{ss} = \mu_B^{ss}$ the ratio in eq. A14 will instead be constant.

Table A1. Definitions and values of used parameters.

Parameter	Value	Reference
e = intracellular concentration of free erythromycin	10^{-8} - 10^{-3} M	
K_E = dissociation constant for erythromycin	10^{-7} M	29 (modelling done before the measurements in ref 30)
K_Q = dissociation constant for a stalled ribosome in the leader ORF of the <i>ermC</i> transcript	10^{-8} - 10^{-3} M	
K_{QM} = normalised k_{cat}/K_m -parameter for ErmC	10^{-8} - 10^{-4} M ⁻¹	
K = Km-parameter for initiation of translation by a ribosome	$5 \cdot 10^{-7}$ M max-value	42, 43
k = constant for a rate-limiting step during initiation of translation	1 s ⁻¹	
N_c = number of codons a ribosome must move before another ribosome may initiate translation on the same mRNA	15	
\bar{N} = the average number of amino acids in a protein	200	40
v_e^{\max} = maximal elongation rate of a ribosome	15 codons·s ⁻¹	40
ρ_0 = concentration of amino acids bound in proteins	2 M	40
r_0 = initial concentration of ribosomes	$4 \cdot 10^{-5}$ M	40
r_0^f = initial concentration of free ribosomes	$8 \cdot 10^{-7}$ M	
p_0 = initial concentration of proteins (all proteins in the cell except ribosomal proteins and ErmC)	$8 \cdot 10^{-3}$ M	40
$[\text{mRNA}]_{\text{ribprot}}$ = concentration of ribosomal mRNA	$2 \cdot 10^{-7}$ M	43
$[\text{mRNA}]_{\text{prot}}$ = concentration of protein mRNA (all mRNA in the cell except ribosomal mRNA and <i>ermC</i> mRNA)	10^{-5} M	43
$[\text{mRNA}]_{\text{met}}$ = concentration of <i>ermC</i> mRNA (when modelled without <i>ermC</i> mRNA stabilisation)	10^{-8} M	
k_s = synthesis rate of <i>ermC</i> mRNA (when modelled with <i>ermC</i> mRNA stabilisation)	$8.3 \cdot 10^{-11}$ Ms ⁻¹	
k_{d1} = degradation rate constant of <i>ermC</i> mRNA without a stalled ribosome in its 5' end (when modelled with <i>ermC</i> mRNA stabilisation)	$8.3 \cdot 10^{-3}$ s ⁻¹	26
k_{d2} = degradation rate constant of <i>ermC</i> mRNA with a stalled ribosome in its 5' end (when modelled with <i>ermC</i> mRNA stabilisation)	$3.7 \cdot 10^{-4}$ s ⁻¹	26



Bi-stable Bacterial Growth Rate in Response to Antibiotics with Low Membrane Permeability

Johan Elf^{1,3,†}, Karin Nilsson^{1,2}, Tanel Tenson⁴ and Måns Ehrenberg^{1‡}

¹Department of Cell and Molecular biology, Uppsala University, Uppsala, Sweden.

²Department of Biometry and Engineering, Swedish University of Agricultural Sciences, Uppsala, Sweden.

³Present affiliation: Department of Chemistry and Chemical Biology, Harvard University, Cambridge, MA.

⁴Institute of Technology, University of Tartu, Tartu, Estonia.

Correspondence: [†]elf@fas.harvard.edu [‡]ehrenberg@xray.bmc.uu.se

We demonstrate that growth rate bi-stability can be expected for bacterial cells growing exponentially at a fixed external antibiotic concentration. Bi-stability requires low membrane permeability and high growth rate sensitivity to the intracellular drug concentration. Rapidly, but not slowly, growing cells will effectively dilute the intracellular drug concentration by volume expansion. Therefore, the former may continue to grow rapidly and the latter to grow slowly at the same external drug concentration. Our findings have implications for the testing of novel antibiotics on growing bacterial strains.

Bacterial infection is a major cause of human suffering and death. Therefore, design of new antibiotics and development of more efficient ways to deliver already existing antibiotics are mandatory. Antibiotics with low membrane permeability for gram-negative bacteria have been regarded as clinically less interesting, although they often are very efficient when they have reached their intracellular targets. The current letter addresses this class of antibiotics and how its members could become clinically more useful by taking into account some striking relations between bacterial growth and intracellular drug concentration. We develop a general dynamic model for the intracellular concentration of these antibiotics and show that the bacterial growth rate will be bi-stable in response to the antibiotic if the membrane permeability is sufficiently small and the intracellular response to the antibiotic is sufficiently sensitive. Accordingly, these bacteria will respond differently to the same antibiotic concentration depending on the state of growth when the drug is administered. Practical consequences for the use of antibiotics and a novel interpretation of the concept of Minimal Inhibitory Concentration (MIC) are suggested.

In general, the total concentration, a , of an antibiotic in a bacterial cell depends on its net-flow over the membrane, J_{mem} , and its dilution by cell volume growth, J_{gr} . When the drug transport in to and out from the cell is passive, we model the time evolution of a by the ordinary differential equation

$$\frac{da}{dt} = \underbrace{c \cdot (a_{ex} - a_{fr})}_{J_{mem}} - \underbrace{\mu \cdot a}_{J_{gr}}. \quad (1)$$

The inflow is proportional to the external antibiotic concentration a_{ex} and the outflow is proportional to the free intracellular concentration of the antibiotic, a_{fr} . The constant of proportionality is defined as the membrane permeability, c . Both the free antibiotic concentration a_{fr} and the growth rate μ will depend on the total intracellular drug concentration a , *i.e.* $a_{fr} = a_{fr}(a)$ and $\mu = \mu(a)$. A mathematically equivalent expression can be obtained when there is active transport by an unsaturated efflux pump system^{1,2}, leading to different permeability for the in-flow and the out-flow: $J_{mem} = c_1 a_{ex} - c_2 a_{fr} = c_2 (c_1 c_2^{-1} a_{ex} - a_{fr})$. Here, c_2 replaces c and $c_1 c_2^{-1}$ is a scale factor for the external concentration a_{ex} in Eq. 1.

We will show that biologically motivated constraints on the functions $a_{fr}(a)$ and $\mu(a)$ in Eq. 1 in conjunction with a sufficiently small permeability c lead to bi-stability for a range of external antibiotic concentrations a_{ex} .

We will first make the natural assumption that the real valued and continuous function $a_{fr} = a_{fr}(a)$ is smaller than the total intracellular concentration a , *i.e.* $a_{fr} \leq a$, and that both the free and the target bound intracellular drug concentrations increase with increasing a , so that $da_{fr}/da = a'_{fr} \leq 1$. We further assume that a_{fr} is concave in a ($a''_{fr} \geq 0$), since a'_{fr} is expected to increase as the target binding sites become saturated. When $a \rightarrow \infty$, all binding sites are occupied so that $a_{fr} \rightarrow a$ and, therefore, $a'_{fr} \rightarrow 1$. Some functions, $a_{fr}(a)$, that fulfill the

criteria for bi-stability are illustrated in Fig 1A and the corresponding convex membrane flow functions $J_{mem}(a) = c(a_{ex} - a_{fr}(a))$ in Fig. 1B. $J_{mem}(0) = ca_{ex}$, the slope of $J_{mem}(a)$ is determined by $-ca'_{fr}$ and $J_{mem}(a)$ is zero when $a_{fr}(a) = a_{ex}$.

The exponential growth rate $\mu = \mu(a)$ is assumed to be a continuous, finite, positive function that decreases monotonically with increasing a , such that the dilution flow $J_{gr} = a\mu < \infty$ and $J'_{gr} = 0$ in the limit $a \rightarrow \infty$. We will, finally, assume that $d(J_{gr})/da < 0$ in some interval of a , implying that here J'_{gr} decreases more rapidly than $1/a$ with increasing a . If, to give an example, the growth rate can be modeled by a Hill function, then $J_{gr} = a\mu = ak_1 / (1 + (a/K_H)^h)$, and the requirement is that $h > 1$, meaning that in this special case $a \cdot \mu = 0$ in the limit $a \rightarrow \infty$. Together, these constraints imply that $J_{gr} = 0$ when $a = 0$, J_{gr} is positive for all values of a , and that J_{gr} reaches a finite asymptote for large values of a . This asymptote may or may not be equal to zero but must be smaller than the maximal value of J_{gr} (Fig 1D).

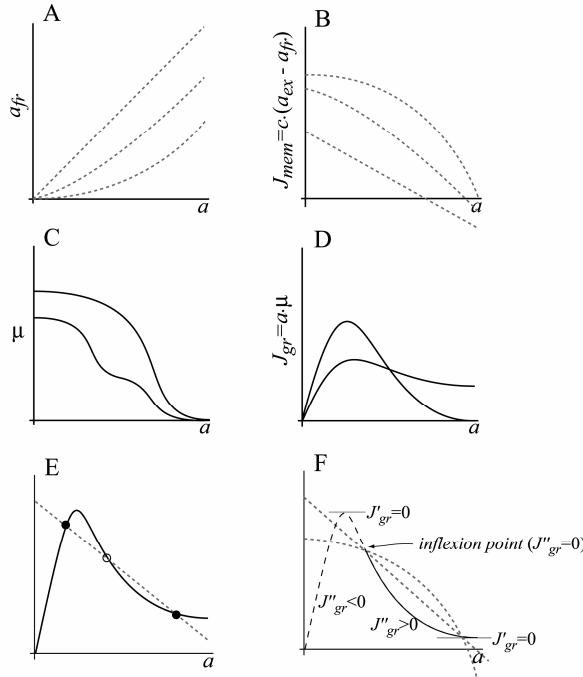


Figure 1. Graphical illustration of the constraints on $a_{fr}(a)$ and $\mu(a)$. A. Examples of how the free intracellular antibiotic concentration, a_{fr} , may depend on the intracellular antibiotic concentration, a . B. Examples of how the flow over the membrane, J_{mem} , may change with a . C. Examples of how the growth rate may depend on a . D. Examples of dilution flows, J_{gr} , compatible with bi-stability. E. Examples of how intersections between J_{gr} and J_{mem} give rise to two stable (filled discs) and one unstable (unfilled disc) steady state(s). F. Graphical demonstration of why multiple steady states always emerge when the convex J_{mem} -curve intersects the inflexion point of the J_{gr} -curve, which is concave to the right of its maximum.

It is now straight forward to show that when these constraints on $a_{fr}(a)$ and $\mu(a)$ are fulfilled and the permeability c is sufficiently small, there will always be values of the external antibiotic concentration a_{ex} for which there exist at least two stable steady state solutions of Eq. (1). To demonstrate this graphically, we first note that for an attracting (stable) steady state, where $a = a^*$ is a solution to the equation $J_{mem}(a^*) = J_{gr}(a^*)$, the inequality $J'_{mem}(a^*) - J'_{gr}(a^*) < 0$ is fulfilled³. This corresponds to intersections between the J_{mem} -curve (*dotted*) and the J_{gr} -curve (*solid*) in Fig 1E, where J_{mem} is larger than J_{gr} just to the left and smaller than J_{gr} just to the right of either steady state point. Under the conditions stated above, J_{gr} will always have an inflection point ($J''_{gr} = 0$) to the right of its maximum, since $J'_{gr} = 0$ also in the limit $a \rightarrow \infty$. Furthermore, by adjusting the external drug concentration a_{ex} it will always be possible to create an intersection of the J_{gr} and J_{mem} curves at the inflection point of J_{gr} , which corresponds to an unstable steady state. By reducing the permeability parameter c it will, finally, always be possible to create additional intersections of the J_{gr} and J_{mem} curves to the left of the maximum and to the right of the inflection point of J_{gr} , both of which fulfill the criteria of a stable steady state (Fig. 1F). Accordingly, the emergence of bi-stability depends critically on the membrane permeability c .

To further illustrate the importance of the permeability parameter c , we will derive an expression for the highest value of c that is compatible with bi-stability for a simple and yet realistic model system, in which the antibiotic drug inhibits ribosome function and thereby reduces the growth rate μ . It can be noted that there is a plethora of clinically useful antibiotics with the ribosome as their target^{4, 5}. In this model, there is a fixed total concentration, r , of ribosomes in the cell, each of which has a single binding site for the drug with the equilibrium dissociation constant K_d , irrespective of the state of the ribosome. We assume rapid intracellular equilibration of drug-bound and drug-free ribosomes with concentrations $(a - a_{fr})$ and $r - (a - a_{fr})$, respectively. The functional relation $a_{fr}(a)$, introduced in Eq. (1), between free and total intracellular concentration of the drug is then given by

$$a_{fr}(r - (a - a_{fr})) = K_d(a - a_{fr}) \Rightarrow a_{fr}(a) = \frac{1}{2} \left(a - K_d - r + \sqrt{4aK_d + (K_d + r - a)^2} \right). \quad (2)$$

On the assumption that the total rate of protein synthesis and the growth rate μ are proportional to the concentration of drug-free ribosomes, the functional dependence $\mu = \mu(a)$ introduced in Eq. (1) is given by^{6, 7}

$$\mu(a) = \frac{v_m(r - (a - a_{fr}(a)))}{\rho_0}. \quad (3)$$

For *E. coli* cells growing in a rich medium, $v_m \approx 20\text{s}^{-1}$, $r=10\ \mu\text{M}$ and the concentration ρ_0 of amino acids in peptide chains $\approx 2M^8$. As long as $K_d < r$, $J_{gr} = a\mu(a)$ fulfills the above stated criteria for potential bi-stability. The J_{mem} and J_{gr} curves that result from this model with $c=0.0001\text{s}^{-1}$, $a_{ex}=2\mu\text{M}$ and $K_d=10\text{nM}$ demonstrate the existence of bi-stable growth rate (Fig. 2A).

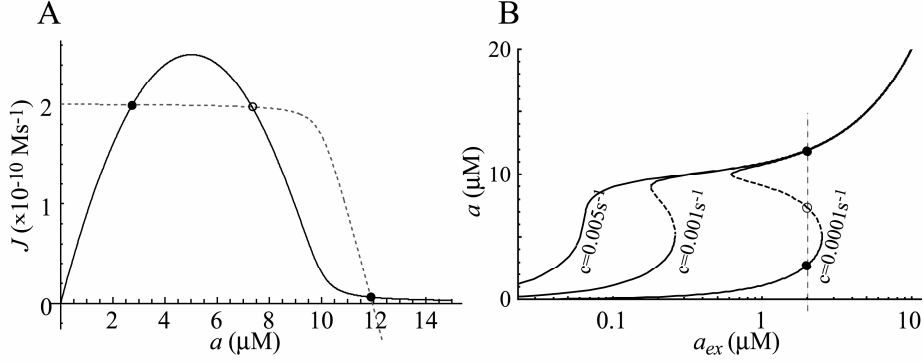


Figure 2 A. The figure shows the flow in through the membrane, J_{mem} (*dashed*) and the dilution flow, J_{gr} (*solid*) for different intracellular concentration of antibiotic, a . The intersections indicate the stationary states. **B.** The stationary states are plotted for three different permeability values, c . Solid lines correspond to stable and dashed lines to unstable states. The stationary states for $a_{ex}=2\mu\text{M}$ on the $c=0.0001\text{s}^{-1}$ curve correspond to the situation in Fig. 2A. Other parameters are $r=10\mu\text{M}$, $K_d=10\text{nM}$, $v_m=20\text{s}^{-1}$

How the region of bi-stability depends on the c and a_{ex} parameters is illustrated in Fig. (2B). Here, the total intracellular drug concentration a is plotted as a function of the external drug concentration a_{ex} for three different values of the permeability c . For the highest c -value (0.005s^{-1}) there is only one stable state, but for the other two c -values (0.001 and 0.0001s^{-1}) there are two. When the permeability c decreases below a critical value c^* , there is a saddle node bifurcation in which the single stable steady state splits into two stable and one unstable steady states. This means that bi-stability exists when $c < c^*$, while there is only a single steady state when $c > c^*$. The critical value c^* is given by the expression

$$c^* = \frac{v_m}{27\rho_0} \frac{(r - K_d)^3}{rK_d} \approx \{K_d \ll r\} \approx \frac{v_m}{27\rho_0} \frac{r^2}{K_d}. \quad (4)$$

The critical c^* value in Eq. (4) was derived by analyzing the solutions to the equation $J'_{mem}(a) - J'_{gr}(a) = 0$ for varying c -values. For small c -values there are two real and positive roots for a , which indicates bi-stability for some a_{ex} -values. For large c -values, in contrast, there are only complex valued roots for a , suggesting lack of bi-stability for all a_{ex} -values. The c -value at which the solutions switch from two

real, positive to complex valued a -roots is c^* . For the parameter values in Fig. 2, $c^* \approx 0.037s^{-1}$.

The bi-stability leads to hysteresis in the growth rate, as demonstrated for $c=0.0001s^{-1}$ in Fig. 3A. The two solid curves illustrate the steady state growth rates as functions of the external drug concentration for bacterial populations initially started out with small (upper curve) or large (lower curve) intracellular drug concentration. It is seen how these different initial conditions lead to two different growth rates in the bi-stable region of a_{ex} ($0.6\mu M - 3\mu M$). The dashed curve illustrates the unstable steady solution. The arrows show the direction in which the growth rate changes if the system is initialized in different regions of the (a_{ex}, μ) -space.

It may take very long times to establish steady state growth in new media with different external drug concentrations, in particular for cells initially containing a large intracellular drug concentration (Fig. 3B, dashed lines). For bacteria, initially growing very slowly in a medium with $10 \mu M$ drug concentration, it takes about fifty hours to attain the fast steady state growth to the left of the bi-stable a_{ex} region. For bacteria, initially growing rapidly in a medium with $0.1 \mu M$ drug concentration, it also takes quite a long time to attain the slow growth to the right of the bi-stable region (solid lines). These long times to establish steady state rates of growth for bacteria with different initial intracellular drug concentrations give rise to an experimental problem. That is, to experimentally identify growth bi-stability and hysteresis, it is essential to allow the growth rates to come near their steady values as the cell populations are shifted from environments with large or small to an intermediate current drug concentration as in Fig. 3B. Since, however, the steady state relaxation times are so long, pleiotropic drug-effects related to mutations or other effects secondary to their primary inhibition of the target obscure the analysis of the long time ($>8h$) growth properties in a fixed external antibiotic concentration (L. Kosenkranius and T. Tenson, unpublished observations).

In conclusion, we have shown how the presence of antibiotics that diffuse slowly over the bacterial cell wall may lead to bi-stability in intracellular drug concentration and bacterial growth rate. We have also shown hysteresis effects, in that bacteria subjected to increasing external drug concentrations will display larger growth rates in the bi-stable region than bacteria subjected to decreasing external drug concentrations. We have outlined the general criteria for when drug-dependent growth bi-stability can arise. We have, in particular, shown that there must be an interval of the intracellular drug concentration a in which the growth rate is reduced more strongly than $1/a$. We have also emphasized the importance of low cell wall permeability for bi-stability to emerge. In addition, we used a simple model system, where the drug binds to ribosomes and inhibits protein synthesis, to derive the critical membrane permeability value below, which bi-stability exists for a range of external drug concentrations.

Non-genetic biochemical memory effects have previously been described for gene-regulatory and signaling circuits with multiple steady states⁹⁻¹⁶. However, the possibility of memory effects directly mediated by the rate of growth has, to our knowledge, not been recognized before.

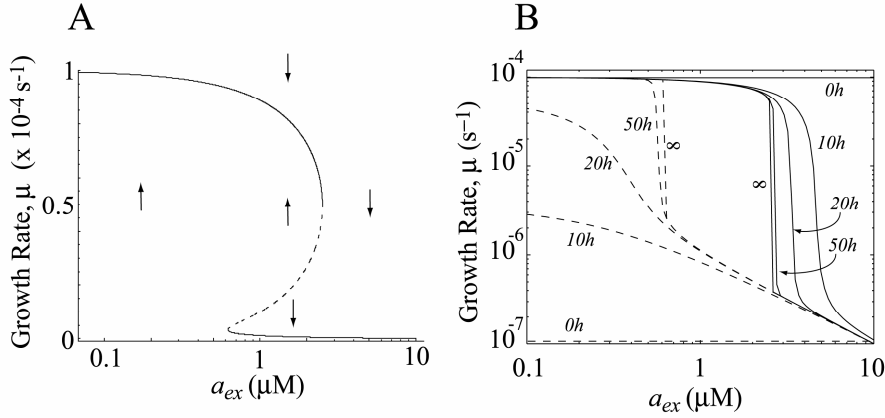


Figure 3 **A.** The steady state growth rate is plotted as a function of the external antibiotic concentration. The solid lines indicate stable and the dashed line indicates unstable steady states. The arrows indicate the direction of growth rate change in different regions for a fixed external concentration of antibiotic. **B.** This panel illustrates the times to establish steady state growth for bacteria exposed to different external drug concentrations and starting out with small (solid lines) or a large (dashed lines) internal drug concentrations. Parameters: $r=10\mu\text{M}$, $K_d=10\text{nM}$, $c=0.0001\text{s}^{-1}$, $v_m=20\text{s}^{-1}$

The starting condition for the growth of a bacterial culture may have profound effects on the growth rate, seen also in the transient phase before steady state has been established (Fig. 3). The Minimal Inhibitory Concentration (MIC) value is commonly used to characterize how susceptible a bacterial strain is to an antibiotic¹⁷. The present finding that responses of bacterial populations to antibiotic drugs may be growth history dependent, could explain why, in some cases, MIC-estimates are hyper-sensitive to experimental conditions¹⁸. When low-permeability drugs are tested, our theory reveals that conditions under which a bacterial growth culture has not reached a large growth rate when the drug is added may result in a low MIC value compared to the MIC value obtained for the very same culture when exposed under maximal growth rate conditions. Normally, MIC values are obtained for cultures growing in rich media with large growth rates, while the growth rates during clinical infections often are very small, suggesting that MIC values should be estimated for bacteria growing in poor, rather than in rich, media. This is particularly relevant for the testing of new antibacterial compounds, which may be discarded as ineffective from rich medium data although they may turn out to be clinically useful.

Acknowledgments

We thank Diarmaid Hughes, Martin Lovmar, Hans Bremer and Arvi Jöers for fruitful discussions. This work was supported by the Swedish Research Council (M.E.), Knut och Alice Wallenbergs Stiftelse (J.E.), the Wellcome Trust International Senior Fellowship (070210/z/03/z) and the Estonian Science Foundation (5311) (T.T.).

References

- 1 X. Li, M. Zolli-Juran, J. D. Cechetto, et al., *Chem Biol* **11**, 1423 (2004).
- 2 K. Poole, *Clin Microbiol Infect* **10**, 12 (2004).
- 3 S. H. Strogatz, *Nonlinear Dynamics and Chaos: With Applications to Physics, Biology, Chemistry, and Engineering* (Addison-Wesley, Cambridge MA, 1994).
- 4 C. Walsh, *Antibiotics: action, origins, resistance* (ASM Press, Washington DC, 2003).
- 5 T. Tenson and A. Mankin, *Mol Microbiol* **59**, 1664 (2006).
- 6 J. Elf, O. G. Berg, and M. Ehrenberg, *J Mol Biol* **313**, 941 (2001).
- 7 M. Ehrenberg and C. G. Kurland, *Q Rev Biophys* **17**, 45 (1984).
- 8 H. Bremer and P. Dennis, in *Escherichia coli and Salmonella Cellular and Molecular Biology*, edited by F. C. Neidhardt, R. Curtiss, J. Ingraham, E. Lin, K. Low, B. Magasanik, W. Reznikoff, M. Riley, M. Schaechter, and H. Umbarger (ASM Press, Washington, D.C., 1996).
- 9 A. Becskei, B. Seraphin, and L. Serrano, *EMBO J* **20**, 2528 (2001).
- 10 J. Elf and M. Ehrenberg, *Systems Biology* **2**, 230 (2004).
- 11 W. Xiong and J. E. Ferrell, Jr., *Nature* **426**, 460 (2003).
- 12 B. M. Shykind, S. C. Rohani, S. O'Donnell, et al., *Cell* **117**, 801 (2004).
- 13 M. Acar, A. Becskei, and A. van Oudenaarden, *Nature* **435**, 228 (2005).
- 14 N. I. Markevich, J. B. Hoek, and B. N. Kholodenko, *J Cell Biol* **164**, 353 (2004).
- 15 T. S. Gardner, C. R. Cantor, and J. J. Collins, *Nature* **403**, 339 (2000).
- 16 M. R. Atkinson, M. A. Savageau, J. T. Myers, et al., *Cell* **113**, 597 (2003).
- 17 J. M. Andrews, *J Antimicrob Chemother* **48 Suppl 1**, 5 (2001).
- 18 R. N. Jones, *Arch Pathol Lab Med* **125**, 1285 (2001).

